Evaluation of the efficacy of the novel varroacide 1-allyloxy-4-propoxybenzene, and assessment of sublethal exposure on honey bee and *Varroa destructor* gene expression

by

Robert Xinzhi Lu

A thesis submitted in partial fulfillment of the requirements for the degree of

Master of Science

Department of Biological Sciences
University of Alberta

ABSTRACT

The ectoparasitic mite *Varroa destructor* ("varroa") poses a major threat to sustainable beekeeping worldwide. Various chemical "varroacides" have been developed to combat infestations in commercial apiaries. While effective, these chemicals can be toxic to honey bees, humans, and leave unwanted residue deposition in beeswax and honey. Furthermore, varroacide-resistant mite populations are increasingly prevalent, necessitating the development of novel solutions. The dialkoxybenzene 1-allyloxy-4-propoxybenzene (codenamed "3c{3,6}") is a promising new varroacide, capable of inducing paralysis and death in varroa *in vitro*. Prior field assays have demonstrated 3c{3,6} treatment to reduce varroa populations and improve overwintering survival in hives. My thesis continued to evaluate the viability of 3c{3,6} as a commercial varroacide.

Across three experimental seasons, I expanded on existing 3c{3,6}field tests to evaluate efficacy and optimize treatment duration, dosage, and applicator design. In the fall of 2021, I tested a 4 g/colony dosage over four weeks, using a wooden applicator was placed on the top bars of each colony's broodnest. In the fall of 2022, the dosage was increased to 8 g/colony, applied over six weeks via a larger applicator consisting of three wooden strips suspended between broodnest frames. Cardboard was also tested as an alternative applicator material in this year. In spring 2023, a 3c{3,6} dosage of 10 g/colony was applied for 6 weeks using the same wooden applicator design as the fall of 2022. In all trials, colonies treated with 3c{3,6} were compared against a negative control containing no active compound, as well as a positive control treated with the commercially available varroacide Thymovar® in 2021 and 2022. In all years, 3c{3,6}-treated colonies exhibited significantly higher mortality of varroa than untreated counterparts, with mortality rates and

efficacy comparable to Thymovar® in 2021 and 2022. Nevertheless, 3c{3,6} treatment efficacy was lower in 2021 (~48%) versus 2022 and 2023 (>90% in all cases), attributable to a combination of lower dosage, reduced applicator surface area, and a shorter treatment duration. Colonies treated with 3c{3,6} showed improved overwinter survival versus negative control colonies in 2022 and 2023, but not 2021. Cardboard applicators, though effective, were destroyed by worker bees within the hive.

Secondly, I used an exposure bioassay coupled with transcriptomics to assess sublethal effects of 3c{3,6} vapour exposure on varroa and honey bees at an EC_{50} dosage (based on the concentration required to kill or paralyze 50% of a sample of varroa mites). I hypothesized greater perturbation in varroa metabolism than in bees, given that 3c{3,6} possesses higher toxicity towards the former. In a 2-by-2 design, cohorts of 10 nurse-age bees were either infested with varroa mites, exposed to 3c{3,6}, had both mites and 3c{3,6}exposure, or neither. I found several hundred differentially-expressed genes between 3c{3,6}-exposed and control honey bees and mites, including putative genes pertaining to detoxification and odorant detection in the bees, and genes encoding calcium-dependent synaptic enzymes in the mites. However, no genes were significantly differentially regulated following a Benjamini-Hochberg correction. Additionally, no significantly differentially regulated ontology pathways were identified.

Overall, my research further demonstrates 3c{3,6} as a promising novel varroacide. In addition, my trials helped optimize dosage and applicator design, though other materials may be tested in the future. However, the precise mode of action of 3c{3,6} on varroa remains unresolved, and further research is needed to investigate the impact of 3c{3,6} exposure on worker bee development and queen fertility.

PREFACE

Chapter 2 of my thesis represents a component of a wider ongoing collaboration between the research groups of Dr. Erika Plettner at Simon Fraser University (SFU), and Dr. Stephen Pernal at Agriculture and Agri-Food Canada (AAFC) Beaverlodge Research Farm. Specifically, the experiments I conducted were part of a set of parallel experiments concurrently running in Beaverlodge, Alberta, and the Fraser Valley, BC. Additionally, I performed the experimental set-up and management of colonies alongside the staff at Beaverlodge Research Farm, who maintained the colonies throughout the year, including during my absence.

Chapter 3 of my thesis represents original work conducted by myself, though with supplies being provided in part by Dr. Erika Plettner at SFU.

ACKNOWLEDGEMENTS

Completion of this thesis project was made possible through the help of numerous individuals and organizations who supported my research and studies. Foremost, I wish to extend my sincerest gratitude to my co-supervisors, Dr. Olav Rueppell at the University of Alberta, and Dr. Stephen F. Pernal at Agriculture and Agri-Food Canada (AAFC), who provided wisdom, feedback, guidance, and perspective throughout the years. Both co-supervisors facilitated the development of my skills in the field and the lab – skills which will no doubt prove indispensable moving forward in my scientific career, no matter the field.

I am grateful to Abdullah Ibrahim at the AAFC, who guided my field activities through all three of my field seasons at the Beaverlodge Research Farm, alongside providing his decades of beekeeping expertise to facilitate my experiments. I gratefully recognize the field assistance of Rassol Bahreini for helping me in my first field season, providing his research expertise in varroacide development towards helping me understand the system which was at the time still unfamiliar to me. I also would like to thank David Ostermann at AAFC, who assisted in the 2023 field season, and managed my experimental colonies during my absence from the Research Farm.

From the Rueppell Research Group, I wished to give special thanks to Jennifer Hofmeyr, who guided me through the laboratory protocols for extracting RNA and creating cDNA libraries. Her extensive expertise and calming demeanor made her an exceptional mentor, as she helped me through each step of our laboratory protocols. I also wish to thank Jacob J. Herman for his assistance in creating and validating the bioinformatics pipeline, leveraging his experience in gene expression analysis to ensure my pipeline functioned from start to end.

I also wish to extend my gratitude to Dr. Erika Plettner and the Plettner Research Group at

Simon Fraser University, who synthesized and supplied 1-allyloxy-4-propoxybenzene for my experiments. They also provided the applicators used in all my field trials.

Very special thanks for all the summer students employed by AAFC who helped me carry out my field work, including Timothy Queva (2021, 2022) and Erik Forsberg from Northwestern Polytechnic (2022, 2023), Shelley Wang (2022) and Natalia Clermont (2022) from the University of British Columbia, Eva-Marie Smith (2022) from the University of Alberta, Olivia Heelan (2023) from the University of Alberta, and Alison Goeres (2023) from the University of the Fraser Valley. All these wonderful individuals not only eased the pressure of managing dozens of honey bee colonies, but also helped make field work a livelier activity for all involved.

I wish to thank Dr. Carolyn Taylor at the University of British Columbia for statistical consulting, helping me design and optimize the linear model used to analyze my field trial data.

Additional thanks to Patricia Wolf Veiga at the National Bee Diagnostics Centre, and Urmila Basu and Yanhong Chen at the University of Alberta, for their assistance in designing a protocol to extract RNA from samples using a tissue disruptor.

I wish to extend thanks to Dr. Jeffrey Harris and Ms. Audrey Sheridan at Mississippi State University for granting me permission to use their diagram of the varroa life cycle, in Chapter 1.

Finally, I wished to thank the Natural Sciences and Engineering Research Council of Canada (NSERC), Project Apis m., and Alberta Innovates for funding me through the course of my master's education. I also wish to thank Project Apis m., the Alberta Beekeepers' Commission (ABC), Results Driven Agricultural Research (RDAR), the Canadian Bee Research Fund, and Bee Maid for providing research funding which enabled us to purchase the necessary supplies and equipment for the field experiment and laboratory analyses

TABLE OF CONTENTS

LIST OF TABLES

LIST OF FIGURES

Chapter 1: Introduction

1.1 General Introduction

Pollinators are a major component of terrestrial ecosystems, owing to their relationship with the many flowering plants whose reproductive cycle is inexorably dependent on the pollen vectoring resulting from their foraging behaviour (Ashman et al. 2004). Among this group, the western honey bee (*Apis mellifera* L.) stands out as the most widespread and populous (Gill 1990). Within agricultural systems in particular, managed honey bee hives are the primary providers of pollination services, allowing for the propagation of economically important crops such as tree fruits, berries, hybrid canola seed, and various legumes (Nye and Anderson 1974, Calderone 2012). In Canada, honey bee dependent crops include tree and stone fruit, various berries, cucurbits, oilseeds, forage legumes (in particular clover), and pulses (CAPA 1995). Furthermore, when present, feral honey bee colonies also play a role in incidental pollination of both crops and wild plants alike (Gill 1990, Kasina et al. 2009). Across its cosmopolitan range (both native and introduced), the honey bee is consistently one of the most ubiquitous pollinators, with its highly generalist foraging breadth linking it to the reproduction of many plant species (Hung et al. 2018).

Honey bees themselves are afflicted by a diverse array of pathogens, including bacteria, viruses, fungi, and parasitic arthropods (Genersch 2010, Evans and Schwarz 2011, Hristov et al. 2020). Historically, these pathogens have led to seasonal losses of honey bee colonies, though these losses appear to have been manageable as evidenced by the net increase of managed honey bee colony numbers from 1961 to 2007 in Canada and worldwide (Aizen and Harder 2009, Meixner 2010). However, in the past 2 decades, high rates of overwintering honey bee loss have raised concerns over the sustainability of beekeeping in Canada and around the globe (Becher et al. 2013, Hristov et al. 2020, Claing et al. 2023). In the past decade, winter colony loss has averaged

between 15-20% across COLOSS surveyed countries (primarily in Europe, but also including the Middle East/North Africa and Mexico) (Brown et al. 2018, Gray et al. 2020, Gray et al. 2023). Winter losses in North America since 2020 have been consistently high, with both Canada and the United States reporting national average winter losses of ~30% annually (Bruckner et al. 2023, Claing et al. 2023). Numerous factors have been reported as contributors to this increased rate of colony loss, including queen failure, starvation, natural disasters, climate change, agricultural pesticide usage, and parasites and pathogens (Brodschneider and Gray 2022, Claing et al. 2023, Gray et al. 2023). However, one particular parasite has become the most significant and consistently identified contributor to colony losses globally – the ectoparasitic mite *Varroa destructor* Anderson and Trueman (2000), alongside its associated vectored viruses (Le Conte et al. 2010, Parveen et al. 2022, Gray et al. 2023).

1.2 The Ectoparasite *Varroa destructor*

Varroa is a genus of ectoparasitic mite affecting bees of the genus *Apis* , though its species are natively endemic to the cavity-nesting honey bee species of Southeast Asia (occasionally referred to as subgenus *Apis*) (Skorikov 1929, Anderson and Trueman 2000). Together with its sister genus *Euvarroa* Delfinado and Baker (1974), *Varroa* has traditionally been placed within its own family Varroidae (Parasitiformes: Mesostigmata: Dermanyssoidea), though recent phylogenetic analyses of superfamily Dermanyssoidea have instead suggested that varroids form a clade nested within the family Laelapidae (Dowling and OConnor 2010, Oh et al. 2024). Historically confined within the range of their native host species *Apis cerana* Fab. in Southeast Asia, a host-shift event occurring in the mid-20th century resulted in populations of *Varroa*

establishing and reproducing within managed *Apis. mellifera* L. colonies for the first time (Oldroyd 1999). Initially, the *A. mellifera*-infesting mites were classified as a distinct lineage of *Varroa jacobsoni* (Oudemans 1904). However, Anderson and Fuchs (1998) observed that the populations established and reproducing on *A. mellifera* differed by approximately 6.8% in their mtDNA COI sequences when compared to the holotype population of *V. jacobsoni* found in Indonesia/Papua New Guinea, whose representatives are also able to establish and reproduce in *A. mellifera* colonies (albeit to a much more restricted extent) (Andino et al. 2016). Consequently, the *A. mellifera*-infesting populations of *Varroa* were reclassified into their own distinct species, *Varroa destructor* Anderson and Trueman (2000), based on differences in in COI sequence and morphology of adult females. It is notable, however, that there are no significant morphological differences distinguishing mature female *V. destructor* and *V. jacobsoni* (Anderson and Trueman 2000). Henceforth, for brevity, I will use the term "varroa" to refer to *V. destructor*. In the decades following the host shift of varroa into managed *A. mellifera* colonies, the mite has attained near-cosmopolitan distribution, emerging as one of the greatest threats to global beekeeping (Rosenkranz et al. 2010, Traynor et al. 2020). Despite control efforts, the range of varroa has nevertheless continued to expand (Giliba et al. 2020, Traynor et al. 2020). Most recently, varroa has expanded into Australia (McFarlane et al. 2024), which was previously considered the last major region for varroa-free beekeeping (Iwasaki et al. 2015, Roberts et al. 2017, Owen et al. 2021).

Varroa is a opportunistic parasite capable of feeding upon both late instar larvae/pupae and adult life cycle stages of their honey bee hosts, with the ventral metasoma being the preferred feeding site for mites infesting pupae and adults (Evans and Cook 2018). Its life cycle can be divided into two distinct stages: dispersing and reproductive (Frey et al. 2013, Piou et al. 2016,

Ramsey et al. 2019, Han et al. 2024) (Fig. 1-1). During the dispersing stage, gravid adult female mites temporarily affix themselves to adult worker bees (typically nursing bees within the brood nest) (Kuenen and Calderone 1997), which allow the mites to be transported in the vicinity of brood cells containing late-instar larvae (5^{th} instar is typically preferred) (Frey et al. 2013). Invasion of cells by mites marks the start of the reproductive stage, and occurs when a gravid foundress enters a 5^{th} instar larval bee cell immediately prior to the application of the wax cap by worker bees – typically 15-20 hours before capping in worker cells, and 40-50 hours before capping in drone cells (Boot et al. 1992). Varroa may also rarely enter queen cells, though foundresses which do so exhibit severely reduced reproductive capacity (Santillán-Galicia et al. 2002). Upon initial entry, the mite will hide submerged in the brood food at the bottom of the cells, before transferring onto the larva and beginning to feed approximately four hours after invasion, immediately after the formation of the pupal cocoon (Dillier et al. 2006, Calderón et al. 2010). As the foundress mite feeds, she both produces a communal feeding site for her offspring, along with constructing faecal accumulations against the walls of the cell to be used as mating platforms upon which her offspring congregate – two forms of parental care behaviour (Donzé and Guerin 1994, Rosenkranz et al. 2010). The reproductive stage begins with production of one egg approximately 60-70 hours after the commencement of feeding activities, with other eggs following at approximate 30 hour intervals (Garedew et al. 2004, Calderón et al. 2009). The foundress mite oviposits a single unfertilized male egg and an average of 4-5 female eggs on each worker pupa, or 5-6 on each drone pupa (Martin 1995). Young mites feed at their mother's feeding wound on the pupal host (as their own chelicerae are too fragile to penetrate the pupal cuticle) and pass through two developmental stages (proto- and deutonymph) before sib-mating (Rosenkranz et al. 2010). The entire post-capping reproductive cycle occurs over approximately 11-12 days on

workers and 15 days on drones (Häußermann et al. 2018, Ardestani 2022, Underwood and López-Uribe 2022), resulting in an average of 2-3 and 3-4 viable daughter mites, respectively (Rosenkranz et al. 2010, Alattal et al. 2017, Odemer 2020).

Varroa primarily feed on fat body tissues and haemolymph of their hosts by piercing the pupal cuticle directly or through the soft intersegmental membrane of the abdomen in adults (Ramsey et al. 2019, Han et al. 2024). This feeding activity is associated with the disease known as "varroosis," characterized by permanent lethargy, shortened lifespans, reduced body mass, and reduced immune fitness in afflicted bees (Rosenkranz et al. 2010, Fanelli and Tizzani 2020, Szczurek et al. 2020). Varroosis symptoms are particularly prominent in bees infested during larval development, although Piou et al. (2016) observed increased rates of wing atrophy/deformation and hyperpigmentation resulting from mite infestation of adult bees as well. Furthermore, varroa mites vector a multitude of severe and debilitating viral diseases, such as deformed wing virus (DWV) and numerous paralysis viruses, among others (Table 1-1) (Kevan et al. 2006, Neumann et al. 2012, Shen et al. 2005a). Moreover, the presence of varroa can worsen the overall viral landscape, by facilitating the selection of higher-virulence virus strains and increasing overall viral titers, even for viruses not vectored by varroa (Martin et al. 2012, Doublet et al. 2024). Once established, these viruses may also be transmitted horizontally among bees through trophallaxis (oral-oral feeding between individuals), food contamination, the fecal-oral route, through adhesion to the surface of eggs laid by infected queens, and through stored sperm (Chen et al. 2006, Chen and Siede 2007, Amiri et al. 2018, Amiri et al. 2020). Many of these viruses can remain as latent asymptomatic infections even in the absence of varroa (Yue and Genersch 2005, Hamiduzzaman et al. 2015, Shen et al. 2005b), which can then be reactivated by stressors, including varroacides used to control the mites (Yang and Cox-Foster 2005, Locke et al. 2012, Nazzi et al. 2012, Di

Prisco et al. 2013, Hou et al. 2014). Acute virus infections may also be facilitated by varroa feeding on the bees' fat body, as the organ plays a crucial role in the synthesis of innate immune proteins, lysozyme, and lectins, among other factors (Wang et al. 2018, Skowronek et al. 2021). At the colony level, the cumulative effects of the varroa-virus dyad further exacerbate other environmental stressors, including non-viral infections (e.g., nosemosis) and agricultural pesticides (Hou et al. 2014, Noël et al. 2020). In regions where overwintering of colonies is required, varroa infestation is a major cause of colony losses during the winter stress period because the weakening and anorexic effects of feeding mites reduces worker bees' thermoregulation capabilities (Amdam et al. 2004, Guzmán-Novoa et al. 2010, Aldea-Sánchez et al. 2021).

Inter-colony dispersal of mites occurs when mites transfer between colonies by drifting (Frey and Rosenkranz 2014, DeGrandi-Hoffman et al. 2017), robbing (Peck and Seeley 2019, Smith and Peck 2023), or switching hosts at flowers (Peck et al. 2016). Horizontal transfer of mites between colonies can either occur by workers from highly-infected and potentially collapsing colonies drifting into other colonies ("mite bomb" hypothesis) or by workers from strong colonies picking up mites during robbing weaker colonies ("robber lure" hypothesis), but the relative importance of either mechanism is current unclear (Peck and Seeley 2019, Kulhanek et al. 2021).

Given the severe impacts of varroa on honey bee health, perennial maintenance of honey bee colonies requires the control of mite populations. Currently, the most common option to control varroa infestations is the use of chemical "varroacides" (Rinkevich 2020). Such chemicals are designed to directly reduce varroa populations by killing mites. For sustainable control of mites, however, a balance is required in that the compounds must maintain their lethality towards mites while also being sufficiently benign towards bees (van der Steen and Vejsnæs 2021). The

most efficient way of accomplishing this goal is to choose compounds that selectively target varroa-specific anatomic or metabolic features (Plettner et al. 2017). Varroacides can generally be divided into two categories: synthetic acaricides, and acaricides derived from natural products (including organic acids). Application of varroacides may occur in the spring, before the start of the nectar flow, and/or in the fall prior to overwintering, depending on infestation levels (Currie and Gatien 2006).

1.3 Synthetic Chemical Varroacides

Synthetic varroacides are manmade chemical compounds used in the control of varroa mites, either being modified from plant-based compounds or synthesized *de novo* (Qadir et al. 2021). These compounds are widely used owing to their high efficacy – typically resulting in over 90% mortality when used against naïve mite populations (Ferrer-Dufol et al. 1991, Hillesheim et al. 1996, Zikic et al. 2020). Currently, three major categories of synthetic varroacides are commercially available in Canada: pyrethroids (tau-fluvalinate and flumethrin), organophosphates (coumaphos), and formamidines (amitraz) (Health Canada 2019, Mitton et al. 2022). In all cases, the typical method of treatment application is through the use of miticide-impregnated plastic strips, hung within the brood nest to facilitate direct contact with dispersing mites on infested nurse bees (Floris et al. 2001, Gregorc et al. 2018, Olmstead et al. 2019).

The pyrethroids tau-fluvalinate and flumethrin have been among the earliest varroacides used in beekeeping and exhibit high efficacies (~99% and 95.4% respectively) against naïve varroa populations (Ferrer-Dufol et al. 1991, Hillesheim et al. 1996). These chemicals have been previously used as agricultural insecticides, targeting voltage-gated sodium channels in arthropod

neurons and causing paralysis and death (Vijverberg and vanden Bercken 1990, Field et al. 2017). Both tau-fluvalinate and flumethrin are registered for use in Canadian apiculture, respectively sold under the trade names Apistan® and Bayvarol® (Currie et al. 2010, Health Canada 2019). Pyrethroid-based miticides are known to exhibit mild non-target toxicity against honey bees resulting in acute neurotoxic symptoms (Johnson et al. 2006, Oruc et al. 2012, Qi et al. 2020). Furthermore, the lipophilic properties of pyrethroids allow miticide residues to sequester in wax and hive products (Johnson et al. 2010, Benito-Murcia et al. 2021). In recent decades, the extensive use of pyrethroids has led to the evolution of pyrethroid-resistant varroa populations globally, which in turn has substantially reduced the overall efficacy of such formulations (Hillesheim et al. 1996, Milani 1999, Rodríguez-Dehaibes et al. 2005, Bąk et al. 2012, González-Cabrera et al. 2016). Tau-fluvalinate resistance in Canada is particularly well-documented, with resistant varroa being reported in the early 2000s (Currie et al. 2010, Morfin et al. 2022). While flumethrin is less widely used than tau-fluvalinate, it too has demonstrated decreased efficacy, likely due to cross-resistance with tau-fluvalinate (Gracia-Salinas et al. 2006).

Also frequently used against varroa are formulations of the organophosphate coumaphos, such as CheckMite+® in Canada (Health Canada 2019). Considered a proinsecticide, coumaphos must be bioactivated intracellularly by cytochrome P450 monooxygenase enzymes into coroxon, which in turn binds to and inhibits acetylcholinesterase (Jeschke 2016, Vlogiannitis et al. 2021). Coumaphos primarily targets the varroa nervous system to induce rapid irreversible paralysis and death, and yields high efficacy rates (96-97%) in naïve varroa populations (Zikic et al. 2020). Efficacy is temperature-dependent, with an optimum efficacy temperature of 32.5° C (Milani and Della Vedova 1996). Treatment dosage must be carefully considered because high concentrations of coumaphos can result in fatal acute toxicity against worker bees, though the toxicity is somewhat

variable depending on exposure route (Gregorc et al. 2018, Bommuraj et al. 2021). Coumaphos is also known to sequester in wax due to its lipophilic properties, which poses second-hand risks to non-nurse bees localized away from brood frames (Johnson et al. 2009, Gregorc et al. 2018). In Canada and various other regions, the efficacy of coumaphos has decreased due to the evolution of coumaphos-resistant varroa mite populations (Elzen and Westervelt 2002, Maggi et al. 2009, Currie et al. 2010, Higes et al. 2020). Additionally, various populations of varroa in Quebec, Ontario, and the West Coast of Canada have developed simultaneous resistance against both coumaphos and tau-fluvalinate (Currie et al. 2010). Coumaphos has shown significant detrimental effects to larval queen development at even low doses, manifesting in elevated queen cell mortality and high rates of deformity in newly-emerging queens after acute doses (Haarmann et al. 2002, Pettis et al. 2004). This shortfall makes coumaphos-based treatments incompatible with colonies reared for queen-breeding purposes.

Currently, formulations of the synthetic formamidine amitraz (specifically Apivar®) are among the most commonly used synthetic varroacides in Canada (Health Canada 2019, Claing et al. 2023). As a non-systemic acaricide, amitraz agonistically targets various receptors of the mite neuronal system, including receptors of the major neurotransmitters octopamine and epinephrine (Kita et al. 2017, Guo et al. 2021, Hernández-Rodríguez et al. 2022). Amitraz-induced stimulation of these receptors results in paralysis and death. Apivar® exhibits very high efficacy against naïve mites *in vivo* (~100% mortality after 3 hours), although the efficacy within an apiary environment is more variable (Rinkevich 2020). This variability is likely due in part to the recent emergence of amitraz-resistant varroa mites, though resistance is not yet as widespread as for other synthetic varroacides (Mitton et al. 2022, Maggi et al. 2010a). Nonetheless, amitraz resistance is becoming more prevalent, particularly in North America where the resistance-inducing Y215H mutation in

the β_2-octopamine target receptor is increasingly reported (Rinkevich 2020, Mitton et al. 2022, Rinkevich et al. 2023). Additionally, the chemical has also been implicated in cases of accidental human poisonings (Yilmaz and Yildizdas 2003, Veale et al. 2011, Herath et al. 2017).

Despite their advantages, synthetic miticides face challenges from decreasing efficacy due to resistance, a problem which will no doubt intensify as use remains extensive (Milani 1999, Mitton et al. 2022). Nonetheless, the evolution of resistance in varroa mites may be somewhat staved off through the employment of rotational varroacide applications, wherein treatments with different active chemical ingredients are used consecutively to reduce selective pressure towards any given varroacide (Maggi et al. 2011, Giacobino et al. 2015). Another notable challenge facing synthetic varroacides is their tendency to contaminate commercial hive products, which renders them incompatible with treatment regimens occurring during the honey flow (Giovenazzo and Dubreuil 2011, Devi et al. 2019). As such, none of these compounds, alone, are a "silver bullet" and need to be integrated with other treatments to form a comprehensive IPM treatment plan.

1.4 Varroacides Derived From Natural Compounds

So-called "natural" varroacides are concentrates of naturally-occurring compounds (often phytochemicals) which are specifically used for killing varroa mites in honey bee colonies. Aside from chemical compositions, natural miticides differ from synthetic miticides in their application mode, with the former more often utilizing vaporization-based methods as opposed to direct contact strips. Such methods may involve wafers that gradually release volatile vapours, or direct fumigation. As the varroa mites respire, varroacide vapours may then be absorbed through the tracheal system spread across the body of the mite (Pugh et al. 1992). Some of these chemicals are

regarded as food-safe and may be used during the honey flow with low risk of honey contamination. Natural miticides approved for use against varroa in Canada fall into two categories: organic acids and phytochemicals (hops beta acids and aromatic essential oils).

Two main organic acids are used as varroa control: formic acid and oxalic acid (Health Canada 2019). Various modes of application are used for both acids, with formic acid being applied in vapour-releasing patches or pads (the "mite wipe" technique) at concentrations of 60-65%, while oxalic acid is directly sprayed, fumigated, or dissolved in sucrose syrup and trickled into the broodnest (Imdorf et al. 1996, van der Steen and Vejsnæs 2021). Formic Pro™, a commercial varroacide formulation using 65% formic acid as the active ingredient, is also available for purchase and use in Canada (Menzies et al. 2019). Upon exposure, these acids induce a high degree of oxidative stress and dehydration in varroa mites, disrupting cellular respiration and leading to death from acute poisoning (Milani 2001, Genath et al. 2021). Formic acid is suitable for use during honey production, and thus is often used while colonies are building up peak populations (Calderón et al. 2000). In contrast, oxalic acid may damage honey bee brood as well as contaminate hive products, and as such, usage occurs in the fall when brood and honey flow are minimal (Gregorc and Planinc 2002, Rademacher et al. 2017). In Europe, typical efficacies of single formic acid treatments range from 60-80%, with multiple treatments spread throughout the year capable of reducing the mite population by 90-95%; oxalic acid regimens can similarly reach efficacies upwards of 96-98% (though are more typically between 80-90%) (Imdorf et al. 1996, Nanetti 1999, Rademacher and Harz 2006). Formic acid in particular is notable for its ability to penetrate the wax caps of sealed brood and kill mites on pupae, though this generally requires concentrations exceeding 80% (Calis et al. 1998). Such treatments may exhibit variable efficacies depending on seasonality and application method – reported mite reduction

rates typically ranged from approximately 30-90% for formic acid, with values as low as 9-20% also being reported (Ostermann and Currie 2004, Underwood and Currie 2005, Menzies et al. 2019, Jack et al. 2020, Jack et al. 2024). Oxalic acid treatments in Canada also vary in efficacy, typically falling between 50-80%, though efficacies above 90% have also been reported (Adjlane et al. 2016, Sabahi et al. 2020). Conversely, high doses of formic acid have been associated with increased rates of queen loss (Underwood and Currie 2007). The corrosive and toxic nature of organic acid vapours poses a risk to beekeepers, and thus their use requires appropriate personal protective equipment (PPE), specifically eye-protection goggles and NIOSH approved respirators (Imdorf et al. 1996, Balint et al. 2010, Imdorf et al. 1999b). While resistance has not been reported for either organic acid, lower temperatures reduce efficacies (Bahreini et al. 2004, Bacandritsos et al. 2007). However, formic acid applications can be adjusted to temperature by varying concentration, with higher-concentration formic acid treatments having lower efficacy drop-offs at lower temperature (Underwood and Currie 2003, Steube et al. 2021). In Canada, both formic and oxalic acids can be applied in either spring/early summer or late fall to reduce the growth of varroa populations in commercial colonies (Giovenazzo and Dubreuil 2011, Plamondon et al. 2024). Organic acid treatments may also have net negative effects on colonies with low infestation levels, as the harm posed against worker bee development may outweigh the benefits of clearing minor varroa infestations (Ostermann and Currie 2004). Finally, though organic-acid based formulations are often cheaper to purchase, they can be much more labour-intensive, particularly in cases involving the use of homemade formic acid applicators, or using direct fumigation. Despite these shortcomings, organic acids remain an effective and widely-used method of varroa control in Canada (Giovenazzo and Dubreuil 2011).

Aside from formic acid, hops beta acids (HBA) derived from the hops plant (*Humulus*

lupulus L.) are also useable for treating varroa infestations during honey flow. Commercially sold as HopGuard® in Canada, the HBA formulation is applied as an impregnated strip hanging between brood frames, and efficacies have been variously reported between 43-88% (Vandervalk et al. 2014, Rademacher et al. 2015, Health Canada 2019).While HBA formulations effectively reduce varroa populations, they tend to exhibit lower efficacies than other commercial miticides (Vandervalk et al. 2014, García-López et al. 2024). While the exact mechanism of HBA action against varroa is not well understood, much of the efficacy appears to be dependent on cuticular contact as opposed to ingestion (DeGrandi-Hoffman et al. 2012, Rademacher et al. 2015, Moškrič et al. 2018). As HBA are a relatively recently developed miticide, there have not yet been any reported issues with resistant mites, though other factors influencing efficacy remain understudied.

Various other plant-derived essential oils (specifically the highly-volatile monoterpene hydrocarbons) have also shown efficacy against varroa mites, with the most common being thymol (Gracia et al. 2017, van der Steen and Vejsnæs 2021, Imdorf et al. 1999a). Thymol may be used as the sole miticidal ingredient, such as in the case of Thymovar®, or in conjunction with other essential oils, as is the case with ApiLife VAR® which uses a mix of thymol, menthol, camphor, and eucalyptol (Imdorf et al. 1995, Bollhalder 1998, Health Canada 2019). These compounds act primarily as volatile organic vapours which dissipate throughout the colony to kill mites (Imdorf et al. 1999a). Accordingly, the application method for treatment formulations is a compound-impregnated wafer placed atop the frames of a hive brood chamber, which slowly releases vapours into the hive environment (Imdorf et al. 1995, Bollhalder 1998). While the precise mechanisms of action regarding toxicity against varroa have not been fully characterized, it is known that monoterpenes can competitively inhibit acetylcholinesterase in the nervous system, and disrupt cell membrane integrity (Brasesco et al. 2017, Youssefi et al. 2019). Compounds used in varroa

control have necessarily required high LC50 values against honey bees; however, there is evidence to suggest chronic toxicity against larval and adult worker bees (Damiani et al. 2009, Gashout and Guzmán-Novoa 2009, Glavan et al. 2020). Thus, thymol-based treatments are best used in colonies with low levels of varroa infestation (Melathopoulos and Gates 2003). Lodesani and Costa (2008) report an efficacy of 78.3-92.4% for thymol-based treatments, though the volatilization of essential oils is temperature dependent. Thus, reported efficacies of thymol vapour treatments in Canada have been highly variable, with Al Naggar et al. (2015) reporting a fall efficacy of 26.7%, while Vandervalk et al. (2014) reported efficacies exceeding 80% in both spring and fall treatment periods. In the case of thymol formulations, optimal ambient temperatures span from 15° C to 35° C for strong colonies and slightly lower upper temperatures for weak colonies (Giacomelli et al. 2016, Imdorf et al. 1999a). Conversely, evaporation rates at high ambient temperatures (>35° C) may induce absconding behaviour (relocation of the queen and adult worker population of a colony) in treated hives (Giacomelli et al. 2016). The temperature-based inconsistencies of vapour-based thymol treatments have led to the development of non-vapour alternatives, such as dust-based treatments involving thymol-impregnated powdered sugar (Melathopoulos et al. 2010, Sabahi et al. 2020). Such methods have demonstrated efficacies comparable to commercially-available vapour-based treatments, though they remain less popular in commercial settings as such applications are comparatively labour-intensive.

As discussed above, natural varroacides have several benefits including low rates of reported resistance and lower risks of hive product contamination. However, many natural varroacide treatment regimens are laborious compared to the single-applicator treatment typical of a synthetic acaricide; both organic acid and essential oil-based regimens require multiple applicators exchanged consecutively throughout the treatment term to achieve comparable

efficacies (Imdorf et al. 1996, Bollhalder 1998). Moreover, natural acaricides tend to have lower immediate efficacies per individual application, with high mortality of mites requiring a protracted length of time and multiple applicators (Imdorf et al. 1996). This is particularly problematic for treating weak colonies with high mite loads, where a rapid response is required to prevent colony loss.

1.5 Determination of Varroacide Efficacy

Studies that have examined the efficacies of candidate acaricides have been centred primarily on mite mortality data (Dennehy et al. 1993, Reddy et al. 2014, Ouyang et al. 2018, Fotoukkiaii et al. 2020, Bahreini et al. 2022, Dawdani et al. 2023). Most commonly, these studies have focused on the concentrations (LC_{50}) or dosages (LD_{50}) required to induce a 50% mortality rate among an experimental population of the study organism (Paramasivam and Selvi 2017). These studies are typically conducted on the pest in question, as well as the host crop/species that the pesticide aims to preserve. Such dose-responses provide information on toxicity, which initially helps inform us about the effectiveness of a compound to kill a target pest while mitigating non-target mortality. However, such studies are often limited in their real-world informativeness, as they are typically performed under controlled *in vitro* laboratory conditions, which are rarely generalizable to an *in situ* system. Moreover, pesticides will often be administered in levels much higher than their LD_{50}/LC_{50} values to maximize the reduction of the pest species' population. Finally, real-world scenarios involve background levels of pest mortality caused by factors unrelated to the treatment itself, and such factors must also be accounted for in long term *in situ* studies. Consequently, studies of field efficacies must examine treatment mortalities against

untreated negative controls, and thus require different analysis formulae to calculate realized efficacies.

Several such formulae exist, with different applicability based on experimental design parameters (Mohiseni et al. 2002, Albeltagy 2021). Four formulae are typically employed in studies of this nature: Abbot's formula (Abbott 1925), Henderson-Tilton's formula (Henderson and Tilton 1955), Sun-Shepard's formula (Püntener 1981), and Schneider-Orelli's formula (Püntener 1981). Selection of the appropriate formula primarily depends on the uniformity of the population sizes across treatments (equal versus unequal population size), and measured input data (infestation level or live test individuals, versus mortality). Details on the usage of these formulae are summarized in Table 1-2.

The first of these formulae, Abbott's formula, simply calculates the efficacy of a treatment as a complement percentage ratio of the survivorship of target pests following treatment over the survivorship in an untreated control population. In Abbott's formula, n_{Treat} and n_{NC} represent the end of experiment pest survivorship in the treated and negative control populations, respectively:

$$\text{Efficacy} = \left(1 - \frac{n_{\text{Treatment}}}{n_{\text{NC}}}\right) * 100\%$$

A disadvantage of Abbott's formula is the requirement for equal starting pest populations, which may not be feasible especially in large-scale studies (Fleming and Retnakaran 1985). Henderson-Tilton's formula was derived from Abbott's formula to accommodate for different treatment and control population sizes, by multiplying the Abbott's formula survivorship ratio with a reciprocal ratio of the starting populations in each treatment group. This enables the formula to base efficacy on the change in a dynamic population size over the treatment term. In Henderson-Tilton's formula, T_{Start} and T_{End} terms represent the respective pre- and post-treatment pest populations of the pesticide-treated group, while NC_{Start} and NC_{End} represent the pre- and post-treatment pest

populations of the negative control:

$$\text{Efficacy} = \left(1 - \frac{T_{\text{End}} * NC_{Start}}{T_{Start} * NC_{\text{End}}}\right) * 100\%$$

Schneider-Orelli's formula serves as a mortality-based counterpart to Abbott's formula, calculating efficacy as a function of mortality rate differences between the treatment and controls. In the following formula, $m_{\text{Treatment}}$ is the mortality rate of the pest population treated with the pesticide, while m_{NC} is the mortality rate of the untreated negative control pest population:

$$\text{Efficacy} = \left(\frac{m_{\text{Treatment}} - m_{\text{NC}}}{100 - m_{\text{NC}}}\right) * 100\%$$

This formula represents efficacy as a corrected mortality rate of the treatment group, taking into consideration the background mortality rates from natural causes as represented by the negative control. Similar to Abbott's formula, Schneider-Orelli's formula assumes a uniform starting population size. Additionally, Schneider-Orelli's formula does not account for possible population growth in the negative control population. The latter is a particularly important consideration, as failure to account for net background population growth artificially inflates efficacy. Sun-Shepard's formula amends these challenges by replacing the mortality rate terms for the treatment and negative control in Schneider-Orelli's formula with a more generalized term representing the change in the population of each treatment *i* (Δn_i). This term can be calculated as such:

$$\Delta n_i = \left(\frac{n_{i(\text{End})} - n_{i(\text{Start})}}{n_{i(\text{Start})}}\right) * 100\%$$

Here, $n_{i(\text{Start})}$ and $n_{i(\text{End})}$ respectively represent the varroa population in colonies with treatment *i* before and after the treatment phase. Respectively substituting m_{NC} and $m_{\text{Treatment}}$ from Schneider-Orelli's formula for Δn_{NC} and $\Delta n_{\text{Treatment}}$ results in Sun-Shepard's formula:

$$\text{Efficacy} = \left(\frac{\Delta n_{\text{Treatment}} - \Delta n_{\text{NC}}}{100 - \Delta n_{\text{NC}}}\right) * 100\%$$

In field studies evaluating varroacide efficacies, calculations must account for a lack of mite population size uniformity across replicate hives, as well as the reproduction of mites during the experimental period (Kanelis et al. 2022). Thus, many such studies utilize a modified version of either Schneider-Orelli's or Sun-Shepard's formula, wherein infestation levels can be established by examining the total varroa mortality during the treatment phase, clean-up phase, or both (Gregorc 2005, Dietemann et al. 2013, Tlak Gajger et al. 2019, Kanelis et al. 2022, Plamondon et al. 2024). The Henderson-Tilton formula may also be used in studies of varroacide efficacy, though the requirement of an initial population size means it is primarily used to analyze *in vitro* assays where a initial population can be inferred due to the static mite populations in such assays (Rinkevich 2020, Bahreini et al. 2022, Bahreini et al. 2024). It may also be used for *in situ* evaluations of efficacy, where the population of live varroa mites is assessed at the start and end of the treatment term through subsampling infested workers or brood from colonies (Girişgin and Aydın 2010, Mert and Yucel 2011, Cook et al. 2024). Values of efficacy such as those provided by the prior formulae act as useful benchmarks for comparisons between different treatment regimens in controlled experimental settings. However, these metrics fail to account for confounding environmental factors that influence outcomes *in situ*, as well as being unable to account for the time-dependent element of treatment regimens. In such cases, generalised linear models are preferred, though these analyses must take into consideration the high degree of autocorrelation associated with time-series data (Gracia et al. 2017, Jack et al. 2020, Kolics et al. 2022, Jack et al. 2024).

1.6 Non-Chemical Methods of Varroa Control

A key aspect of sustainable long-term honey bee management is the maintenance of low baseline varroa levels throughout the year (Devi et al. 2019). To this end, beekeepers may engage in cultural control techniques to interrupt varroa life cycles and stifle reproductive rates. Such methods target and disrupt the varroa life cycle to pre-emptively reduce infestation levels and population growth (Jack and Ellis 2021). Additionally, honey bees can be selectively bred for sanitary behaviours that reduce varroa loads or to resist/tolerate infestations, as a form of hands-free control (Rinderer et al. 2010). When used in conjunction with one another, beekeepers can establish effective integrated pest management (IPM) regimens which minimize the need for chemical varroacides.

In colonies of *A. cerana*, the original host of varroa, the reproductive stage of varroa is limited to drone brood cells, as sealed worker brood infested with varroa mites are quickly uncapped and removed from the colony – a social immunity adaptation termed "varroa-sensitive hygiene" (VSH) (Lin et al. 2016, Page et al. 2016, Lin et al. 2018). Varroa mites infesting *A. mellifera* colonies will reproduce within worker cells more frequently than mites infesting *A. cerana* colonies due to the former's much higher worker to drone brood ratio, longer worker post-capping period, and lower rates of VSH (Boot et al. 1997, Boot et al. 1999, Martin et al. 2020, Ardestani 2022). It was previously believed that varroa exhibited a distinct preference for drone brood regardless of host species (Le Conte et al. 1989, Otten and Fuchs 2021). However, Reams et al. (2024) also found varroa to have more opportunity to infest drone cells versus worker cells, due to drone brood being more frequently attended by nurse bees that might be carrying varroa and taking longer to develop, resulting in a longer infection window. Thus, it is uncertain to what extent host preference plays in contributing to the greater prevalence of varroa in drone cells,

versus being due to natural hive circumstances. The placement of drone frames can therefore be used as a cultural control against varroa, with the drone brood acting as a "lure" that concentrates varroa foundresses away from worker brood (Calderone 2005). This both allows beekeepers to easily remove capped cells containing varroa mites and shifts mites away from developing workers.

Brood breaks are another method of cultural control, whereby the queen is placed in a cage or entirely removed from the hive for a three-week span, to allow all brood to develop and metamorphose while preventing oviposition (Gabel et al. 2023, Meikle et al. 2023). The subsequent lack of brood in the colony forces varroa mites onto adult worker bees, which limits the population growth of the mites and makes them susceptible to removal by grooming (Arechavaleta-Velasco and Guzmán-Novoa 2001, Currie and Tahmasbi 2008, Hunt et al. 2016). Colonies undergoing brood breaks may also be equipped with a screen bottom board (featuring a coarse mesh layer at the hive floor) equipped with adhesive sticky boards, which capture falling mites and prevent reestablishment (Pettis and Shimanuki 1999). Dispersing mites are also susceptible to contact-based varroacides, thus the coupling of a brood break regimen with a varroacide treatment can improve efficacy of the varroacide (Evans et al. 2022). One downside to the use of brood breaks is the interference to colony growth during the nectar flow, with the prevention of brood production by the queen for a period of weeks potentially leading to reduced worker populations and overall honey productivity (Kovačić et al. 2023). The former in particular means brood break treatment may be unsuitable for use in colonies with already weakened worker populations due to heavy varroa infestations or otherwise.

Both allogrooming and autogrooming (self-grooming) behaviours are important forms of honey bee social immune behaviour, functioning as both a form of communication and to maintain

routine hygiene (Land and Seeley 2004, Stevanovic et al. 2012). Grooming is also an effective defence against varroa, potentially resulting in severe damage to varroa mites, such as the destruction of limbs and damaging the idiosomal cuticle, which can compromise the mite's reproductive and feeding capabilities (Bąk et al. 2012, Bąk and Wilde 2015, Pritchard 2016). In the context of selective breeding against varroa, emphasis is placed on the relative frequency at which grooming-damaged mites are observed in a colony (Jack and Ellis 2021). While grooming has shown low heritability in prior studies (Stanimirović et al. 2010, Pritchard 2016), recent studies have estimated heritability to be higher, which may facilitate the development of grooming-intensive bees (Arechavaleta-Velasco et al. 2012, Morfin et al. 2023).

Another potential cultural control mechanism which may be selected for is that of small brood cell sizes. Historically, small brood cells were posited to be a key resistance mechanism of Africanized strains of *Apis mellifera*, which are generally more resistant to varroa than other genetic stocks (Piccirillo and De Jong 2003). The proposed mechanism to explain this proposed phenomenon is that the smaller volume of a narrower cell limits the growth and reproduction of varroa mites, in addition to making mite movement and feeding more difficult (Heaf 2011). Studies have also found some negative correlation between reduced brood cell size and presence of brood-infesting varroa, as well as lower rates of varroa fecundity within narrower cells (Oddie et al. 2019, Maggi et al. 2010b). However, other studies have failed to reproduce these findings (Ellis et al. 2009, Coffey et al. 2010, Seeley and Griffin 2011), and further still, Zhang et al. (2024) found that larger cells apparently suppressed the reproduction of foundress mites versus smaller cell sizes. Thus, the effect of brood cell size on varroa infestation and reproductive rates remains inconclusive to date.

Many varroa-focused breeding programs aim to enhance existing VSH behaviour in *A.*

mellifera stocks, as the VSH trait is known to possess high heritability (Ibrahim and Spivak 2006, Tsuruda et al. 2012, Kirrane et al. 2015). Aside from decreasing varroa loads, hygienic behaviour has been associated with more general colony health benefits, including upregulation of immune genes (*PGRP-S2*, *hymenoptaecin*, and others from various immune pathways) and lower virus prevalence, which likely relates to the decreased presence of varroa vectors (Erez et al. 2022). Breeding programs can also aim to directly decrease pathologies caused by varroa-associated viruses, notably deformed wing virus (Bouuaert et al. 2021). Such breeding programs act by increasing tolerance, mitigating the indirect pathological effects of varroa infestations.

Another behaviour that may confer resistance against varroa is the uncapping and recapping of sealed brood cells, with heightened uncapping/recapping behaviour seemingly correlating with lower mite fecundity at the cell level (Oddie et al. 2018, Hawkins and Martin 2021). It has been proposed that the uncapping/recapping of sealed brood results in fluctuations of temperature and humidity, in turn disrupting the reproductive cycle of varroa mites (Martin et al. 2020, Jack and Ellis 2021). However, the impact of uncapping/recapping behaviour on varroa mite populations has not been resolved, with Guichard et al. (2023) reporting minimal differences in mite fecundity at the colony level in contrast to Oddie et al. (2021), who notes that mite-resistant honey bee populations exhibit higher rates of uncapping/recapping behaviour than mite-susceptible populations.

1.7 Biocontrols Against Varroa

Biological control agents ("biocontrols") are natural enemies or pathogens of a pest species used by humans to reduce the population of said pest (Ram et al. 2018). Such biocontrols are

broadly used in agriculture, and include bacteria, viruses, fungi, and predatory arthropods. These biocontrols are frequently incorporated into IPM programs when available, as they typically lack the non-target toxicity of chemical controls. While such products would undoubtedly assist in varroa control, there are no such biocontrols to date which prove effective against varroa. Nevertheless, numerous avenues are being researched, as will be discussed below.

Pseudoscorpions are predatory arthropods that naturally occur inside honey bee hive environments (Girişgin et al. 2013, Fombong et al. 2016, Lin et al. 2020). In experimental conditions, pseudoscorpions have demonstrated the ability to remove and consume varroa mites directly off infested brood, without harming the bees themselves (Fagan et al. 2012, Read et al. 2014, van Toor et al. 2015). Their generalist feeding habits also allow pseudoscorpion-based varroa biocontrols to manage other pest species, including small hive beetle, *Tropilaelaps* mites, and tracheal mites (Donovan and Paul 2005). However, this behaviour appears to be highly variable across different pseudoscorpion species – notably, *Ellingsenius indicus* found in *A. cerana* colonies will rarely feed on varroa in experimental settings, and may even preferentially target bee eggs and young larvae (Donovan and Paul 2006, Thapa et al. 2013). There is also a lack of data on pseudoscorpion behaviour and interactions with honey bees and the hive environment as a whole, which limits their current applicability (Donovan and Paul 2005). The laelapid mite *Stratiolaelaps scimitus* has also shown promise against varroa mites, with Rangel and Ward (2018) showing a 97.1% mortality of varroa exposed to *S. scimitus in vitro* over a span of 24 hours. Despite the initial success of the petri dish assays, Rondeau et al. (2019) found no significant decrease in varroa mite populations within colonies where *S. scimitus* were introduced. Additionally, *S. scimitus* refrain from attacking dispersing-stage mites, which further limits their utility as a biocontrol (Rondeau et al. 2018).

Arthropod pathogens provide another promising pathway to finding a varroa biocontrol, with the bacterium *Bacillus thuringiensis* (Bt) already being widely used against various agricultural pest arthropods (Porcar et al. 2009, Chougule et al. 2013, Schünemann et al. 2014, Plata-Rueda et al. 2020). Moreover, Bt exhibits no notable virulence against honey bees, making them an attractive prospective varroa biocontrol (Tsagou et al. 2004, Alquisira-Ramírez et al. 2014). Mortality rates of between 90-100% in varroa mites sprayed with isolated cultures of *B. thuringiensis* serovar *tenebrionis* and serovar *kurstaki* have been reported in *in vitro* studies, though it is not yet known how this efficacy translates to the hive environment (Alquisira-Ramírez et al. 2014, Saccà and Lodesani 2020). Entomopathogenic fungi provide an additional candidate pathogen taxon, with Kanga et al. (2002) finding both *Hirsutella thompsonii* and *Metarhizium anisopliae* to have significant pathogenicity towards varroa, while being benign to honey bees. In contrast, Davidson et al. (2003) found many strains of entomopathogenic fungi to have significantly decreased *in situ* performance, likely owing to the high temperature of the hive environment. Thus, further *in situ* research is required to develop a deployable pathogenic biocontrol against varroa.

A promising emergent avenue of varroa biocontrol is the use of RNA interference (RNAi) technology. RNAi methods involve the use of molecular mechanisms to disrupt the expression of target genes – by utilizing these mechanisms against critical functional genes in a target pathogen, it becomes possible to target critical functions within the target organism with theoretically high specificity (Niu et al. 2018). In the past, RNAi has been deployed against Israeli Acute Paralysis Virus (IAPV) and Deformed Wing Virus (DWV), wherein bees fed with double-stranded RNA (dsRNA) corresponding to target viral genomes have resulted in a decrease in haemolymph viral titers (Desai et al. 2012, Chen et al. 2014, Jack and Ellis 2021). Against varroa, early trials of RNAi

have yielded potential gene targets, causing impaired reproductive capacity and mortality in mites injected with dsRNA (Garbian et al. 2012, Huang et al. 2019). As a large-scale deployment approach, it has been suggested that varroa-targeting dsRNA could be fed to hives en masse, wherein the dsRNA would enter the honey bee haemolymph to be picked up by varroa mites during feeding (Jack and Ellis 2021). A proprietary product utilizing such dsRNA-containing syrup is currently undergoing development by GreenLight Biosciences (https://www.greenlightbiosciences.com/). Alternatively, engineered dsRNA-producing symbionts could be inoculated into honey bee microbiomes, where they would actively and continuously produce varroa-targeting dsRNA (Leonard et al. 2020). In such cases, care must be taken to ensure that varroa-targeting dsRNA sequences to not overlap with functional honey bee gene sequences, as well as potential other mesostigmatan mite species, to avoid cross-toxicity in bees and other non-target species.

1.8 Thesis Objective

With the global expansion of miticide-resistant varroa, novel treatments are becoming an increasingly urgent necessity. This thesis will focus on the development of a novel varroacide: 1-allyloxy-4-propoxybenzene, codenamed 3c{3,6} (Singh et al. 2020, Dawdani et al. 2023).

In Chapter 2, I will discuss assessment of the efficacy of 3c{3,6} in a commercial apicultural setting. This was achieved through a series of *in situ* experiments conducted from 2021 to 2023, wherein 3c{3,6} was deployed via various application modes in honey bee colonies at Beaverlodge Research Farm, Beaverlodge AB, Canada. These studies sought to quantify the mortality-based efficacy of 3c{3,6}, as well as model and compare differences in varroa mortality

over time of colonies treated with 3c{3,6}, a negative control, or a positive control (Thymovar®). Additionally, I will discuss how different colony parameters (brood, food, bee population, winter survival) differed across treatment groups to provide a holistic view of the suitability of 3c{3,6} as a commercial varroacide.

Chapter 3 will more narrowly explore the sublethal effects of 3c{3,6} vapour exposure on the physiological state of mites and honey bees. To achieve this, I employed *in vitro* exposure assays in which honey bees and mites were placed into glass jars containing either a low dose of volatilised 3c{3,6} or a control. High-throughput transcriptome analyses of honey bees and mites were performed to study global gene expression levels in two honey bee body compartments and in varroa and identify potential 3c{3,6}-induced sub-lethal effects at a molecular scale.

Table 1-1: Major varroa-vectored viruses infecting *Apis mellifera*, including known transmission routes and reported symptoms.

Virus	Transmission Avenues	Symptoms in Infected Bees	References
Acute bee paralysis virus (ABPV)	Vectored by varroa during feeding Horizontally transmitted to queens in semen Potential oral infection routes including larvae, workers, faecal-oral infection, and cannibalized infected brood	Highly virulent, accumulating in brain and hypopharyngeal gland of adult bees rapidly leading to paralysis and death. Thoraces and abdomens darken and loses setae. Severe outbreaks lead to a decline in the adult bee population at the colony level.	Bailey et al. (1963) de Miranda et al. (2010a) Erban et al. (2015) Kevan et al. (2006)
Deformed wing virus (DWV)	Vectored by varroa during feeding Horizontally transmitted to queens in semen Vertical transmission by binding to egg surface Transmission to larvae in contaminated food Horizontal transmission via trophallaxis Potentially through contaminated pollen	Three master strains globally: DWV-A, DWV-B, DWV-C. DWV-A and DWV-B predominate, while DWV-C remains comparatively rare. Infected pupae exhibit increased mortality (especially for DWV-B) and may develop deformed/atrophied wings. Adults exhibit decreased flight capabilities regardless of wing morphology, and bloated abdomens. Minimal reported impacts on queens.	Kevill et al. (2019) Martin and Brettell (2019) Mazzei et al. (2014) Penn et al. (2022)
Israeli acute paralysis virus (IAPV)	Vectored by varroa during feeding Venereal transmission to queens Foodborne and trophallaxis transmission Apparent vertical transmission to eggs and young brood	Early infection characterized by shivering, convulsion of wings, and setae loss in adult bees. Rapidly leads to paralysis/death in symptomatic workers. May persist asymptomatically at a colony level, though virus can rapidly become virulent with the advent of environmental stressors.	Chen et al. (2014) de Miranda et al. (2012) Reynaldi et al. (2011)
Kashmir bee virus (KBV)	Vectored by varroa during feeding Vertical transmission on the surface of eggs Oral transmission via ingesting contaminated food, or faecal-oral route	Highly virulent and causes rapid death of infected bees, though with few preceding symptoms. Capable of infecting all life stages, and may also infect queens. Infections are often asymptomatic.	de Miranda et al. (2010a) de Miranda et al. (2012)

Table 1-1 (Cont.)

Virus	Transmission Avenues	Symptoms in Infected Bees	References
Slow bee paralysis virus (SBPV)	Vectored by varroa during feeding Relatively minor role of bee-to-bee direct horizontal transmission in influencing outbreaks	Slow onset of paralytic symptoms in adult bees, particularly the external extremities. Symptom onset takes up to ~10 days.	de Miranda et al. (2010b) (Santillán-Galicia et al. 2014)

Table 1-2: Four commonly-used formulae to calculate efficacy, and their associated experimental design parameters.

		Population Uniformity	
		Uniform	**Non-Uniform**
Measured Response	**Infestation**	Abbott Formula	Henderson-Tilton Formula
	Mortality	Schneider-Orelli Formula	Sun-Shepard Formula

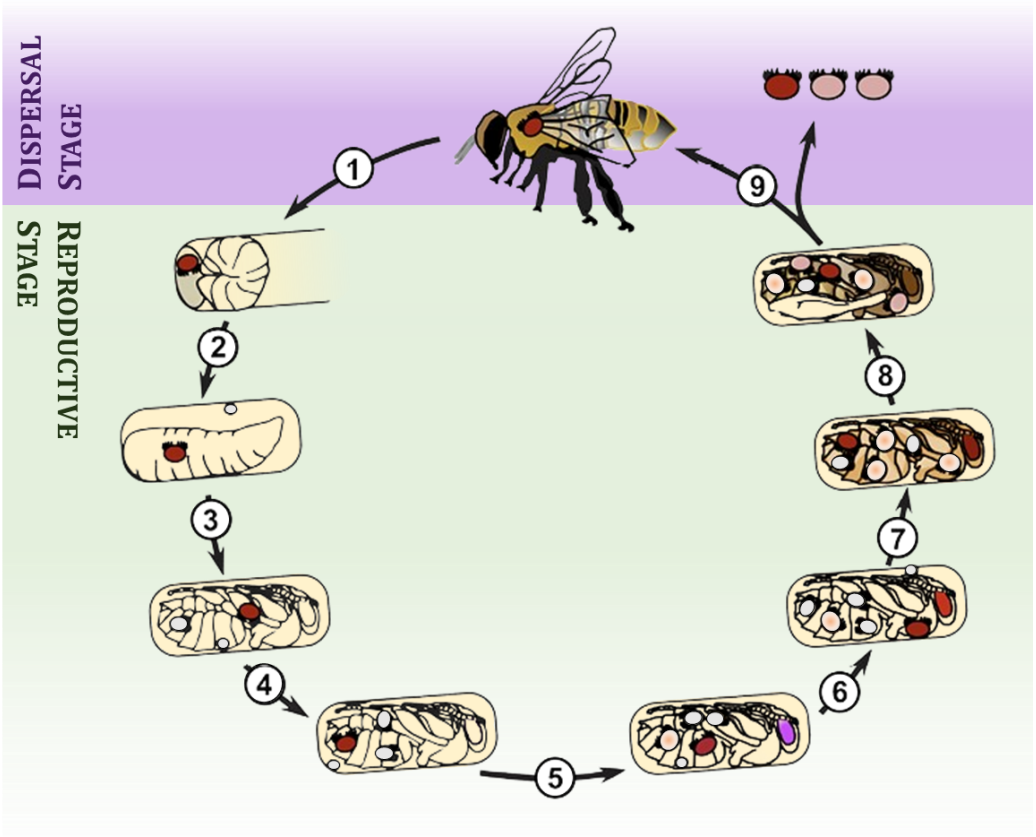

Figure 1-1: Life cycle of *Varroa destructor* within the colony environment, with the dispersal stage highlighted purple and the reproductive stage highlighted green. [1] Adult female varroa invades the cell prior to capping and hides in brood food. [2] Foundress mite creates communal feeding site and begins feeding, lays first (male) egg. [3] Foundress mite continues feeding and lays female eggs, male hatches into protonymph. [4] Subsequent female eggs hatch; all offspring molt twice before maturing. [5] Male varroa matures before female offspring. [6] First daughter matures, mates with male offspring. [7] Other daughters mature, mate with male, and continue to darken in colour. [8] Bee pupa completes development and emerges. [9] Mated daughter mites emerge and disperse atop worker bees, male dies. Reproduced from Harris and Sheridan (2023) with permission.

Chapter 2: Field Trials of the Novel Miticide 1-Allyloxy-4-Propoxybenzene (3c{3,6}) Against *Varroa destructor*

2.1 Introduction

Across terrestrial ecosystems, pollinators play a vital role facilitating flowering plant reproduction (Ashman et al. 2004, Klein et al. 2007). Within this guild, the western honey bee (*Apis mellifera* L.) stands out as the most prolific, providing extensive pollination services to wild and agricultural plant ecosystems alike (Gill 1990, Gallai et al. 2009, Garibaldi et al. 2013). The latter is especially important for global food supplies as up to one third of all food consumed globally is produced through insect pollination, accounting for high proportions of dietary vitamins and antioxidants (Klein et al. 2007, Eilers et al. 2011). However, the compounding effects of multiple emergent honey bee diseases has resulted in increasing colony mortality rates in recent decades, straining the sustainability of the global beekeeping industry (Cornman et al. 2012, Smith et al. 2013, Bruckner et al. 2023, Claing et al. 2023, Gray et al. 2023).

Of the pathogens afflicting honey bees, none are as severe a threat as the ectoparasitic mite *Varroa destructor* Anderson and Trueman (2000), hereon referred to as "varroa" (Le Conte et al. 2010, Rosenkranz et al. 2010). Varroa feeds on the fat bodies and haemolymph of both developing and adult bees, causing weakness, immunosuppression, and reduced foraging capacity (Yang and Cox-Foster 2005, Ramsey et al. 2019, Peck 2021, Han et al. 2024). The array of pathologies caused directly by varroa feeding activities (known as "varroosis") is worsened by the various viruses vectored by varroa mites (Kevan et al. 2006, Ullah et al. 2021, de Miranda et al. 2010a). The varroa life cycle primarily occurs within sealed brood cells, where female foundresses lay 1 male and an average of 4-5 female eggs on workers, or 5-6 on drones, which feed upon the developing brood

(Martin 1995, Evans and Cook 2018). At the end of this cycle, males die shortly after maturing and mating, while a respective average of 2-3 (worker brood) or 3-4 (drone brood) viable daughter mites mature (Alattal et al. 2017, Odemer 2020). This cycle takes place over 11-12 days in worker cells, and 15 days in drone cells (Häußermann et al. 2018, Ardestani 2022). Emerging mature females then disperse on adult worker bees, which they feed on and cause pathology to their hosts (Piou et al. 2016). The short reproductive cycle of varroa allow their populations to rapidly expand within a colony, potentially leading to colony loss, especially during overwintering (Amdam et al. 2004, Guzmán-Novoa et al. 2010).

Numerous chemical miticides have been developed to control varroa (termed "varroacides"), typically falling into two categories: synthetic varroacides, and varroacides derived from natural compounds (Mitton et al. 2022). Synthetic compounds were the first to be used broadly and include pyrethroids (tau-fluvalinate and flumethrin), organophosphates (coumaphos), and formamidines (amitraz). These compounds are popular due to their simple application protocol and high efficacies on naïve mite populations (>90%) (Ferrer-Dufol et al. 1991, Zikic et al. 2020). However, they have also been associated with non-target toxicity against honey bees and humans and may contaminate honey and wax due to their lipophilicity (Yilmaz and Yildizdas 2003, Benito-Murcia et al. 2021). Moreover, extensive use of these treatments has resulted in the emergence of miticide-resistant varroa populations (Martin 2004, Pettis 2004, Currie et al. 2010, Rinkevich 2020). Varroacides derived from natural compounds include organic acid solutions (typically formic and oxalic acids), as well as phytochemicals (hops beta acids and essential oils, notably thymol) (Mitton et al. 2022). These tend to pose lower risks to consumer health and so far have remained effective against varroa, though they may cause non-target toxicity against honey bees when used at high dosages, such as increased queen mortality (notable in formic acid treatments)

(Underwood and Currie 2007, Giovenazzo and Dubreuil 2011, Charpentier et al. 2014). Several other challenges exist regarding their use, including lower efficacies per individual treatment, thus requiring repeat administrations of compound to eliminate mites (Imdorf et al. 1996). In the case of organic acids, treatment application requires use of personal protective equipment (PPE) to mitigate potential health hazards, typically involving a respirator, eye protection, and gloves (Imdorf et al. 1996, Balint et al. 2010). Furthermore, as both organic acids and phytochemicals rely heavily on volatile vapours, the efficacy of such treatments depends on ambient temperature and humidity (DeGrandi-Hoffman et al. 2012). Given the varied shortcomings of different chemical varroacides, long-term varroa management regimens should utilize different treatment in rotation, which reduces the evolution of resistance (Maggi et al. 2011). Treatments should also be used in integrated pest management (IPM) frameworks, being combined with cultural controls (such as brood breaks) to further mitigate the evolution of varroacide resistance (Jack and Ellis 2021). In addition to killing varroa mites, IPM-friendly chemical treatments may also seek to disrupt varroa behaviours, such as host-finding and mating (Vilarem et al. 2021). Thus, novel varroacides play a key role in expanding the suite of treatment options available.

One candidate chemical with demonstrated potential as a novel varroacide is 1-allyloxy-4-propoxybenzene, also known as 3c{3,6} (Dawdani et al. 2023). As a low-molecular weight dialkoxybenzene, 3c{3,6} is a structural mimic of phytochemical odorants and was first explored as a feeding deterrent against cabbage looper caterpillars (*Trichoplusia ni*) (Plettner and Gries 2010, Ebrahimi et al. 2013). Further *in vitro* bioassays involving topical application of 3c{3,6} onto varroa mites rapidly induced acute paralysis and death in mites exposed to the chemical (Singh et al. 2020, Dawdani et al. 2023). At sublethal doses, 3c{3,6} has been demonstrated to interrupt varroa host-finding, by disrupting the activity of foreleg chemoreceptors and reducing

the mites' ability to navigate toward host bees, as well as causing varroa to arrest while locating their hosts (Singh et al. 2020, Dawdani et al. 2023). In comparison with structurally-similar dialkoxybenzenes, 3c{3,6} possesses greater and more rapid varroacidal activity and yields the highest mortality rates (90% mortality *in vitro* after 6h) (Dawdani et al. 2023).

The acute toxic and chemoreceptor-disruptive effects of 3c{3,6} do not appear to occur in exposed honey bees, whose behaviour remains unchanged following both acute and long-term oral exposure to high doses of 3c{3,6} administered in syrup (Singh et al. 2020, Dawdani et al. 2023). However, 3c{3,6} has been demonstrated to allosterically interact with at least one honey bee acetylcholinesterase (*Am*AChE), though the effects of this are unknown; human acetylcholinesterase (*h*AChE) was shown to be unaffected by 3c{3,6} exposure (Dawdani et al. 2023). Nevertheless, the potential toxicity of 3c{3,6} against AChE is less than that of DEET, a comparable chemical pesticide which produces similar physiological outcomes against varroa and which competitively inhibits both mammal and honey bee AChE (Corbel et al. 2009). The potential of 3c{3,6} to be a pollutant in the environment is low, as 3c{3,6} has been shown to be metabolized and biodegraded by common strains of the cosmopolitan soil bacterium *Pseudomonas putida* (Dos Santos et al. 2004, Loh and Cao 2008, Ebrahimi and Plettner 2014).

In this study, I sought to build upon previous field trials and further evaluate the *in situ* efficacy of 3c{3,6} over the course of three experimental seasons. The first and second experiments occurred in the late summer to early fall of 2021 and 2022 respectively, while a third experiment took place during the spring and entire summer of 2023. Field experiments aimed to quantify the mortality-based efficacy of 3c{3,6} in comparison to the existing varroacide Thymovar®, which functioned as a positive control. Across different years, per-colony dosages of 3c{3,6} and applicator mechanisms were bewere modified, to optimize the treatment dosage and

delivery method. In each season, two parallel experiments occurred in Beaverlodge, AB, and Langley, BC. In this chapter of my thesis, I will report on the three AB experimental trials, for which I had direct involvement.

2.2 Materials and Methods

2.2.1 Experimental Colony Management and Selection

Across all three years, experimental colonies were managed in standard-sized Langstroth deep hive boxes with nine frames. Colonies were managed as single-brood chamber hives, and during the honey flow season from July to mid-August when they were equipped with honey supers. All honey supers were standard-sized Langstroth deep hive boxes with nine frames, separated from the broodnest via a metal queen excluder. Colonies were grouped on wooden pallets in groups of two to four.

Prior to the experiment, all colonies were assessed for their dispersing-stage mite infestation levels using the alcohol wash method. This method involves loading adult worker bees into a mesh-bottomed container, which is then nested in a solid-bottomed container (De Jong et al. 1982, Gregorc and Sampson 2019) and filled with enough 70% ethanol to fully submerge all sampled bees before being sealed with a lid. Bees were then agitated for three cycles of five, five, and ten minutes using an orbital shaker (MBIMS-NOR-30, Montréal Biotech Inc., Montréal, QC) to dislodge mites from the bees, with the number of dislodged mites summed. Fifty of the sampled bees were also counted out and weighed at the end of the wash, and a weight regression was used to estimate the total number of worker bees in the sample. These values were then used to calculate percent dispersing mite infestation. The use of the weight-regression based varroa alcohol wash

allowed my colony assessment technique to be consistent with methods commonly used by beekeepers *in situ* (Ghasemi et al. 2024). Colony selection was based on treatment thresholds laid out by Currie and Gatien (2006) and Currie (2008), with colonies in fall experiments (2021 and 2022) requiring a minimum of 3% dispersing mite infestation, while spring experiment colonies (2023) required a minimum infestation level of 1%.

Supplemental pollen patties containing 15% pollen by weight (Global Patties, Airdrie, AB) were provided to colonies in mid-April, with each colony receiving a full patty split into two halves. During periods of low nectar flow starting in late September, colonies were fitted with colony-top feeders (BeeMaid Bee Supplies, Spruce Grove, AB) and fed 66% Brix sucrose syrup. Colonies were provisioned with 12-16 L sugar syrup at a time, supplemented with ~190 mg/colony fumagillin dicyclohexylamine (fumagillin) to prevent nosemosis (Peirson and Pernal 2024). Feeders were continuously refilled until syrup was no longer being consumed.

Colonies used in 2021 were constituted using worker bees split on 20 May 2021 from mixed Italian and New World Carniolan-stock colonies bred locally in Beaverlodge, and re-queened with New World Carniolan queens (Olivarez Honey Bees, Orland, CA) bred in 2021. Prior to the start of the experiment, all colonies were equalized to a nominal colony size of 14 frame sides of adult worker bees and 2-3 frame sides of brood (open and capped combined), with the remaining consisting of food stores. In total, 30 colonies were divided into three treatment groups of 10 colonies each.

In 2022, colonies were founded using 1-kg New Zealand package bees (Kintail Honey Ltd., New Zealand) installed on 21 April 2022, and the New Zealand Queens were subsequently replaced with newly-bred New World Carniolan queens (Olivarez Honey Bees, Orland, CA). As these newly established colonies did not contain varroa mites in levels detectable via alcohol wash,

varroa mites for inoculation were sourced from local colonies in Beaverlodge. First, dispersing mites were collected live using the sugar shake method, whereby frames of bees from varroa-infested brood colonies would be shaken into bins of powdered sugar and agitated to dislodge mites, which were sieved out using a coarse mesh (Gregorc et al. 2017). These infesting mites were then collected, gently wiped clean of sugar using a damp fine-tip paintbrush, and manually placed onto nurse bees within the broodnest of experimental colonies using a fine-tipped paintbrush. However, post-inoculation mite infestation levels remained below fall treatment thresholds, and thus some colonies were substituted with local Beaverlodge colonies containing locally-bred one- to two-year-old queens, which exhibited infestation levels above the minimum treatment threshold. The mixture of assembled California-queened colonies and local Beaverlodge-queened colonies were evenly distributed across all treatment groups, such that no treatment group had colony composition biased toward either queen stock. Colonies in the 2022 experiment had a nominal starting size of 16-17 frame sides of worker bees and 3.5 frame sides of combined brood, with the rest consisting of food stores. In total, 40 colonies (11 Californian queen colonies and 29 local colonies) were distributed into five treatment groups of eight replicate colonies each.

Colonies in 2023 were sourced locally, being selected from surviving overwintered colonies from 2022. These included colonies established for the 2022 experiment that were previously excluded due to low mite levels, alongside colonies of local Beaverlodge bees. None of the colonies used in the 2023 experiment were used in the 2022 3c{3,6} experiment. The nominal start size of colonies in the 2023 experiment was 5 frame sides of adult worker bees and 3 frame sides of combined brood, with the remaining consisting of food stores. A total of 20 colonies were equally distributed among two treatment groups..

2.2.2 General Experimental Overview

As my study builds on the results of Dawdani et al. (2023), my experiments follow a similar experimental protocol. The general experimental timeline was divided into three distinct phases: setup, treatment, and clean-up. The dates and durations of each phase varied depending on the experiment year. Experimental colonies were placed atop mesh screen bottom boards (Propolis-etc… [sic], St-Mathieu de Beloeil, Québec), within which varroa mite sticky boards (Dadant and Sons Inc., Hamilton, IL) were placed to monitor rates of mite mortality. The first sticky board was placed at the start of experimental set-up, and was exchanged with a fresh board at the beginning of the treatment phase. Subsequently, sticky boards would be exchanged at seven-day intervals, except during the first week of both treatment and clean-up phases, where the first exchange occurred after a single day, followed by three, two-day exchange intervals. An exception to this pattern was in the Spring 2023 experiment clean-up phase onward, where sticky boards were replaced at four- to five-day intervals to coincide with formic acid pad exchanges. Daily mite mortality was determined via dividing counts of mites stuck to sticky boards at each collection interval, by the length (in days) of the interval.

During the setup phase, experimental colonies were randomized to treatment groups in a stratified manner based on the dispersing mite infestation levels calculated from mite alcohol washes, as described above. This was done to ensure all treatment groups had similar average pre-experimental mite infestation levels. In addition, several other colony-level factors relating to overall colony health were assessed (Table 2-1) to verify that colonies were nominally equal across treatment groups. Specifically, I evaluated brood and food stores based on surface area of frames occupied, and the adult worker bee populations were evaluated based on surface area coverage of frame sides. I also evaluated capped brood cell infestation levels, by pulling frames of capped

pupal brood from each colony and uncapping 100 cells from each frame (Harbo and Harris 2009, Harris et al. 2012). Pupae were extracted from the cells following uncapping and cells containing live varroa foundresses were scored.

At the beginning of the treatment phase (experimental day 0), a second mite alcohol wash was performed to establish the dispersing mite infestation level at the start of the experiment. Additionally, applicators of 3c{3,6}, negative controls, and Thymovar® positive controls (when used) were applied to each colony in accordance with their assigned treatment group. Sticky board exchanges were performed as previously detailed. Another set of colony evaluations were performed at the end of the treatment phase, examining dispersing mite infestation level, brood and food stores, adult worker bee population, and brood infestation level via the same methods detailed previously.

At the start of the clean-up phase, new sticky boards were inserted, and all treatment applicators were removed and exchanged with the clean-up treatment (Apivar® in 2021 and 2022, formic acid in 2023). All colonies received the same clean-up treatment regimen irrespective of treatment group. Details of treatments and experimental procedures, per year, are described below. At the end of the clean-up phase, a third mite alcohol wash was performed to evaluate the final dispersing mite infestation levels across all colonies.

2.2.3 Colony Overwintering

In the 2021 and 2022 field seasons, colonies were overwintered indoors (Currie et al. 2015). The overwintering room was kept at 4-5° C, with air circulation provided via ceiling-mounted fans and excess heat removed using a thermostatically-controlled two-stage exhaust fan. In 2021, overwintering occurred immediately after the end of the clean-up phase, while the extended 2022

experimental term of 12 weeks resulted in colonies being moved into the overwintering room while the clean-up phase was still ongoing.

Pre-winter cluster evaluations for all experimental colonies occurred immediately following the move into the overwintering room, on 12 November 2021, 6 December 2022, and 1 November 2023 across the three respective years' experiments. These evaluations entailed opening hives and visually examining and scoring the size of overwintering bee clusters, based on the number of inter-frame spaces occupied. These measurements (rounded to the nearest quarter-space) were conducted following the procedure laid out by Borba et al. (2022), and replicate a protocol which beekeepers may use to assess colony population/strength entering winter. In 2021 and 2023, colonies were evaluated from both the top and bottom of the broodnest box, while in 2022 the bottom box cluster evaluation was not possible due to the screened bottom boards having metal fixtures which locked them into the broodnest box (removed the subsequent year). In the early spring of the following year, colonies were re-evaluated for survival. Colonies were considered to have survived if they had a live queen and any quantity of worker bees present.

2.2.4 Fall 2021 3c{3,6} Field Efficacy Experiment Details and Timeline

The fall 2021 experiment included 30 colonies distributed into three different treatment groups (n = 10 for all groups): 3c{3,6}, negative control (untreated), and Thymovar® (positive control). All colonies selected had pre-existing levels of naturally-occurring varroa mites exceeding the minimum fall treatment threshold (3%), and thus no mite inoculations were required. Colonies in 2021 were housed at the "Varroa Yard" bee yard (55.30007° N, 119.28215° W) during the 2021 season.

In 2021, the 3c{3,6} applicators were wooden strips (15.3 cm × 5.1 cm × 0.5 cm), with a

total of 4 g of 3c{3,6} (Fig. 2-1). Compound 3c{3,6} was applied to the strips by dissolving the compound in 40 mL of isopropanol with 2% glycerol, and brushing on in several layers, allowing to dry out between applications. Negative control applicators used the same wooden strips, though were only treated with of 2% glycerol-isopropanol solvent. The positive control colonies received Thymovar® (an approved compound used to treat varroa in Canada) applied per label instructions, whereby each strip contained 15 g of thymol. 3c{3,6} and negative control strips were laid flat over the top bars of the frames at the centre of the broodnest. In the positive control cohort, a single Thymovar® strip per colony was cut into two halves, with each half placed on opposite corners of the hive box, placed on top of the frames.

The 2021 experiment treatment phase lasted 28 days, beginning with day 0 on 3 September 2021 and ending with day 28 on 1 October 2021. On day 14, all treatment applicators (3c{3,6}, negative control, and Thymovar®) were inverted. Immediately following the end of the treatment phase, a 42-day varroa clean-up was performed using Apivar® per label instructions, with two strips being placed into each colony, oriented towards opposing corners hanging between frames. Full colony assessments (food, brood, bees, brood infestation) were performed on days 0 (3 September 2021) and 28 (1 October 2021), while dispersing mite alcohol washes were performed on days 0 (3 September 2021), 28 (1 October 2021), and 70 (12 November 2021). A comprehensive timeline of the fall 2021 experiment, including dates, sticky board intervals, and experimental days, can be found in Table 2-2.

2.2.5 Fall 2022 3c{3,6} Field Efficacy Experiment Details and Timeline

The fall 2022 experiment included 40 colonies distributed into five treatment groups (n = 8 for all groups). All colonies initially featured undetectable varroa mite levels, and thus

required inoculation to establish infesting varroa populations. Inoculations took place two months prior to the commencement of the experiment, from 8 July 2022 to 14 July 2022, to allow for varroa mite population expansion. In each experimental colony, 42 dispersing mites collected from highly-infested donor colonies were introduced over four inoculations (8 July 2022, 11 July 2022, 13 July 2022, 14 July 2022). The 2022 experiment began on 13 September 2022 (day 0), when treatment applicators were installed into the experimental colonies. Colonies in the 2022 experiment were initially housed at the "Anderson Lake" bee yard (55.20135° N, 119.15251° W) until 11 October 2022 (experimental day 28), at which point they were moved to the "Home Yard" bee yard (55.20278° N, 119.39644° W) where they remained until overwintering. Colony transport occurred before bee flight commenced in the morning, and colony entrances were sealed with metal hardware cloth and duct tape.

A new 3c{3,6} applicator design was utilized in the fall 2022 experiment season, using two different materials: wood and cardboard. Thus, the treatment groups were stratified by both treatment compound and applicator type: 3c{3,6} (wood), negative control (wood), 3c{3,6} (cardboard), negative control (cardboard), and Thymovar® (positive control). The 2022 treatment applicator design included three 3c{3,6}-impregnated strips of wood (24.0cm × 5.0cm × 0.5cm) (Fig. 2-2A) or corrugated cardboard (24.0 cm × 5.0 cm × 0.3 cm) (Fig. 2-2C) hung vertically between the frames of the broodnest and supported horizontally by a fourth untreated strip of the same material and dimensions (Fig. 2-2B). A total dosage of 8 g 3c{3,6} was applied evenly across the three hanging strips of the applicator, with the first 6 g being dissolved in 60 mL isopropanol with 2% glycerol and brushed on, and the final 2 g dissolved in 20 mL of 100% isopropanol. Control applicator strips were treated with only carrier solvent. The total treatment phase for the 2022 experiment was 42 days. Thymovar® was once again used as the positive control treatment.

In compliance with label instructions for the 6-week treatment term, two single Thymovar® strips were used. Single Thymovar® strips were cut into half lengthwise and placed at opposite corners on top of the frames of the broodnest on day 0 (13 September 2022) and replaced on day 21 (4 October 2022) with a new halved strip.

Immediately after the end of the treatment phase on day 42 (25 October 2022), a 42-day varroa clean-up phase was performed once again using two Apivar® strips hung between the frames towards opposite corners. Due to cold weather, full colony assessments were performed on days 0 (13 September 2022) and 35 (18 October 2022), while dispersing mite alcohol washes were performed on days 0 (13 September 2022), 42 (25 October 2022), and 84 (6 December 2022). A comprehensive timeline of the fall 2022 experiment, including dates, sticky boards, and experimental days, can be found in Table 2-3.

2.2.6 Spring 2023 3c{3,6} Field Efficacy Experiment Details and Timeline

A follow-up experiment to the fall 2022 trials was planned and carried out in Spring 2023. From the 2022 experiment, the same wooden 3c{3,6} applicator design was selected for the 2023 experiment. A total of 20 colonies were stratified into two groups (n = 10 for all groups): 3c{3,6} (wood), and negative control (wood). Due to a lack of surviving colonies with significant mite loads after the winter of 2022, no positive control was included. All colonies in the 2023 experiment were housed in the "Home Yard" (55.20278° N, 119.39644° W) for the entire season.

Though the treatment applicators used were identical to the fall 2022 experimental applicators, the 3c{3,6} total dosage was increased to 10 g for spring 2023. A total of 8 g of 3c{3,6} was initially dissolved in 80 mL of isopropanol with 2% glycerol and brushed onto the hanging wooden strips. A further 2 g of 3c{3,6} was then dissolved in 20 mL of 100% isopropanol. Control

applicator strips were treated with an equal amount of carrier solvent.

The 2023 experiment began on 11 May 2023 (day 0), with the treatment phase lasting 42 days (until 22 June 2023), followed by a 43-day varroa clean-up phase (ending on Day 85, dating 4 August 2023). Because the clean-up phase coincided with the honey flow, as well as the detection of potential amitraz-resistance within the Beaverlodge varroa mite population, Apivar® could not be used in the 2023 experiment. Instead, formic acid was applied to all colonies at intervals of 4-5 days per treatment. Clean absorbent Dri-Loc® brand meat pads (fluid capacity of ~20 mL) were soaked in 65% formic acid solution to create "mite wipes," which were placed above the frames along the periphery of the broodnest. During the clean-up phase, sticky board exchange intervals were set to occur on the same days as mite wipe exchange intervals. Full colony assessments (food, brood, bees, brood infestation) were performed on days 0 (11 May 2023) and 42 (22 June 2023), while dispersing mite alcohol washes were performed on days 0 (11 May 2023), 42 (22 June 2023), and 91 (10 August 2023).

Sticky board exchanges continued after the removal of the final mite wipe on day 90 (9 August 2023) to further monitor mite populations throughout the year, being exchanged at weekly intervals. Due to increasing mite populations across all colonies post-experiment, oxalic acid fumigation was used as a pre-wintering mite treatment beginning in September 2023. Seven rounds of oxalic acid fumigation were performed using a ProVap applicator with 1 g oxalic acid per colony, and occurred on the following dates: 7 September (Day 119), 13 September (Day 125), 4 October (Day 146), 12 October (Day 154), 18 October (Day 160), 25 October (Day 167). After 25 October 2023, oxalic acid treatments were discontinued in Beaverlodge as colonies were prepared for wintering. A comprehensive timeline of the Spring 2023 experiment is found in Table 2-4.

2.2.7 Statistical Analyses

To determine data structure of colony metrics, a Shapiro-Wilk test was employed for normality analysis, while Levene's test was used to assess variance structure. In the 2021 and 2022 data, comparisons of colony metrics across the treatment groups were performed using a Kruskal-Wallis test followed by Dunn's post-hoc test for nonnormal and/or heteroscedastic variables, or a one-Way ANOVA with a Tukey's post-hoc test for variables exhibiting normality and homoscedasticity. As the 2023 experiment only included two treatment groups allowing for direct pairwise comparison, colony metrics were compared directly. This involved a two-sided, two-sample Student's *t*-test for variables with normality and homoscedasticity, a Welch's *t*-test for normal but heteroscedastic variables, or Mann-Whitney U-test if normality (and homoscedasticity) assumptions were not met. Additionally, Student's *t*-tests were used to evaluate changes to dispersing mite and brood infestation levels between the start and end of the experimental term across all treatment cohorts.

Comparisons of wintering cluster sizes between treatment groups was performed similarly to other colony metrics, with comparisons in 2021 and 2022 being made using the Kruskal-Wallis and Dunn's post-hoc tests (as all cluster distributions deviated significantly from normality, though maintained homoscedasticity). Meanwhile, the 2023 colonies maintained normality and homoscedasticity in both top and bottom clusters, so analysis was carried out using a two-sided, two-sample Student's *t*-test. In early spring, colonies were re-evaluated for survival.

Efficacies for each 3c{3,6} treatment season and applicator were calculated using a modified version of Sun-Shepard's formula, to take into consideration differences in both varroa mortality and dispersing mite load changes across treatment groups (Kanelis et al. 2022). This method is advantageous as it can accommodate non-uniform population sizes across treatment

cohorts, and account for both mortality and reproduction. From Püntener (1981), calculation of corrected efficacy via Sun-Shepard's formula as applied to my experimental design is as follows:

$$\text{Efficacy} = \left(\frac{\Delta Inf_{\text{Treat}} - \Delta Inf_{\text{NC}}}{100 - \Delta Inf_{\text{NC}}}\right) * 100\%$$

Where $\Delta Inf_{\text{Treat}}$ and ΔInf_{NC} is the average change in dispersing mite infestation levels of the 3c{3,6} or Thymovar®, and negative control colony cohorts respectively. The change in infestation can be calculated using the following formula:

$$\Delta Inf = \frac{Inf_{\text{Start}} - Inf_{\text{End}} * \left(\frac{Bees_{\text{End}}}{Bees_{\text{Start}}}\right)}{Inf_{\text{Start}}}$$

Where Inf_{Start} and Inf_{End} are the dispersing infestation levels at the start and end of the treatment term, respectively, and $Bees_{\text{Start}}$ and $Bees_{\text{End}}$ respectively represent the adult bee population (by frame sides) at the start and end of the treatment term. The inclusion of the $\left(\frac{Bees_{\text{End}}}{Bees_{\text{Start}}}\right)$ term to the equation accounts for the change in the adult bee population, which influences the total population of mites within the colony alongside the infestation level.

Comparisons between the efficacy of 3c{3,6} and the Thymovar® positive control (when included) were performed using a two-tailed Student's *t*-test. Due to each applicator having its own respective negative control in the fall 2022 experiment, Thymovar® efficacy was calculated twice (once corresponding to each negative control). fall 2022 comparisons between 3c{3,6} treatment efficacies against Thymovar® were performed using the Thymovar® efficacy values calculated using the respective negative controls (i.e., 3c{3,6} wood applicator efficacy was compared to Thymovar® efficacy calculated using the wood negative control, and vice versa for cardboard).

Mite mortality was determined by calculating daily mite fall per sticky board, dividing the

total mite fall per board by the number of days of the respective sticky board interval. Mite mortality was determined by calculating daily mite fall per sticky board, dividing the total mite fall per board by the number of days of the respective sticky board interval. A generalized least squares (GLS) approach was used to model mite mortality per treatment over each measurement interval, to determine interactive effects between treatment and time. To account for temporal autocorrelation stemming from repeated measurements, a first-order autoregression term was incorporated into the models for all years, based upon colony ID. Three models were constructed in the R statistical environment v4.1.1, corresponding to each year, with the following formulae input into the *gls* command in the "nlme" package v3.1-151 (Pinheiro et al. 2021):

```
gls(mites ~ treat*day, data=mitefall[year], correlation=corAR1(form= ~1 | Colony),
    weights=varIdent(form= ~ 1 | treat*day_int), method= "ML")
```

Pairwise comparisons of mite mortalities between treatment groups at each sticky board date were performed with the "emmeans" package v1.10.2 (Lenth 2024). *P*-values were globally adjusted across all pairwise comparisons at all days, using the Benjamini-Hochberg method with a false discovery rate (FDR) of 5% (0.05) (Dai et al. 2023).

2.3 Results

2.3.1 Fall 2021 Experiment Testing 3c{3,6} Field Efficacy

To determine the varroacidal activity of 4-g treatments of 3c{3,6} in comparison to Thymovar® and an untreated negative control, I examined daily varroa mortality levels and changes in varroa populations throughout the experimental treatment period (28 days). At the start of the experiment on day 0 (3 September 2021), colonies began with 15.0 ± 1.33% dispersing mite

infestation levels (range 2.8 to 29.3%). Infestation levels on adult bees did not differ among any of the treatment groups at the start of the experiment ($F = 1.67$; df = 2, 27; $P = 0.206$) (Table 2-5), and also remained similar on day 28 (1 October 2021) ($H = 0.94$; df = 2; $P = 0.626$). At the end of the experiment on day 70 (12 November 2021), dispersing mite levels differed among treatments ($H = 6.33$; df = 2; $P = 0.042$), with the 3c{3,6}-treated colonies having significantly fewer mites than the Thymovar®-treated colonies ($P = 0.036$).

The proportion of brood cells infested with mites were also similar across treatment groups on day 0 ($F = 0.31$; df = 2, 27; $P = 0.738$). Likewise, brood cell infestations remained similar on day 28 among the three treatment groups ($F = 0.58$; df = 2, 27; $P = 0.566$).

The 3c{3,6}-treated colonies had no significant changes in either dispersing mite ($t = 1.04$; df = 18; $P = 0.156$) or brood infestation levels ($t = 1.39$; df = 18; $P = 0.091$) when compared between the start of the treatment phase (day 0) and the end (day 28). Thymovar®-treated colonies experienced no change in dispersing mite infestations ($t = 0.54$; df = 18; $P = 0.702$), but saw a significant increase in brood infestation levels ($t = 2.12$; df = 18; $P = 0.024$). In the control colonies, significant increases were observed in both the dispersing mite ($t = 1.75$; df = 18; $P = 0.048$) and brood infestation levels ($t = 3.61$; df = 18; $P = 0.001$) between day 0 to day 28.

In 2021, changes were not observed among treatments for the quantity of food stores in colonies before and after the treatment period. On day 0, treatment groups did not differ significantly in their pollen stores ($H = 0.46$; df = 2; $P = 0.796$) (Table 2-5), though honey stores varied slightly at the start of the experiment ($H = 9.60$; df = 2; $P = 0.008$), with 3c{3,6}-treated colonies possessing smaller honey stores than negative control colonies ($P = 0.007$). Nevertheless, these differences disappeared on day 28, with no significant differences in honey or pollen stores observed between treatment groups.

GLS analysis of the daily varroa mortality counted from sticky boards during the duration of the fall 2021 experiment revealed a significant interaction between the Treatment and Day terms ($F = 3.29$; df = 32, 459; $P < 0.001$). However, while the 3c{e,6} and Thymovar® treated-colonies generally exhibited higher mite mortality than the negative control colonies during the treatment phase, and vice versa during the clean-up phase (Fig. 2-3), these differences were only significant on days 14 (17 September 2021) and 31 (4 October 2021).

Using the Sun-Shepard formula, the fall 2021 3c{3,6} treatment achieved a mean corrected experimental efficacy of 48.1% ± 7.36%, while the Thymovar® treatments in positive control colonies had a mean efficacy of 40.2% ± 21.92%. There was no significant difference in efficacy between the 3c{3,6} and positive control treatment ($t = 0.65$; df = 18; $P = 0.739$).

Three colonies died between the end of the experiment (day 70) and the cluster evaluation date (two treated with 3c{3,6}, one negative control), and were thus excluded from cluster comparisons. Surviving 3c{3,6}-treated top and bottom cluster scores spanned an average of 2.6 ± 0.41 and 0.8 ± 0.46 inter-frame spaces, respectively, negative control colony top and bottom clusters spanned an average of 2.3 ± 0.37 and 0.9 ± 0.30 inter-frame spaces, and Thymovar®-treated colony top and bottom clusters spanned an average of 3.0 ± 0.73 inter-frame spaces and 1.5 ± 0.47 inter-frame spaces. Treatment groups were all similar in both their top ($H = 0.65$; df = 2; $P = 0.721$) and bottom cluster scores ($H = 3.05$; df = 2; $P = 0.218$). Following wintering on 26 April 2022, the fall 2021 3c{3,6}-treated colony cohort experienced 100% mortality, the negative control cohort experienced 90% mortality (1 surviving colony), and the Thymovar®-treated cohort experienced 80% colony mortality (2 surviving colonies).

2.3.2 Fall 2022 Experiment Testing 3c{3,6} Field Efficacy

In 2022, I modified the 2021 experimental design by increasing the 3c(3,6) dosage per colony from 4 to 8 g and the duration of treatment application from 28 to 42 days. In addition, modifications were made in the applicator design. On day 0 of the 2022 experiment (13 September 2022), the average infestation level across all experimental colonies was 4.7 ± 0.65%. Initial dispersing mite infestation levels did not differ across the five treatment groups ($H = 0.03$; df = 4; $P > 0.999$) (Table 2-7). By day 42 (25 October 2022), however, significant differences were observed ($H = 23.85$; df = 4; $P < 0.001$). Specifically, colonies with 3c{3,6}wood or 3c{3,6}cardboard applicators exhibited similar dispersing mite infestations, and had significantly lower levels than negative control colonies with either type of applicator; the latter two treatment groups also had comparable dispersing mite loads between them. Dispersing mite infestations in Thymovar®-treated colonies did not differ significantly from 3c{3,6} wood or 3c{3,6} cardboard-treated colonies, nor negative control colonies with cardboard applicators, but were significantly lower than negative control colonies with wood applicators. On day 84, differences among treatments remained significant ($H = 13.71$; df = 4; $P = 0.008$) for dispersing mite loads. Dunn's post-hoc test revealed significantly lower mite levels in 3c{3,6} colonies with cardboard applicators and Thymovar-treated colonies, than negative control colonies with wooden applicators; no other pairwise differences were significant.

Day 0 differences in brood infestation levels were also consistent among treatment groups ($H = 0.61$; df = 4; $P = 0.962$). On day 35 (18 October 2022), significant differences were observed in the brood infestation levels ($H = 22.67$; df = 4; $P < 0.001$) across the five treatments, as Dunn's post-hoc test revealed significantly lower rates of brood infestation in Thymovar® and 3c{3,6}-treated colonies with wood or cardboard applicators, versus either negative control. Thymovar®

and 3c{3,6}-treated colonies with wood or cardboard applicators showed similar levels of brood infestation, while infestation levels between negative control colonies with wood and cardboard applicators were also comparable.

Over the treatment period, colonies having 3c{3,6}-treated wooden applicators experienced significant decreases in both dispersing mite (t = 2.30; df = 14; P = 0.019) and brood infestation levels (t = 1.84; df = 11; P = 0.046), while colonies containing untreated wooden applicators had no change in mite levels on adult bees (t = 0.66; df = 14; P = 0.262) nor infesting their capped brood (t = 0.17; df = 13; P = 0.432). Likewise, colonies having 3c{3,6}-treated cardboard applicators saw significant decreases in both dispersing mite (t = 2.46; df = 14; P = 0.014) and brood infestation levels (t = 1.93; df = 13; P = 0.038), while colonies with untreated cardboard applicators saw no changes in mites on adult bees (t = 1.73; df = 14; P = 0.047) nor mites in their capped brood cells (t = 153; df = 14; P = 0.074). In the Thymovar®-treated colonies, both dispersing mite (t = 2.45; df = 14; P = 0.014) and brood infestation levels (t = 1.87; df = 14; P = 0.042) were significantly lower at the end of the treatment phase than at the start.

It is worth noting that, though colonies provided cardboard applicators experienced comparable levels of mite mortality and treatment efficacy compared to their wood applicator-provisioned counterparts, cardboard applicators quickly disintegrated within the hive environment (Fig. 2-2C). The subsequent cardboard shavings settled to the bottom of the hives, where it became trapped on the sticky boards. This degradation began immediately following the installation of the applicators. By the end of the treatment phase on day 42, all cardboard applicators (both negative control and 3c{3,6}) showed severe degradation.

All colony metrics (food, brood, adult bee populations) (Table 2-7) were similar among treatments on day 0. On day 35 (18 October 2022), only differences in the area of open brood

between treatments were different (H = 10.44; df = 4; P = 0.034). Specifically, the Thymovar®-treated and negative control wooden treatment had significantly more open brood than both 3c{3,6} cardboard and negative control cardboard treatment, while the 3c{3,6} wooden treatment had significantly less open brood than the Thymovar®-treated colonies; no other pairwise comparisons were significant.

The GLS analysis of the fall 2022 mite mortality data revealed a significant interaction between the Treatment and Day main effects (F = 2.49; df = 72, 665; P < 0.001). A strong peak in mite mortality within the 3c{3,6} treated colonies with both wood and cardboard applicators, with these two treatments exhibiting similar levels of mite mortality which were significantly higher than both negative control and the Thymovar®-treated colonies (Fig. 2-4). In Thymovar®-treated colonies, mite mortality slowly increased during the treatment phase, peaking on day 21 (4 October 2022) when the Thymovar® treatment cohort exhibited significantly higher mortality than all other cohorts, before subsequently decreasing towards the end of the treatment phase. Entering the clean-up phase, both wood and cardboard negative control cohorts showed similar mite mortalities to one another, being significantly higher than both 3c{3,6}-treated and the Thymovar®-treated colonies. However, these differences would taper off towards the end of the experiment.

Using the Sun-Shepard formula, the average corrected efficacy of the 3c{3,6} cardboard applicator across 8 colonies in fall 2022 was 90.1% ± 6.11%, which did not significantly differ from the average Thymovar® efficacy of 89.5% ± 5.65%, calculated from the negative control cardboard colonies (t = 1.77; df = 14; P = 0.951). The average mortality-based efficacy of the 3c{3,6} wooden applicator colonies was 98.1% ± 1.09%, which also did not differ significantly from Thymovar® efficacy of 95.5% ± 2.46%, when calculated against the negative controls with wooden applicators (t = 0.01; df = 14; P = 0.339).

Average top clusters ranged from 1.7 ± 0.44 inter-frame spaces in the Thymovar® cohort, 2.0 ± 0.51 inter-frame spaces in the 3c{3,6} wood cohort, 2.3 ± 0.59 inter-frame spaces in the 3c{3,6} cardboard cohort, 3.4 ± 1.02 inter-frame spaces in the negative control cardboard cohort, up to 3.9 ± 1.02 inter-frame spaces in the negative control wood cohort. However, these differences were not significant across treatment groups ($H = 4.23$; df = 4; $P = 0.368$). During the following evaluation of overwinter survivorship on 1 May 2023, the 3c{3,6} cardboard, 3c{3,6} wood, and Thymovar®-treated cohorts each experienced 12.5% winter mortality (7 surviving colonies). Overwinter mortality was highest in the negative control wood cohort at 25% (6 surviving colonies), and lowest in the negative control cardboard cohort at 0% (8 surviving colonies).

2.3.3 Spring 2023 Experiment Testing 3c{3,6} Field Efficacy

To assess the efficacy of 3c{3,6} as a spring treatment for controlling overwintering mite buildup, I performed a third experiment in spring 2023 comparing varroa populations in 3c{3,6}-treated colonies against untreated negative control colonies. This experiment applied 10 g of 3c{3,6} per colony using a wooden applicator, over a 42-day treatment period, The average dispersing mite infestation level across all colonies on day 0 of the Spring 2023 experiment (11 May 2023) was 2.5% ± 0.37%, with no significant differences between treatment groups ($U = 49.5$; $P > 0.999$) (Table 2-9). On day 42 (22 June 2023), 3c{3,6}-treated colonies showed significantly lower levels of dispersing mites than negative control colonies ($U = 9.0$; $P = 0.001$), and on day 92 (11 August 2023), 3c{3,6}-treated colonies continued to maintain lower mite levels than negative control colonies ($U = 8.5$; $P = 0.008$).

Brood infestation levels did not differ significantly across the treatment groups ($t = 0.13$; df = 18; $P = 0.895$) at the start of the experiment on day 0 (Table 2-9). However on day 42,

3c{3,6}-treated colonies showed significantly lower brood infestation levels than negative control colonies ($U = 18.0$; $P = 0.009$) on day 42.

Throughout the treatment phase, the 3c{3,6}-treated colonies experienced significant decreases in both dispersing mite ($t = 3.38$; df = 17; $P = 0.002$) and brood infestation levels ($t = 3.51$; df = 17; $P = 0.001$). No significant changes to dispersing mite ($t = 0.72$; df = 18; $P = 0.239$) or brood infestation levels ($t = 1.46$; df = 18; $P = 0.080$) were observed in the negative control colonies.

On day 0, all colony metrics (brood, food, adult bees) were similar between the 3c{3,6}-treated and negative control colonies (Table 2-9). On day 42, only adult bee populations differed significantly across treatment groups, with 3c{3,6}-treated colonies having significantly lower adult bee populations than negative control colonies ($t = 3.03$; df = 18; $P = 0.009$) – specifically, 3c{3,6}-treated colonies exhibited a nearly two-fold reduction in the adult worker population (6.5 ± 0.98 frame sides) in comparison to the negative control colonies (12.2 ± 1.60 frame sides). All other colony metrics were similar across groups, although the differences in capped brood were only marginally significant ($P = 0.054$).

The Spring 2023 GLS model indicated a significant interaction between Treatment and Day terms ($F = 4.81$; df = 21, 396; $P < 0.001$). Figure 2-5 illustrates that after the installation of treatments on day 0, 3c{3,6}-treated colonies had an immediate peak in mite mortality, remaining greater than the negative control colonies up to day 14 (25 May 2023). From day 21 (1 June 2023) to day 97 (16 August 2023), negative control colonies exhibited higher mite mortality than 3c{3,6}-treated colonies. A mortality peak was observed in the negative control cohort on day 43 (23 June 2023), immediately after the installation of formic acid pads.

Calculating the Sun-Shepard corrected efficacy for the Spring 2023 applications of 3c{3,6}

treatments, up to the end of formic acid treatment on day 90 (9 August 2023), yielded an average efficacy of 100% ± 0.0% across 10 colonies.

Prior to overwintering on 1 November 2023, two colonies from the 3c{3,6} cohort and one colony from the negative control cohort had died . The surviving 3c{3,6} colonies had average top and bottom cluster sizes of 4.0 ± 1.03 inter-frame spaces and 3.7 ± 0.86 inter-frame spaces respectively, while the surviving negative control colonies had average top and bottom cluster sizes of 3.4 ± 1.43 inter-frame spaces and 3.7 ± 1.27 inter-frame spaces respectively. Neither top (t = 0.69; df = 15; P = 0.504) nor bottom (t = 0.03; df = 15; P = 0.979) clusters differed significantly between treatment cohorts. Mortality during overwintering was equivalent in both the 3c{3,6}-treated and negative control cohorts, with one colony dying from each. In total, seven 3c{3,6}-treated and eight negative control colonies survived until spring 2024.

2.4 Discussion

The results of my study demonstrate the acaricidal activity of 3c{3,6} against *V. destructor* in managed honey bee colonies located on the Canadian prairies. Moreover, I found that 3c{3,6} can perform at efficacy levels comparable to other registered varroacides, with 3c{3,6} attaining measures of efficacy and mite mortality comparable to or exceeding the Thymovar® positive control in both 2021 and 2022. This performance was recapitulated in both the GLS model of mortality, and the calculations of corrected efficacy based on the change in infestation level over the course of the experiment. Furthermore, the efficacies found in 2022 and 2023 were comparable to or exceeded field efficacies of varroacide formulations based on thymol, tau-fluvalinate, flumethrin, amitraz, and hops organic acids reported across Canada and the United States

(Vandervalk et al. 2014, Gregorc et al. 2018, Bąk et al. 2021, Hýbl et al. 2021, Morfin et al. 2022, Jack et al. 2024). Additionally, my experimental treatments of 3c{3,6} in fall 2022 and spring 2023 yielded similar *in situ* efficacies as those reported by (Dawdani et al. 2023) (51.2% in British Columbia, Canada, and 81.1% in Alberta, Canada), and by (Cook et al. 2024) (72.8% in Maryland, USA). Differences between these treatments with one another, as well as with my experimental findings, may be attributable to a climate, dosage, applicator design, or a combination of these reasons, though it is not possible to disentangle these factors.

Our findings suggest that 3c{3,6} is most efficacious at killing varroa when administered at a dosage of 8-10g, on applicators hanging between frames as per those used in my 2022 and 2023 experiments. It is also notable that in the case of the between-frame hanging applicators used in 2022 and 2023, I observed a large spike in mite mortality immediately following the installation of the applicators. This observation, in conjunction with a decreasing rate of mortality in 3c{3,6}-treated colonies as the treatment phase progressed, implies a strong and immediate effect of 3c{3,6} against varroa mites *in situ*. However, this pattern was noticeably absent in the 2021 experiment. In comparing the applicators used in the 2022 and 2023 experiments versus the 2021 experiment, differences in four experimental parameters may explain the lower efficacy in the latter. First, the 2021 applicator had a much lower dosage than the other two years, at 4 g of 3c{3,6}. Second, the 4-week treatment window in 2021 was 2 weeks shorter than the 6-week treatment window in 2022 and 2023, which allowed less time for the miticidal activity of 3c{3,6} to act on varroa populations. Third, the larger surface area of the 2022 and 2023 applicators may have enabled more complete volatilization of 3c{3,6} than in 2021. Fourth, the hanging applicators used in 2022 and 2023 were positioned between broodnest frames, which may have provided more opportunities for varroa-infested bees to come into direct contact with 3c{3,6} residues on the

surface of the applicators alongside vapours. In addition, the particularly high mite infestation levels in 2021 may have contributed to a reduction in efficacy (van der Steen and Vejsnæs 2021). Because adjustments to each of the four parameters were performed simultaneously, disentangling the effect of each individual parameter on efficacy between years was not possible.

In 2021, the high varroa infestation level along with the 100% colony loss across all treatment groups suggest that 3c{3,6} treatment is unable to prevent colony death in cases of exceptionally high varroa infestation and lower colony application rates. In 2022, much higher proportions of colonies across all treatment cohorts survived the overwintering process, though the 3c{3,6}-treated colonies experienced comparable low mortality rates to the negative controls. Survival of these negative control colonies may be attributable to the elimination of varroa following the application of Apivar®, given the lower 2022 varroa densities versus 2021 and the high mortality counts during the clean-up phase. In the Spring 2023 experiment, mite levels in the negative control remained high even past the clean-up phase with formic acid treatments, necessitating a fall-time oxalic acid fumigation as a follow-up treatment. Meanwhile, the 3c{3,6}-treated colonies in 2023 maintained low mite levels from the end of formic acid on day 92 until approximately day 125, after which there was a resurgence in the varroa population. While it is unknown if this resurgence was due to the continued reproduction of remaining mites, or to the secondary acquisition of mites from drifting or cross-infestation during foraging, these results suggest a springtime treatment of 3c{3,6} alone is not sufficient in preventing the recovery of mite populations by the end of the season. Despite the high end-season varroa populations in negative control colonies, overwintering survival rates in 2023 were similar in both the 3c{3,6}-treated (70%) and negative control (80%) cohorts. In this case, survival of the negative control colonies may be attributable to their large worker populations entering winter.

Corrected efficacy calculations provide a numerical quantification of the effectiveness of a given compound in acting as a pesticide, relative to natural pest mortality levels found within negative controls (Parsad 2010, Bahreini et al. 2024, Özüiçli et al. 2024). Applying such formulae to field experiments is challenging as pest population sizes during the treatment period are unknown, and therefore must be estimated using subsampling (Sudo et al. 2019). Regarding varroa, alcohol washes provide a rapid and reliable means to determine the infestation level from a sample of honey bees, which may then be extrapolated to the entire colony to estimate an infestation level (Owen et al. 2022). However, like all subsampling methods, alcohol wash may suffer from decreased detection power at lower mite population densities, as the probability of sampling mites within a relatively small subset of bees diminishes. This may ultimately lead to overinflated efficacy measurements in colonies with particularly high efficacy, such as the 3c{3,6} treatment in my 2023 experiment. One method of overcoming this challenge is to collect a larger sample of bees, but as alcohol washes kill the collected, the maximum size of a sample cannot be too large or the health of the colony will be negatively affected. An alternative is the use of a non-destructive method to dislodge dispersing bees (such as briefly exposing bees to high levels of CO_2, or rolling them in powdered sugar), which can be employed on the scale of entire frames or colonies (Macedo et al. 2002, Aliano and Ellis 2005, Gregorc and Sampson 2019, Noble et al. 2021). Such methods are able to detect up to >90% of the dispersing varroa population within a sampled bees, though this detection sensitivity can decrease with increasing infestation levels (Gregorc and Sampson 2019, Owen et al. 2022). However, while these larger-scale sampling methods are more likely to detect mites in colonies with low infestation levels, they are much more time-intensive and may not be feasible for all experimental designs. Ultimately, efficacy calculations provide a useful quantification of the pesticidal effectiveness of a compound and serve

as a metric for comparison between different treatments. Nonetheless, given the shortcomings in methods used for *in situ* population size estimation, efficacy calculations should be coupled with more sensitive analyses (such as mortality modelling) which can recapitulate and support efficacy calculations and comparisons.

In the 2021 experiment to test 3c{3,6} efficacy *in situ*, no treatment group exhibited significant decreases to dispersing mite or brood infestation levels from the start to the end of the treatment phase, while in 2022 and 2023, all 3c{3,6} and Thymovar®-treated cohorts saw significant decreases in both dispersing mite and brood infestation levels. Meanwhile, negative control cohorts in 2022 and 2023 saw insignificant changes to both dispersing mite and brood infestation levels. These results align with the calculated efficacies of 3c{3,6} and its putative miticidal activity. As proposed by Dawdani *et al.* (2023), decreases in brood infestation may be a result of fewer varroa mites entering cells (due to lower varroa populations), fewer mites capable of properly entering cells to begin with, or a combination of both. There is currently no evidence to suggest that 3c{3,6} is capable of diffusing through the wax cap of sealed brood at sufficient levels to kill reproducing varroa mites, though this topic remains to be experimentally investigated, as does the permeability of 3c{3,6} vapour through the cap itself (Kubásek et al. 2022).

Throughout all three years, treatment groups were stratified into groups with emphasis on ensuring approximately-equal average conditions during the pre-experimental set-up phase with regard to colony metrics (brood, food, adult bee population). The only exception to this was the per-colony honey content in the 2021 experiment which differed significantly across treatment cohorts, however the addition of an initial honey term did not improve the 2021 model. These metrics remained similar between treatments throughout all three years' experiment, with the exception of day 35 open-brood proportions in fall 2022, and day 42 adult bee populations in the

Spring 2023 experiment. The latter observation is particularly noteworthy as the 3c{3,6}-treated colonies possessed significantly lower adult bee populations and numerically lower capped brood levels, despite significantly lower varroa infestation levels. This observation suggests the possible existence of sublethal toxic effects of 3c{3,6} against honey bees, though the nature and mechanism of this toxicity was not investigated in this study. Nevertheless, should such toxicity be present, a dosage of 10 g/single box colony may be the lower threshold for significant toxic effects to manifest, representing an upper limit to 3c{3,6} treatment dosages.

2.5 Conclusion

3c{3,6} has continued to demonstrate promise in its ability to control *Varroa destructor* in an outdoor colony setting, across both spring and fall treatment terms. Additionally, treatment with 3c{3,6} does not appear to disrupt the nectar and pollen foraging capabilities of colonies based on measure food stores, nor does it significantly impact the reproductive rates of queens based on measurements of brood area. Across all experiments, 3c{3,6}-treated colonies bore significantly higher daily mite mortality rates than their untreated negative control counterparts, and 3c{3,6} performed equivalently to a commercial varroacide (Thymovar®). I found 3c{3,6} to be effective at preventing overwintering colony loss when mite levels were slightly above the recommended treatment thresholds, though it was not effective at preventing mortality at exceptionally high mite levels. At high dosages (10 g per colony), it is possible that 3c{3,6} may hinder growth of the worker bee population, though the causative mechanism is unknown. The high field efficacy of 3c{3,6} is comparable to commercial varroacides, making it a promising new candidate treatment against *V. destructor*. Nevertheless, further studies will help optimize dosage and application modality to maximize mite mortality while minimizing non-target effects on honey bees.

Table 2-1: Colony metrics assessed for all experimental colonies, and units of measurements per experimental year.

Colony Metric	Unit of Measurement Used	
	2021	**2022 and 2023**
Dispersing mite infestation (mite wash)	Dispersing mites per 100 bees (%)	Dispersing mites per 100 bees (%)
Brood infestation level	Foundress mites per 100 capped brood cells (%)	Foundress mites per 100 capped brood cells (%)
Colony honey stores	Frame sides (rounded to nearest 0.25 frame side)	Percent frame sides (approximate %)
Colony pollen stores	Frame sides (rounded to nearest 0.25 frame side)	Percent frame sides (approximate %)
Colony open brood	Number of 10cm × 10cm squares covered (rounded to nearest square)	Percent frame sides (approximate %)
Colony capped brood	Number of 10cm × 10cm squares covered (rounded to nearest square)	Percent frame sides (approximate %)
Worker bee population	Frame sides (rounded to nearest 0.25 frame side)	Frame sides (rounded to nearest 0.25 frame side)

Table 2-2: Fall 2021 experimental timeline, including dates, experimental days, and sticky boards.

Sticky Board	Experimental Day 2021	Treatment Actions	Other Actions	Calendar Date 2021	Collection Interval (d)
1	-4		First assessment of food/brood, brood infestation Mite wash I	30-August	
2	0	Installation of 3c{3,6} and Thymovar®		03-September	4
3	1			04-September	1
4	3			06-September	2
5	5			08-September	2
6	7			10-September	2
7	14			17-September	7
8	21			24-September	7
9	28	Removal of 3c{3,6} and Thymovar® treatments Clean-up phase and Apivar® begin	Second assessment of food/brood, brood infestation Mite wash II	01-October	7
10	29			02-October	1
11	31			04-October	2
12	33			O6-October	2
13	35			08-October	2
14	42			15-October	7
15	49			22-October	7
16	56			29-October	7
17	63			05-November	7
	70	End of clean-up, removal of Apivar®	Mite wash III Final sticky board removed, no replacement	12-November	7

Table 2-3: Fall 2022 experimental timeline, including dates, experimental days, and sticky boards.

Sticky Board	Experimental Day 2022	Treatment Actions	Other Actions	Calendar Date 2022	Collection Interval (d)
1	-5		First assessment of food/brood, brood infestation Mite wash I	08-September	
2	0	Installation of 3c{3,6} and Thymovar®		13-September	5
3	1			14-September	1
4	3			16-September	2
5	5			18-September	2
6	7			20-September	2
7	14			27-September	7
8	21	Thymovar® strips switched		04-October	7
9	28			11-October	7
10	35		Second assessment of food/brood, brood infestation (performed early due to cold weather)	18-October	7
11	42	Removal of 3c{3,6} and Thymovar® treatments Clean-up phase and Apivar® begin	Mite wash II	25-October	7
12	43			26-October	1
13	45			28-October	2
14	47			30-October	2
15	49			01-November	2
16	56			08-November	7
17	63			15-November	7
18	70			22-November	7
19	77			29-November	7
	84	End of clean-up, removal of Apivar®	Mite wash III Final sticky board removed, no replacement	06-December	7

Table 2-4: Spring 2023 experimental timeline, including dates, experimental days, and sticky boards.

Sticky Board	Experimental Day 2023	Treatment Actions	Other Actions	Calendar Date 2023	Collection Interval (d)
1	-6		First assessment of food/brood, brood infestation Mite wash I	05-May	
2	0	Installation of 3c{3,6}		11-May	6
3	1			12-May	1
4	3			14-May	2
5	5			16-May	2
6	7			18-May	2
7	14			25-May	7
8	21			01-June	7
9	28			08-June	7
10	35			15-June	7
11	42	Removal of 3c{3,6} treatments Clean-up phase and formic acid begin	Second assessment of food/brood, brood infestation Mite wash II	22-June	7
12	43			23-June	1
13	45			25-June	2
14	47			27-June	2
15	52			02-July	5
16	57			07-July	5
17	62			12-July	5
18	67			17-July	5
19	71			21-July	4
20	76			26-July	5
21	81			31-July	5
22	85			04-August	4
23	90	End of clean-up, removal of formic acid		09-August	5
	92		Mite wash III	11-August	
24	97		Ongoing monitoring of post-experiment mite populations	16-August	7
25	104			23-August	7
26	111			30-August	7
27	118			06-September	7
	119	Oxalic acid fumigation I		07-September	
28	125	Oxalic acid fumigation II		13-September	7
29	132			20-September	7
30	139			27-September	7
31	146	Oxalic acid fumigation III		04-October	7
32	153			11-October	7
	154	Oxalic acid fumigation IV		12-October	
33	160			18-October	7
34	167	Oxalic acid fumigation V		25-October	7
	174		Final sticky board removed, no replacement	01-November	7

Table 2-5: Fall 2021 colony evaluation metrics, and statistical comparisons. Post-hoc significance was corrected using the Bonferroni method.

Day	Metric	Treatment	*n*	Mean	Standard Error	Test	DF	Test Statistic	*p*-Value	Post-Hoc Significance
0	Pollen (Frame Sides)	3c{3,6}	10	2.0	0.33	Kruskal-Wallis + Dunn	2	0.46	0.796	n/a
		Negative Control	10	1.9	0.42					
		Thymovar®	10	1.7	0.34					
	Honey (Frame Sides)	3c{3,6}	10	3.0	0.75	Kruskal-Wallis + Dunn	2	9.60	0.008	a
		Negative Control	10	6.5	0.98					b
		Thymovar®	10	3.8	0.73					ab
	Capped Brood (10cm × 10cm Squares)	3c{3,6}	10	21.6	2.43	One-Way ANOVA + Tukey	2, 27	2.63	0.090	n/a
		Negative Control	10	15.1	1.91					
		Thymovar®	10	19.1	1.58					
	Open Brood (10cm × 10cm Squares)	3c{3,6}	10	6.8	1.34	Kruskal-Wallis + Dunn	2	0.94	0.626	n/a
		Negative Control	10	5.8	1.44					
		Thymovar®	10	7.0	0.96					
	Adult Bees (Frame Sides)	3c{3,6}	10	13.8	1.33	Kruskal-Wallis + Dunn	2	0.05	0.973	n/a
		Negative Control	10	13.8	0.99					
		Thymovar®	10	14.2	0.72					
	Mite-Infested Brood Cells (%)	3c{3,6}	10	26.3	5.51	One-Way ANOVA + Tukey	2, 27	0.31	0.738	n/a
		Negative Control	10	21.2	3.52					
		Thymovar®	10	24.4	4.71					
	Dispersing Mite Infestation (%)	3c{3,6}	10	15.0	1.79	One-Way ANOVA + Tukey	2, 27	1.67	0.206	n/a
		Negative Control	10	12.2	2.09					
		Thymovar®	10	18.0	2.75					

Table 2-5 (Cont.)

Day	Metric	Treatment	*n*	Mean	Standard Error	Test	DF	Test Statistic	*p*-Value	Post-Hoc Significance
28	Pollen (Frame Sides)	3c{3,6}	10	2.1	0.38	One-Way ANOVA + Tukey	2, 27	0.06	0.942	n/a
		Negative Control	10	1.9	0.37					
		Thymovar®	10	2.1	0.41					
	Honey (Frame Sides)	3c{3,6}	10	3.3	0.42	One-Way ANOVA + Tukey	2, 27	0.21	0.810	n/a
		Negative Control	10	3.8	0.49					
		Thymovar®	10	3.7	0.66					
	Capped Brood (10cm × 10cm Squares)	3c{3,6}	10	6.1	1.83	Kruskal-Wallis + Dunn	2	2.17	0.338	n/a
		Negative Control	10	7.5	1.57					
		Thymovar®	10	4.5	1.10					
	Open Brood (10cm × 10cm Squares)	3c{3,6}	10	1.9	1.14	Kruskal-Wallis + Dunn	2	1.29	0.524	n/a
		Negative Control	10	2.4	0.88					
		Thymovar®	10	1.2	0.31					
	Adult Bees (Frame Sides)	3c{3,6}	10	6.8	0.68	Kruskal-Wallis + Dunn	2	2.25	0.325	n/a
		Negative Control	10	8.1	0.91					
		Thymovar®	10	6.4	0.61					
	Mite-Infested Brood Cells (%)	3c{3,6}	10	40.8	5.96	One-Way ANOVA + Tukey	2,27	0.58	0.566	n/a
		Negative Control	10	48.3	5.66					
		Thymovar®	10	41.2	4.93					
	Dispersing Mite Infestation (%)	3c{3,6}	10	20.1	2.88	Kruskal-Wallis + Dunn	2	0.94	0.626	n/a
		Negative Control	10	22.4	4.23					
		Thymovar®	10	19.3	2.12					
70	Dispersing Mite Infestation (%)	3c{3,6}	6	0.1	0.12	Kruskal-Wallis + Dunn	2	6.33	0.042	a
		Negative Control	9	0.6	0.23					ab
		Thymovar®	8	1.9	0.86					b

Table 2-6: Pairwise comparisons of Fall 2021 GLS Treatment effects for different groups, performed post-hoc via Tukey's HSD.

Comparison	Estimate	Std. Error	DF	*t*-Statistic	*p*-Value
3c{3,6} – Negative	53.6	11.5	189	4.65	< 0.001
Thymovar® – Negative	67.6	11.5	189	5.86	< 0.001
Thymovar® – 3c{3,6}	14.0	11.5	189	1.21	0.449

Table 2-7: Fall 2022 colony evaluation metrics, and statistical comparisons. Post-hoc significance was corrected using the Bonferroni method.

Day	Metric	Treatment	*n*	Mean	Standard Error	Test	DF	Test Statistic	*P*-Value	Post-Hoc Significance
0	Pollen (Frame Sides)	3c{3,6} Cardboard	8	2.8	0.75	Kruskal-Wallis + Dunn	4	3.80	0.434	n/a
		Negative Control Cardboard	8	0.9	0.53					
		3c{3,6} Wood	8	2.3	0.84					
		Negative Control Wood	8	2.6	0.80					
		Thymovar®	8	2.4	0.90					
	Honey (Frame Sides)	3c{3,6} Cardboard	8	7.0	0.88	One-Way ANOVA + Tukey	4, 35	1.10	0.373	n/a
		Negative Control Cardboard	8	8.5	1.15					
		3c{3,6} Wood	8	7.4	0.90					
		Negative Control Wood	8	5.8	0.94					
		Thymovar®	8	7.7	0.78					
	Capped Brood (Frame Sides)	3c{3,6} Cardboard	8	2.9	0.51	One-Way ANOVA + Tukey	4, 35	0.40	0.806	n/a
		Negative Control Cardboard	8	3.2	0.44					
		3c{3,6} Wood	8	2.5	0.31					
		Negative Control Wood	8	3.1	0.33					
		Thymovar®	8	2.9	0.45					
	Open Brood (Frame Sides)	3c{3,6} Cardboard	8	0.5	0.16	Kruskal-Wallis + Dunn	4	3.04	0.551	n/a
		Negative Control Cardboard	8	0.4	0.15					
		3c{3,6} Wood	8	0.6	0.15					
		Negative Control Wood	8	0.9	0.24					
		Thymovar®	8	0.4	0.09					
	Adult Bees (Frame Sides)	3c{3,6} Cardboard	8	16.7	0.64	Kruskal-Wallis + Dunn	4	0.73	0.948	n/a
		Negative Control Cardboard	8	16.4	1.14					
		3c{3,6} Wood	8	17.0	0.92					
		Negative Control Wood	8	16.1	0.86					
		Thymovar®	8	17.9	2.11					
	Mite-Infested Brood Cells (%)	3c{3,6} Cardboard	8	9.1	3.50	Kruskal-Wallis + Dunn	4	0.61	0.962	n/a
		Negative Control Cardboard	8	5.5	1.05					
		3c{3,6} Wood	8	4.3	0.77					
		Negative Control Wood	8	7.8	3.54					
		Thymovar®	8	6.6	1.97					
	Dispersing Mite Infestation (%)	3c{3,6} Cardboard	8	4.0	1.34	Kruskal-Wallis + Dunn	4	0.03	1.000	n/a
		Negative Control Cardboard	8	4.1	1.59					
		3c{3,6} Wood	8	4.1	1.52					
		Negative Control Wood	8	4.0	1.47					
		Thymovar®	8	4.2	1.70					

Table 2-7 (Cont.)

Day	Metric	Treatment	*n*	Mean	Standard Error	Test	DF	Test Statistic	*p*-Value	Post-Hoc Significance
35	Pollen (Frame Sides)	3c{3,6} Cardboard	8	2.2	0.37	One-Way ANOVA + Tukey	4, 35	0.13	0.972	n/a
		Negative Control Cardboard	8	2.3	0.74					
		3c{3,6} Wood	8	1.7	0.74					
		Negative Control Wood	8	2.0	0.75					
		Thymovar®	8	2.1	0.56					
	Honey (Frame Sides)	3c{3,6} Cardboard	8	14.1	0.63	Kruskal-Wallis + Dunn	4	0.34	0.987	n/a
		Negative Control Cardboard	8	13.5	0.83					
		3c{3,6} Wood	8	14.1	0.54					
		Negative Control Wood	8	13.5	0.88					
		Thymovar®	8	13.6	0.84					
	Capped Brood (Frame Sides)	3c{3,6} Cardboard	8	1.0	0.18	Kruskal-Wallis + Dunn	4	1.44	0.838	n/a
		Negative Control Cardboard	8	1.0	0.11					
		3c{3,6} Wood	8	0.9	0.29					
		Negative Control Wood	8	1.0	0.18					
		Thymovar®	8	0.8	0.16					
	Open Brood (Frame Sides)	3c{3,6} Cardboard	8	0.2	0.12	Kruskal-Wallis + Dunn	4	10.44	0.034	a
		Negative Control Cardboard	8	0.1	0.07					a
		3c{3,6} Wood	8	0.1	0.04					a
		Negative Control Wood	8	0.4	0.14					a
		Thymovar®	8	0.3	0.08					a
	Adult Bees (Frame Sides)	3c{3,6} Cardboard	8	9.5	0.67	One-Way ANOVA + Tukey	4, 35	0.78	0.545	n/a
		Negative Control Cardboard	8	8.9	0.60					
		3c{3,6} Wood	8	8.1	0.34					
		Negative Control Wood	8	8.7	0.79					
		Thymovar®	8	9.4	0.77					
	Mite-Infested Brood Cells (%)	3c{3,6} Cardboard	7	0.4	0.30	Kruskal-Wallis + Dunn	4	22.67	< 0.001	a
		Negative Control Cardboard	8	10.9	2.57					b
		3c{3,6} Wood	5	1.8	0.58					a
		Negative Control Wood	7	12.6	4.92					b
		Thymovar®	8	1.0	0.38					a
42	Dispersing Mite Infestation (%)	3c{3,6} Cardboard	8	0.2	0.07	Kruskal-Wallis + Dunn	4	23.85	< 0.001	a
		Negative Control Cardboard	8	3.9	1.19					bc
		3c{3,6} Wood	8	0.1	0.05					a
		Negative Control Wood	8	7.3	2.43					b
		Thymovar®	8	0.3	0.14					ac

Table 2-7 (Cont.)

Day	Metric	Treatment	*n*	Mean	Standard Error	Test	DF	Test Statistic	*p*-Value	Post-Hoc Significance
84	Dispersing Mite Infestation (%)	3c{3,6} Cardboard	8	0.2	0.12	Kruskal-Wallis + Dunn	4	13.71	0.008	a
		Negative Control Cardboard	8	0.5	0.16					ab
		3c{3,6} Wood	8	0.2	0.08					ab
		Negative Control Wood	8	2.0	0.70					b
		Thymovar®	8	0.1	0.06					a

Table 2-8: Pairwise comparisons of fall 2022 GLS Treatment effects for different groups, performed post-hoc via Tukey's HSD.

Comparison	Estimate	Std. Error	DF	*t*-Statistic	*p*-Value
3c{3,6} Card – 3c{3,6} Wood	20.8	9.6	315	2.16	0.197
3c{3,6} Card – Negative Card	62.4	9.6	315	6.49	< 0.001
3c{3,6} Card – Negative Wood	58.8	9.6	315	6.12	< 0.001
3c{3,6} Card – Thymovar®	43.2	9.6	315	4.49	< 0.001
3c{3,6} Wood – Negative Card	41.6	9.6	315	4.32	< 0.001
3c{3,6} Wood – Negative Wood	38.0	9.6	315	3.95	< 0.001
3c{3,6} Wood – Thymovar®	22.4	9.6	315	2.33	0.140
Negative Card – Negative Wood	3.6	9.6	315	0.37	0.996
Negative Card – Thymovar®	19.2	9.6	315	2.00	0.270
Negative Wood – Thymovar®	15.7	9.6	315	1.63	0.481

Table 2-9: Spring 2023 colony evaluation metrics, and statistical comparisons. Post-hoc significance was corrected using the Bonferroni method.

Day	Metric	Treatment	*n*	Mean	Standard Error	Test	DF	Test Statistic	*p*-Value
0	Pollen (Frame Sides)	3c{3,6}	10	2.3	0.37	Two-sided two-sample Mann-Whitney U (with continuity correction)	18	46.5	0.8203
		Negative Control	10	2.4	0.36				
	Honey (Frame Sides)	3c{3,6}	10	8.8	1.02	Two-sided two-sample Student's t-test	18	0.19	0.851
		Negative Control	10	8.5	0.74				
	Capped Brood (Frame Sides)	3c{3,6}	10	2.0	0.18	Two-sided two-sample Student's t-test	18	-0.09	0.931
		Negative Control	10	2.0	0.35				
	Open Brood (Frame Sides)	3c{3,6}	10	1.5	0.36	Two-sided two-sample Mann-Whitney U (with continuity correction)	18	63.5	0.324
		Negative Control	10	1.0	0.21				
	Adult Bees (Frame Sides)	3c{3,6}	10	5.6	0.96	Two-sided two-sample Student's t-test	18	0.35	0.730
		Negative Control	10	5.2	0.85				
	Mite-Infested Brood Cells (%)	3c{3,6}	10	4.9	1.12	Two-sided two-sample Student's t-test	18	0.13	0.895
		Negative Control	10	4.7	0.99				
	Dispersing Mite Infestation (%)	3c{3,6}	10	2.5	0.54	Two-sided two-sample Mann-Whitney U (with continuity correction)	n/a	49.5	1.000
		Negative Control	10	2.5	0.53				
42	Pollen (Frame Sides)	3c{3,6}	10	4.1	0.74	Two-sided two-sample Student's t-test	18	1.30	0.211
		Negative Control	10	2.8	0.65				
	Honey (Frame Sides)	3c{3,6}	10	5.8	0.64	Two-sided two-sample Student's t-test	18	1.44	0.166
		Negative Control	10	4.5	0.63				
	Capped Brood (Frame Sides)	3c{3,6}	10	2.6	0.60	Two-sided two-sample Student's t-test	18	-2.06	0.054
		Negative Control	10	4.3	0.56				
	Open Brood (Frame Sides)	3c{3,6}	10	1.0	0.24	Two-sided two-sample Student's t-test	18	-1.30	0.213
		Negative Control	10	1.6	0.35				
	Adult Bees (Frame Sides)	3c{3,6}	10	6.5	0.98	Two-sided two-sample Student's t-test	18	-3.03	0.009
		Negative Control	10	12.2	1.60				
	Mite-Infested Brood Cells (%)	3c{3,6}	9	0.0	0.00	Two-sided two-sample Mann-Whitney U (with continuity correction)	n/a	18	0.009
		Negative Control	10	2.2	0.92				
	Dispersing Mite Infestation (%)	3c{3,6}	9	0.0	0.00	Two-sided two-sample Mann-Whitney U (with continuity correction)	n/a	9	0.001
		Negative Control	10	1.6	0.50				

Table 2-9 (Cont.)

Day	Metric	Treatment	*n*	Mean	Standard Error	Test	DF	Test Statistic	*p*-Value
92	Dispersing Mite Infestation (%)	3c{3,6}	8	0.2	0.13	Two-sided two-sample Mann-Whitney U (with continuity correction)	n/a	8.5	0.008
		Negative Control	9	2.1	0.52				

Figure 2-1: Photo of vapour-based 3c{3,6} applicator used in the fall 2021 experiment within a colony undergoing varroacide treatment. The single 15.3 cm × 5.1 cm × 0.5 cm wooden strip was impregnated with 4 g 3c{3,6}, and placed centrally across the top bars of the broodnest.

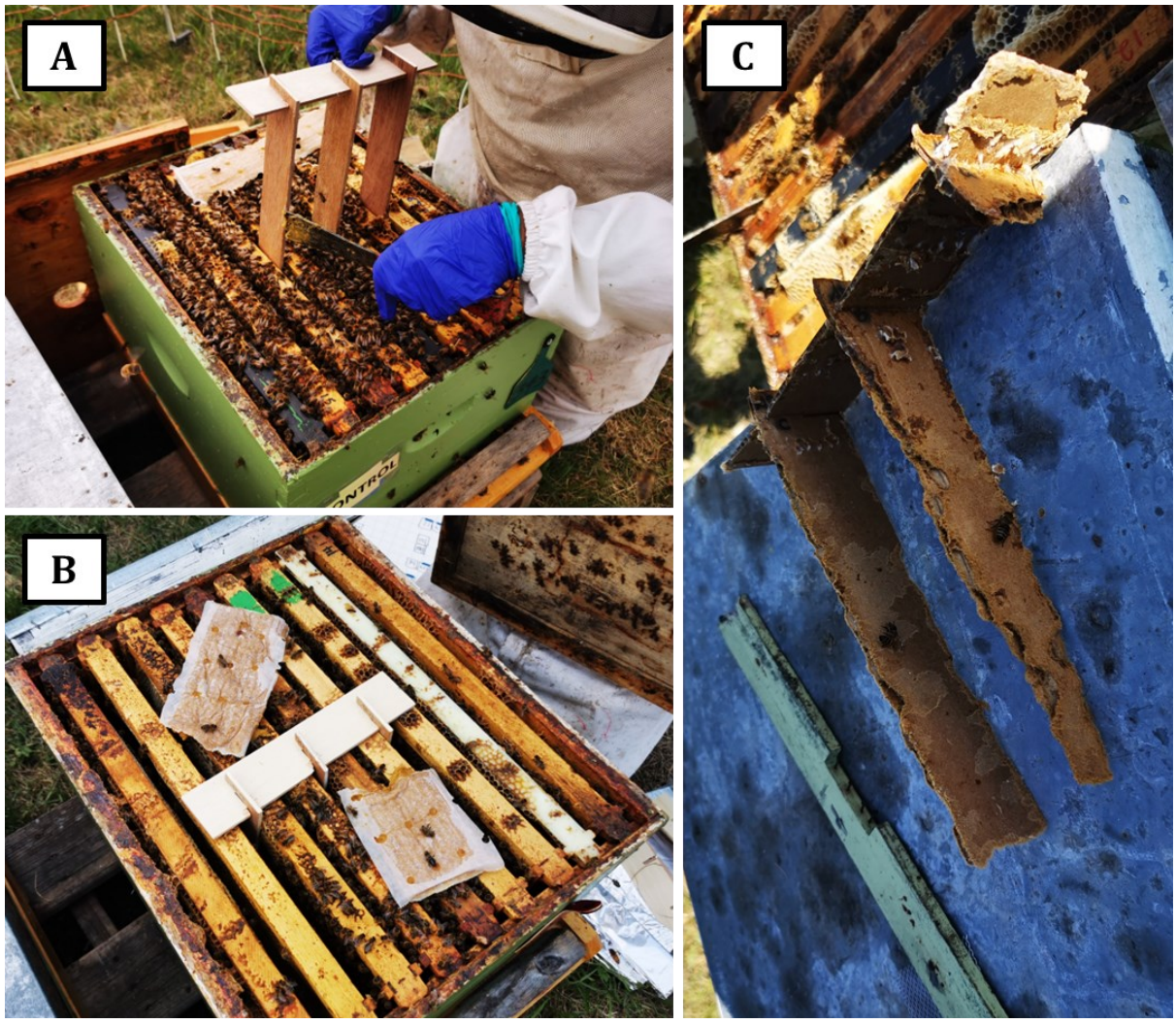

Figure 2-2: Photos of applicators used in the fall 2022 and spring 2023 experiments. Three strips (24.0cm × 5.0cm × 0.5cm wood, or 24.0cm × 5.0cm × 0.3cm cardboard) were impregnated with a total of 8 g (2022) or 10 g (2023) 3c{3,6} between them, and suspended between frames attached to a fourth untreated strip. [A] A wooden 3c{3,6} applicator being inserted into an experimental colony. [B] Placement and positioning of a fully-inserted wooden 3c{3,6} applicator. [C] A heavily-degraded cardboard 3c{3,6} applicator, having been removed for examination following 21 days within the colony.

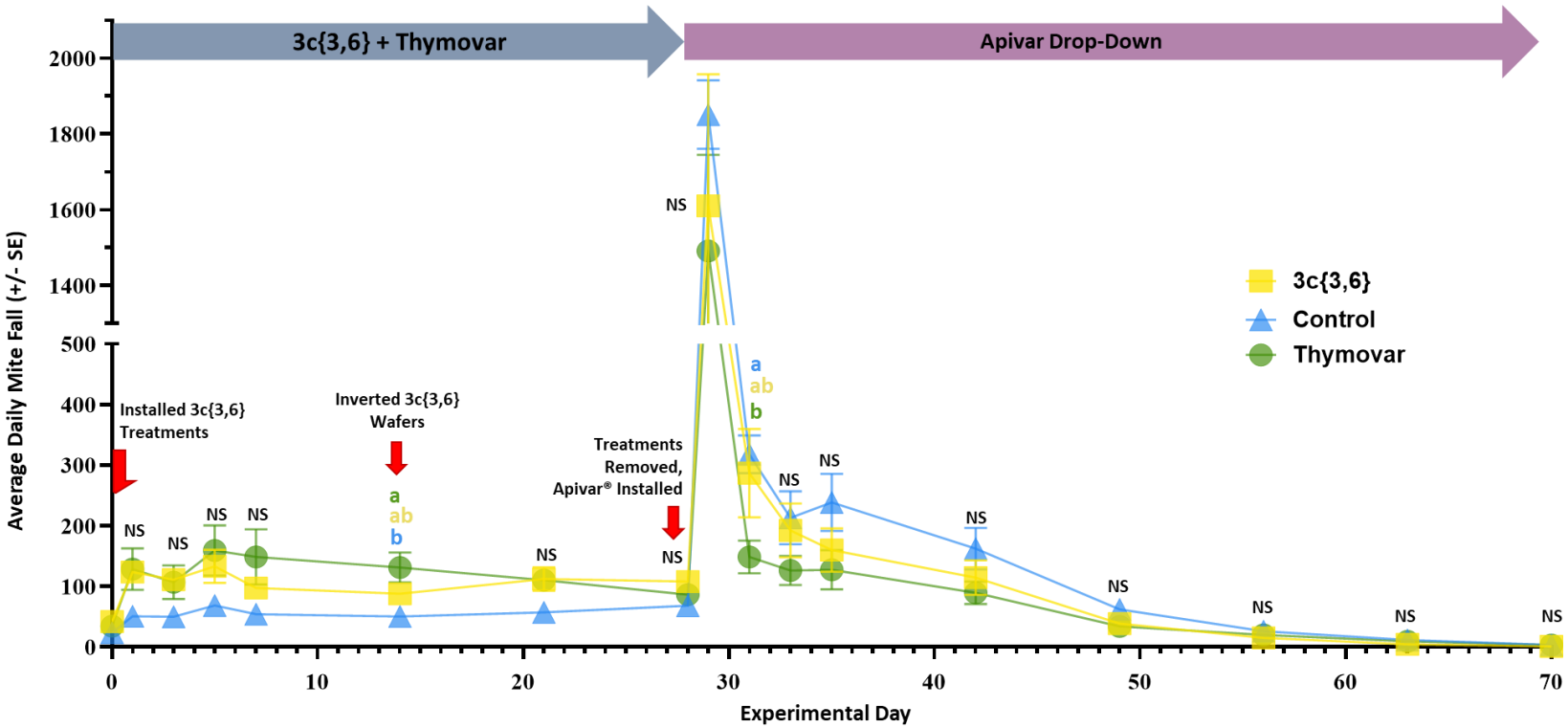

Figure 2-3: Daily varroa mortality per sticky board interval, for each treatment group within the fall 2021 experimental field trials. Mortality data were tracked from Day 0 (3 September 2021) to Day 70 (12 November 2021). Points represent average ± standard error of 10 replicate colonies per treatment group. Three-way comparisons of daily mite fall across treatment groups were calculated using an ANOVA, followed by a Tukey's HSD for pairwise significance comparisons (NS = not significant, letters represent pairwise significance $p < 0.05$).

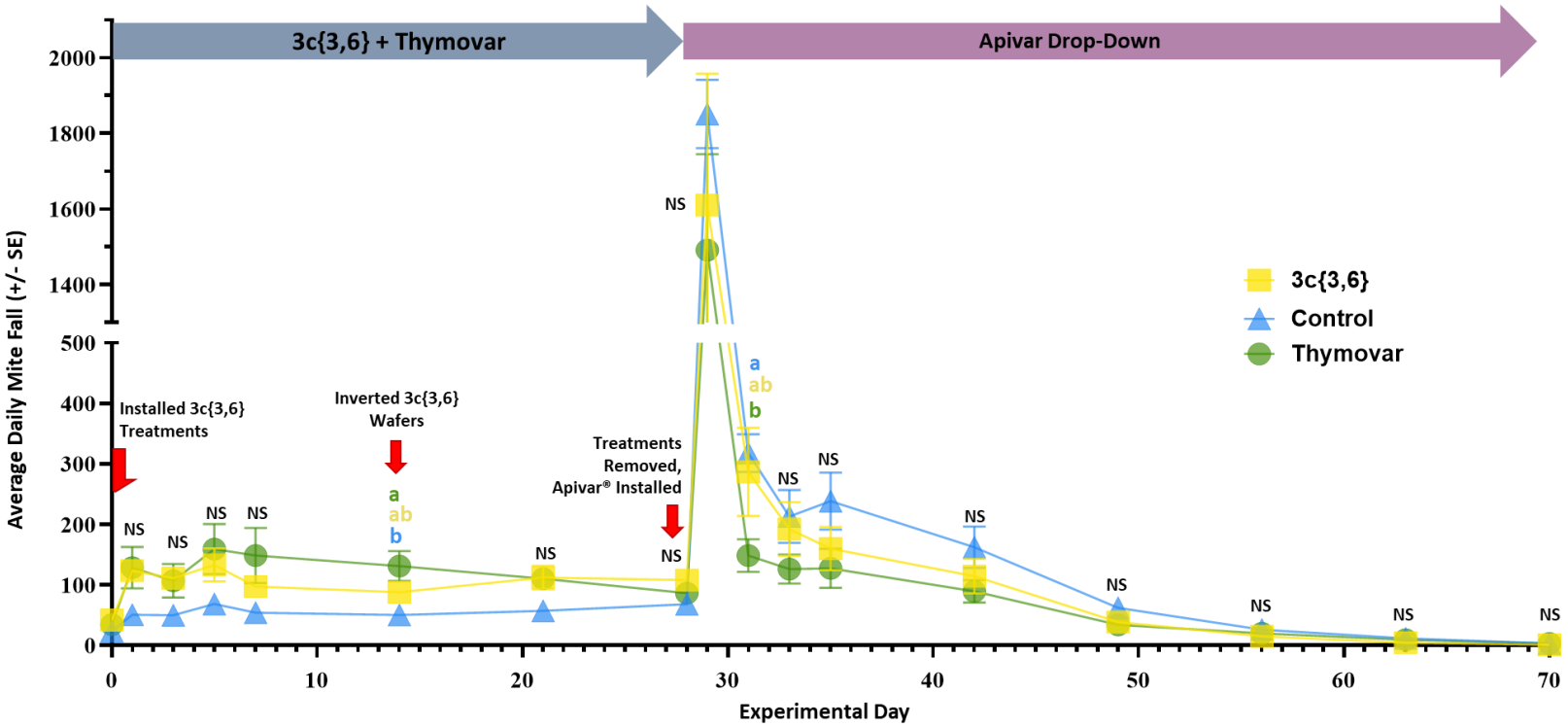

Figure 2-4: Daily varroa mortality per sticky board interval, for each treatment group within the fall 2022 experimental field trials. Mortality data were tracked from Day 0 (13 September 2022) to Day 84 (6 December 2022). Points represent average ± standard error of 8 replicate colonies per treatment group. Five- way comparisons of daily mite fall across treatment groups were calculated using an ANOVA, followed by a Tukey's HSD for pairwise significance comparisons (NS = not significant, letters represent pairwise significance $p < 0.05$).

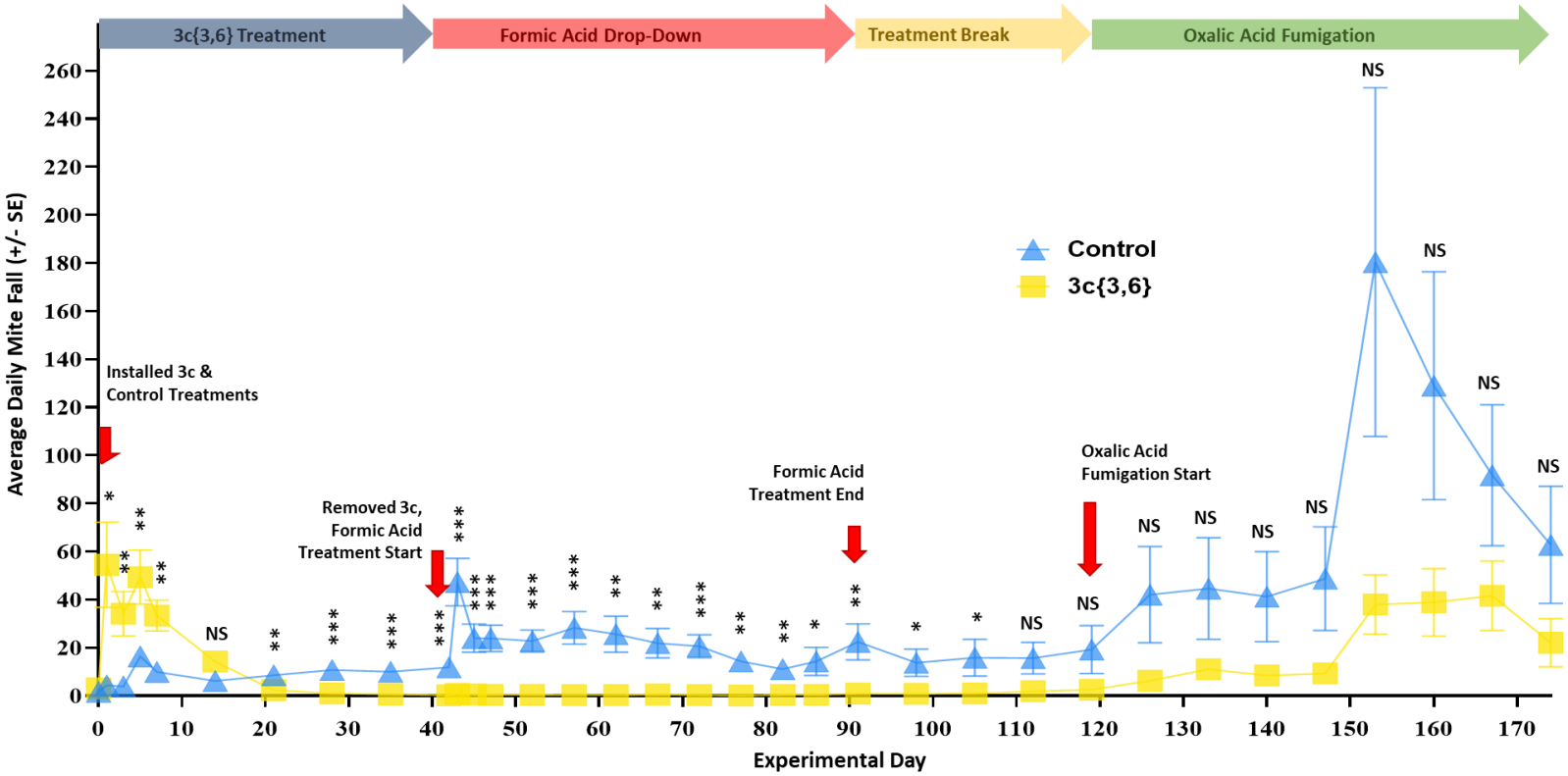

Figure 2-5: Daily varroa mortality per sticky board interval, for each treatment group within the Spring 2023 experimental field trials. Mortality data were tracked from Day 0 (11 May 2023) to the experimental end on Day 85 (4 July 2023), and post-treatment mortality tracking continued until Day 174 (1 November 2023). Points represent average ± standard error of 10 replicate colonies per treatment group. Pairwise comparisons between the 3c{3,6} and control treatment cohorts were performed (two-sampled two-tailed *t*-tests; NS = not significant, * = $p < 0.05$, ** = $p < 0.01$, *** = $p < 0.001$).

Chapter 3: Transcriptomic Assessment of the Sublethal Effects of 1-Allyloxy-4-Propoxybenzene on Honey Bees and *Varroa destructor*

3.1 Introduction

The parasitic *Varroa destructor* mite ("varroa") is a major threat to global beekeeping, as its feeding activity on honey bee workers results in virus infections, weakness, diminished foraging capability, and reduced productivity, ultimately leading to colony death in cases of severe mite infestations (Yang and Cox-Foster 2005, Le Conte et al. 2010, Peck 2021). Varroa infestations can be controlled through varroa-targeting chemical pesticides ("varroacides") applied to infested honey bee colonies (Rinkevich 2020). Development of varroacides is focussed on their ability to kill mites while having low toxicity towards bees (Riva et al. 2019). Varroacides may also exert sublethal effects against varroa, such as interfering with important metabolic and behavioural functions (Lindberg et al. 2000, Plettner et al. 2017). Though sublethal effects remain understudied in varroa, they are known to enhance pesticide efficacy against target pests in other systems by impeding pest population growth (Leviticus et al. 2020). Therefore, it is worth examining the possibility that such effects are recapitulated in varroa exposed to 3c{3,6} as well.

Many varroacides are also have sublethal effects in honey bees. For instance, Gashout et al. (2020) found an exposure dosage of LD_{05} (10% of LD_{50}) against honey bees to formic acid, coumaphos, amitraz, and *tau*-fluvalinate to significantly reduce long-term memory retention in worker bees, specifically regarding learned stimuli associated with food sources. The non-target toxicity of coumaphos is particularly pertinent due to its ability to accumulate in wax, resulting in heightened developmental mortality of brood and smaller adults – an effect particularly pronounced in reared queens (Collins et al. 2004, Kast et al. 2023). Another commonly used

varroacide, oxalic acid, has been shown to induce degeneration of the gastrointestinal epithelia in worker bees following ingestion, alongside reductions in nursing behaviour and shortened overall lifespan (Schneider et al. 2012, Rademacher et al. 2017). Prolonged exposure to volatile oil-based varroacides including thymol or carvacrol can cause upregulation of glutathione S-transferase (GST) genes responsible for detoxification, and the acetylcholinesterase gene (AChE) responsible for neurotransmission (Loucif-Ayad et al. 2008, Glavan et al. 2020). Additionally, varroacides may synergize with one another through interactions with common metabolic pathways (Johnson et al. 2013). For instance, oxalic acid may agonistically increase the toxicity of other varroacides through facilitating cuticular penetrance and absorption, and/or through the production of reactive oxygen species. Over time, chronic exposure to varroacides in the hive environment can lead to accumulation within developing bees, which may result in increased mortality and reduced productivity (Johnson et al. 2009, Berry et al. 2013).

Despite the non-target toxicity of varroacides, they remain a crucial component of sustained beekeeping as the detriments of untreated varroa infestations outweigh the costs imposed by well-managed treatment regimens (Hernandez et al. 2022). Nevertheless, decreasing efficacies of existing treatments resulting from emerging varroacide-resistant varroa populations necessitate the development of new treatment options (Bąk et al. 2012, Rinkevich 2020). One compound that has shown promise as a novel varroacide is the dialkoxybenzene 1-allyloxy-4-propoxybenzene (also known as "3c{3,6}"), which is capable of inducing paralysis and death in varroa mites at a low topical EC_{50} of 0.06 ng/mite after 6 hours (Singh et al. 2020, Dawdani et al. 2023). Laboratory assays indicate volatilised 3c{3,6} to have a similar structure-activity relationship to the known varroacide thymol (Dawdani et al. 2023). Initial field experiments have additionally demonstrated the potential of 3c{3,6} as an *in situ* varroacide, as colonies treated with 5 g of 3c{3,6} per colony

experienced significantly higher mite mortality and lower winter mortality compared to untreated control colonies (Dawdani et al. 2023, Cook et al. 2024). Fluorescent probe analysis indicates a neurotoxic activity of 3c{3,6}, with the central nervous system and tarsal olfactory chemoreceptors being key binding sites of 3c{3,6} molecules (Dawdani 2020). This also disrupts the feeding activity of varroa mites, preventing them from accurately targeting their preferred feeding location of the ventral abdominal region of adult bees. The exact mechanism by which 3c{3,6} induces paralysis in varroa is currently not fully understood, and Dawdani et al. (2023) did not find 3c{3,6} to inhibit acetylcholinesterase activity in the central nervous system. Additionally, it remains uncertain whether 3c{3,6} disrupts other organ systems within varroa, though 3c{3,6} has not been observed to significantly impact fecundity of varroa foundresses (Dawdani et al. 2023).

The compound 3c{3,6} should additionally be evaluated for its sublethal effects on honey bees, as doing so will provide two key benefits. Firstly, understanding the toxicological risks of 3c{3,6} on honey bee health will facilitate the development of treatment regimens that maximize varroa mortality and minimize damage to honey bees (Gregorc et al. 2018). Secondly, understanding these toxicological effects can enable beekeepers to design integrative pest management (IPM) regimens by accounting for potential non-target toxicity of 3c{3,6}, such as avoiding toxic synergy with other compounds (Lindberg et al. 2000). Thus far, honey bee cytochrome P450 enzymes have been demonstrated to dealkylate 3c{3,6} into hydroquinone and 1-hydroxy-4-allyloxybenzene (Gkaleni 2021). However, it remains unknown whether cytochrome P450 expression is upregulated in honey bees as a consequence of 3c{3,6} exposure. Additionally, toxicity against other honey bee metabolic pathways has yet to be assessed.

Here, I used transcriptome analysis to comprehensively evaluate the effects of sublethal 3c{3,6} exposure in honey bees and mites. Specifically, I used high-throughput mRNA sequencing

to compare the gene expression profiles of varroa mites and heads and abdomens of honey bees acutely exposed to 3c{3,6} against unexposed controls. Honey bee heads were selected to evaluate the effect of 3c{3,6} exposure on the honey bee nervous system, as 3c{3,6} induces feeding deterrence in insect pests (Akhtar et al. 2007, Akhtar et al. 2010, Cameron et al. 2014), and interrupts host-finding mechanisms and feeding behaviour in varroa (Singh et al. 2020, Dawdani et al. 2023). Bee abdomens were selected because the majority of detoxification processes occur in the honey bee digestive system and fat body (Berenbaum and Johnson 2015, Gong and Diao 2017, Maiwald et al. 2023).

We tested 3c{3,6} in vapour form, consistent with the deployment of the primarily vapour-based 3c{3,6} applicators in previous field experiments (see Chapter 2). I hypothesize that exposure to sublethal levels of 3c{3,6} vapours results in greater toxicity against metabolic processes in varroa mites than in honey bees. Thus, I predict a greater quantity of differentially expressed genetic pathways in 3c{3,6}-exposed varroa mites than in bees, compared to an unexposed negative control, and that these gene pathways will be associated with a wider degree of metabolic processes in mites than in bees. Conversely, if honey bees possess mechanisms which enable the detoxification of 3c{3,6} better than in varroa, I would predict such mechanisms to be significantly upregulated versus other genes, and to a much greater extent in the bees versus the mites.

3.2 Materials and Methods

3.2.1 Preparation of Nurse-Age Honey Bees and Varroa Mites

Colony infestation level was determined by the alcohol wash method, wherein samples of

~300 adult worker bees from the broodnest of each hive were collected for assessment (De Jong et al. 1982, Gregorc and Sampson 2019). Bees were then loaded into mesh-bottom containers, which were then nested into solid-bottom containers with 70% ethanol. Nested containers were sealed and agitated for two 5-minutes cycles and a final 10-minute cycle on an orbital shaker (MBIMS-NOR-30, Montréal Biotech Inc., Montréal, QC), to dislodge dispersing-phase varroa mites which sank to the bottom of the solid-bottom container. Afterward, mites were counted, and fifty worker bees were counted out and weighed. Weight regression of the fifty workers was used to estimate the total sampled workers. These values were used to calculate the percent infestation level.

Five experimental colonies with undetectable mite loads were established in April 2022 using 1 kg New Zealand package bees (Kintail Honey Ltd.). The original New Zealand queens included in the packages were subsequently replaced with newly mated New World Carniolan queens (Olivarez Honey Bees, Orland, CA). All colonies were maintained in single full-sized Langstroth deep hive boxes with nine frames per box. Experimental colonies were housed in the "Lagoon" apiary site at Agriculture and Agri-Food Canada's Beaverlodge Research Farm, in Beaverlodge, Alberta (55.20355°N, 119.39011°W), between April and November 2022. This location was selected for its isolation from other bee yards, minimizing risks of varroa mite cross-infestation. During the main nectar flow, from July 2022 until mid-August 2022, each colony was provided with a queen excluders and a honey super. On 18 August 2022, colony 611 was discovered to be queenless and subsequently requeened with another mated New World Carniolan queen. Thus, trials from colony 611 are separated into two separate replicates, based on queen source – worker bees emerged prior to 21 August 2022 will hereafter be referred to as originating from colony 611a, while worker bees emerging after 21 August 2022 will be referred to as

originating from colony 611b to account for possible worker turnover.

Two varroa donor colonies were selected from untreated colonies, established in Beaverlodge 2021 and overwintered. Both donor colonies were maintained as single-box Langstroth deeps containing nine frames and founded with New World Carniolan queens in 2021 (Olivarez Honey Bees, Orland, CA). Due to their low worker population and food stores, mite donor colonies did not receive supers during the honey flow. Varroa populations in both colonies were established in summer 2021, through inoculations of local Beaverlodge varroa mites. Only one donor colony survived to the start of the experiment. This donor colony was located at the "Home Yard" apiary site at Beaverlodge Research Farm (55.20278°N, 119.39644°W) from April 2022 to November 2022.

Nurse-age bees were selected as the experimental system, as nurse bees in the colony broodnest are most likely to be continually exposed to 3c{3,6} applications. As nursing age typically spans from between 5 to 16 days post-emergence (Haydak 1963), frames of purple-eyed sealed brood were collected from experimental colonies and housed at 33° C and 40% relative humidity (RH) within a programmable incubator (model I36NLC9, Percival Scientific Inc., Perry, IA) to allow for controlled emergence at a temperature consistent with the conditions within a colony broodnest (Becher et al. 2010). Cohorts of 80-120 newly-emerged teneral worker bees were collected from incubating frames and marked on the top of their thorax with a distinct paint colour, before being returned to their home colonies and allowed to age for a minimum of six days. This number ensured that at least 40 bees from each marked cohort could be found and retrieved from within their hives of origin. All bees were between 6-16 days old when collected.

Live dispersing varroa mites, found on adult bees, were collected from the mite donor colony using the sugar shake technique (Aliano and Ellis 2005, Gregorc et al. 2017). The

dispersing life stage was selected because mites at this stage face the greatest exposure to 3c{3,6} *in situ*. Collected mites were wiped clean of powdered sugar using a damp fine-tip paintbrush and provisioned with pin-killed drone pupae as nourishment during the interim between collection and experimentation, which lasted between 1-2 hours.

In total, twelve pairwise assays of the experiment were conducted, two replicates for each of the six source colonies of donor bees. All mites were collected from the same donor colony.

3.2.2 Preparation of 3c{3,6}-Hexane Solution

A total of 232.95 mg (=1.2 mmol) crystalline 3c{3,6,} synthesized and provided by the Plettner Lab at Simon Fraser University, was dissolved in 1.20 mL of HPLC-grade hexane, to create a 100× stock solution with a concentration of 1 M. Between experimental trials, the stock solution was stored in an airtight container, refrigerated at 4° C. A 1× experimental solution was prepared by diluting 10 µL of 100× stock solution in 990 µL HPLC-grade hexane.

3.2.3 Sublethal 3c{3,6} Exposure Jar Bioassay

The bioassay consisted of a two-by-two design, with live nurse-aged bees divided along two treatment groups (3c{3,6} and negative control hexane), and two varroa groups (varroa-infested and varroa free). Bees in the varroa-infested group were infested with a single varroa mite per bee, administered using a fine-tip hair paintbrush. Each treatment-by-varroa group contained ten replicate bees and ten varroa mites (when applicable). Glass mason jars with 120 mL internal volume were used as the experimental containers, with glass being preferred over plastic for its low reactivity towards both 3c{3,6} and the hexane solvent (Fig. 3-1).

Using soft-tip forceps (BioQuip Products, Inc.), bees were placed into jars labelled with

the appropriate treatment and varroa group and covered with the upside-down lid cover (but not sealed with the lid ring). A 2 cm × 2 cm parafilm square was attached to the inner face of each lid cover, and the treatment solution was dispensed into the center of the square (1× 3c{3,6} stock solution, or HPLC-grade hexane for the negative controls) (Fig. 3-1). Corresponding to the 3c{3,6} 3-hour EC_{50} of 1.68 nmol/mL (326.2 ng/mL) against isolated varroa mites (Dawdani et al. 2023), 20.2 µL of treatment solution was applied. Hexane solvent was allowed to evaporate off the lids for one minute under a fume hood, before the lid cover was placed right-side up and loosely sealed with the lid ring (allowing for air flow). Consistent with previous experiments (Dawdani et al. 2023), jars were placed into incubators for 3 hours, at 33° C and 40% RH.

Afterwards, bees were gently separated from mites with soft forceps as applicable. Bees and varroa were immediately frozen on dry ice and stored at -80° C until further processing. Though all bees were collected and frozen, only bees from the mite-free cohort were used in my study, as I primarily aimed to isolate the effects of 3c{3,6} exposure on honey bees. In addition, mite-free bees better represented the majority of the population of workers in colonies during fall and spring periods when traditional miticides would be applied (Currie and Gatien 2006, Currie 2008). No mortality was observed for either mites or bees included in my experimental trials.

3.2.4 RNA Extraction

Samples of five pooled honey bee heads, corresponding abdomens, and varroa mites from twelve pairs of 3c{3,6)} treatment and control groups were suspended in TRIzol (400 µL per varroa pool, 1 mL per bee head or abdomen pool), and homogenized using an MP Biomedicals™ FastPrep-24™ 5G Bead Beating Grinder and Lysis System (MP Biomedicals, Santa Ana, CA) with ten 2.3 mm diameter zirconia lysis beads per sample pool (BioSpec Products, Bartlesville,

OK). All samples were ground at 4.0 m/s frequencies in 30-second intervals, with 10-second breaks between intervals. Mites were ground over the course of two intervals, while bee samples were ground over four intervals. Total RNA was extracted from each homogenized pool using the Zymo® Research Direct-zol RNA Miniprep kits (Zymo Research, Irvine, CA), following the manufacturer protocol and reprecipitated into DNase/Rnase-free water (20 µL per varroa pool, 50 µL per bee pool). Sample quality was evaluated with a NanoDrop™ One© spectrophotometer (Thermo Fisher Scientific Inc., Waltham, MA) and concentrations were verified to be within 1-10 ng/µL (with higher concentrations being better), before being stored at -80° C. A total of 72 samples were generated: 6 colony/queen sources × 2 replicates × 2 treatments (3c{3,6} and control) × 3 sample types (honey bee heads, honey bee abdomens, varroa mites).

3.2.5 cDNA Synthesis and Amplification

An incubation master mix was first prepared as per Table 3-1, with gentle inversion to mix the reagents. A primer mix was created by mixing equal volumes of ILL_BC (Integrated DNA Technologies, Inc., Coralville, IA) and TruSeq UN (Illumina, Inc., San Diego, CA) oligo solutions (targeting the poly-A tail of mRNA), each diluted to 2 µM in 10 mM TRIS-HCl pH 8.0. A 96-well PCR plate was labelled, and 72 wells (corresponding to the number of samples) were filled with 10 µL extracted RNA (between 10-100 ng total RNA per well), 6 µL of primer mix, and 8 µL master mix, before being sealed with aluminum foil tape. The sealed plate was placed in a preheated thermocycler and incubated at 70° C for 10 minutes, before being chilled on ice for 2 minutes. Unused primer mix was stored at -20° C.

To synthesize first-strand cDNA, samples were centrifuged at 700 ×g for 1 minute at room temperature in a Sorvall™ ST 8R Benchtop Centrifuge (Thermo Fisher Scientific Inc., Waltham,

MA), before the foil seal was removed. 1 µL Switch-Oligo-mix (New England BioLabs Ltd., Ipswich, MA) and 1 µL SuperScript™ III reverse transcriptase (Invitrogen by Thermo Fisher Scientific Inc., Waltham, MA) was added to each sample and mixed with a pipette, before the plate was resealed. Plates were then placed into a Mastercycler® Nexus Gradient thermal cycler (Eppendorf SE, Hamburg, Germany) preheated to 42° C, incubated for 1 hour, and then held at 65° C for 15 minutes. Subsequently, 30 µL nuclease-free water was added to each well, followed by 50 µL room-temperature SparQ PureMag® magnetic beads (Quantabio BioSciences, Inc., Beverly, MA), and incubated at room temperature for 15 minutes to enable cDNA binding. The plate was then placed atop a magnet plate for 5 minutes to collect the cDNA-bound beads at the bottom of each well, and 90 µL of supernatant was removed. Each sample well was then washed twice with 80% ethanol, with a 30-second room-temperature incubation between washes. The supernatant was removed with a pipette after each wash, with residual ethanol allowed to evaporate off over a 3-minute room-temperature incubation following the final wash. Dried samples were resuspended with 12 µL nuclease-free water, incubated for 2 minutes, and then placed on a magnet plate for 5 minutes to collect beads. 10 µL of purified cDNA solution was transferred to a new 96-well plate on ice.

To amplify the cDNA, a second master mix (Table 3-2) was prepared and added to the purified cDNA and mixed with a pipette. Samples were amplified in a polymerase chain reaction programme consisting of 19x 5-minute cycles (94° C for 1 minute, 63° C for 2 minutes, 72° C for 2 minutes) and subsequently stored at 4° C.

Amplified cDNA was purified via a second round of magnetic bead cleanup, as described previously. The clean cDNA was resuspended in 23 µL nuclease-free water. 22 µL of the cDNA-containing supernatant was transferred into a new 96-well plate, and dsDNA was quantified using

an HS Qubit kit (Thermo Fisher Scientific Inc., Waltham, MA).

3.2.6 cDNA Barcoding and Size Selection

A barcoding master mix was prepared prior to the start of the barcoding process (Table 3-3). In a new 96-well plate, purified cDNA samples produced from the prior PCR amplifications were diluted to 5 ng/µL and 20 µL was mixed with 14 µL barcoding master mix, and 6 µL primer mix left over from the cDNA synthesis step described previously. Another polymerase chain reaction was performed to attach the barcodes to the cDNA, consisting of 4x 5-minute cycles (95° C for 40 seconds, 63° C for 2 minutes, 72° C for 2 minutes). Eight random samples of 5 µL were analysed by 2% gel electrophoresis to assess DNA fragment size distribution and confirm successful and uniform amplification.

Aliquots of 5 µL from each sample were pooled into a 1.5 mL microcentrifuge tube, and an equal volume of magnetic beads (360 µL for 72 samples) was added before incubating the mixture for 15 minutes at room temperature. Beads were collected at the bottom of the tube using a magnetic plate, and the supernatant was removed. Beads were then washed twice with 300 µL of 80% ethanol, before being air-dried for 5 minutes. cDNA was then resuspended in 70 µL nuclease-free water, the beads were removed, and 60 µL of the final cDNA solution was collected. Size selection and quality control of the final cDNA libraries was performed by the Molecular Biology Service Unit (MBSU) at the University of Alberta, Department of Biological Sciences (https://www.ualberta.ca/biological-sciences/services/mbsu/index.html). RNA sequences can be found on the National Institute of Health (NIH) Sequence Read Archive (SRA) database (Leinonen et al. 2010) (reference number to be assigned at time of thesis completion).

3.2.7 Tag-Seq Transcriptome Analysis

The pooled sample was submitted to the North Carolina State University's Genomics Sciences Laboratory (https://research.ncsu.edu/gsl/) for sequencing on a NovaSeq™ S4 (Illumina, Inc., San Diego, CA) sequencer (⅔ lane of 150 bp paired-end sequencing). Due to the large size of the raw read files, a random subset of six files from each of the bee head, bee abdomen, and varroa datasets (representing 25% of the total sequencing data) were input into FastQC v0.12.1 (Andrews 2010) to verify overall quality of the reads, and determine the length of the adapters and tags to be trimmed.

Computational processing of sequencing data was performed on the Digital Research Alliance of Canada's Narval cluster. Count tables were generated using only the forward read sequences, due to the low quality of the reverse read Tag-Seq sequences. Reads were first cleaned using custom Tag-Seq scripts, as per previous studies involving the Tag-Seq method (https://github.com/z0on/tag-based_RNAseq; (Meyer et al. 2011). PCR duplicates were removed with the RemovePCRDups.pl script with default parameters, followed by the removal of 5' cDNA tags introduced during library preparation using the TagTrimmer.pl script. HiSat2 v2.2.1 was then used to construct a transcriptome index from the Amel_HAv3.1 (Wallberg et al. 2019) and Vdes_3.0 (Techer et al. 2019) assemblies for honey bee and varroa mite data respectively, against which the reads were mapped (Kim et al. 2019). Unmapped reads were identified using NCBI BLAST to determine their origin (Altschul et al. 1990). SAMtools v1.20 was then used to order the reads positionally along the respective reference genomes based on the HiSat2 indices (Danecek et al. 2021), and feature count tables were generated using the HTSeq-count command, from the HTSeq v2.0.7 module (Anders et al. 2015). Genes with fewer than 10 counts across all

samples were considered low-expression and removed from the datasets.

Differential expression analysis of individual genes based on log2 fold change was performed using the DESeq2 package (Love et al. 2014) in the R statistical environment v4.4.0. The unadjusted *P*-values (obtained via the Wald test) were adjusted for multiple testing using the Benjamini-Hochberg method, with a default false discovery rate of 10% (FDR = 0.10) (van Iterson et al. 2010, Galbraith et al. 2015, Palmer et al. 2017). All differential gene expression analyses were performed in pairwise comparisons, with treatment pairs stratified by trial. All genes with an unadjusted Wald test *P*-value below the $\alpha = 0.05$ significance threshold were queried for function, regardless of whether the adjusted *P*-value fell below $\alpha = 0.05$. Queries of honey bee head and abdomen genes were performed in the HymenopteraMine Genome Database v1.6 (Walsh et al. 2022), while varroa gene queries were performed using a list of annotated genes from the Vdes_3.0 varroa genome assembly (Techer et al. 2019) and NCBI BLAST (Altschul et al. 1990).

Principal component analyses (PCA) were performed on the varroa, bee head, and bee abdomen datasets to compare variation between experimental groups (3c{3,6} versus negative control), using DESeq2 (Love et al. 2014). Additional PCA analyses were performed to test whether varroa mites cluster by experimental trial, and whether either honey bee dataset exhibited clustering by colony source, date of emergence of worker bees, or age of worker post-emergence at time of experiment. Gene expression clustering heatmaps were also generated for each dataset using the ComplexHeatmap package v3.19 in R v4.4.0 (Gu et al. 2016), and compared all samples by their per-gene differential expression using normalized z-scores of gene up- or downregulation. Once again, varroa were evaluated on their clustering by treatment and trial, while honey bee heads and abdomens were evaluated based on treatment, colony source, emergence date, and age.

Gene ontology analyses to compare 3c{3,6} and negative control groups in all three

datasets were performed inclusive of all data regardless of significance threshold. This was conducted using the GO_MWU package in R (https://github.com/z0on/GO_MWU), and were based upon orthologous gene ontology pathways characterized in *Drosophila melanogaster* (Ashburner et al. 2000, The Gene Ontology Consortium et al. 2023). The FDR threshold was set to a default 10% to determine if GO terms were significantly up- or down-regulated.

3.3 Results

3.3.1 Data Processing; mapping sequence reads to transcriptome

To determine the coverage of sequence reads from bee head and abdomen and varroa mites, reads were mapped to a dataset of known protein-encoding genes of each respective organism. An average of 15,860,748.7 ± 1,046,464.81 reads (mean ± SE) were sequenced from the honey bee head pools (range: 8,072,138 – 32,265,286 reads). Of these, an average of 9,095,598.7 ± 612,797.66 reads mapped to the honey bee transcriptome index, representing an average mapping rate of 57.31 ± 0.72% (range: 50.43 – 63.32%). In the honey bee abdomen pools, an average of 15,959,143.3 ± 536,449.47 reads were sequenced (range: 12,588,277 – 22,634,320 reads), with a mean 9,018,253.7 ± 374,098.09 reads mapping to the transcriptome index for an average mapping rate of 56.35 ± 0.91% (range: 47.55 – 65.65%). Varroa mites averaged 12,670,002.4 ± 399,702.10 sequenced reads per pool (range: 7,865,658 – 16,817,555 reads), with an average of 4,683,577.7 ± 326,567.88 reads mapping to the transcriptome index for a mean mapping rate of 34.83 ± 1.50% (range: 26.27 – 56.49%). BLAST analysis revealed the unmapped sequences to be mostly viral RNA, with DWV-B representing the >90% of sequences that did not map to the target genomes.

Aligned reads from honey bee heads and abdomens were mapped to a set of 9,940

annotated genes in HTSeq, with each dataset retaining a respective 9,326 and 9,424 genes following the filtering of low-expression genes. Aligned reads from varroa mites were mapped to a set of 10,265 annotated genes, of which 8,542 genes were retained after filtering low-expression genes.

3.3.2 Sublethal Exposure to 3c{3,6} Effects on Gene Expression

No genes in either the honey bee head or abdomen datasets had adjusted *P*-values below the FDR = 0.10 threshold. However, the honey bee head dataset featured 370 genes with unadjusted *P*-values below the $\alpha = 0.05$ threshold (Appendix A), and the honey bee abdomen dataset included 251 genes with unadjusted *P*-values below $\alpha = 0.05$ (Appendix B). In the varroa mite dataset, there were no genes with an adjusted *P*-value below $\alpha = 0.05$. A total of 253 genes in the varroa dataset had unadjusted *P*-values below $\alpha = 0.05$ (Appendix C). Several of the putative candidate genes with unadjusted *P*-values below $\alpha = 0.05$ from both honey bees and varroa mites had interesting functional annotations and will be discussed below.

3.3.3 PCA and Gene Clustering Analyses

The first principal component (PC1) of the honey bee heads dataset accounted for 45% of observed variance, while PC2 accounted for 16%. While heads did not exhibit any distinct treatment-based clusters (Fig. 3-2A), clusters could be observed by colony source (Fig. 3-2B). Specifically, samples from colony 374 clustered away from all other samples along the PC1 axis, while the remaining head data points formed two additional clusters along the PC2 axis. However, these clusters were not distinct in terms of colony source, though they did separate along differences in emergence date (Fig. 3-2C). Meanwhile, PC1 of the honey bee abdomens dataset

accounted for 46% of observed variance, and PC2 accounted for 14%. No treatment-based clustering was observed (Fig. 3-3A), and the data points from colony 374 again clustered away from all other data points along PC1 (Fig. 3-3B). Data points from all other colonies formed a separate cluster, which showed organization by emergence date (Fig. 3-3C). Both heads (Fig. 3-2D) and abdomens (Fig. 3-3D) also displayed a gradient along PC2 with regards to the age of bees, though it is worth noting that both honey bee heads and abdomens displayed correlation between age and emergence date, with younger experimental bees having emerged earlier in the year.

In the varroa dataset, PC1 explained 55% of the multivariate variance across samples while PC2 accounted for an additional 9% of total variance. There were no distinct clusters observed between the negative control and 3c{3,6}-treated samples in the varroa mite data (Fig. 3-4A). When analysing by trial, pairs of negative control and 3c{3,6}-treated varroa also showed no distinct clustering with counterparts (Fig. 3-4B).

Likewise, no clustering by treatment was observed in any of the bee head, bee abdomen, and varroa mite heatmaps. However, samples from colony 374 continued to cluster together in the dendrograms of head (Fig. 3-5) and abdomen (Fig. 3-6) data heatmaps. Additionally, all bee samples showed strong clustering by emergence date in heads and abdomens. The varroa mite heatmap dendrogram (Fig. 3-7) did not show treatment-based or chronological clustering, nor was there pairwise clustering of 3c{3,6}-treated mites with negative control counterparts.

3.3.4 Gene Ontology Pathway Analysis

Even though the GO-MWU analysis does not rely on significant differences in gene expression, no gene ontology terms were identified as being significantly differentially regulated between the treatment and control groups in any of the three datasets based on the $\alpha = 0.05$

threshold following a Benjamini-Hochberg correction with FDR = 0.10.

3.4 Discussion

The lack of significant differentially expressed genes following the Benjamini-Hochberg correction ($P < 0.05$, FDR = 0.10) between 3c{3,6}-treated and unexposed varroa mites and honey bees does not support my initial hypothesis that 3c{3,6} vapour exposure impacts varroa mites more broadly than honey bees, nor the hypothesis that bees may possess an innate detoxification method against 3c{3,6} which may be upregulated upon exposure. This is further suggested by the lack of significant gene ontology terms ($P < 0.05$, FDR = 0.10) in all three datasets, as well as a lack of clustering by treatment in the PCAs and gene expression heatmaps of both organisms.

While neither varroa mite PCA nor heatmap plots exhibited any clustering patterns by treatment, honey bees exhibited noticeable clustering by both colony source and chronology. Samples from colony 374 consistently clustered away from all other colonies' samples in both head and abdomen PCA plots. This clustering pattern among honey bees was recapitulated in the gene expression heatmaps, which also featured a much more pronounced chronological effect. Colony-level clustering patterns are not unusual, as substantial evidence demonstrates the role played by both genealogy and hive environmental conditions on gene expression profiles of honey bee workers (Decanini et al. 2007, Rittschof and Robinson 2013, Anderson and Maes 2022). However, in my experiment, effects of either variable cannot be disentangled from one another. As the experiment occurred at the end of summer into the fall, chronological differences in gene expression profile may be explained by differences in date of emergence which spanned the shift from summer to overwintering bees (Doeke et al. 2015). This shift is known to be accompanied

by numerous physiological changes, which result in differential expression of metabolic gene pathways, including in the head and abdominal tissues (Steinmann et al. 2015, Wang et al. 2020, Bresnahan et al. 2022). Also of note is the fact that honey bee imagoes exhibit ontogenetic gene expression changes in various pathways, especially preceding the onset of foraging activity (Whitfield et al. 2006). As my experimental design resulted in a strong correlation between emergence date and age post-emergence and bees were not monitored for their behaviour prior to the assay, the two chronological factors cannot be disentangled. Samples designated 611a and 611b could represent the same genotype in addition to the same hive history, as the 611b workers were collected between 22-54 days post-requeening. As worker turnover following requeening typically occurs between 3-6 weeks following introduction of the new queen, it is uncertain as to the extent which genetic factors play into differences between 611a and 611b samples – especially given the large timespan of post-requeening collection. Nevertheless, even if a change in genetics occurred during my experimental time frame, such a change correlates with the progression from summer to fall season as well, further entangling the relationships between the different variables.

One possible explanation for my lack of significant differentially expressed genes may be an experimental dosage that was too low to elicit any physiological responses in bees or varroa, which is particularly remarkable because the latter is particularly susceptible to 3c{3,6} (Singh et al. 2020, Dawdani et al. 2023, Cook et al. 2024). While the 3-hour EC_{50} dosage I selected had previously elicited paralysis and death in varroa, it is nonetheless a conservative dose relative to other exposure studies of 3c{3,6} against the mite (Dawdani et al. 2023, Cook et al. 2024) intended to target sublethal effects. Potentially compounding the low dosage was the pre-experimental placement of varroa on live worker bees, which differs from the prior studies used to determine the EC_{50} of 3c{3,6} in which mites began the experiment completely isolated from bees (Dawdani

et al. 2023). In my experiment, varroa were situated beneath the workers' abdominal sternites, which is the preferred feeding site on adult bees (Rosenkranz et al. 2010, Li et al. 2019, Ramsey et al. 2019). This location is likely to have shielded mites from 3c{3,6} exposure to some degree (Bahreini et al. 2021), especially with respect to their forelimb chemoreceptors (though the forelimbs were not specifically analyzed). It is noteworthy that this shielded feeding position is the primary location of mites on adult bees during whole-colony field experiments, which in turn have demonstrated efficacy against varroa (Dawdani et al. 2023, Cook et al. 2024). However, such trials exposed the mites to substantially higher doses of 3c{3,6} for longer periods of time than my bioassays.

Though no genes were significantly differentially expressed after the Benjamini-Hochberg adjustment, several hundred genes in both the honey bee head and abdomen datasets had unadjusted *P*-values below $\alpha = 0.05$. Notable candidates among these are six genes belonging to the cytochrome P450 enzyme superfamily, with four of these genes located in the head and two in the abdomen. Cytochrome P450s contribute to xenobiotic metabolism and detoxification in a wide variety of insect species (Lu et al. 2021), and honey bee cytochrome P450s are able to metabolize 3c{3,6} (Gkaleni 2021). Exposure to xenobiotics (including the varroacide tau-fluvalinate) is known to increase P450 expression in bees once certain exposure thresholds have been reached (Alptekin et al. 2016, Wu et al. 2020, Wu et al. 2022). However, I found five of the six cytochrome P450s to be downregulated in the 3c{3,6}-exposed bees, with only the unnamed gene encoding cytochrome P450 4c3 in the abdomens being more expressed in the 3c{3,6}-exposed bees versus the controls. Moreover, the cytochrome P450 expression differences between 3c{3,6}-exposed and control bees were minor, being below a two-fold difference in all cases. Thus, it is unlikely that the differential expression of cytochrome P450s was meaningfully affected by 3c{3,6} vapour

exposure. It is possible that the 3c{3,6} dosage used in my study was too low to elicit detoxification responses within honey bees. Thus, future studies should evaluate the expression levels of cytochrome P450s at different levels of 3c{3,6} exposure in honey bees.

Another notable result of differentially-expressed genes in the head dataset with unadjusted *P*-values below $\alpha = 0.05$ are three downregulated odorant receptors/binding proteins. This group includes the G-protein coupled olfactory receptor *Or115* (Zhang et al. 2022), alongside two odorant binding proteins (*Obp4* and *Obp19*) which function in binding odor molecules (Forêt and Maleszka 2006, Song et al. 2018). Additionally, the *Or115* gene was the ninth most downregulated gene in the 3c{3,6} treated bees, with a 2.06-fold downregulation compared to the controls. The two odorant binding protein genes were only moderately downregulated, with under two-fold downregulation. Olfaction plays a key role in foraging behaviour, allowing bees to identify nectar-rich flowers (Wright and Schiestl 2009, Lusebrink et al. 2015). Olfaction also contributes to social immunity, with nurse bees relying on olfactory cues to detect the presence of pathogens in brood, including varroa (Mondet et al. 2015, McAfee et al. 2017). Olfactory interference of 3c{3,6} in honey bees could challenge its implementation as a commercial varroacide if confirmed, as such effects might impair foraging efficiency and thus honey production (Drezner-Levy et al. 2009, Klein et al. 2019), and potentially be incompatible with IPM regimens involving varroa-sensitive hygiene (Mondet et al. 2015). Moreover, the importance of pheromonal communication within honey bee colonies means any disruptions to pheromone reception can have drastic implications on colony-level function, leading to downstream impacts on colony health and productivity (Mumoki and Crewe 2021). Such effects are also notable because 3c{3,6} has demonstrated a feeding deterrence effect against another insect, *Trichoplusia ni* (though the mechanism remains unknown) (Plettner and Gries 2010, Ebrahimi et al. 2013, Cameron et al. 2014). While the

substrates of my detected odorant receptors and binding proteins currently are unknown, and their function as a whole remains understudied in *Apis mellifera*, similar proteins are known to play a role in the detection of floral volatiles and pheromones in the eastern honey bee *Apis cerana* (Li et al. 2013, Song et al. 2018, Zhao et al. 2021). However, preliminary field experiments have failed to indicate lower honey and pollen production in hives treated with 3c{3,6} compared to untreated controls (Dawdani et al. 2023), suggesting that 3c{3,6} does not impact foraging efficiency at field-relevant dosages. Regardless, future investigations should evaluate the impact of 3c{e,6} exposure on honey bee olfactory sensitivity, including potential detoxification mechanisms proximal to the olfactory receptors. Such studies may aim to directly test olfactory responses in bees to floral volatiles or pheromone stimuli before and after an acute antennal exposure to 3c{3,6}, or compare the differences in response to olfactory stimuli between a 3c{3,6}-exposed and an unexposed control cohort.

The compound 3c{3,6} has previously been shown to affect the electrophysiological activity of chemoreceptors on the varroa forelegs, interrupting their host-finding ability (Singh et al. 2020). However, my study found no differentially expressed genes with unadjusted *P*-values below $\alpha = 0.05$ that were associated with chemoreception between negative control varroa and varroa exposed to 3c{3,6} vapours. There were also no differentially expressed genes associated with reproductive functions between treatments in varroa, which reinforces field observations that 3c{3,6} does not significantly impact varroa foundress fecundity (Dawdani et al. 2023). Nevertheless, there were still several downregulated genes with unadjusted *P*-values below $\alpha = 0.05$ worth noting. Foremost was a group of three genes which encoded proteins putatively identified as neurosynaptic calcium receptors modulating neurotransmitter release. These include a calcium-dependent secretion activator (CAPS)-like protein (Elhamdani et al. 1999, Vonhoff and

Keshishian 2017), the synaptotagmin-1-like isoform (DiAntonio and Schwarz 1994, Gruget et al. 2020), and a regulating synaptic membrane exocytosis protein 2 (RIMS)-like isoform (Dresbach et al. 2001). In addition, a fourth downregulated gene was discovered to encode a protocadherin Fat 4-like isoform – a calcium-driven adhesion protein that functions in the formation of neural circuits, including adhesion at neural synapses (Molumby et al. 2017). These findings suggest that the potential mode of action of 3c{3,6} in inducing paralysis in varroa mites involves the disruption of calcium-dependent regulatory proteins at the synapse. However, all four genes expressed less than a 2-fold downregulation in 3c{3,6}-exposed mites compared to the controls and none of the experimental mites exhibiting paralysis symptoms following their removal from host bees. Given the suggestive nature of my results, future studies comparing differences calcium-dependent synaptic protein activity between 3c{3,6}-paralyzed, 3c{3,6}-exposed but unparalyzed, and unexposed control mites are necessary before a mechanism of paralysis can be inferred.

A core question that my study failed to resolve is understanding the mechanisms which cause differential toxicity between honey bees and mites. Though my experiment yielded inconclusive results regarding the role of P450s, Genath et al. (2020) has shown that exposure to formic acid induces P450 upregulation in both bees and varroa mites, though it is unclear if the P450 upregulation is directly due to formic acid exposure or a knock-on effect. There may also be non-P450 detoxification enzymes which underpins differences in 3c{3,6} toxicity, such as reductases (Genath et al. 2021). One key aspect to understanding the effects of 3c{3,6} on detoxification pathways in honey bees in particular, is to avoid synergistic toxicity with other varroacides (Gong and Diao 2017). For instance, both thymol and amitraz are known to interact with detoxification enzymes, resulting in increased toxicity of other varroacides (notably P450-detoxified pyrethroids) to bees, if follow-up exposures happen within a short time span (Johnson

et al. 2013). Thus, when interpreting the results of future studies, it is important to consider potential synergies with other varroacides, especially with regards to overlapping detoxification mechanisms.

The challenge of optimizing my exposure regimen in terms of dosage and time led to inconclusive results in this experiment with regards to the central question whether varroa's physiology is more disrupted by sublethal 3c{3,6} exposure than the physiology of its honey bee host. Exposure optimizations will likely be the greatest challenge for future sublethal effect experiments as well. Unlike the majority of varroacide studies wherein an optimal regimen maximizes toxicity towards the mites and minimizes non-target effects (Riva et al. 2019), sublethal effect studies must strike a balance between a sufficient dosage to elicit toxic effects, and a dosage low enough to avoid introducing survivorship bias into the results (Qi et al. 2017, Gagliardi et al. 2019). The question of applicability must also be addressed in designing future studies, as both bees and varroa mites in honey bee colonies will likely fluctuate between different dosages of vapour exposure when they move through the colony, as is the case for other volatile varroacides (Lodesani and Costa 2008). Though there have been relatively few studies examining sublethal effects of varroacides on varroa, numerous such studies exist for honey bees which aim to address these concerns.

Employing a serial dilution of 3c{3,6} in a series of parallel exposure experiments, such as the assay used by Bahreini et al. (2020), is an approach that could be employed with two key benefits. First, serial dilutions can help find an optimal dosage which elicits acute sublethal toxicity in mites without crossing the mortality threshold. Second, resultant samples from such an assay will likely exhibit a gradient of sublethal symptoms, which can then be compared at the transcriptomic level. Another valuable technique to employ is the use of a time gradient, whereby

bees and mites exposed to a constant sublethal dosage of 3c{3,6} are incubated over a series of time frames before being collected (Dawdani et al. 2023). Comparing the transcriptomes of samples within a time series will reveal a transcriptome chronology, enabling us to distinguish immediate acute effects of 3c{3,6} exposure from potential knock-on effects not directly caused by the varroacide.

Multiple avenues of application should also be explored, as both varroa and bees treated with 3c{3,6} in an apicultural context will almost certainly encounter the compound through different modalities. Furthermore, such studies can target specific systems of interest. For instance, ingestion experiments with 3c{3,6}-containing sugar syrup can provide detailed insights into honey bee detoxification mechanisms against 3c{3,6} within the honey bee digestive system (Berenbaum and Johnson 2015). Alternatively, direct topical application of 3c{3,6} onto the honey bee antennae can reveal important details of the impact of 3c{3,6} on olfaction.

Finally, colonies *in situ* themselves can be treated with 3c{3,6} (see Chapter 2), and bees and varroa can directly be sampled from these field assays after relevant exposures that are effective against varroa. *In situ* studies will not only be useful in evaluating effects of long-term exposure, but could also reveal the effects of larval 3c{3,6} exposure on subsequent adult bee physiology. Though a managed hive is a less controlled environment compared to a laboratory assay, results from such experiments are highly informative as to the generalizability of laboratory results. However, care should be taken to collect paralyzed mites from field studies as well, to mitigate survivorship bias. Such collections may be achieved using screened bottom boards with a removable varroa mite tray, such as those used by Dawdani et al. (2023). In such an experiment, care should be taken to avoid collecting dead varroa mites with degraded RNA (Gallego Romero et al. 2014). This can potentially be avoided by frequently checking mite trays, and testing for

paralysis with a fine-tipped paintbrush similar to the tests performed by Dawdani et al. (2023)

Overall, this study did not find a significant effect of 3c{3,6} vapours on gene expression of honey bees or dispersing mites on worker bees, at an EC_{50} dosage. However, this does not rule out possible effects of 3c{3,6} on honey bee and varroa metabolisms at higher dosages. Future experiments should focus on testing a greater variety of dosages, different exposure avenues (vapour, oral, cutaneous application, etc.), and different time frames. It is also important to account for potential difficulties in creating unbiased exposure experiments, as bees and mites may not be exposed to equal dosages during contact assays, nor do lab assays translate equivalently to *in situ* exposure within the colony environment. Thus, lab experimentation should be complimented with transcriptome analyses of bees and mites collected in the field. With many questions still remaining regarding the mode of action of 3c{3,6}, respondent detoxification mechanisms in mites and honey bees, and the organisms' metabolic responses to 3c{3,6} exposures, acute and chronic, evaluation of these questions should be achieved through multiple diverse experimental approaches. Ultimately, future studies should strive for a balance between understanding the sublethal interactions of the chemical with relevant organisms, and generating results that are applicable to field-relevant dosages.

3.5 Conclusion

An acute exposure to 3c{3,6} vapour at EC_{50} dosage was insufficient to elicit significant responses at the transcriptional level in mites and honey bees, when statistical *P*-values are adjusted for multiple hypothesis testing. However, unadjusted *P*-values indicate significantly downregulated genes pertaining to detoxification (specifically belonging to the P450 superfamily

of monooxygenase enzymes) and of odorant reception in exposed honey bees, and genes encoding calcium-dependent synaptic proteins in varroa mites. These findings are suggestive of potential effects in both honey bees and mites, though none of these pathways were recovered using a gene ontology Mann-Whitney U analysis of all genes. The inconclusive results may have been due to a dosage which was too low for the experimental design. 3c{3,6} is known to exhibit low toxicity against bees relative to mites, and the vapour EC_{50} of 3c{3,6} against varroa was determined using isolated mites, as opposed to the mites on host bees used in my study. Given that the genes I uncovered in honey bees are putatively relevant to foraging and social immunity, while the mite genes may help explain the mode of action of 3c{3,6} the results indicate a need for future studies to examine if the observed effects can be confirmed at different exposure regimens.

Table 3-1: Overview of the master mix (MM) used in the first incubation cycle of cDNA synthesis at 70° C, with reagent volumes per well, as well as for a 72-well run (with 10% extra master mix included in the preparation to account for fluid loss during pipetting).

Reagent	Volume per well (µL)	Total volume in MM for 72 wells (µL)
dNTP (10mM each)	1	79.2
DTT (0.1M)	2	158.4
5X First Strand Buffer	4	316.8
3ILL-30TV (10µM)	1	79.2

Table 3-2: Overview of the master mix (MM) used in the cDNA amplification step, with reagent volumes per well, as well as for a 72-well run (with 10% extra master mix included in the preparation to account for fluid loss during pipetting).

Reagent	**Volume per well (μL)**	**Total volume in MM for 72 wells (μL)**
H_2O	4.6	364.3
dNTP (2.5mM each)	2	158.4
10X PCR buffer	2	158.4
3ILL-30TV oligo (10μM)	0.45	35.6
5ILL oligo (10μM)	0.45	35.6
Klentaq DNA polymerase	0.5	39.6

Table 3-3: Overview of the barcoding master mix (MM), with reagent volumes per well, as well as for a 72-well run (with 10% extra master mix included in the preparation to account for fluid loss during pipetting).

Reagent	Volume per well (μL)	Total volume in MM for 72 wells (μL)
H_2O	7.4	586.1
dNTP (2.5mM each)	3	237.6
10X PCR buffer	3	237.6
Klentaq DNA polymerase	0.6	47.5

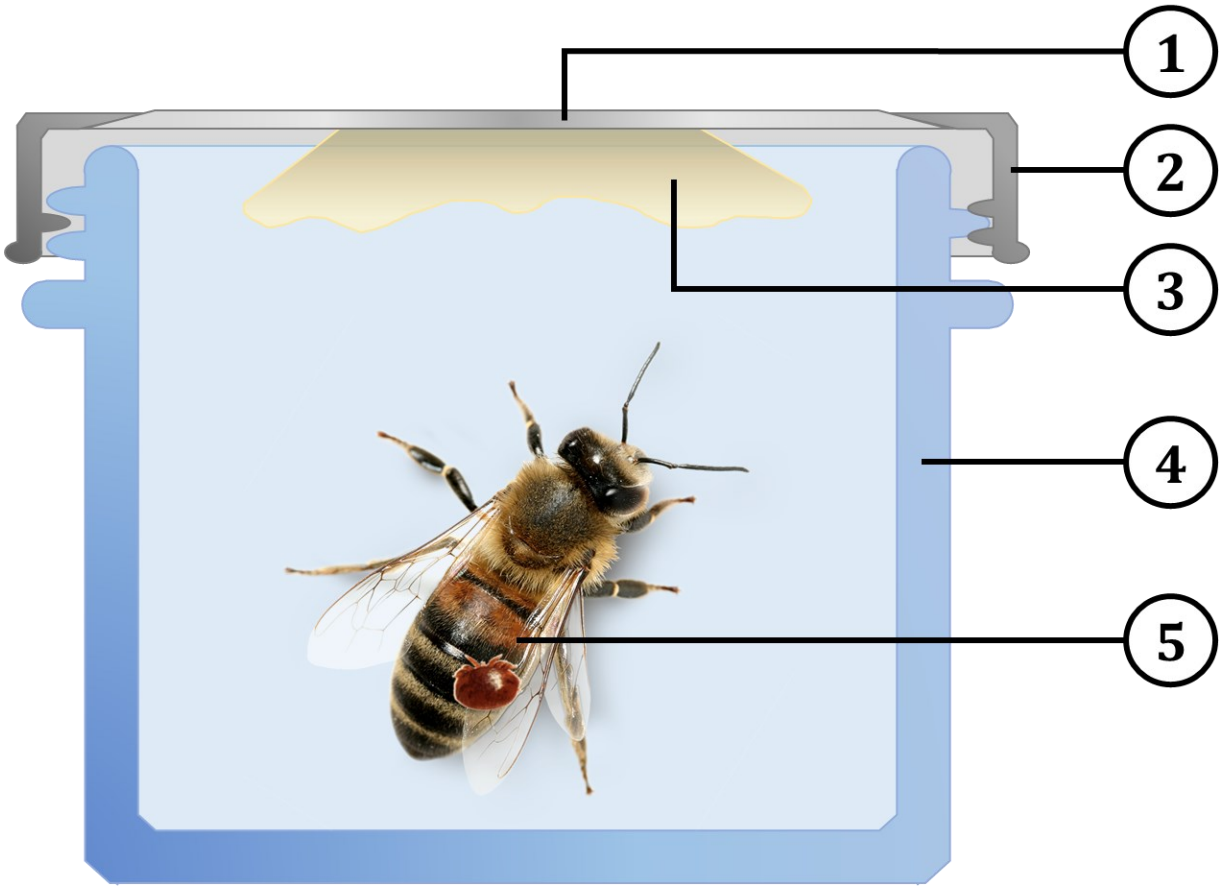

Figure 3-1: Diagrammatic representation of the jar bioassay cage used in the experiment, including labelled components. [1] Jar lid cover. [2] Jar lid ring (holds the lid cover in place; held loosely in place to permit ventilation). [3] Parafilm square stuck to bottom of lid cover, with 3c{3,6} or negative control hexane dispensed in centre. [4] Glass mason jar. [5] Ten nurse-age honey bees (depicted with one varroa mite per bee, though bees in only two of four jars per assay trial included mites). Honey bee photo courtesy of https://freepnglogos.com.

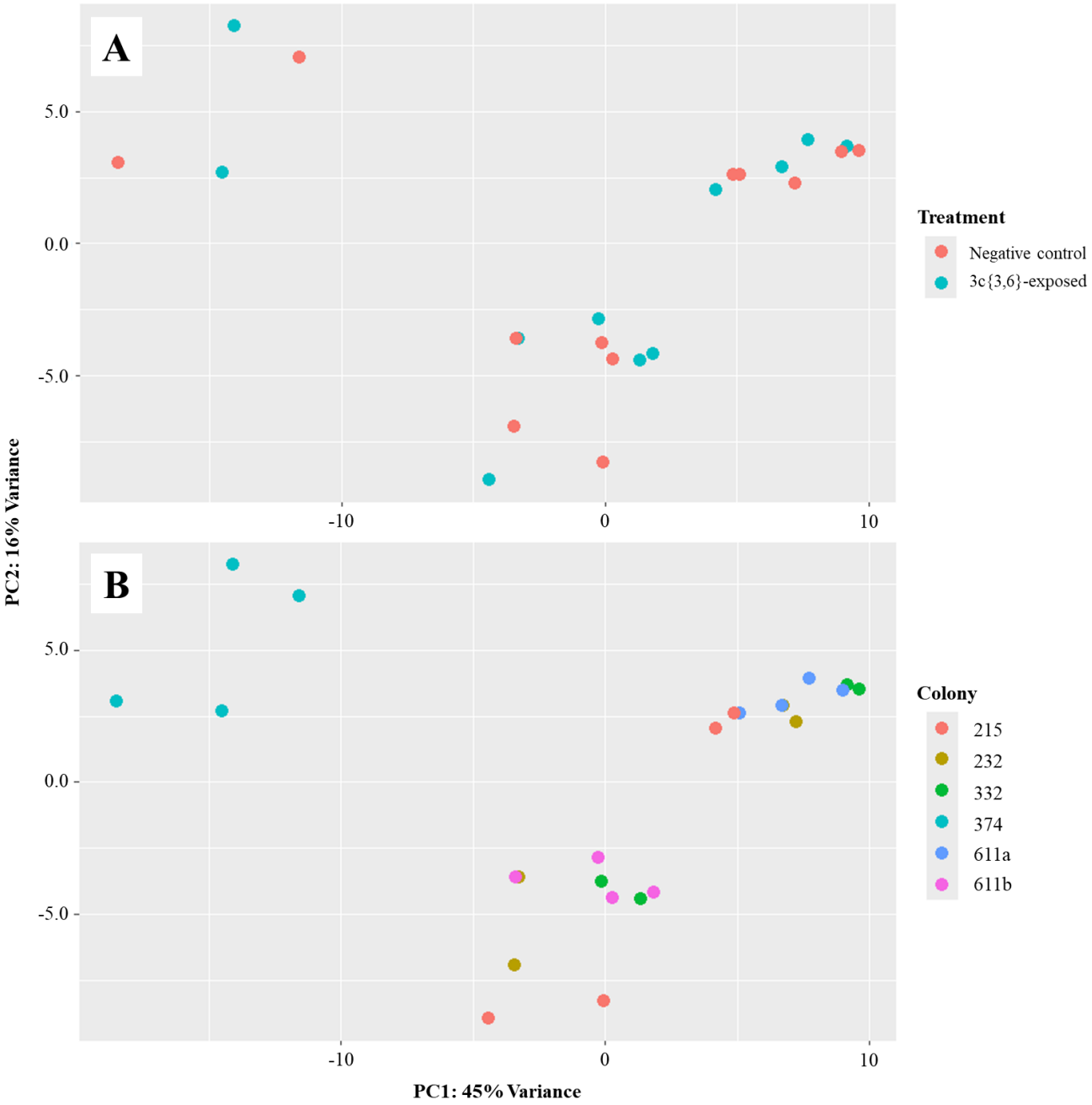

Figure 3-2: Principal component analysis (PCA) plots of honey bee head samples, colour-coded by [A] 3c{3,6} treatment, [B] colony source, [C] emergence date, and [D] post-emergence age (days).

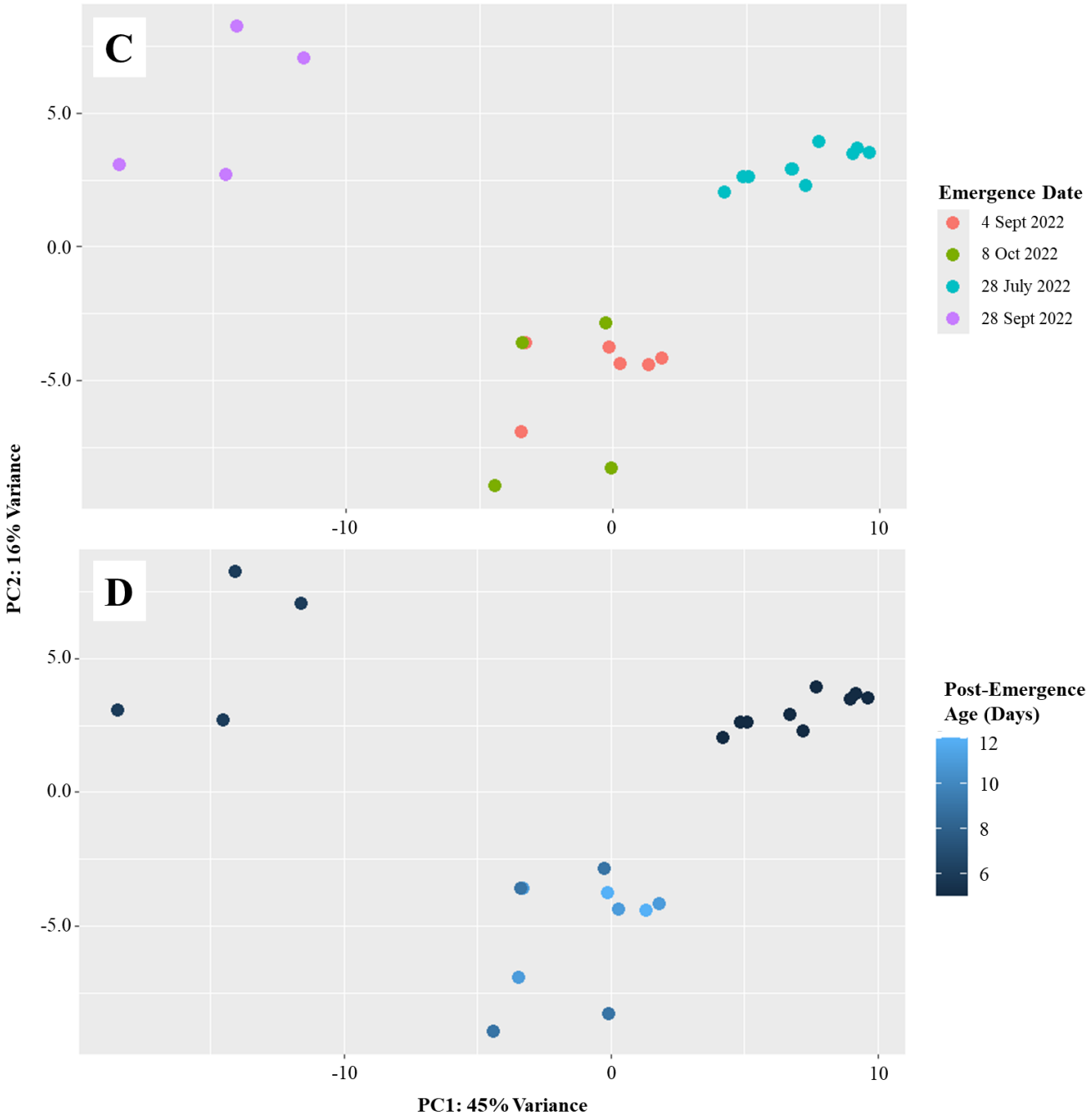

Figure 3-2 (Cont.)

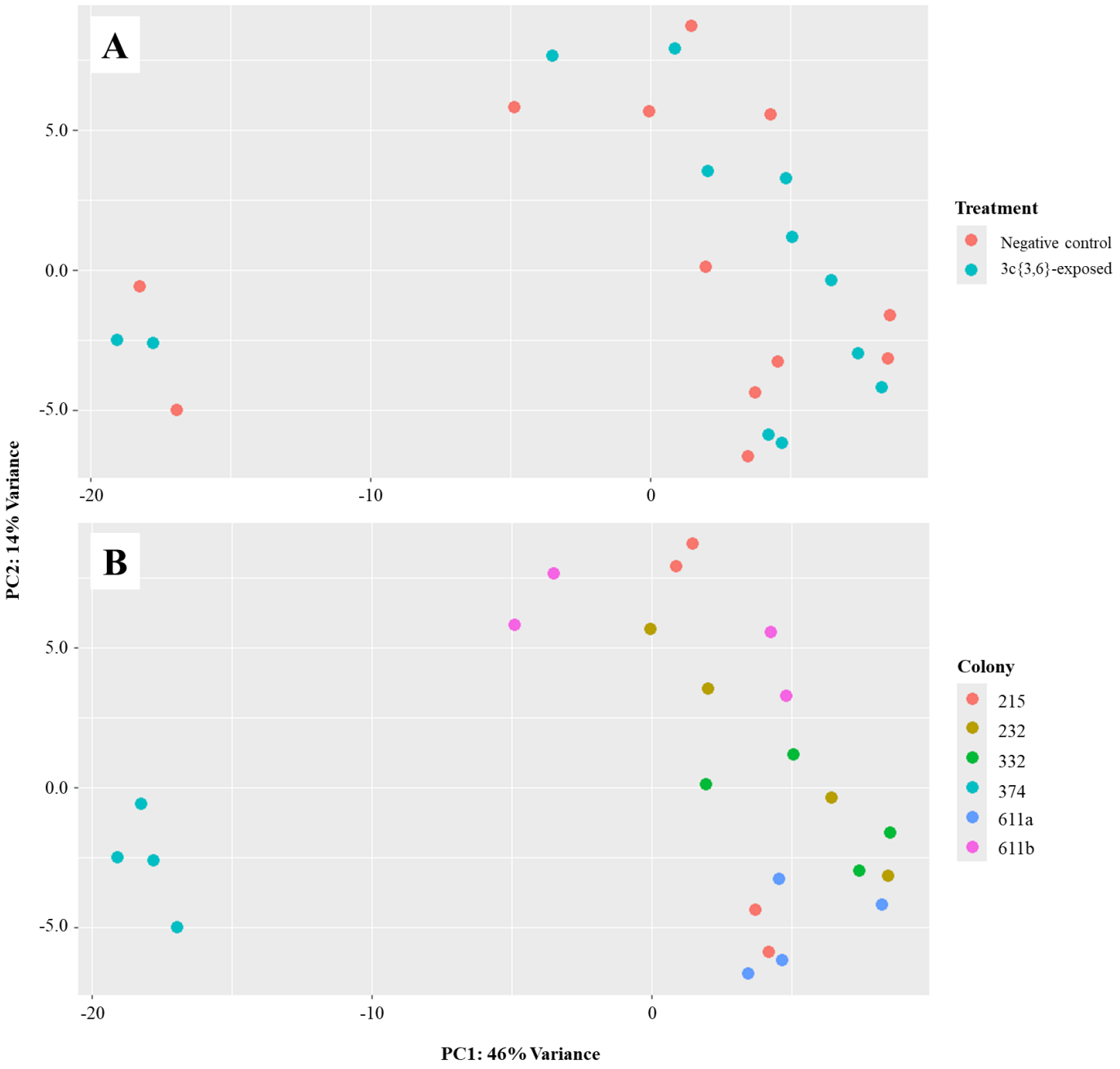

Figure 3-3: Principal component analysis (PCA) plots of honey bee abdomen samples, colour-coded by [A] 3c{3,6} treatment, [B] colony source, [C] emergence date, and [D] post-emergence age (days).

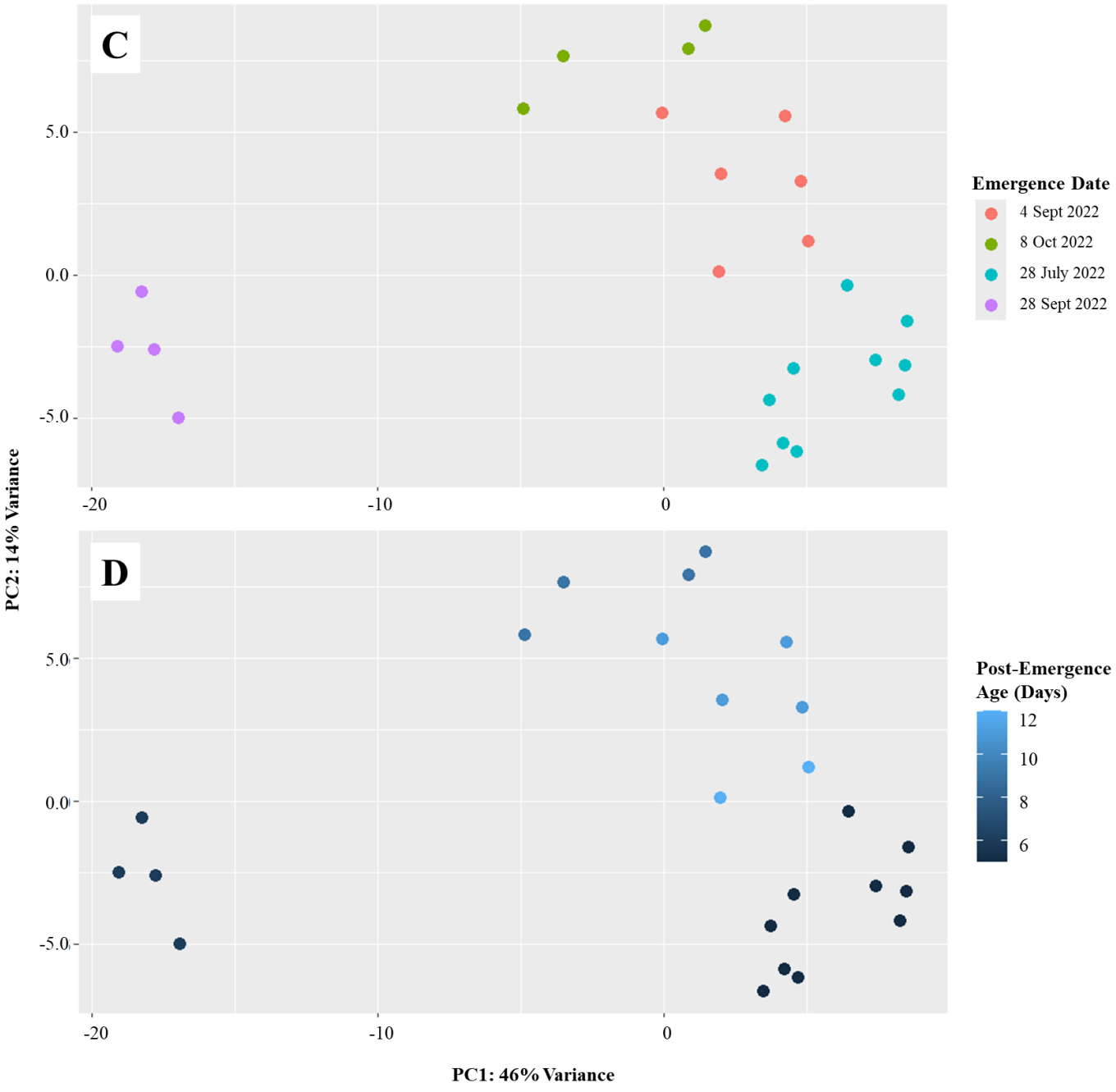

Figure 3-3 (Cont.)

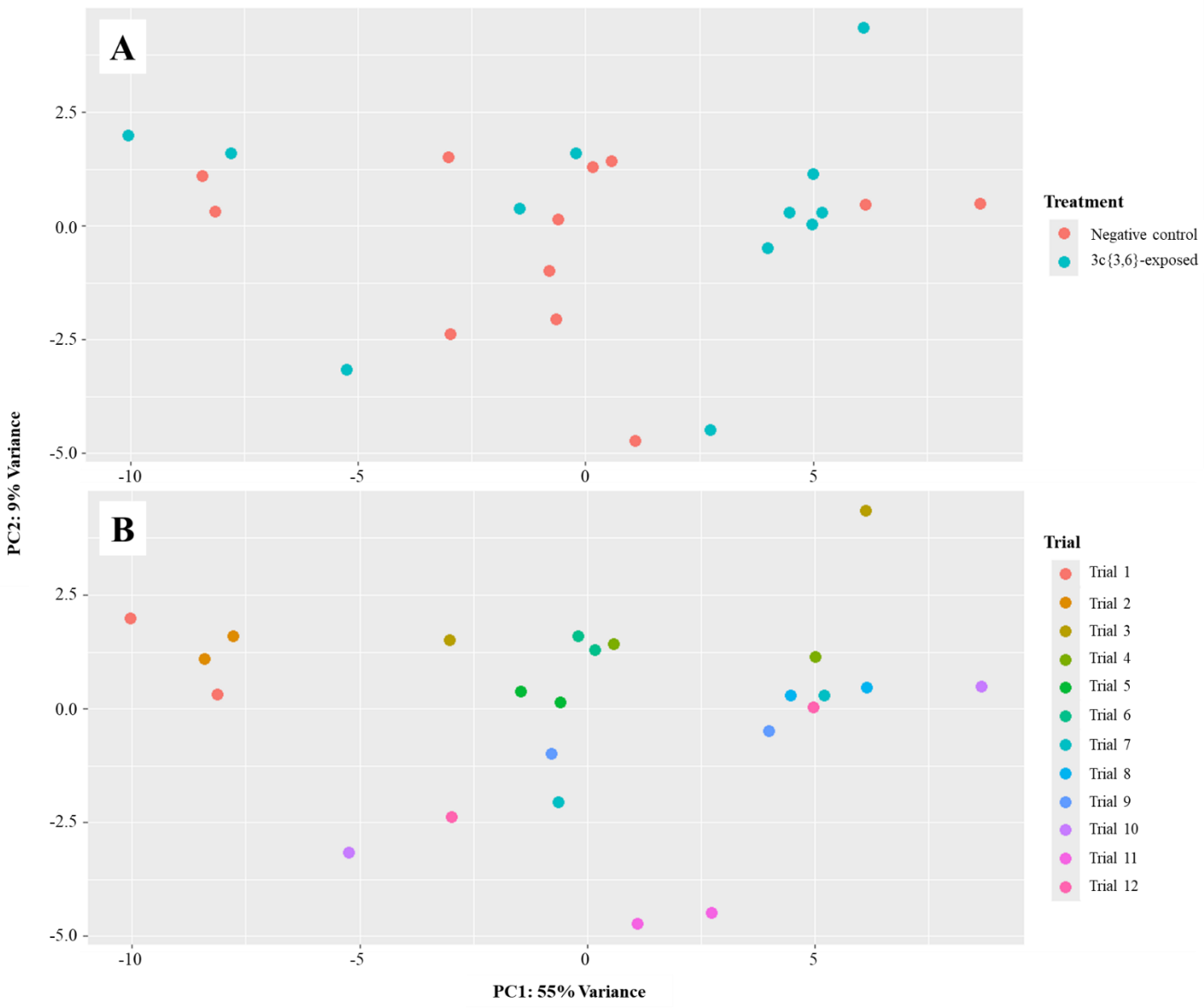

Figure 3-4: Principal component analysis (PCA) plots of varroa mite samples, colour-coded by [A] 3c{3,6} treatment, and [B] experimental trial.

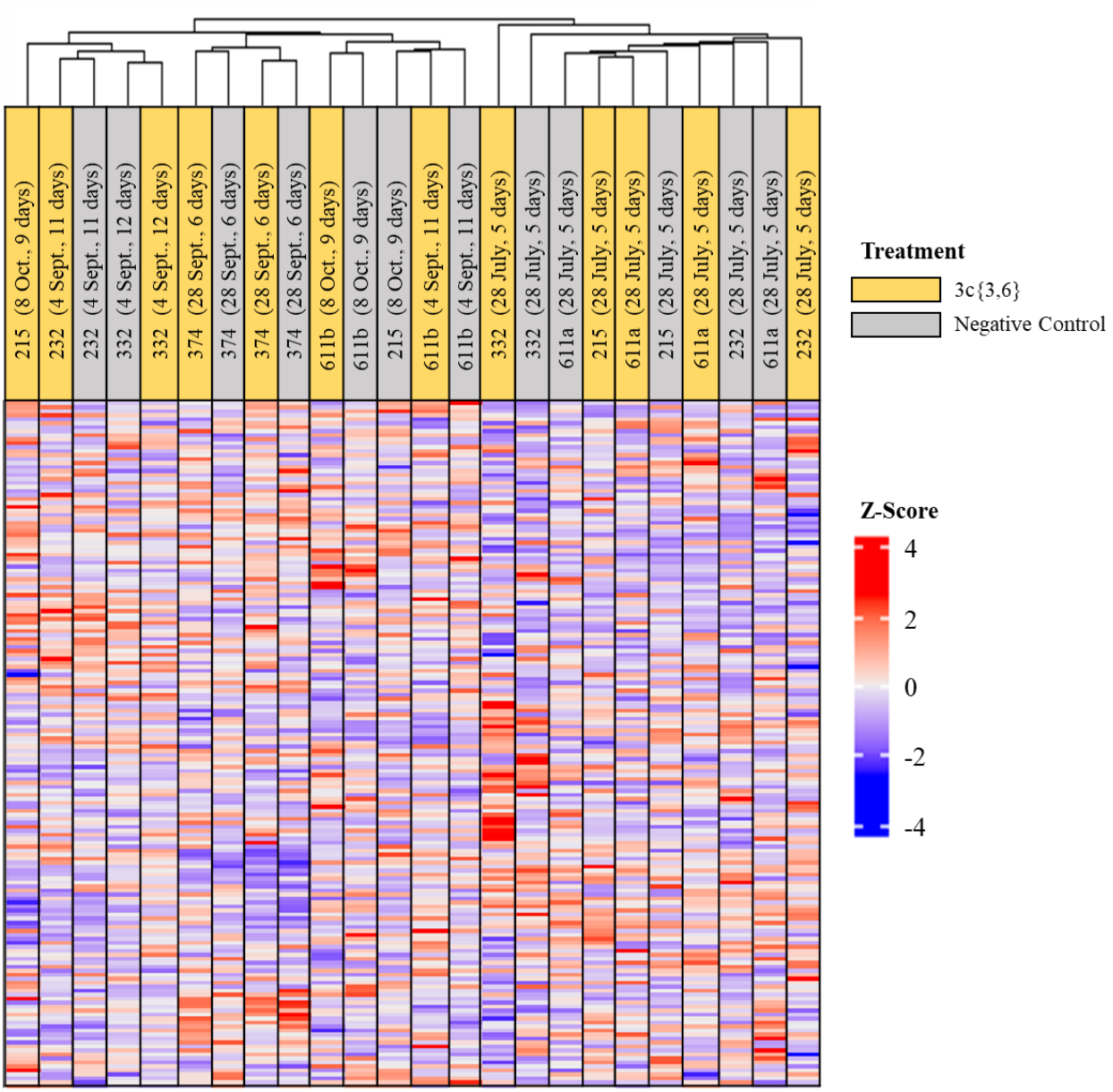

Figure 3-5: Gene expression clustering heatmaps and dendrogram of honey bee heads, with normalized z-scores of relative per-gene expression levels. Samples are identified by treatment, colony, emergence date, and post-emergence age.

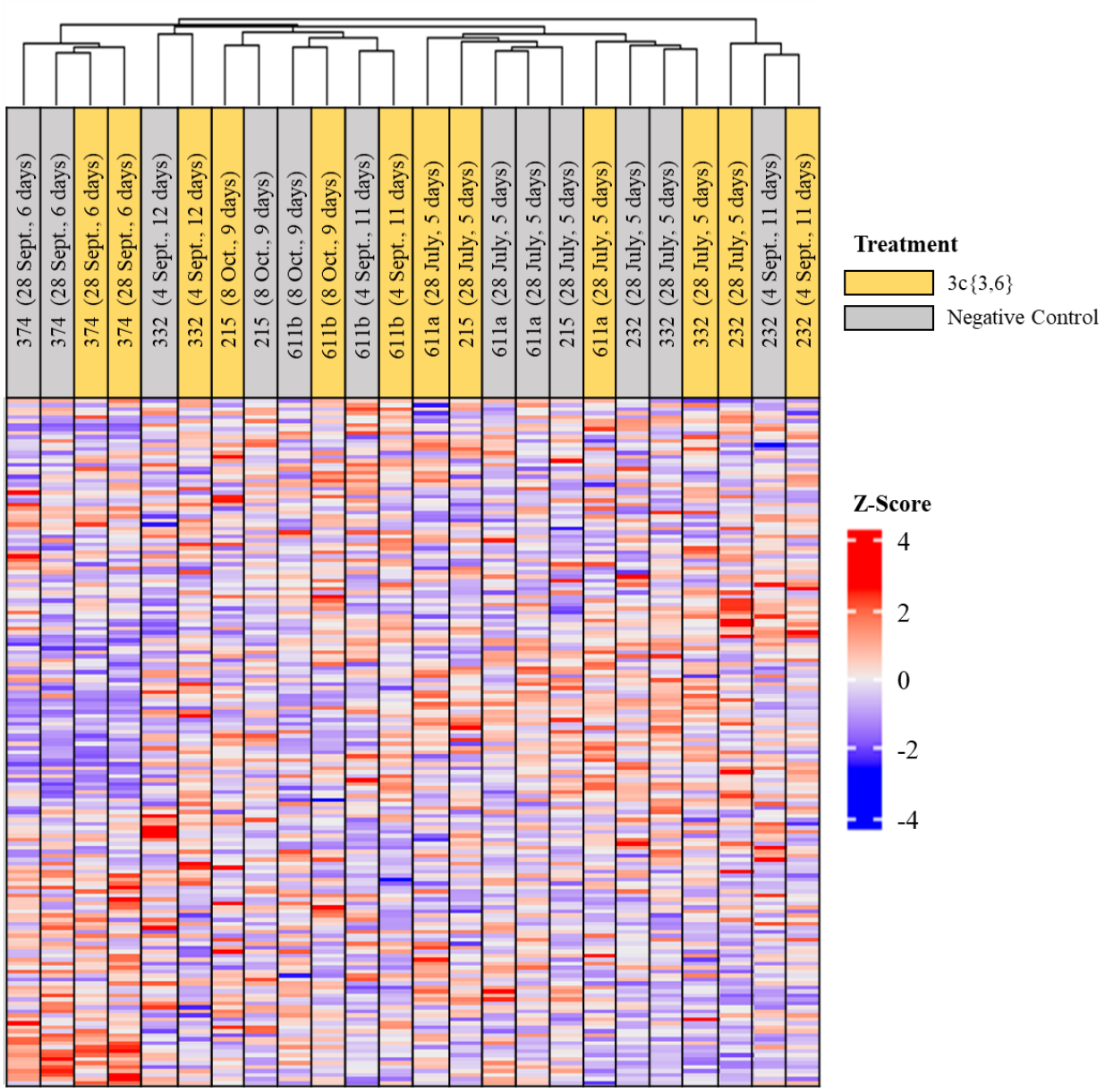

Figure 3-6: Gene expression clustering heatmaps and dendrogram of honey bee abdomens, with normalized z-scores of relative per-gene expression levels. Samples are identified by treatment, colony, emergence date, and post-emergence age.

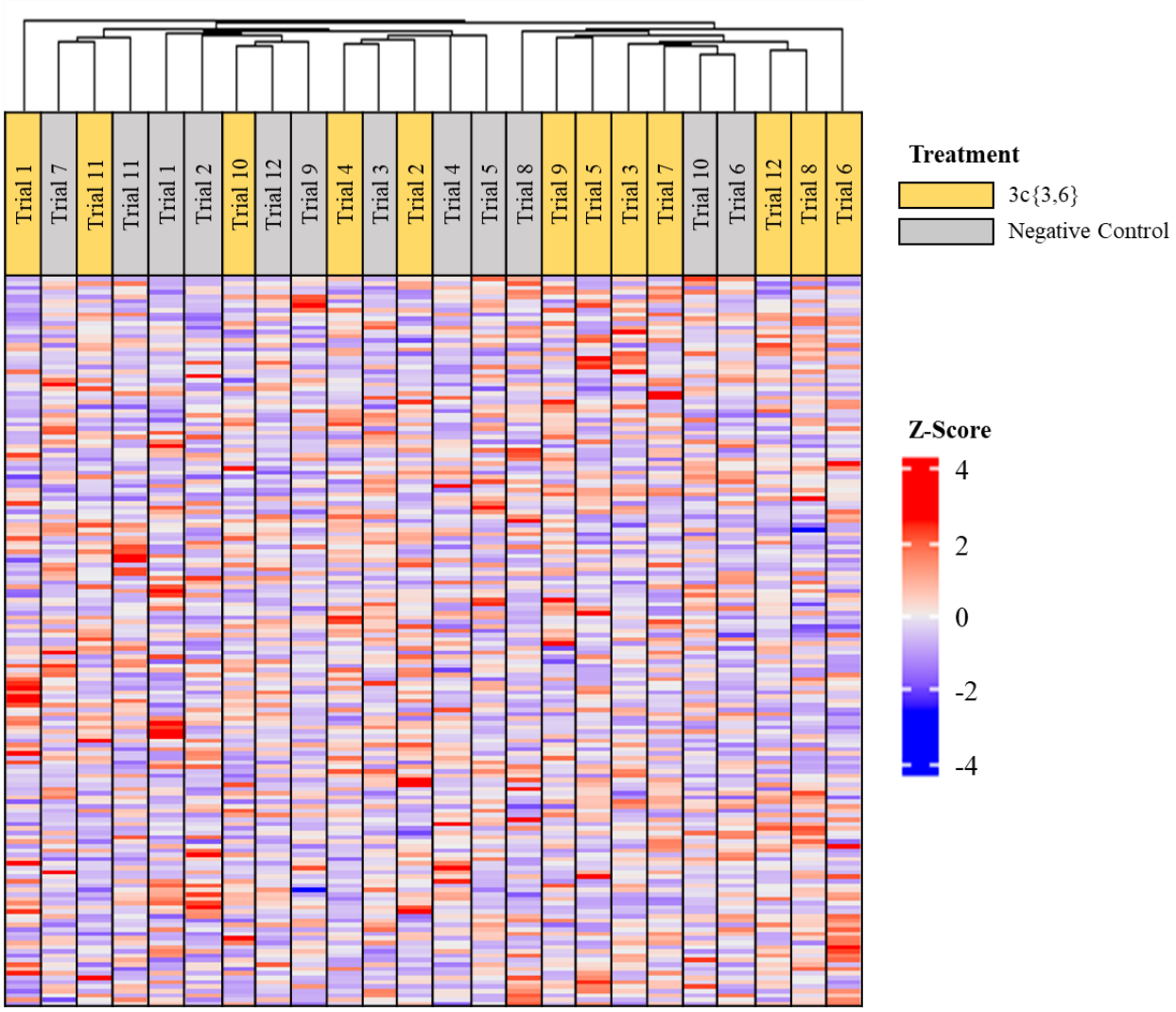

Figure 3-7: Gene expression clustering heatmaps and dendrogram of varroa mites, with normalized z-scores of relative per-gene expression levels. Samples are identified by treatment, and trial.

Chapter 4: Conclusion

4.1 General Conclusion

The main objective of this thesis was to evaluate the potential for the novel compound 1-allyloxy-4-propoxybenzene (codenamed 3c{3,6}) to act as a miticide against the parasitic honey bee mite *Varroa destructor*. Specifically, I pursued two main avenues of research. First, I assessed the varroacidal efficacy of 3c{3,6} through a series of field assays. Secondly, I analyzed the effects of sublethal 3c{3,6} vapour exposure on the physiology of both honey bees and varroa, comparing the degree of gene expression perturbation in each organism.

In Chapter 2, I outline the three field experimental trials (occurring in the 2021, 2022, and 2023 field seasons) wherein 3c{3,6} was deployed in colonies within commercial apiaries in Northern Alberta. Miticidal efficacy was evaluated based on linear modelling of daily mite mortality over the treatment phase, while changes to the dispersing-stage mite infestation levels from the start of the treatment phase to the end was calculated with a modified version of Sun-Shepard's formula (Püntener 1981). To evaluate the effect of dosage and applicator design on efficacy, I varied the per-colony 3c{3,6} dosage throughout the years. Additionally, I also sought to optimize the applicator design and achieve a balance between ease of use and efficacy. Through these variations, I sought to optimize the treatment design for maximum varroacidal efficacy in commercial settings, while minimizing non-target effects on the honey bee colonies themselves. Varroacidal efficacy of 3c{3,6} was comparable to or exceeded that of Thymovar® in all comparisons, with 3c{3,6}-treated colonies exhibiting increased mite mortality versus the controls in all three years. Additionally, efficacy was much higher in 2022 and 2023 versus 2021, though whether this was attributable to differences in applicator design, dosage, treatment term length, or

a combination could not be determined. Additionally, cardboard applicators performed comparably to wood applicators in 2022 despite being rapidly degraded within the hive environment. The high efficacy of cardboard applicator material may indicate that most varroacidal activities of 3c{3,6} are front-loaded, occurring in the days immediately following the installation of applicators – a model which is supported by my observations (Fig. 2-4). Alternatively, the degradation of cardboard may have facilitated the vaporization of 3c{3,6} within the material, though this could not be determined from my findings. Colonies treated with 3c{3,6} also exhibited improved overwintering survivorship in 2022 and 2023 compared to negative controls, though this was not the case in 2021. However, I were unable to statistically compare these differences in survivorship, due to there only being a single cohort of each treatment per year. It is also notable that the 3c{3,6}-treated colonies in 2023 exhibited significant reductions to the worker bee population from the start of the treatment phase to the end, potentially indicating that a 10 g/colony dosage exceeds the upper limit of 3c{3,6} treatment levels of bee hives without negative side effects. While I sought to optimize the *in situ* application method throughout the three experiments, overlaps in differences between infestation rates, season, dosage, applicator design, and treatment length made disentangling different factors difficult. Thus, future experiments seeking to primarily optimize the deployment method should focus on varying individual factors to isolate the effects on miticidal efficacy of individual changes made to the treatment regimen. Overall, 3c{3,6} was shown to be an effective varroacide for use *in situ*, effectively killing varroa mites and improving colony overwintering success at levels comparable to other commercial varroacides.

In Chapter 3, I sought to uncover the transcriptome-level effects of an acute sublethal exposure to 3c{3,6} vapours on nurse-age bees and dispersing-stage mites. Given the intended

function of 3c{3,6} as a varroacide, I specifically sought to test the hypothesis that 3c{3,6} exposure perturbs metabolic pathways in varroa mites to a greater intensity and diversity than in honey bees. In contrast to the previous study conducted by Dawdani et al. (2023), I did not observe any mortality in bees or mites, nor did I observe arrestment/paralysis of 3c{3,6}-exposed mites. I analyzed gene expression differences in the heads and abdomens of exposed mite-free honey bees, and of whole varroa mites. High-throughput RNA-seq is a useful tool for evaluating sublethal pesticide exposures as it enables the evaluation of a wide array of different metabolic pathways simultaneously (Wang et al. 2009). Furthermore, analyzing gene expression changes allows us to relate gene expression patterns directly to changes in metabolic function within the organisms (Shi et al. 2017). This enables us to not only make inferences about modes of action against varroa, but also let us identify other potential pathways of interest in the non-target honey bee system, providing a starting point for future investigations into the long-term effects of 3c{3,6} usage on colonies. The analysis of 3c{3,6}-exposed honey bees suggested a potential downregulation of genes pertaining to detoxification (via the cytochrome P450-mediated pathways) and odorant reception in honey bees, alongside calcium-dependent enzymes at the neuronal synapses in mites. However, each dataset also contained hundreds of other genes with stronger log2-fold changes and lower unadjusted *P*-values, with many of these genes being putatively unrelated to the aforementioned pathways, and others having unknown functions. Furthermore, none of these changes were significant when a 10% false discovery rate correction was applied. To identify potential ontological pathways that were differentially expressed between 3c{3,6}-exposed and control mites and bees, I employed a gene ontology Mann-Whitney U (GO MWU) analysis. This analysis differs from a traditional gene ontology analysis in its ability to detect differentially-regulated pathways involving non-significantly differentially expressed genes, and not just

significantly differential genes as is the case with the latter method. my GO MWU analysis did not recover any significantly differentially expressed genetic pathways in either bees or mites. These results failed to support my prediction that the varroa transcriptome would more perturbed by 3c{3,6} exposure than that of honey bees, as both organisms expressed equivalent levels of differential gene expression based off the unadjusted *P*-values, and no genes in either organism were significant upon adjustment with the 10% FDR correction.

The overall findings of my exposure experiment fail to support my hypothesis that exposure to 3c{3,6} at sublethal levels induces perturbations to the metabolic pathways of honey bees and varroa, at least at the level of gene expression. Alternatively, it is possible that the lack of significant differential expression is due to my dosage being too low to elicit detectable effects following a statistical correction. Nevertheless, the putative functions of the aforementioned genes are highly relevant to both honey bee health (detoxification, foraging, social immunity) and against varroa (potential mechanism of 3c{3,6}-induced paralysis), and thus future studies should aim to analyze these whether these pathways remain differentially expressed at different exposure dosages. This is especially pertinent to the functionality of 3c{3,6} as a potential varroacide, as such compounds should ideally have very minimal toxic effects on the metabolism of honey bees, while strongly impacting varroa at even sublethal dosages. Moreover, studies examining the sublethal effects of mites and bees exposed to field-relevant dosages may help us understand how sublethal effects may contribute to reducing mite levels and potentially compromise bee health in the environment of a commercial bee yard.

Taken together, I found 3c{3,6} to be an effective varroacide, albeit one with remaining unknowns regarding the specific mode of action. I found optimal varroacidal efficacy when applying 3c{3,6} at a dosage of 8-10 g using applicators that facilitate increased volatilization and

direct contact of mite-infested bees against the compound through surface are and positioning (i.e., those used in 2022 and 2023). Meanwhile, decreased efficacy observed in colonies equipped with a smaller applicator in 2021 implies higher contact-based efficacy with the 2022 and 2023 applicators, although a higher dosage and greater surface area enabling increased volatilization may also have contributed to increased efficacy. These findings are seemingly supported by the relatively mild differences in gene expression profiles seen in 3c{3,6}-exposed and control mites within my exposure bioassay. However, it is important to note that changes in applicator design coincided with changes in dosage, treatment duration, and applicator surface area, with the effect of each individual modification being impossible to disentangle from one another. Additionally, 3c{3,6}-treated colonies in the Spring 2023 experiment exhibited diminished worker bee populations versus the negative control, despite the former also possessing significantly lower mite infestation levels than the latter cohort. Thus, it is possible that 10 g/colony exceeds an upper limit to a honey bee-safe field dosage, with the upper dosage limit of safety for bees being between 8 g/colony and 10 g/colony. It remains unclear why this phenomenon occurred, as I found no explanatory metabolic changes caused by 3c{3,6} vapours in honey bees within my lab-based bioassay study on adult workers. Furthermore, I did not evaluate the effect of 3c{3,6}-exposure on different stages of honey bee development, nor did I assess for effects against queens (especially fertility), which may have provided additional explanatory reasons for the reduced worker population.

Overall, the future of 3c{3,6} as a commercial varroacide candidate remains promising. The high efficacy demonstrated in my study, coupled with prior studies demonstrating low risk to users and the environment (Ebrahimi and Plettner 2014, Dawdani et al. 2023), reinforce the candidacy of 3c{3,6} as a candidate varroacide. In Canada, commercial varroacides must meet

registration requirements laid out by the Pest Management Regulatory Agency (PMRA) of Health Canada (Health Canada 2019). These generally concern human safety, target animal safety, safety to the environment, and evidence of value, with the latter point focusing on sustainable chronic exposure of honey bees to a varroacide. These guidelines are a good roadmap to ensuring a varroacide is safe and commercially viable, as the challenge of varroa is urgent and new solutions are urgently needed to ensure the future of beekeeping. Nonetheless, it is important to identify and address more subtle sublethal effects of a novel varroacide such as 3c{3,6}, which can prove informative as to potential incompatibilities with other treatments. This is especially true given that sustainable long-term control of varroa should not be reliant on varroacides alone, but instead deploy them alongside other means of varroa prevention in integrated pest management (IPM) regimens (Jack and Ellis 2021). The integrated pest and pollinator management (IPPM) framework is particularly pertinent, seeking to balance long-term varroa control with the preservation of pollinator health through methods of reducing harmful effects of chemical pest controls (Biddinger and Rajotte 2015). To this end, questions of how 3c{3,6} differentially influences varroa and honey bee metabolism are crucial for designing and optimizing a treatment regimen. Such differential expression studies will also inform best practices for combining or rotating 3c{3,6} regimens with other mite control techniques, to improve long-term varroacidal outcomes while understanding and minimizing the risks to pollinator communities in areas of high beekeeping intensity. Though my thesis was unable to resolve these questions conclusively, the research I have conducted may hopefully provide a useful scaffolding upon which future studies can be built.

4.2 Study Limitations and Future Research

A key limitation in the field trials was the inability to test differences in treatment applicator design, dosage, and applicator surface area independently of one another. Such limitations are often inevitable, being brought about by budget, time, and resource limitations, notably the number of colonies available for experimentation. Should large-scale studies be conducted in the future, emphasis should first be placed on testing different applicator designs. Applicators should be designed with increased surface area compared to those used in the fall 2021 experiment, with different positioning options explored as well (such as two separate applicators being placed at opposing corners of the broodnest, vis-à-vis Thymovar®). Aside from wood and cardboard, other materials should be explored, especially materials with a more consistent matrix structure that provides more consistent long-term vaporization rates (such as cellulose wafer used in Thymovar® treatments).

The 3c{3,6} exposure assays were quite limited in their design, exploring only one dosage, one time frame, and one exposure avenue. Future experiments may explore a graded array of different 3c{3,6} vapour dosages and time spans to which honey bees and varroa mites may be exposed. Alongside vapour, different avenues of testable exposure includes topical (bees and mites), and oral (bees) exposure routes. Topical applications on bees may be further focused on evaluating the effects of direct 3c{3,6} contact against antennae, and the consequences for olfaction at both the behavioural and transcriptomic levels, specifically examining response capacities to sugar syrup and floral volatiles. Honey bees and mites (paralyzed and on nurse bees) may also be collected directly from field trials, to determine the evaluate the effects of 3c{3,6} at field-relevant dosages. Finally, focus can be expanded to other life history stages of honey bees, looking at the ways larval exposure to 3c{3,6} vapour influences gene expression profiles of adult

workers, irrespective of adult 3c{3,6} exposure. Such studies could be performed both in labs by rearing larvae in controlled cages alongside 3c{3,6} vapour applicators, or alongside field assays via collecting brood frames directly from 3c{3,6} treated colonies. Larvae exposed to 3c{3,6} may then have their gene expression profiles analyzed outright, or be allowed to metamorphose and emerge in an unexposed environment. Post-exposure adults in the latter case may be used in behavioural assays to evaluate locomotory/olfactory capabilities outright, or be evaluated for transcriptomic changes resulting from larval 3c{3,6} exposure (or both).

One additional experimental avenue which may be worth exploring is the potential for 3c{3,6} to affect varroa mites within capped brood. As the majority of the varroa life cycle occurs under the wax cap (notably, the entirety of the reproductive stage), understanding potential varroacidal effects during this period is of particular interest (Han et al. 2024). For such studies, frames of recently-capped brood from untreated varroa-infested colonies should be collected and incubated alongside different dosages of 3c{3,6} vapour. Towards the end of the incubation period, as capped brood develop into purple-eyed or pre-emergent pupae, brood infestation assessments can be performed in accordance with the protocols laid out by Harbo and Harris (2009) and Harris et al. (2012) (similar to the brood infestation assessment protocol that I employed in Chapter 2). Numbers of varroa mites in each group of 100 uncapped cells should be counted, and varroa mites should be scored based on survival and reproductive status. Comparisons can then be made across treatment and control frames, to determine the effects of different 3c{3,6} dosages on capped mite survivorship and fecundity, while controlling for 3c{3,6} exposure during the dispersing stage of the varroa life cycle.

Moving forward, future registration of 3c{3,6} will require further testing of chronic exposure effects against honey bees. Specifically, I should seek to fill knowledge gaps regarding

effects on brood development within colonies, worker longevity and overall health (especially regarding disease immunity), task ontogeny, and behaviours that may impact long-term hive productivity. Moreover, any risks to human safety must be thoroughly evaluated, including identifying a potential genetic targets for 3c{3,6} in varroa, and evaluating the same targets in humans. As managed honey bees are a food-producing organism, significant evaluation should be undertaken to assess the possibility of 3c{3,6} residues sequestering in hive products, particularly wax and honey, but also potentially bee pollen and royal jelly.

REFERENCES

Abbott WS. **1925**. A method of computing the effectiveness of an insecticide. Journal of Economic Entomology. 18(2):265–267. doi:10.1093/jee/18.2.265a.

Adjlane N, Tarek E-O, Haddad N. **2016**. Evaluation of oxalic acid treatments against the mite *Varroa destructor* and secondary effects on honey bees *Apis mellifera*. Journal of Arthropod-Borne Diseases. 10(4):501. PMID:28032102

Aizen MA, Harder LD. **2009**. The global stock of domesticated honey bees is growing slower than agricultural demand for pollination. Current biology. 19(11):915–918. doi:10.1016/j.cub.2009.03.071.

Akhtar Y, Isman MB, Paduraru PM, Nagabandi S, Nair R, Plettner E. **2007**. Screening of dialkoxybenzenes and disubstituted cyclopentene derivatives against the cabbage looper, *Trichoplusia ni*, for the discovery of new feeding and oviposition deterrents. Journal of agricultural and food chemistry. 55(25):10323–10330. doi:10.1021/jf071636d.

Akhtar Y, Yu Y, Isman MB, Plettner E. **2010**. Dialkoxybenzene and dialkoxyallylbenzene feeding and oviposition deterrents against the cabbage looper, *Trichoplusia ni*: potential insect behavior control agents. Journal of agricultural and food chemistry. 58(8):4983–4991. doi:10.1021/jf9045123

Al Naggar Y, Tan Y, Rutherford C, Connor W, Griebel P, Giesy JP, Robertson AJ. **2015**. Effects of treatments with Apivar® and Thymovar® on *V. destructor* populations, virus infections and indoor winter survival of Canadian honey bee (*Apis mellifera* L.) colonies. Journal of Apicultural Research. 54(5):548–554. doi:10.1080/00218839.2016.1186917.

Alattal Y, AlGhamdi A, Single A, Ansari MJ, Alkathiri H. **2017**. Fertility and reproductive rate of *Varroa* mite, *Varroa destructor*, in native and exotic honeybee, *Apis mellifera* L., colonies under Saudi Arabia conditions. Saudi journal of biological sciences. 24(5):992–995. doi:10.1016/j.sjbs.2016.12.018.

Albeltagy M. **2021**. A new formula for evaluating the effectiveness of insecticides against cotton bollworm under Egyptian conditions, instead of the Henderson and Tilton (1955) formula Abdallah. 4:499–504.

Aldea-Sánchez P, Ramírez-Cáceres GE, Rezende EL, Bozinovic F. **2021**. Heat tolerance, energetics, and thermal treatments of honeybees parasitized with *Varroa*. Frontiers in Ecology and Evolution. 9:656504. doi:10.3389/fevo.2021.656504.

Aliano NP, Ellis MD. **2005**. A strategy for using powdered sugar to reduce varroa populations in honey bee colonies. Journal of Apicultural Research. 44(2):54–57. doi:10.1080/00218839.2005.11101148.

Alptekin S, Bass C, Nicholls C, Paine MJ, Clark SJ, Field L, Moores GD. **2016**. Induced thiacloprid insensitivity in honeybees (*Apis mellifera* L.) is associated with up-regulation of detoxification genes. Insect Molecular Biology. 25(2):171–180. doi:10.1016/j.envpol.2020.115297.

Alquisira-Ramírez EV, Paredes-Gonzalez JR, Hernández-Velázquez VM, Ramírez-Trujillo JA, Peña-Chora G. **2014**. In vitro susceptibility of *Varroa destructor* and *Apis mellifera* to native strains of *Bacillus thuringiensis*. Apidologie. 45:707–718. doi:10.1007/s13592-014-0288-z.

Altschul SF, Gish W, Miller W, Myers EW, Lipman DJ. **1990**. Basic local alignment search tool. Journal of molecular biology. 215(3):403–410. doi:10.1016/S0022-2836(05)80360-2.

Amdam GV, Hartfelder K, Norberg K, Hagen A, Omholt SW. **2004**. Altered physiology in worker honey bees (Hymenoptera: Apidae) infested with the mite *Varroa destructor* (Acari: Varroidae): a factor in colony loss during overwintering? Journal of Economic Entomology. 97(3):741–747. doi:10.1093/jee/97.3.741. doi:10.1093/jee/97.3.741.

Amiri E, Kryger P, Meixner MD, Strand MK, Tarpy DR, Rueppell O. **2018**. Quantitative patterns of vertical transmission of deformed wing virus in honey bees. PLoS One. 13(3):e0195283. doi:10.1371/journal.pone.0195283.

Amiri E, Strand MK, Tarpy DR, Rueppell O. **2020**. Honey bee queens and virus infections. Viruses. 12(3):322. doi:10.3390/v12030322.

Anders S, Pyl PT, Huber W. **2015**. HTSeq—a Python framework to work with high-throughput sequencing data. bioinformatics. 31(2):166–169. doi:10.1093/bioinformatics/btu638.

Anderson DL, Fuchs S. **1998**. Two genetically distinct populations of *Varroa jacobsoni* with contrasting reproductive abilities on *Apis mellifera*. Journal of Apicultural Research. 37(2):69–78. doi:10.1080/00218839.1998.11100957.

Anderson DL, Trueman JWH. **2000**. *Varroa jacobsoni* (Acari: Varroidae) is more than one species. Experimental & Applied Acarology. 24(3):165–189. doi:10.1023/A:1006456720416.

Anderson KE, Maes P. **2022**. Social microbiota and social gland gene expression of worker honey bees by age and climate. Scientific Reports. 12(1):10690. doi:10.1038/s41598-022-14442-0.

Andino GK, Gribskov M, Anderson DL, Evans JD, Hunt GJ. **2016**. Differential gene expression in *Varroa jacobsoni* mites following a host shift to European honey bees (*Apis mellifera*). BMC Genomics. 17(1):926. doi:10.1186/s12864-016-3130-3.

Andrews S. **2010**. FastQC: a quality control tool for high throughput sequence data. https://www.bioinformatics.babraham.ac.uk/projects/fastqc/.

Ardestani MM. **2022**. Investigating the influence of postcapping period on varroa mite infestation. Journal of Apicultural Research. 54(4):335–341. doi:10.1080/00218839.2016.1159788.

Arechavaleta-Velasco ME, Guzmán-Novoa E. **2001**. Relative effect of four characteristics that restrain the population growth of the mite *Varroa destructor* in honey bee (*Apis mellifera*) colonies. Apidologie. 32(2):157–174. doi:10.1051/apido:2001121.

Arechavaleta-Velasco ME, Alcala-Escamilla K, Robles-Rios C, Tsuruda JM, Hunt GJ. **2012**. Fine-scale linkage mapping reveals a small set of candidate genes influencing honey bee grooming behavior in response to *Varroa* mites. PLoS One. 7(11):e47269. doi:10.1371/journal.pone.0047269.

Ashburner M, Ball CA, Blake JA, Botstein D, Butler H, Cherry JM, Davis AP, Dolinski K, Dwight SS, Eppig JT, et al. 2000. Gene Ontology: tool for the unification of biology. Nature Genetics. 25(1):25–29. doi:10.1038/75556.

Ashman T-L, Knight TM, Steets JA, Amarasekare P, Burd M, Campbell DR, Dudash MR, Johnston MO, Mazer SJ, Mitchell RJ, et al. 2004. Pollen limitation of plant reproduction: Ecological and evolutionary causes and consequences. Ecology. 85(9):2408–2421. doi:10.1890/03-8024.

Bacandritsos N, Papanastasiou I, Saitanis C, Nanetti A, Roinioti E. **2007**. Efficacy of repeated trickle applications of oxalic acid in syrup for varroosis control in *Apis mellifera*: Influence of meteorological conditions and presence of brood. Veterinary Parasitology. 148(2):174–178. doi:10.1016/j.vetpar.2007.06.001.

Bahreini R, Currie RW. **2015**. The potential of bee-generated carbon dioxide for control of varroa mite (Mesostigmata: Varroidae) in indoor overwintering honey bee (Hymenoptera: Apidae) colonies. Journal of Economic Entomology. 108(5):2153–2167. doi:10.1093/jee/tov202.

Bahreini R, Tahmasebi G, Nowzari J, Talebi M. **2004**. A study of the efficacy of formic acid in controlling *Varroa destructor* and its correlation with temperature in Iran. Journal of Apicultural Research. 43(4):158–161. doi:10.1080/00218839.2004.11101129.

Bahreini R, Nasr M, Docherty C, de Herdt O, Muirhead S, Feindel D. **2020**. Evaluation of potential miticide toxicity to *Varroa destructor* and honey bees, *Apis mellifera*, under laboratory conditions. Scientific Reports. 10(1):21529. doi:10.1038/s41598-020-78561-2.

Bahreini R, Nasr M, Docherty C, Feindel D, Muirhead S, de Herdt O. 2021. New bioassay cage methodology for in vitro studies on *Varroa destructor* and *Apis mellifera*. PLoS One. 16(4):e0250594. doi:10.1371/journal.pone.0250594.

Bahreini R, Nasr M, Docherty C, Muirhead S, de Herdt O, Feindel D. **2022**. Miticidal activity of fenazaquin and fenpyroximate against *Varroa destructor*, an ectoparasite of *Apis mellifera*. Pest Management Science. 78:1686–1679. doi:10.1002/ps.6788.

Bahreini R, Docherty C, Feindel D, Muirhead S. **2024**. Comparing the efficacy of synthetic varroacides and *Varroa destructor* phenotypic resistance using apiarium and mason jar bioassay techniques. Pest Management Science. 80(3):1577–1592. doi:10.1002/ps.7891.

Bailey L, Gibbs A, Woods R. **1963**. Two viruses from adult honey bees (*Apis mellifera* Linnaeus). Virology. 21(3):390–395. doi:10.1016/0042-6822(63)90200-9.

Bąk B, Wilde J. **2015**. Grooming behavior by worker bees of various subspecies of honey bees to remove *Varroa destructor* mites. Journal of Apicultural Research. 54(3):207–215. doi:10.1080/00218839.2016.1147791.

Bąk B, Wilde J, Siuda M. **2012**. Characteristics of north-eastern population of *Varroa destructor* resistant to synthetic pyrethroids. Medycyna Weterynaryjna. 68(10):603–6.

Bąk B, Wilde J, Siuda M, Wilk J. **2021**. *Varroa*cide effectiveness of polyvar yellow (flumethrin 275 mg) preparation. Journal of Apicultural Science. 65(1):189–193. doi:10.2478/jas-2021-0011.

Balint A, DĂRĂBUŞ G, Oprescu I, Morariu S, MEDERLE N, Ilie M, Imre K, HOTEA I, Indre D, SORESCU D. **2010**. In vitro effectiveness study of some acaricides substances used in the *Varroa destructor* mite control. Lucrari Stiintifice-Universitatea de Stiinte Agricole a Banatului Timisoara, Medicina Veterinara. 43(1):45–48.

Becher MA, Hildenbrandt H, Hemelrijk CK, Moritz RF. **2010**. Brood temperature, task division and colony survival in honeybees: A model. Ecological Modelling. 221(5):769–776.

Becher MA, Osborne JL, Thorbek P, Kennedy PJ, Grimm V. **2013**. REVIEW: Towards a systems approach for understanding honeybee decline: a stocktaking and synthesis of existing models. Journal of Applied Ecology. 50(4):868–880. doi:10.1111/1365-2664.12112.

Benito-Murcia M, Bartolomé C, Maside X, Bernal J, Bernal JL, Del Nozal MJ, Meana A, Botías C, Martín-Hernández R, Higes M. **2021**. Residual tau-fluvalinate in honey bee colonies is coupled with evidence for selection for *Varroa destructor* resistance to pyrethroids. Insects. 12(8):731. doi:10.3390/insects12080731.

Berenbaum MR, Johnson RM. **2015**. Xenobiotic detoxification pathways in honey bees. Current Opinion in Insect Science. 10:51–58. doi:10.1016/j.cois.2015.03.005.

Berry JA, Hood WM, Pietravalle S, Delaplane KS. **2013**. Field-level sublethal effects of approved bee hive chemicals on honey bees (*Apis mellifera* L). PLoS One. 8(10):e76536. doi:10.1371/journal.pone.0076536.

Biddinger DJ, Rajotte EG. **2015**. Integrated pest and pollinator management—adding a new dimension to an accepted paradigm. Current Opinion in Insect Science. 10:204–209. doi:10.1016/j.cois.2015.05.012

Bollhalder F. **1998**. Thymovar for *Varroa* control. Schweiz Bienen-Zeitung. 121(3):148–151.

Bommuraj V, Chen Y, Birenboim M, Barel S, Shimshoni JA. **2021**. Concentration- and time-dependent toxicity of commonly encountered pesticides and pesticide mixtures to honeybees (*Apis mellifera* L.). Chemosphere. 266:128974. doi:10.1016/j.chemosphere.2020.128974.

Boot WJ, Calis JN, Beetsma J. **1992**. Differential periods of *Varroa* mite invasion into worker and drone cells of honey bees. Experimental & applied acarology. 16:295–301. doi:10.1007/bf01218571.

Boot WJ, Calis JN, Beetsma J, Hai DM, Lan NK, Toan TV, Trung LQ, Minh NH. **1999**. Natural selection of *Varroa jacobsoni* explains the different reproductive strategies in colonies of *Apis cerana* and *Apis mellifera*. Experimental & applied acarology. 23:133–144. doi:10.1023/A:1006050527004.

Boot WJ, Tan NQ, Dien PC, Huan LV, Dung NV, Long LT, Beetsma J. **1997**. Reproductive success of *Varroa jacobsoni* in brood of its original host, *Apis cerana*, in comparison to that of its new host, *A. mellifera* (Hymenoptera: Apidae). Bulletin of Entomological Research. 87(2):119–126. doi:10.1017/S0007485300027255. doi:10.1017/S0007485300027255.

Borba RS, Hoover SE, Currie RW, Giovenazzo P, Guarna MM, Foster LJ, Zayed A, Pernal SF. **2022**. Phenomic analysis of the honey bee pathogen-web and its dynamics on colony productivity, health and social immunity behaviors. PLoS One. 17(1):e0263273. doi:10.1371/journal.pone.0263273.

Bouuaert DC, De Smet L, de Graaf DC. **2021**. Breeding for virus resistance and its effects on deformed wing virus infection patterns in honey bee queens. Viruses. 13(6):1074. doi:10.3390/v13061074.

Brasesco C, Gende L, Negri P, Szawarski N, Iglesias A, Eguaras M, Ruffinengo S, Maggi M. **2017**. Assessing in vitro acaricidal effect and joint action of a binary mixture between essential oil compounds (thymol, phellandrene, eucalyptol, cinnamaldehyde, myrcene, carvacrol) over ectoparasitic mite *Varroa destructor* (Acari: Varroidae). Journal of Apicultural Science. 61(2):203–215. doi:10.1515/jas-2017-0008.

Bresnahan ST, Döke MA, Giray T, Grozinger CM. **2022**. Tissue-specific transcriptional patterns underlie seasonal phenotypes in honey bees (*Apis mellifera*). Molecular ecology. 31(1):174–184. doi:10.1111/mec.16220.

Brodschneider R, Gray A. **2022**. How COLOSS monitoring and research on lost honey bee colonies can support colony survival. Bee World. 99(1):8–10. doi:10.1080/0005772X.2021.1993611.

Brown P, Newstrom-Lloyd LE, Foster BJ, Badger PH, McLean JA. **2018**. Winter 2016 honey bee colony losses in New Zealand. Journal of Apicultural Research. 57(2):278–291. doi:10.1080/00218839.2018.1430980.

Bruckner S, Wilson M, Aurell D, Rennich K, vanEngelsdorp D, Steinhauer N, Williams GR. **2023**. A national survey of managed honey bee colony losses in the USA: results from the Bee Informed Partnership for 2017–18, 2018–19, and 2019–20. Journal of Apicultural Research. 62(3):429–443. doi:10.1080/00218839.2022.2158586.

Calderón RA, Fallas N, Zamora LG, van Veen JW, Sánchez LA. **2009**. Behavior of varroa mites in worker brood cells of Africanized honey bees. Experimental and Applied Acarology. 49(4):329–338. doi:10.1007/s10493-009-9266-y.

Calderón RA, Ortiz RA, Arce HG, van Veen JW, Quan J. **2000**. Effectiveness of formic acid on varroa mortality in capped brood cells of Africanized honey bees. Journal of Apicultural Research. 39(3–4):177–179. doi:10.1080/00218839.2000.11101039.

Calderón RA, van Veen JW, Sommeijer MJ, Sanchez LA. **2010**. Reproductive biology of *Varroa destructor* in Africanized honey bees (*Apis mellifera*). Experimental and Applied Acarology. 50(4):281–297. doi:10.1007/s10493-009-9325-4.

Calderone NW. **2005**. Evaluation of drone brood removal for management of *Varroa destructor* (Acari: Varroidae) in colonies of *Apis mellifera* (Hymenoptera: Apidae) in the northeastern United States. Journal of Economic Entomology. 98(3):645–650. doi:10.1603/0022-0493-98.3.645.

Calderone NW. **2012**. Insect pollinated crops, insect pollinators and US agriculture: Trend analysis of aggregate data for the period 1992–2009. PLoS One. 7(5):e37235. doi:10.1371/journal.pone.0037235.

Calis J, Boot W, Beetsma J, van Den Eijnde J, De Ruijter A, van Der Steen J. **1998**. Control of varroa by combining trapping in honey bee worker brood with formic acid treatment of the capped brood outside the colony: putting knowledge on brood cell invasion into practice. Journal of Apicultural Research. 37(3):205–215. doi:10.1080/00218839.1998.11100973.

Cameron LM, Rogers M, Aalhus M, Seward B, Yu Y, Plettner E. **2014**. Feeding deterrence of cabbage looper (Lepidoptera: Noctuidae) by 1-allyloxy-4-propoxybenzene, alone and blended with neem extract. Journal of Economic Entomology. 107(6):2119–2129. doi:10.1603/EC14259.

Canadian Association of Professional Apiculturists (CAPA). **1995**. A guide to managing bees for crop pollination.

Charpentier G, Vidau C, Ferdy J, Tabart J, Vetillard A. **2014**. Lethal and sub-lethal effects of thymol on honeybee (*Apis mellifera*) larvae reared in vitro. Pest management science. 70(1):140–147. doi:10.1002/ps.3539.

Chen YP, Siede R. **2007**. Honey bee viruses. Advances in Virus Research. 70:33–80. doi:10.1016/S0065-3527(07)70002-7.

Chen Y, Evans J, Feldlaufer M. **2006**. Horizontal and vertical transmission of viruses in the honey bee, *Apis mellifera*. Journal of Invertebrate Pathology. 92(3):152–159. doi:10.1016/j.jip.2006.03.010.

Chen YP, Pettis JS, Corona M, Chen WP, Li CJ, Spivak M, Visscher PK, DeGrandi-Hoffman G, Boncristiani H, Zhao Y, et al. 2014. Israeli acute paralysis virus: Epidemiology, pathogenesis and implications for honey bee health. PLOS Pathogens. 10(7):e1004261. doi:10.1371/journal.ppat.1004261.

Chougule NP, Li H, Liu S, Linz LB, Narva KE, Meade T, Bonning BC. **2013**. Retargeting of the *Bacillus thuringiensis* toxin Cyt2Aa against hemipteran insect pests. Proceedings of the National Academy of Sciences. 110(21):8465–8470. doi:10.1073/pnas.1222144110.

Claing G, Kempers M, Kozak P, Maund C, Menzies C, Micholson D, Morfin N, Muirhead S, Nasr M, Pernal S, et al. 2023. Statement on honey bee wintering losses in Canada for 2023. https://capabees.com/shared/CAPA-Statement-on-Colony-Losses-2022-2023.pdf.

Coffey MF, Breen J, Brown MJ, McMullan JB. **2010**. Brood-cell size has no influence on the population dynamics of *Varroa destructor* mites in the native western honey bee, *Apis mellifera* mellifera. Apidologie. 41(5):522–530. doi:10.1051/apido/2010003.

Collins AM, Pettis JS, Wilbanks R, Feldlaufer MF. **2004**. Performance of honey bee (*Apis mellifera*) queens reared in beeswax cells impregnated with coumaphos. Journal of Apicultural Research. 43(3):128–134. doi:10.1080/00218839.2004.11101123.

Cook SC, Johnson JD, Rogers CW, Sachs IE, Feng X, Plettner E. **2024**. The efficacy of 1-allyloxy-4-propoxybenzene (3c{3,6}) against *Varroa destructor* mites in honey bee colonies from Maryland, USA. Journal of Insect Science. 24(3):9. doi:10.1093/jisesa/iead111.

Corbel V, Stankiewicz M, Pennetier C, Fournier D, Stojan J, Girard E, Dimitrov M, Molgó J, Hougard J-M, Lapied B. **2009**. Evidence for inhibition of cholinesterases in insect and mammalian nervous systems by the insect repellent DEET. BMC Biology. 7(1):1–11. doi:10.1186/1741-7007-7-47.

Cornman RS, Tarpy DR, Chen Y, Jeffreys L, Lopez D, Pettis JS, Vanengelsdorp D, Evans JD. **2012**. Pathogen webs in collapsing honey bee colonies. PLoS One. 7(8): e43562. doi:10.1371/journal.pone.0043562.

Currie R. **2008**. Economic threshold for *Varroa* on the Canadian Prairies. Canadian Association of Professional Apiculturists (CAPA) http://capabeesorg/content/uploads/2013/02/varroathresholdpdf.

Currie R, Gatien P. **2006**. Timing acaricide treatments to prevent *Varroa destructor* (Acari: Varroidae) from causing economic damage to honey bee colonies. The Canadian Entomologist. 138(2):238–252. doi:10.4039/n05-024.

Currie R, Tahmasbi G. **2008**. The ability of high-and low-grooming lines of honey bees to remove the parasitic mite *Varroa destructor* is affected by environmental conditions. Canadian Journal of Zoology. 86(9):1059–1067. doi:10.1139/Z08-083.

Currie RW, Pernal SF, Guzmán-Novoa E. **2010**. Honey bee colony losses in Canada. Journal of Apicultural Research. 49(1):104–106. doi:10.3896/IBRA.1.49.1.18. doi:10.3896/IBRA.1.49.1.18.

Dai C, Lin B, Xing X, Liu JS. **2023**. A scale-free approach for false discovery rate control in generalized linear models. Journal of the American Statistical Association. 118(543):1551–1565. doi:10.1080/01621459.2023.2165930.

Damiani N, Gende LB, Bailac P, Marcangeli JA, Eguaras MJ. **2009**. Acaricidal and insecticidal activity of essential oils on *Varroa destructor* (Acari: Varroidae) and *Apis mellifera* (Hymenoptera: Apidae). Parasitology Research. 106(1):145–152. doi:10.1007/s00436-009-1639-y.

Danecek P, Bonfield JK, Liddle J, Marshall J, Ohan V, Pollard MO, Whitwham A, Keane T, McCarthy SA, Davies RM, et al. 2021. Twelve years of SAMtools and BCFtools. GigaScience. 10(2):giab008. doi:10.1093/gigascience/giab008.

Davidson G, Phelps K, Sunderland K, Pell J, Ball B, Shaw K, Chandler D. **2003**. Study of temperature–growth interactions of entomopathogenic fungi with potential for control of *Varroa destructor* (Acari: Mesostigmata) using a nonlinear model of poikilotherm development. Journal of Applied Microbiology. 94(5):816–825. doi:10.1046/j.1365-2672.2003.01871.x.

Dawdani S. **2020**. Evaluating the effects of 1-allyloxy-4-propoxybenzene on the parasitic mite *Varroa destructor* and synthesis of fluorescent probes to visualize the binding location(s) of the active compound in the mite. Master's thesis. https://summit.sfu.ca/item/34430.

Dawdani S, O'Neill M, Castillo C, Sámano JEM, Higo H, Ibrahim A, Pernal SF, Plettner E. **2023**. Effects of dialkoxybenzenes against *Varroa destructor* and identification of 1-allyloxy-4-propoxybenzene as a promising acaricide candidate. Scientific Reports. 13(1):11195. doi:10.1038/s41598-023-38187-6.

De Jong D, Roma DDA, Goncalves L. **1982**. A comparative analysis of shaking solutions for the detection of *Varroa jacobsoni* on adult honeybees. Apidologie. 13(3):297–306. doi:10.1051/apido:19820308.

Decanini LI, Collins AM, Evans JD. **2007**. Variation and heritability in immune gene expression by diseased honeybees. Journal of Heredity. 98(3):195–201. doi:10.1093/jhered/esm008.

DeGrandi-Hoffman G, Ahumada F, Probasco G, Schantz L. **2012**. The effects of beta acids from hops (*Humulus lupulus*) on mortality of *Varroa destructor* (Acari: Varroidae). Experimental and Applied Acarology. 58(4):407–421. doi:10.1007/s10493-012-9593-2. doi:10.1007/s10493-012-9593-2.

DeGrandi-Hoffman G, Ahumada F, Graham H. **2017**. Are dispersal mechanisms changing the host–parasite relationship and increasing the virulence of *Varroa destructor* (Mesostigmata: Varroidae) in managed honey bee (Hymenoptera: Apidae) colonies? Environmental Entomology. 46(4):737–746. doi:10.1093/ee/nvx077.

Delfinado MD, Baker EW. **1974**. Varroidae, a new family of mites on honey bees (Mesostigmata: Acarina). Journal of the Washington Academy of Sciences. 4–10. https://www.jstor.org/stable/24535743.

Dennehy TJ, Farnham AW, Denholm I. **1993**. The microimmersion bioassay: a novel method for the topical application of pesticides to spider mites. Pesticide Science. 39(1):47–54. doi:10.1002/ps.2780390107.

Desai SD, Eu Y-J, Whyard S, Currie RW. **2012**. Reduction in deformed wing virus infection in larval and adult honey bees (*Apis mellifera* L.) by double-stranded RNA ingestion. Insect Molecular Biology. 21(4):446–455. doi:10.1111/j.1365-2583.2012.01150.x.

Devi S, Devi M, Barwar C. **2019**. Different methods for the management of varroa mite (*Varroa destructor*) in honey bee colony. Journal of Entomology and Zoology StudiesStud. 7:178–182. E-ISSN:2320-7078.

Di Prisco G, Cavaliere V, Annoscia D, Varricchio P, Caprio E, Nazzi F, Gargiulo G, Pennacchio F. **2013**. Neonicotinoid clothianidin adversely affects insect immunity and promotes replication of a viral pathogen in honey bees. Proceedings of the National Academy of Sciences. 110(46):18466–18471. doi:10.1073/pnas.1314923110.

DiAntonio A, Schwarz TL. **1994**. The effect on synaptic physiology of synaptotagmin mutations in drosophila. Neuron. 12(4):909–920. doi:10.1016/0896-6273(94)90342-5.

Dietemann V, Nazzi F, Martin SJ, Anderson DL, Locke B, Delaplane KS, Wauquiez Q, Tannahill C, Frey E, Ziegelmann B, et al. 2013. Standard methods for varroa research. Journal of Apicultural Research. 52(1):1–54. doi:10.3896/IBRA.1.52.1.09.

Dillier F-X, Fluri P, Imdorf A. **2006**. Review of the orientation behaviour in the bee parasitic mite *Varroa destructor*: sensory equipment and cell invasion behaviour. Revue suisse de zoologie. 113(4):857–878. doi:10.5962/bhl.part.80381.

Doeke MA, Frazier M, Grozinger CM. **2015**. Overwintering honey bees: biology and management. Current Opinion in Insect Science. 10:185–193. doi:10.1016/j.cois.2015.05.014.

Donovan BJ, Paul F. **2005**. Pseudoscorpions: the forgotten beneficials inside beehives and their potential for management for control of varroa and other arthropod pests. Bee World. 86(4):83–87. doi:10.1080/0005772X.2005.11417322.

Donovan BJ, Paul F. **2006**. Pseudoscorpions to the rescue? American Bee Journal. 146(10):867–869. ISSN:0002-7626.

Donzé G, Guerin PM. **1994**. Behavioral attributes and parental care of *Varroa* mites parasitizing honeybee brood. Behavioral Ecology and Sociobiology. 34:305–319. doi:10.1007/BF00197001.

Dos Santos VM, Heim S, Moore E, Strätz M, Timmis K. **2004**. Insights into the genomic basis of niche specificity of *Pseudomonas putida* KT2440. Environmental microbiology. 6(12):1264–1286. doi:10.1111/j.1462-2920.2004.00734.x.

Doublet V, Oddie MAY, Mondet F, Forsgren E, Dahle B, Furuseth-Hansen E, Williams GR, De Smet L, Natsopoulou ME, Murray TE, et al. 2024. Shift in virus composition in honeybees (*Apis mellifera*) following worldwide invasion by the parasitic mite and virus vector *Varroa destructor*. Royal Society Open Science. 11(1):231529. doi:10.1098/rsos.231529.

Dowling APG, OConnor BM. **2010**. Phylogeny of Dermanyssoidea (Acari: Parasitiformes) suggests multiple origins of parasitism. Acarologia. 50(1):113–129. doi:10.1051/acarologia/20101957.

Dresbach T, Qualmann B, Kessels M, Garner C, Gundelfinger E. **2001**. The presynaptic cytomatrix of brain synapses. Cellular and Molecular Life Sciences CMLS. 58:94–116. doi:10.1007/PL00000781.

Drezner-Levy T, Smith BH, Shafir S. **2009**. The effect of foraging specialization on various learning tasks in the honey bee (*Apis mellifera*). Behavioral Ecology and Sociobiology. 64:135–148. doi:10.1007/s00265-009-0829-z.

Ebrahimi P, Plettner E. **2014**. Biodegradation of 1-allyloxy-4-propoxybenzene by selected strains of *Pseudomonas putida*. Biodegradation. 25:31–39. doi:10.1007/s10532-013-9638-1.

Ebrahimi P, Spooner J, Weinberg N, Plettner E. **2013**. Partition, sorption and structure activity relation study of dialkoxybenzenes that modulate insect behavior. Chemosphere. 93(1):54–60. doi:10.1016/j.chemosphere.2013.04.065.

Eilers EJ, Kremen C, Smith Greenleaf S, Garber AK, Klein A-M. **2011**. Contribution of pollinator-mediated crops to nutrients in the human food supply. PLoS One. 6(6):e21363. doi:10.1371/journal.pone.0021363.

Elhamdani A, Martin TF, Kowalchyk JA, Artalejo CR. **1999**. Ca^{2+}-dependent activator protein for secretion is critical for the fusion of dense-core vesicles with the membrane in calf adrenal chromaffin cells. Journal of Neuroscience. 19(17):7375–7383. doi:10.1523/JNEUROSCI.19-17-07375.1999.

Ellis A, Hayes G, Ellis J. **2009**. The efficacy of small cell foundation as a varroa mite (*Varroa destructor*) control. Experimental and Applied Acarology. 47(4):311–316. doi:10.1007/s10493-008-9221-3.

Elzen P, Westervelt D. **2002**. Detection of coumaphos resistance in *Varroa destructor* in Florida. American Bee Journal. 142(4):291–292. ISSN:0002-7626.

Erban T, Harant K, Hubalek M, Vitamvas P, Kamler M, Poltronieri P, Tyl J, Markovic M, Titera D. **2015**. In-depth proteomic analysis of *Varroa destructor*: Detection of DWV-complex, ABPV, VdMLV and honeybee proteins in the mite. Scientific Reports. 5(1):13907. doi:10.1038/srep13907.

Erez T, Bonda E, Kahanov P, Rueppell O, Wagoner K, Chejanovsky N, Soroker V. **2022**. Multiple benefits of breeding honey bees for hygienic behavior. Journal of Invertebrate Pathology. 193:107788. doi:10.1016/j.jip.2022.107788.

Evans JD, Cook SC. **2018**. Genetics and physiology of *Varroa* mites. Current Opinion in Insect Science. 26:130–135. doi:10.1016/j.cois.2018.02.005.

Evans JD, Schwarz RS. **2011**. Bees brought to their knees: microbes affecting honey bee health. Trends in microbiology. 19(12):614–620. doi:10.1016/j.tim.2011.09.003.

Evans KC, Underwood RM, López-Uribe MM. **2022**. Combined effects of oxalic acid sublimation and brood breaks on *Varroa* mite (*Varroa destructor*) and deformed wing virus levels in newly established honey bee (*Apis mellifera*) colonies. Journal of Apicultural Research. 61(2):197–205. doi:10.1080/00218839.2021.1985260.

Fagan L, Nelson W, Meenken E, Howlett B, Walker M, Donovan B. **2012**. *Varroa* management in small bites. Journal of Applied Entomology. 136(6):473–475. doi:10.1111/j.1439-0418.2011.01666.x.

Fanelli A, Tizzani P. **2020**. Spatial and temporal analysis of varroosis from 2005 to 2018. Research in Veterinary Science. 131:215–221. doi:10.1016/j.rvsc.2020.04.017.

Ferrer-Dufol M, Martinez-Vinuales AI, Sanchez-Acedo C. **1991**. Comparative tests of fluvalinate and flumethrin to control *Varroa jacobsoni* Oudemans. Journal of apicultural research. 30(2):103–106. doi:10.1080/00218839.1991.11101241.

Field LM, Emyr Davies TG, O'reilly AO, Williamson MS, Wallace BA. **2017**. Voltage-gated sodium channels as targets for pyrethroid insecticides. European biophysics journal. 46:675–679. doi:10.1007/s00249-016-1195-1.

Fleming R, Retnakaran A. **1985**. Evaluating single treatment data using Abbott's formula with reference to insecticides. Journal of Economic Entomology. 78(6):1179–1181. doi:10.1093/jee/78.6.1179.

Floris I, Cabras P, Garau VL, Minelli EV, Satta A, Troullier J. **2001**. Persistence and effectiveness of pyrethroids in plastic strips against *Varroa jacobsoni* (Acari: Varroidae) and mite resistance in a Mediterranean area. Journal of Economic Entomology. 94(4):806–810. doi:10.1603/0022-0493-94.4.806.

Fombong AT, Cham DT, Nkoba K, Neethling JA, Raina SK. **2016**. Occurrence of the pseudoscorpions Ellingsenius ugandanus and Paratemnoides pallidus in honey bee colonies in Cameroon. Journal of Apicultural Research. 55(3):247–250. doi:10.1080/00218839.2016.1227553.

Forêt S, Maleszka R. **2006**. Function and evolution of a gene family encoding odorant binding-like proteins in a social insect, the honey bee (*Apis mellifera*). Genome research. 16(11):1404–1413. doi:10.1101/gr.5075706.

Fotoukkiaii SM, Mermans C, Wybouw N, Van Leeuwen T. **2020**. Resistance risk assessment of the novel complex II inhibitor pyflubumide in the polyphagous pest *Tetranychus urticae*. Journal of Pest Science. 93(3):1085–1096. doi:10.1007/s10340-020-01213-x.

Frey E, Rosenkranz P. **2014**. Autumn invasion rates of *Varroa destructor* (Mesostigmata: Varroidae) into honey bee (Hymenoptera: Apidae) colonies and the resulting increase in mite populations. Journal of Economic Entomology. 107(2):508–515. doi:10.1603/EC13381.

Frey E, Odemer R, Blum T, Rosenkranz P. **2013**. Activation and interruption of the reproduction of *Varroa destructor* is triggered by host signals (*Apis mellifera*). Journal of Invertebrate Pathology. 113(1):56–62. doi:10.1016/j.jip.2013.01.007.

Gabel M, Scheiner R, Büchler R. **2023**. Immediate and long-term effects of induced brood interruptions on the reproductive success of *Varroa destructor*. Apidologie. 54(2):20. doi:10.1007/s13592-023-00998-x.

Gagliardi B, Long SM, Pettigrove VJ, Griffin PC, Hoffmann AA. **2019**. A re-evaluation of chironomid deformities as an environmental stress response: Avoiding survivorship bias and testing noncontaminant biological factors. Environmental Toxicology and Chemistry. 38(8):1658–1667. doi:10.1002/etc.4446.

Galbraith DA, Yang X, Nino EL, Yi S, Grozinger C. **2015**. Parallel epigenomic and transcriptomic responses to viral infection in honey bees (*Apis mellifera*). PLoS Pathogens. 11(3):e1004713. doi:10.1371/journal.ppat.1004713.

Gallai N, Salles J-M, Settele J, Vaissière BE. **2009**. Economic valuation of the vulnerability of world agriculture confronted with pollinator decline. Ecological Economics. 68(3):810–821. doi:10.1371/journal.ppat.1004713.

Gallego Romero I, Pai AA, Tung J, Gilad Y. **2014**. RNA-seq: impact of RNA degradation on transcript quantification. BMC Biology. 12:1–13. doi:10.1186/1741-7007-12-42.

Garbian Y, Maori E, Kalev H, Shafir S, Sela I. **2012**. Bidirectional transfer of RNAi between honey bee and *Varroa destructor*: *Varroa* gene silencing reduces *Varroa* population. PLoS pathogens. 8(12):e1003035. doi:10.1371/journal.ppat.1003035.

García-López J, Herrera-Medina R, Rendón-Huerta J, Negrete-Sánchez L, Lee-Rangel H, Álvarez-Fuentes G. 2024. Acaricide potential of creosote bush (*Larrea tridentata*) extracts in the control of *Varroa destructor* in *Apis mellifera*. Journal of Applied Life Sciences International. 27(3):7–20. doi:10.9734/jalsi/2024/v27i3643.

Garedew A, Schmolz E, Lamprecht I. 2004. The energy and nutritional demand of the parasitic life of the mite *Varroa destructor*. Apidologie. 35(4):419–430. doi:10.1051/apido:2004032.

Garibaldi LA, Steffan-Dewenter I, Winfree R, Aizen MA, Bommarco R, Cunningham SA, Kremen C, Carvalheiro LG, Harder LD, Afik O. 2013. Wild pollinators enhance fruit set of crops regardless of honey bee abundance. science. 339(6127):1608–1611. doi:10.1126/science.1230200.

Gashout HA, Guzmán-Novoa E. 2009. Acute toxicity of essential oils and other natural compounds to the parasitic mite, *Varroa destructor*, and to larval and adult worker honey bees (*Apis mellifera* L.). Journal of apicultural research. 48(4):263–269. doi:10.3896/IBRA.1.48.4.06.

Gashout HA, Guzman-Novoa E, Goodwin PH, Correa-Benítez A. 2020. Impact of sublethal exposure to synthetic and natural acaricides on honey bee (*Apis mellifera*) memory and expression of genes related to memory. Journal of insect physiology. 121:104014. doi:10.1016/j.jinsphys.2020.104014.

Genath A, Sharbati S, Buer B, Nauen R, Einspanier R. 2020. Comparative transcriptomics indicates endogenous differences in detoxification capacity after formic acid treatment between honey bees and varroa mites. Scientific Reports. 10(1):21943. doi:10.1038/s41598-020-79057-9.

Genath A, Petruschke H, von Bergen M, Einspanier R. 2021. Influence of formic acid treatment on the proteome of the ectoparasite *Varroa destructor*. PLoS One. 16(10):e0258845. doi:10.1371/journal.pone.0258845.

Genersch E. 2010. Honey bee pathology: current threats to honey bees and beekeeping. Applied Microbiology and Biotechnology. 87:87–97. doi:10.1007/s00253-010-2573-8.

Ghasemi V, Zarbaf Z, Amini M. 2024. Comparing the efficacy of alcohol wash and powdered sugar methods to dislodge the *Varroa* mite from the body of the adult honey bee. Journal of Entomological Society of Iran.(Articles in Press).

Giacobino A, Molineri A, Cagnolo NB, Merke J, Orellano E, Bertozzi E, Masciángelo G, Pietronave H, Pacini A, Salto C. 2015. Risk factors associated with failures of *Varroa* treatments in honey bee colonies without broodless period. Apidologie. 46:573–582. doi:10.1016/j.prevetmed.2018.09.011.

Giacomelli A, Pietropaoli M, Carvelli A, Iacoponi F, Formato G. 2016. Combination of thymol treatment (Apiguard®) and caging the queen technique to fight *Varroa destructor*. Apidologie. 47(4):606–616. doi:10.1007/s13592-015-0408-4.

Giliba RA, Mpinga IH, Ndimuligo SA, Mpanda MM. **2020**. Changing climate patterns risk the spread of *Varroa destructor* infestation of African honey bees in Tanzania. Ecological processes. 9:1–11. doi:10.1186/s13717-020-00247-4.

Gill RA. **1990**. The value of honeybee pollination to society. Acta Horticulturae. 288:62–68. doi:10.17660/ActaHortic.1991.288.4.

Giovenazzo P, Dubreuil P. **2011**. Evaluation of spring organic treatments against *Varroa destructor* (Acari: Varroidae) in honey bee *Apis mellifera* (Hymenoptera: Apidae) colonies in eastern Canada. Experimental and Applied Acarology. 55:65–76. doi:10.1007/s10493-011-9447-3.

Girişgin AO, Aydın L. **2010**. Determining the Efficacy of Flumethrin (Varostop) Against to *Varroa* Testructor in Honey Bee Colonies in Fall Season. Uludağ Arıcılık Dergisi. 10(2):70–73.

Girişgin AO, Girişgin O, Harvey M. **2013**. The first record of pseudoscorpions in honeybee hives in Turkey. Turkish Journal of Veterinary & Animal Sciences. 37(5):608–610. doi:10.3906/vet-1207-7.

Gkaleni N. **2021**. Studies of bacterial and insect cytochromes P450 in degradation of pesticides. Master's Thesis. https://summit.sfu.ca/item/34618.

Glavan G, Novak S, Božič J, Jemec Kokalj A. **2020**. Comparison of sublethal effects of natural acaricides carvacrol and thymol on honeybees. Pesticide Biochemistry and Physiology. 166:104567. doi:10.1016/j.pestbp.2020.104567.

Gong Y, Diao Q. **2017**. Current knowledge of detoxification mechanisms of xenobiotic in honey bees. Ecotoxicology. 26(1):1–12. doi:10.1007/s10646-016-1742-7.

González-Cabrera J, Rodríguez-Vargas S, Davies TE, Field LM, Schmehl D, Ellis JD, Krieger K, Williamson MS. **2016**. Novel mutations in the voltage-gated sodium channel of pyrethroid-resistant *Varroa destructor* populations from the Southeastern USA. PLoS One. 11(5):e0155332. doi:10.1371/journal.pone.0155332.

Gracia-Salinas MJ, Ferrer-Dufol M, Latorre-Castro E, Monero-Manera C, Castillo-Hernández J, Lucientes-Curd J, Peribáñez-López MA. **2006**. Detection of fluvalinate resistance in *Varroa destructor* in Spanish apiaries. Journal of Apicultural Research. 45(3):101–105. doi:10.1080/00218839.2006.11101326.

Gracia MJ, Moreno C, Ferrer M, Sanz A, Peribáñez MÁ, Estrada R. **2017**. Field efficacy of acaricides against *Varroa destructor*. PLoS One. 12(2):e0171633. doi:10.1371/journal.pone.0171633.

Gray A, Adjlane N, Arab A, Ballis A, Brusbardis V, Charrière J-D, Chlebo R, Coffey MF, Cornelissen B, Amaro da Costa C. **2020**. Honey bee colony winter loss rates for 35 countries participating in the COLOSS survey for winter 2018–2019, and the effects of a new queen on the risk of colony winter loss. Journal of Apicultural Research. 59(5):744–751. doi:10.1080/00218839.2020.1797272.

Gray A, Adjlane N, Arab A, Ballis A, Brusbardis V, Bugeja Douglas A, Cadahía L, Charrière J-D, Chlebo R, Coffey MF, et al. 2023. Honey bee colony loss rates in 37 countries using the COLOSS survey for winter 2019–2020: the combined effects of operation size, migration and queen replacement. Journal of Apicultural Research. 62(2):204–210. doi:10.1080/00218839.2022.2113329.

Gregorc A. **2005**. Efficacy of oxalic acid and apiguard against *Varroa* mites in honeybee (*Apis mellifera*) colonies. Acta Veterinaria Brno. 74(3):441–447. doi:10.2754/avb200574030441.

Gregorc A, Planinc I. **2002**. The Control of *Varroa destructor* Using Oxalic Acid. The Veterinary Journal. 163(3):306–310. doi:10.1053/tvjl.2001.0675.

Gregorc A, Sampson B. **2019**. Diagnosis of *Varroa* Mite (*Varroa destructor*) and Sustainable Control in Honey Bee (*Apis mellifera*) Colonies—A Review. Diversity. 11(12). doi:10.3390/d11120243.

Gregorc A, Knight PR, Adamczyk J. **2017**. Powdered sugar shake to monitor and oxalic acid treatments to control varroa mites (*Varroa destructor* Anderson and Trueman) in honey bee (*Apis mellifera*) colonies. Journal of Apicultural Research. 56(1):71–75. doi:10.1080/00218839.2017.1278912.

Gregorc A, Alburaki M, Sampson B, Knight PR, Adamczyk J. **2018**. Toxicity of selected acaricides to honey bees (*Apis mellifera*) and varroa (*Varroa destructor* Anderson and Trueman) and their use in controlling varroa within honey bee colonies. Insects. 9(2). doi:10.3390/insects9020055.

Gruget C, Bello O, Coleman J, Krishnakumar SS, Perez E, Rothman JE, Pincet F, Donaldson SH. **2020**. Synaptotagmin-1 membrane binding is driven by the C2B domain and assisted cooperatively by the C2A domain. Scientific Reports. 10(1):18011. doi:10.1038/s41598-020-74923-y.

Gu Z, Eils R, Schlesner M. **2016**. Complex heatmaps reveal patterns and correlations in multidimensional genomic data. Bioinformatics. 32(18):2847–2849. doi:10.1093/bioinformatics/btw313.

Guichard M, von Virag A, Dainat B. **2023**. Evaluating the potential of brood recapping to Select *Varroa destructor* (Acari: Varroidae) resistant honey bees (Hymenoptera: Apidae). Journal of Economic Entomology. 116(1):56–67. doi:10.1093/jee/toac186.

Guo L, Fan X, Qiao X, Montell C, Huang J. **2021**. An octopamine receptor confers selective toxicity of amitraz on honeybees and *Varroa* mites. eLife. 10:e68268. doi:10.7554/eLife.68268.

Guzmán-Novoa E, Eccles L, Calvete Y, Mcgowan J, Kelly PG, Correa-Benítez A. **2010**. *Varroa destructor* is the main culprit for the death and reduced populations of overwintered honey bee (*Apis mellifera*) colonies in Ontario, Canada. Apidologie. 41(4):443–450. doi:10.1051/apido/2009076.

Haarmann T, Spivak M, Weaver D, Weaver B, Glenn T. **2002**. Effects of fluvalinate and coumaphos on queen honey bees (Hymenoptera: Apidae) in two commercial queen rearing operations. Journal of Economic Entomology. 95(1):28–35. doi:10.1603/0022-0493-95.1.28.

Hamiduzzaman MM, Guzman-Novoa E, Goodwin PH, Reyes-Quintana M, Koleoglu G, Correa-Benítez A, Petukhova T. **2015**. Differential responses of Africanized and European honey bees (*Apis mellifera*) to viral replication following mechanical transmission or *Varroa destructor* parasitism. Journal of Invertebrate Pathology. 126:12–20. doi:10.1016/j.jip.2014.12.004.

Han B, Wu J, Wei Q, Liu F, Cui L, Rueppell O, Xu S. **2024**. Life-history stage determines the diet of ectoparasitic mites on their honey bee hosts. Nature Communications. 15(1):725. doi:10.1038/s41467-024-44915-x.

Harbo JR, Harris JW. **2009**. Responses to *Varroa* by honey bees with different levels of *Varroa* Sensitive Hygiene. Journal of Apicultural Research. 48(3):156–161. doi:10.3896/IBRA.1.48.3.02.

Harris JW, Sheridan AB. **2023**. Managing varroa mites in honey bee colonies. Mississippi State University Extension. Accessed 2024 Jul 1. https://extension.msstate.edu/publications/managing-varroa-mites-honey-bee-colonies.

Harris JW, Danka RG, Villa JD. **2012**. Changes in infestation, cell cap condition, and reproductive status of *Varroa destructor* (Mesostigmata: Varroidae) in brood exposed to honey bees with *Varroa* sensitive hygiene. Annals of the Entomological Society of America. 105(3):512–518. doi:10.1603/AN11188.

Häußermann CK, Ziegelmann B, Rosenkranz P. **2018**. Spermatozoa production in male *Varroa destructor* and its impact on reproduction in worker brood of *Apis mellifera*. Experimental and Applied Acarology. 74:43–54. doi:10.1007/s10493-018-0216-4.

Hawkins GP, Martin SJ. **2021**. Elevated recapping behaviour and reduced *Varroa destructor* reproduction in natural *Varroa* resistant *Apis mellifera* honey bees from the UK. Apidologie. 52:647–657. doi:10.1007/s13592-021-00852-y.

Haydak MH. **1963**. Age of nurse bees and brood rearing. Journal of Apicultural Research. 2(2):101–103. doi:10.1080/00218839.1963.11100067.

Heaf D. **2011**. Do small cells help bees cope with *Varroa*. A review. The Beekeepers Quarterly. 104:39–45.

Health Canada. **2019**. Pesticide Label Search - Health Canada. [accessed 2023 Jul 18]. https://pr-rp.hc-sc.gc.ca/ls-re/index-eng.php.

Henderson CF, Tilton EW. 1955. Tests with acaricides against the brown wheat mite. Journal of Economic Entomology. 48(2):157–161. doi:10.1093/jee/48.2.157.

Herath H, Pahalagamage S, Yogendranathan N, Wijayabandara M, Kulatunga A. **2017**. Amitraz poisoning: A case report of an unusual pesticide poisoning in Sri Lanka and literature review. BMC Pharmacology and Toxicology. 18(1):1–6. doi:10.1186/s40360-016-0114-5.

Hernandez J, Hattendorf J, Aebi A, Dietemann V. **2022**. Compliance with recommended *Varroa destructor* treatment regimens improves the survival of honey bee colonies over winter. Research in veterinary science. 144:1–10. doi:10.1016/j.rvsc.2021.12.025.

Hernández-Rodríguez CS, Moreno-Martí S, Almecija G, Christmon K, Johnson JD, Ventelon M, vanEngelsdorp D, Cook SC, González-Cabrera J. **2022**. Resistance to amitraz in the parasitic honey bee mite *Varroa destructor* is associated with mutations in the β-adrenergic-like octopamine receptor. Journal of Pest Science. 1–17. doi:10.1007/s10340-021-01471-3.

Higes M, Martín-Hernández R, Hernández-Rodríguez CS, González-Cabrera J. **2020**. Assessing the resistance to acaricides in *Varroa destructor* from several Spanish locations. Parasitology Research. 119(11):3595–3601. doi:10.1007/s00436-020-06879-x.

Hillesheim E, Ritter W, Bassand D. **1996**. First data on resistance mechanisms of *Varroa jacobsoni* (Oud.) against tau-fluvalinate. Experimental & Applied Acarology. 20:283–296. doi:10.1007/BF00052878.

Hou C, Rivkin H, Slabezki Y, Chejanovsky N. **2014**. Dynamics of the presence of Israeli acute paralysis virus in honey bee colonies with colony collapse disorder. Viruses. 6(5):2012–2027. doi:10.3390/v6052012.

Hristov P, Shumkova R, Palova N, Neov B. **2020**. Factors associated with honey bee colony losses: A mini-review. Veterinary Sciences. 7(4):166. doi:10.3390/vetsci7040166.

Huang ZY, Bian G, Xi Z, Xie X. **2019**. Genes important for survival or reproduction in *Varroa destructor* identified by RNAi. Insect Science. 26(1):68–75. doi:10.1111/1744-7917.12513.

Hung K-LJ, Kingston JM, Albrecht M, Holway DA, Kohn JR. **2018**. The worldwide importance of honey bees as pollinators in natural habitats. Proceedings of the Royal Society B: Biological Sciences. 285(1870):20172140. doi:10.1098/rspb.2017.2140.

Hunt G, Given JK, Tsuruda JM, Andino GK. **2016**. Breeding mite-biting bees to control *Varroa*. Bee Culture. 8:41–47.

Hýbl M, Bohatá A, Rádsetoulalová I, Kopecký M, Hoštičková I, Vaníčková A, Mráz P. **2021**. Evaluating the efficacy of 30 different essential oils against *Varroa destructor* and honey bee workers (*Apis mellifera*). Insects. 12(11):1045. doi:10.3390/insects12111045.

Ibrahim A, Spivak M. **2006**. The relationship between hygienic behavior and suppression of mite reproduction as honey bee (*Apis mellifera*) mechanisms of resistance to *Varroa destructor*. Apidologie. 37(1):31–40. doi:10.1051/apido:2005052.

Imdorf A, Bogdanov S, Kilchenmann V, Maquelin C. **1995**. Apilife VAR: a new varroacide with thymol as the main ingredient. Bee World. 76(2):77–83. doi:10.1080/0005772X.1995.11099245.

Imdorf A, Charriere J-Da, Maqueln C, Kilchenmann V, Bachofen B. **1996**. Alternative varroa control. American Bee Journal. 136(3):189–194.

Imdorf A, Bogdanov S, Ochoa RI, Calderone NW. **1999a**. Use of essential oils for the control of *Varroa jacobsoni* Oud. in honey bee colonies. Apidologie. 30(2–3):209–228. doi:10.1051/apido:19990210.

Imdorf A, Charrière J-D, Rosenkranz P. **1999b**. *Varroa* control with formic acid. FAIR CT97-3686. 24.

van Iterson M, Boer JM, Menezes RX. **2010**. Filtering, FDR and power. BMC Bioinformatics. 11:1–11. doi:10.1186/1471-2105-11-450.

Iwasaki JM, Barratt BI, Lord JM, Mercer AR, Dickinson KJ. **2015**. The New Zealand experience of varroa invasion highlights research opportunities for Australia. Ambio. 44:694–704. doi:10.1007/s13280-015-0679-z.

Jack CJ, Ellis JD. **2021**. Integrated pest management control of *varroa destructor* (acari: varroidae), the most damaging pest of (*Apis mellifera* L. (Hymenoptera: Apidae)) colonies. Journal of Insect Science. 21(5):6. doi:10.1093/jisesa/ieab058.

Jack CJ, van Santen E, Ellis JD. **2020**. Evaluating the efficacy of oxalic acid vaporization and brood interruption in controlling the honey bee pest *Varroa destructor* (Acari: Varroidae). Journal of Economic Entomology. 113(2):582–588. doi:10.1093/jee/toz358.

Jack CJ, Boncristiani H, Prouty C, Schmehl DR, Ellis JD. **2024**. Evaluating the seasonal efficacy of commonly used chemical treatments on *Varroa destructor* (Mesostigmata: Varroidae) population resurgence in honey bee colonies. Journal of Insect Science. 24(3):11. doi:10.1093/jisesa/ieae011. doi:10.1093/jisesa/ieae011.

Jeschke P. **2016**. Propesticides and their use as agrochemicals. Pest Management Science. 72(2):210–225. doi:10.1002/ps.4170.

Johnson RM, Wen Z, Schuler MA, Berenbaum MR. **2006**. Mediation of pyrethroid insecticide toxicity to honey bees (Hymenoptera: Apidae) by cytochrome P450 monooxygenases. Journal of Economic Entomology. 99(4):1046–1050. doi:10.1093/jee/99.4.1046.

Johnson RM, Pollock HS, Berenbaum MR. **2009**. Synergistic interactions between in-hive miticides in *Apis mellifera*. Journal of Economic Entomology. 102(2):474–479. doi:10.1603/029.102.0202.

Johnson RM, Ellis MD, Mullin CA, Frazier M. **2010**. Pesticides and honey bee toxicity–USA. Apidologie. 41(3):312–331. doi:10.1051/apido/2010018.

Johnson RM, Dahlgren L, Siegfried BD, Ellis MD. **2013**. Acaricide, fungicide and drug interactions in honey bees (*Apis mellifera*). PLoS One. 8(1):e54092. doi:10.1371/journal.pone.0054092.

Kanelis D, Tananaki C, Liolios V, Rodopoulou M. **2022**. Evaluation of oxalic acid with glycerin efficacy against *Varroa destructor* (Varroidae): a four year assay. Journal of Apicultural Research. 1–9. doi:10.1080/00218839.2023.2169368.

Kanga LHB, James RR, Boucias DG. **2002**. Hirsutella thompsonii and Metarhizium anisopliae as potential microbial control agents of *Varroa destructor*, a honey bee parasite. Journal of Invertebrate Pathology. 81(3):175–184. doi:10.1016/S0022-2011(02)00177-5.

Kasina JM, Mburu J, Kraemer M, Holm-Mueller K. **2009**. Economic benefit of crop pollination by bees: A case of Kakamega small-holder farming in Western Kenya. Journal of Economic Entomology. 102(2):467–473. doi:10.1603/029.102.0201.

Kast C, Droz B, Kilchenmann V. **2023**. Toxicity of coumaphos residues in beeswax foundation to the honey bee brood. Environmental Toxicology and Chemistry. 42(8):1816–1822. doi:10.1002/etc.5645.

Kevan PG, Hannan MA, Ostiguy N, Guzman-Novoa E. **2006**. A summary of the *Varroa*-virus disease complex in honey bees. American Bee Journal. 146(8):694–697.

Kevill JL, de Souza FS, Sharples C, Oliver R, Schroeder DC, Martin SJ. **2019**. DWV-A lethal to honey bees (*Apis mellifera*): A colony level survey of DWV variants (A, B, and C) in England, Wales, and 32 states across the US. Viruses. 11(5):426. doi:10.3390/v11050426.

Kim D, Paggi JM, Park C, Bennett C, Salzberg SL. 2019. Graph-based genome alignment and genotyping with HISAT2 and HISAT-genotype. Nature Biotechnology. 37(8):907-915. doi:10.1038/s41587-019-0201-4.

Kirrane MJ, de Guzman LI, Holloway B, Frake AM, Rinderer TE, Whelan PM. **2015**. Phenotypic and genetic analyses of the *Varroa* sensitive hygienic trait in Russian honey bee (Hymenoptera: Apidae) colonies. PLoS One. 10(4):e0116672. doi:10.1371/journal.pone.0116672.

Kita T, Hayashi T, Ohtani T, Takao H, Takasu H, Liu G, Ohta H, Ozoe F, Ozoe Y. **2017**. Amitraz and its metabolite differentially activate α-and β-adrenergic-like octopamine receptors. Pest Management Science. 73(5):984–990. doi:10.1002/ps.4412.

Klein A-M, Vaissière BE, Cane JH, Steffan-Dewenter I, Cunningham SA, Kremen C, Tscharntke T. 2007. Importance of pollinators in changing landscapes for world crops. Proceedings of the Royal Society B: Biological Sciences. 274(1608):303–313. doi:10.1038/s41598-019-42677-x.

Klein S, Pasquaretta C, He XJ, Perry C, Søvik E, Devaud J-M, Barron AB, Lihoreau M. 2019. Honey bees increase their foraging performance and frequency of pollen trips through experience. Scientific Reports. 9(1):6778. doi:10.1038/s41598-019-42677-x.

Kolics B, Kolics É, Mátyás K, Taller J, Specziár A. 2022. Comparison of alternative application methods for anti-varroa lithium chloride treatments. Insects. 13(7). doi:10.3390/insects13070633.

Kovačić M, Uzunov A, Tlak Gajger I, Pietropaoli M, Soroker V, Adjlane N, Benko V, Charistos L, Dall'Olio R, Formato G. 2023. Honey vs. Mite—A trade-off strategy by applying summer brood interruption for *Varroa destructor* control in the Mediterranean region. Insects. 14(9):751. doi:10.3390/insects14090751.

Kubásek J, Svobodová K, Půta F, Krejčí AB. 2022. Honeybees control the gas permeability of brood and honey cappings. iScience. 25(11):105445. doi:10.1016/j.isci.2022.105445.

Kuenen LPS, Calderone NW. 1997. Transfers of *Varroa* mites from newly emerged bees: Preferences for age- and function-specific adult bees (Hymenoptera: Apidae). Journal of Insect Behavior. 10(2):213–228. doi:10.1007/BF02765554.

Kulhanek K, Garavito A, VanEngelsdorp D. 2021. Accelerated *Varroa destructor* population growth in honey bee (*Apis mellifera*) colonies is associated with visitation from non-natal bees. Scientific Reports. 11(1):7092. doi:10.1038/s41598-021-86558-8.

Land BB, Seeley TD. 2004. The grooming invitation dance of the honey bee. Ethology. 110(1):1–10. doi:10.1046/j.1439-0310.2003.00947.x.

Le Conte Y, Arnold G, Trouiller J, Masson C, Chappe B, Ourisson G. 1989. Attraction of the parasitic mite *Varroa* to the drone larvae of honey bees by simple aliphatic esters. Science. 245(4918):638–639. doi:10.1126/science.245.4918.638.

Le Conte Y, Ellis M, Ritter W. 2010. *Varroa* mites and honey bee health: can *Varroa* explain part of the colony losses? Apidologie. 41(3):353–363. doi:10.1051/apido/2010017.

Leinonen R, Sugawara H, Shumway M, International Nucleotide Sequence Database Collaboration. 2010. The sequence read archive. Nucleic acids research. 39(database issue):D19–D21. doi:10.1093/nar/gkq1019.

Lenth RV. 2024. emmeans: Estimated marginal means, AKA least-squares means. https://CRAN.R-project.org/package=emmeans.

Leonard SP, Powell JE, Perutka J, Geng P, Heckmann LC, Horak RD, Davies BW, Ellington AD, Barrick JE, Moran NA. **2020**. Engineered symbionts activate honey bee immunity and limit pathogens. Science. 367(6477):573–576. doi:10.1126/science.aax9039.

Leviticus K, Cui L, Ling H, Jia Z, Huang Q, Han Z, Zhao C, Xu L. **2020**. Lethal and sublethal effects of fluralaner on the two-spotted spider mites, *Tetranychus urticae* Koch (Acari: Tetranychidae). Pest management science. 76(3):888–893. doi:10.1002/ps.5593.

Li H, Zhang L, Ni C, Shang H, Zhuang S, Li J. **2013**. Molecular recognition of floral volatile with two olfactory related proteins in the Eastern honeybee (*Apis cerana*). International Journal of Biological Macromolecules. 56:114–121. doi:10.1016/j.ijbiomac.2013.01.032.

Li AY, Cook SC, Sonenshine DE, Posada-Florez F, Noble NI, Mowery J, Gulbronson CJ, Bauchan GR. **2019**. Insights into the feeding behaviors and biomechanics of *Varroa destructor* mites on honey bee pupae using electropenetrography and histology. Journal of insect physiology. 119:103950. doi:10.1016/j.jinsphys.2019.103950.

Lin Z, Page P, Li L, Qin Y, Zhang Y, Hu F, Neumann P, Zheng H, Dietemann V. **2016**. Go east for better honey bee health: *Apis cerana* is faster at hygienic behavior than *A. mellifera*. PLoS One. 11(9):e0162647. doi:10.1371/journal.pone.0162647.

Lin Z, Qin Y, Page P, Wang S, Li L, Wen Z, Hu F, Neumann P, Zheng H, Dietemann V. **2018**. Reproduction of parasitic mites *Varroa destructor* in original and new honeybee hosts. Ecology and evolution. 8(4):2135–2145. doi:10.1002/ece3.3802.

Lin Z, Chen H, Page P, Wang K, Ji T, Chen G. **2020**. First record of pseudoscorpions in the Eastern honey bee colonies in China. Journal of Apicultural Research. 59(4):515–518. doi:10.1080/00218839.2019.1673577.

Lindberg CM, Melathopoulos AP, Winston ML. **2000**. Laboratory evaluation of miticides to control *Varroa jacobsoni* (Acari: Varroidae), a honey bee (Hymenoptera: Apidae) parasite. Journal of Economic Entomology. 93(2):189–198. doi:10.1603/0022-0493-93.2.189.

Locke B, Forsgren E, Fries I, de Miranda JR. **2012**. Acaricide treatment affects viral dynamics in *Varroa destructor*-infested honey bee colonies via both host physiology and mite control. Applied and Environmental Microbiology. 78(1):227–235. doi:10.1128/AEM.06094-11.

Lodesani M, Costa C. **2008**. Maximizing the efficacy of a thymol based product against the mite *Varroa destructor* by increasing the air space in the hive. Journal of Apicultural Research. 47(2):113–117. doi:10.1080/00218839.2008.11101436.

Loh K-C, Cao B. **2008**. Paradigm in biodegradation using *Pseudomonas putida*—a review of proteomics studies. Enzyme and Microbial Technology. 43(1):1–12. doi:10.1016/j.enzmictec.2008.03.004.

Loucif-Ayad W, Aribi N, Soltani N. **2008**. Evaluation of secondary effects of some acaricides on *Apis mellifera* intermissa (Hymenoptera, Apidae): acetylcholinesterase and glutathione S-transferase activities. European Journal of Scientific Research. 21(4):642–649. ISSN:1450-216X.

Love MI, Huber W, Anders S. **2014**. Moderated estimation of fold change and dispersion for RNA-seq data with DESeq2. Genome Biology. 15(12):550. doi:10.1186/s13059-014-0550-8.

Lu K, Song Y, Zeng R. **2021**. The role of cytochrome P450-mediated detoxification in insect adaptation to xenobiotics. Current Opinion in Insect Science. 43:103–107. doi:10.1016/j.cois.2020.11.004.

Lusebrink I, Girling RD, Farthing E, Newman TA, Jackson CW, Poppy GM. **2015**. The effects of diesel exhaust pollution on floral volatiles and the consequences for honey bee olfaction. Journal of Chemical Ecology. 41:904–912. doi:10.1007/s10886-015-0624-4.

Macedo PA, Wu J, Ellis MD. **2002**. Using inert dusts to detect and assess varroa infestations in honey bee colonies. Journal of Apicultural Research. 41(1–2):3–7. doi:10.1080/00218839.2002.11101062.

Maggi MD, Ruffinengo SR, Damiani N, Sardella NH, Eguaras MJ. **2009**. First detection of *Varroa destructor* resistance to coumaphos in Argentina. Experimental and Applied Acarology. 47:317–320. doi:10.1007/s10493-008-9216-0.

Maggi MD, Ruffinengo SR, Negri P, Eguaras MJ. **2010a**. Resistance phenomena to amitraz from populations of the ectoparasitic mite *Varroa destructor* of Argentina. Parasitology Research. 107:1189–1192. doi:10.1007/s00436-010-1986-8.

Maggi M, Damiani N, Ruffinengo S, De Jong D, Principal J, Eguaras M. **2010b**. Brood cell size of *Apis mellifera* modifies the reproductive behavior of *Varroa destructor*. Experimental and Applied Acarology. 50(3):269–279. doi:10.1007/s10493-009-9314-7.

Maggi MD, Ruffinengo SR, Mendoza Y, Ojeda P, Ramallo G, Floris I, Eguaras MJ. **2011**. Susceptibility of *Varroa destructor* (Acari: Varroidae) to synthetic acaricides in Uruguay: *Varroa* mites' potential to develop acaricide resistance. Parasitology Research. 108:815–821. doi:10.1007/s00436-010-2122-5.

Maiwald F, Haas J, Hertlein G, Lueke B, Roesner J, Nauen R. **2023**. Expression profile of the entire detoxification gene inventory of the western honeybee, *Apis mellifera* across life stages. Pesticide Biochemistry and Physiology. 192:105410. doi:10.1016/j.pestbp.2023.105410.

Martin SJ. **1995**. Ontogenesis of the mite *Varroa jacobsoni* Oud. in drone brood of the honeybee *Apis mellifera* L. under natural conditions. Experimental & Applied Acarology. 19(4):199–210. doi:10.1007/BF00130823.

Martin SJ. **2004**. Acaricide (pyrethroid) resistance in *Varroa destructor*. Bee World. 85(4):67–69. doi:10.1080/0005772X.2004.11099632.

Martin SJ, Brettell LE. **2019**. Deformed wing virus in honeybees and other insects. Annual Review of Virology. 6(Volume 6, 2019):49–69. doi:10.1146/annurev-virology-092818-015700.

Martin SJ, Highfield AC, Brettell L, Villalobos EM, Budge GE, Powell M, Nikaido S, Schroeder DC. **2012**. Global honey bee viral landscape altered by a parasitic mite. Science. 336(6086):1304–1306. doi:10.1126/science.1220941.

Martin SJ, Hawkins GP, Brettell LE, Reece N, Correia-Oliveira ME, Allsopp MH. **2020**. *Varroa destructor* reproduction and cell re-capping in mite-resistant *Apis mellifera* populations. Apidologie. 51:369–381. doi:10.1007/s13592-019-00721-9.

Mazzei M, Carrozza ML, Luisi E, Forzan M, Giusti M, Sagona S, Tolari F, Felicioli A. **2014**. Infectivity of DWV associated to flower pollen: experimental evidence of a horizontal transmission route. PLoS One. 9(11):e113448. doi:10.1371/journal.pone.0113448.

McAfee A, Collins TF, Madilao LL, Foster LJ. **2017**. Odorant cues linked to social immunity induce lateralized antenna stimulation in honey bees (*Apis mellifera* L.). Scientific Reports. 7(1):46171. doi:10.1038/srep46171.

McFarlane GR, Robinson KL, Whitaker K, Webster J, Drysdale L, Brancalion L, Webster A, O'Rourke B, Bogema DR. 2024. Amplicon and Cas9-targeted nanopore sequencing of *Varroa destructor* at the onset of an outbreak in Australia. Frontiers in Bee Science. 2:1334543. doi:10.3389/frbee.2024.1334543.

Meikle WG, Corby-Harris V, Ricigliano V, Snyder L, Weiss M. **2023**. Cold storage as part of a *Varroa* management strategy: effects on honey bee colony performance, mite levels and stress biomarkers. Scientific Reports. 13(1):11842. doi:10.1038/s41598-023-39095-5.

Meixner MD. **2010**. A historical review of managed honey bee populations in Europe and the United States and the factors that may affect them. Journal of Invertebrate Pathology. 103:S80–S95. doi:10.1016/j.jip.2009.06.011.

Melathopoulos AP, Gates J. **2003**. Comparison of two thymol-based acaricides, API LIFE VAR® and Apiguard™, for the control of *Varroa* mites. American Bee Journal, 143(6): 489–493.

Melathopoulos A, Pernal S, Moller E, Baumgartner W, Guzman-Novoa E. **2010**. A spring evaluation of thymol formulated in a sucrose dust for the control of *Varroa destructor*, a parasite of the honey bee (*Apis mellifera*) in Alberta, Canada. Science of Bee Culture. 2(2):2–6.

Menzies C, Olmstead S, McCallum R, Cutler C. **2019**. The efficacy of Formic Pro™ and 65% liquid formic acid against *Varroa* mite (*Varroa destructor*) in honey bee (*Apis mellifera*) colonies in autumn in Nova Scotia, Canada. Journal of the Acadian Entomological Society. 15.

Mert G, Yucel B. **2011**. Efficacy levels of organic acids are used for controlling *Varroa* (*Varroa jacobsoni* Oudmans) and their effects on colony development of honey bees (*Apis mellifera* L.). Journal of Animal and Veterinary Advances. 10(9):1106–1111. doi:10.3923/javaa.2011.1106.1111.

Meyer E, Aglyamova G, Matz M. **2011**. Profiling gene expression responses of coral larvae (*Acropora millepora*) to elevated temperature and settlement inducers using a novel RNA-Seq procedure. Molecular Ecology. 20(17):3599–3616. doi:10.1111/j.1365-294X.2011.05205.x.

Milani N. **1999**. The resistance of *Varroa jacobsoni* Oud. to acaricides. Apidologie. 30(2–3):229–234. doi:10.1051/apido:19990211.

Milani N. **2001**. Activity of oxalic and citric acids on the mite *Varroa destructor* in laboratory assays. Apidologie. 32(2):127–138. doi:10.1051/apido:2001118.

Milani N, Della Vedova G. **1996**. Determination of the LC50 in the mite *Varroa jacobsoni* of the active substances in Perizin® and Cekafix®. Apidologie. 27(3):175–184. doi:10.1051/apido:19960306.

de Miranda JR, Cordoni G, Budge G. **2010a**. The acute bee paralysis virus–Kashmir bee virus–Israeli acute paralysis virus complex. Journal of Invertebrate Pathology. 103:S30–S47. doi:10.1016/j.jip.2009.06.014.

de Miranda JR, Dainat B, Locke B, Cordoni G, Berthoud H, Gauthier L, Neumann P, Budge GE, Ball BV, Stoltz DB. **2010b**. Genetic characterization of slow bee paralysis virus of the honeybee (*Apis mellifera* L.). Journal of General Virology. 91(10):2524–2530. doi:10.1099/vir.0.022434-0.

de Miranda JR, Gauthier L, Ribière M, Chen YP. **2012**. Honey bee viruses and their effect on bee and colony health. Honey Bee Colony Health: Challenges and Sustainable Solutions. 71–102. doi:10.1201/b11318-8.

Mitton GA, Meroi Arcerito F, Cooley H, Fernández de Landa G, Eguaras MJ, Ruffinengo SR, Maggi MD. **2022**. More than sixty years living with *Varroa destructor*: a review of acaricide resistance. International Journal of Pest Management. 1–18. doi:10.1080/09670874.2022.2094489.

Mohiseni AA, Jaafari V, Zare A, Maleki M. **2002**. Effect of emulsifiable oil in controlling olive *Psylla euphyllum* (Costa) (Hom. Aphalaridae) and phytotoxicity of olive trees. Food and Agricultural Organization of the United Nations.

Molumby MJ, Anderson RM, Newbold DJ, Koblesky NK, Garrett AM, Schreiner D, Radley JJ, Weiner JA. **2017**. γ-Protocadherins interact with neuroligin-1 and negatively regulate dendritic spine morphogenesis. Cell Reports. 18(11):2702–2714. doi:10.1016/j.celrep.2017.02.060.

Mondet F, Alaux C, Severac D, Rohmer M, Mercer AR, Le Conte Y. **2015**. Antennae hold a key to *Varroa*-sensitive hygiene behaviour in honey bees. Scientific Reports. 5(1):10454. doi:10.1038/srep10454.

Morfin N, Rawn D, Petukhova T, Kozak P, Eccles L, Chaput J, Pasma T, Guzman-Novoa E. **2022**. Surveillance of synthetic acaricide efficacy against *Varroa destructor* in Ontario, Canada. The Canadian Entomologist. 154(1):e17. doi:10.4039/tce.2022.4.

Morfin N, Harpur BA, De la Mora A, Guzman-Novoa E. **2023**. Breeding honey bees (*Apis mellifera* L.) for low and high *Varroa destructor* population growth: Gene expression of bees performing grooming behavior. Frontiers in Insect Science. 3:951447. doi:10.3389/finsc.2023.951447.

Moškrič A, Bubnič J, Škerl MIS, Prešern J. **2018**. Potential positive effects of hop beta acids on parasitic mite *Varroa destructor* control in honey bee colonies. Journal of Hygienic Engineering and Design. 24:21–28.

Mumoki FN, Crewe RM. **2021**. Pheromone communication in honey bees (*Apis mellifera*). In: Blomquist GJ, Vogt RG. Insect Pheromone Biochemistry and Molecular Biology. 2nd ed. Elsevier. p. 183–204. doi:10.1016/B978-0-12-819628-1.00006-7.

Nanetti A. **1999**. Oxalic acid for mite control—results and review. Coordination in Europe of research on integrated varroa mites in honey bee colonies. 9–15. https://hal.science/hal-00892183.

Nazzi F, Brown SP, Annoscia D, Del Piccolo F, Di Prisco G, Varricchio P, Della Vedova G, Cattonaro F, Caprio E, Pennacchio F. **2012**. Synergistic parasite-pathogen interactions mediated by host immunity can drive the collapse of honeybee colonies. PLoS pathogens. 8(6):e1002735. doi:10.1371/journal.ppat.1002735.

Neumann P, Yañez O, Fries I, de Miranda JR. **2012**. Varroa invasion and virus adaptation. Journal of Invertebrate Pathology. 103:96–119. doi:10.1016/j.pt.2012.06.004.

Niu J, Shen G, Christiaens O, Smagghe G, He L, Wang J. **2018**. Beyond insects: current status and achievements of RNA interference in mite pests and future perspectives. Pest Management Science. 74(12):2680–2687. doi:10.1002/ps.5071. doi:10.1002/ps.5071.

Noble NI, Stuhl C, Nesbit M, Woods R, Ellis JD. **2021**. A comparison of *Varroa destructor* (Acari: Varroidae) collection methods and survivability in in vitro rearing systems. Florida Entomologist. 104(1):13–17.

Noël A, Le Conte Y, Mondet F. **2020**. *Varroa destructor*: how does it harm *Apis mellifera* honey bees and what can be done about it? Emerging Topics in Life Sciences. 4(1):45–57. doi:10.1042/ETLS20190125.

Nye WP, Anderson JL. **1974**. Insect pollinators frequenting strawberry blossoms and the effect of honey bees on yield and fruit quality. Journal of the American Society for Horticultural Science. 99(1):40–44. doi:10.21273/JASHS.99.1.40. doi:10.21273/JASHS.99.1.40.

Oddie M, Büchler R, Dahle B, Kovacic M, Le Conte Y, Locke B, De Miranda JR, Mondet F, Neumann P. **2018**. Rapid parallel evolution overcomes global honey bee parasite. Scientific Reports. 8(1):7704. doi:10.1007/s13592-018-0610-2.

Oddie MA, Neumann P, Dahle B. **2019**. Cell size and *Varroa destructor* mite infestations in susceptible and naturally-surviving honeybee (*Apis mellifera*) colonies. Apidologie. 50:1–10.

Oddie MAY, Burke A, Dahle B, Le Conte Y, Mondet F, Locke B. **2021**. Reproductive success of the parasitic mite (*Varroa destructor*) is lower in honeybee colonies that target infested cells with recapping. Scientific Reports. 11(1):9133. doi:10.1038/s41598-021-88592-y.

Odemer R. **2020**. Reproductive capacity of *Varroa destructor* in four different honey bee subspecies. Saudi Journal of Biological Sciences. 27(1):247–250. doi:10.1016/j.sjbs.2019.09.002.

Oh J, Lee Seunghyun, Kwon W, Joharchi O, Kim S, Lee Seunghwan. **2024**. Molecular phylogeny reveals *Varroa* mites are not a separate family but a subfamily of Laelapidae. Scientific Reports. 14(1):13994. doi:10.1038/s41598-024-63991-z.

Oldroyd BP. **1999**. Coevolution while you wait: *Varroa jacobsoni*, a new parasite of western honeybees. Trends in Ecology & Evolution. 14(8):312–315. doi:10.1016/S0169-5347(99)01613-4.

Olmstead S, Menzies C, McCallum R, Glasgow K, Cutler C. **2019**. Apivar® and Bayvarol® suppress varroa mites in honey bee colonies in Canadian Maritime Provinces. Journal of the Acadian Entomological Society. 15:46–49.

Oruc H, Hranitz J, Sorucu A, Duell M, Cakmak I, Aydin L, Orman A. **2012**. Determination of acute oral toxicity of flumethrin in honey bees. Journal of Economic Entomology. 105(6):1890–1894. doi:10.1603/ec12055.

Ostermann DJ, Currie RW. **2004**. Effect of formic acid formulations on honey bee (Hymenoptera: Apidae) colonies and influence of colony and ambient conditions on formic acid concentration in the hive. Journal of Economic Entomology. 97(5):1500–1508. doi:10.1603/0022-0493-97.5.1500.

Otten C, Fuchs S. **2021**. Individual differences in *Varroa jacobsoni* of preference for drone larvae to worker bee larvae. In: Commission of the European Committees. European Research on Varroatosis Control. 1st ed. CRC Press. p. 69–71.

Oudemans A. 1904. Nog iets aangaande de "Afbeeldingen met beschrijving van insecten, schdelijk voor naaldhout." Berichten. 18:156–164.

Ouyang J, Tian Y, Jiang C, Yang Q, Wang H, Li Q. **2018**. Laboratory assays on the effects of a novel acaricide, SYP-9625 on *Tetranychus cinnabarinus* (Boisduval) and its natural enemy, *Neoseiulus californicus* (McGregor). PLoS One. 13(11):e0199269. doi:10.1371/journal.pone.0199269.

Owen R, Stevenson M, Scheerlinck J-P. **2021**. *Varroa destructor* detection in non-endemic areas. Apidologie. 52:900–914. doi:10.1007/s13592-021-00873-7.

Owen R, Stevenson M, Scheerlinck J-P. **2022**. Comparing sugar shake to alcohol wash: Is alcohol wash the gold standard? Bee World. 99(2):66–67. doi:10.1080/0005772x.2022.2046367.

Özüiçli M, Girişgin AO, Kısadere İ, Demirbaş Ö, Baykalır Y. **2024**. Determination of the efficacy of thymol, eucalyptus and oxalic acid in the control of varroosis in honey bees. Balıkesir Sağlık Bilimleri Dergisi. 13(1):45–50. doi:10.53424/balikesirsbd.1339642.

Page P, Lin Z, Buawangpong N, Zheng H, Hu F, Neumann P, Chantawannakul P, Dietemann V. **2016**. Social apoptosis in honey bee superorganisms. Scientific Reports. 6(1):27210. doi:10.1038/srep27210.

Palmer A, Phapale P, Chernyavsky I, Lavigne R, Fay D, Tarasov A, Kovalev V, Fuchser J, Nikolenko S, Pineau C. **2017**. FDR-controlled metabolite annotation for high-resolution imaging mass spectrometry. Nature Methods. 14(1):57–60. doi:10.1038/nmeth.4072.

Paramasivam M, Selvi C. **2017**. Laboratory bioassay methods to assess the insecticide toxicity against insect pests-A review. Journal of Entomology and Zoology Studies. 5(3):1441–1445. E-ISSN:2320-7078.

Parsad R. **2010**. Some statistical techniques for bio-efficacy trials. Indian Journal of Agricultural Science. 16:62–76.

Parveen N, Miglani R, Kumar A, Dewali S, Kumar K, Sharma N, Bisht SS. **2022**. Honey bee pathogenesis posing threat to its global population: A short review. Proceedings of the Indian National Science Academy. 88(1):11–32. doi:10.1007/s43538-022-00062-9.

Peck DT, Smith ML, Seeley TD. **2016**. *Varroa destructor* mites can nimbly climb from flowers onto foraging honey bees. PLoS One. 11(12):e0167798. doi:10.1371/journal.pone.0167798.

Peck DT, Seeley TD. **2019**. Mite bombs or robber lures? The roles of drifting and robbing in *Varroa destructor* transmission from collapsing honey bee colonies to their neighbors. PLoS One. 14(6):e0218392. doi:10.1371/journal.pone.0218392.

Peck DT. **2021**. The parasitic mite *Varroa destructor*: history, biology, monitoring, and management. Honey Bee Medicine for the Veterinary Practitioner. 235–251. doi:10.1002/9781119583417.ch20.

Peirson M, Pernal SF. **2024**. A systematic review of fumagillin field trials for the treatment of Nosema disease in honeybee colonies. Insects. 15(1). doi:10.3390/insects15010029.

Penn HJ, Simone-Finstrom MD, Chen Y, Healy KB. **2022**. Honey bee genetic stock determines deformed wing virus symptom severity but not viral load or dissemination following pupal exposure. Frontiers in Genetics. 13:909392. doi:10.3389/fgene.2022.909392.

Pettis JS. **2004**. A scientific note on *Varroa destructor* resistance to coumaphos in the United States. Apidologie. 35(1):91–92. doi:10.1051/apido:2003060.

Pettis JS, Shimanuki H. **1999**. A hive modification to reduce varroa populations. American Bee Journal. 139(6):471–473.

Pettis JS, Collins AM, Wilbanks R, Feldlaufer MF. **2004**. Effects of coumaphos on queen rearing in the honey bee, *Apis mellifera*. Apidologie. 35(6):605–610. rearing in the honey bee, *Apis mellifera*. *Apidologie*, *35*(6), 605–610. doi:10.1051/apido:2004056.

Piccirillo GA, De Jong D. **2003**. The influence of brood comb cell size on the reproductive behavior of the ectoparasitic mite *Varroa destructor* in Africanized honey bee colonies. Genetics and Molecular Research. 2(1):36–42. PMID:12917800

Pinheiro J, Bates D, DebRoy S, Sarkar D, R Core Team. **2021**. nlme: Linear and nonlinear mixed effects models. https://CRAN.R-project.org/package=nlme.

Piou V, Tabart J, Urrutia V, Hemptinne J-L, Vétillard A. **2016**. Impact of the phoretic phase on reproduction and damage caused by *Varroa destructor* (Anderson and Trueman) to its host, the European honey bee (*Apis mellifera* L.). PLoS One. 11(4):e0153482. doi:10.1371/journal.pone.0153482.

Plamondon L, Paillard M, Julien C, Dubreuil P, Giovenazzo P. **2024**. Effects of summer treatments against *Varroa destructor* on viral load and colony performance of *Apis mellifera* colonies in Eastern Canada. Journal of Insect Science. 24(3):14. doi:10.1093/jisesa/ieae042.

Plata-Rueda A, Quintero HA, Serrão JE, Martínez LC. **2020**. Insecticidal activity of *Bacillus thuringiensis* strains on the nettle caterpillar, *Euprosterna elaeasa* (Lepidoptera: Limacodidae). Insects. 11(5):310. doi:10.3390/insects11050310.

Plettner E, Gries R. **2010**. Agonists and antagonists of antennal responses of gypsy moth (*Lymantria dispar*) to the pheromone (+)-disparlure and other odorants. Journal of Agricultural and Food Chemistry. 58(6):3708–3719. doi:10.1021/jf904139e.

Plettner E, Eliash N, Singh NK, Pinnelli GR, Soroker V. **2017**. The chemical ecology of host-parasite interaction as a target of *Varroa destructor* control agents. Apidologie. 48(1):78–92. doi:10.1007/s13592-016-0452-8.

Porcar M, Grenier A-M, Federici B, Rahbé Y. **2009**. Effects of *Bacillus thuringiensis* δ-endotoxins on the pea aphid (*Acyrthosiphon pisum*). Applied and Environmental Microbiology. 75(14):4897–4900. doi:10.1128/AEM.00686-09.

Pritchard DJ. **2016**. Grooming by honey bees as a component of varroa resistant behavior. Journal of Apicultural Research. 55(1):38–48. doi:10.1080/00218839.2016.1196016.

Pugh P, King P, Fordy M. **1992**. The respiratory system of the female *Varroa jacobsoni* (Oudemans): its adaptations to a range of environmental conditions. Experimental & applied acarology. 15:123–139. doi:10.1007/BF01275523.

Püntener W. **1981**. Manual for field trials in plant protection. 2nd ed. Basel, Switzerland: Agricultural Division, Ciba-Geigy Limited.

Qadir ZA, Idrees A, Mahmood R, Sarwar G, Bakar MA, Ahmad S, Raza MM, Li J. **2021**. Effectiveness of different soft acaricides against honey bee ectoparasitic mite *Varroa destructor* (Acari: Varroidae). Insects. 12(11):1032. doi:10.3390/insects12111032.

Qi Y, Yan B, Fu G, Guan X, Du L, Li J. **2017**. Germination of seeds and seedling growth of *Amaranthus retroflexus* L. following sublethal exposure of parent plants to herbicides. Scientific Reports. 7(1):157. doi:10.1038/s41598-017-00153-4.

Qi S, Zhu L, Wang D, Wang C, Chen X, Xue X, Wu L. **2020**. Flumethrin at honey-relevant levels induces physiological stresses to honey bee larvae (*Apis mellifera* L.) in vitro. Ecotoxicology and Environmental Safety. 190:110101. doi:10.1016/j.ecoenv.2019.110101.

Rademacher E, Harz M. **2006**. Oxalic acid for the control of varroosis in honey bee colonies–a review. Apidologie. 37(1):98–120. doi:10.1051/apido:2005063.

Rademacher E, Harz M, Schneider S. **2015**. The development of HopGuard® as a winter treatment against *Varroa destructor* in colonies of *Apis mellifera*. Apidologie. 46(6):748–759. doi:10.1007/s13592-015-0363-0.

Rademacher E, Harz M, Schneider S. **2017**. Effects of oxalic acid on *Apis mellifera* (Hymenoptera: Apidae). Insects. 8(3):84. doi:10.3390/insects8030084.

Ram RM, Keswani C, Bisen K, Tripathi R, Singh SP, Singh HB. **2018**. Biocontrol technology: eco-friendly approaches for sustainable agriculture. In: Barh D, Azevedo V. Omics Technologies and Bio-Engineering. 1st ed. Elsevier. p. 177–190.

Ramsey SD, Ochoa R, Bauchan G, Gulbronson C, Mowery JD, Cohen A, Lim D, Joklik J, Cicero JM, Ellis JD, et al. 2019. *Varroa destructor* feeds primarily on honey bee fat body tissue and not hemolymph. Proceedings of the National Academy of Sciences of the United States of America. 116(5):1792–1801. doi:10.1073/pnas.1818371116.

Rangel J, Ward L. **2018**. Evaluation of the predatory mite *Stratiolaelaps scimitus* for the biological control of the honey bee ectoparasitic mite *Varroa destructor*. Journal of Apicultural Research. 57(3):425–432. doi:10.1080/00218839.2018.1457864.

Read S, Howlett B, Donovan B, Nelson W, Van Toor R. **2014**. Culturing chelifers (Pseudoscorpions) that consume *Varroa* mites. Journal of applied entomology. 138(4):260–266. doi:10.1111/jen.12096.

Reams T, Rueppell O, Rangel J. **2024**. Honey bee (*Apis mellifera*) nurse bee visitation of worker and drone larvae increases *Varroa destructor* mite cell invasion. Journal of Insect Science. 24(3):16. doi:10.1093/jisesa/ieae044.

Reddy DS, Nagaraj R, Latha MP, Chowdary R. **2014**. Comparative evaluation of novel acaricides against two spotted spider mite, *Tetranychus urticae* Koch. infesting cucumber (Cucumis sativus) under laboratory and green house conditions. The Bioscan. 9(3):1001–1005.

Reynaldi FJ, Sguazza GH, Tizzano MA, Fuentealba N, Galosi CM, Pecoraro MR. **2011**. First report of Israeli acute paralysis virus in asymptomatic hives of Argentina. Revista Argentina de Microbiología. 43(2):84–6. doi:10.1590/S0325-75412011000200003.

Rinderer TE, Harris JW, Hunt GJ, De Guzman LI. **2010**. Breeding for resistance to *Varroa destructor* in North America. Apidologie. 41(3):409–424. doi:10.1051/apido/2010015.

Rinkevich FD. **2020**. Detection of amitraz resistance and reduced treatment efficacy in the *Varroa* Mite, *Varroa destructor*, within commercial beekeeping operations. PLoS One. 15(1):1–12. doi:10.1371/journal.pone.0227264. doi:10.1371/journal.pone.0227264.

Rinkevich FD, Moreno-Martí S, Hernández-Rodríguez CS, González-Cabrera J. **2023**. Confirmation of the Y215H mutation in the β2-octopamine receptor in *Varroa destructor* is associated with contemporary cases of amitraz resistance in the United States. Pest Management Science. 79(8):2840–2845. doi:10.1002/ps.7461.

Rittschof CC, Robinson GE. **2013**. Manipulation of colony environment modulates honey bee aggression and brain gene expression. Genes, Brain and Behavior. 12(8):802–811.

Riva C, Suzanne P, Charpentier G, Dulin F, Halm-Lemeille M-P, Sopkova-de Oliveira Santos J. **2019**. In silico chemical library screening and experimental validation of novel compounds with potential varroacide activities. Pesticide Biochemistry and Physiology. 160:11–19. doi:10.1016/j.pestbp.2019.05.012.

Roberts JM, Anderson DL, Durr PA. **2017**. Absence of deformed wing virus and *Varroa destructor* in Australia provides unique perspectives on honeybee viral landscapes and colony losses. Scientific Reports. 7(1):6925. doi:10.1038/s41598-017-07290-w.

Rodríguez-Dehaibes SR, Otero-Colina G, Sedas VP, Jiménez JAV. **2005**. Resistance to amitraz and flumethrin in *Varroa destructor* populations from Veracruz, Mexico. Journal of Apicultural Research. 44(3):124–125. doi:10.1080/00218839.2005.11101162.

Rondeau S, Giovenazzo P, Fournier V. **2018**. Risk assessment and predation potential of *Stratiolaelaps scimitus* (Acari: Laelapidae) to control *Varroa destructor* (Acari: Varroidae) in honey bees. PLoS One. 13(12):e0208812. doi:10.1371/journal.pone.0208812.

Rondeau S, Giovenazzo P, Fournier V. **2019**. The use of the predatory mite *Stratiolaelaps scimitus* (Mesostigmata: Laelapidae) to control *Varroa destructor* (Mesostigmata: Varroidae) in honey bee colonies in early and late fall. Journal of Economic Entomology. 112(2):534–542. doi:10.1093/jee/toy418.

Rosenkranz P, Aumeier P, Ziegelmann B. **2010**. Biology and control of *Varroa destructor*. Journal of Invertebrate Pathology. 103(SUPPL. 1):S96–S119. doi:10.1016/j.jip.2009.07.016.

Sabahi Q, Morfin N, Emsen B, Gashout HA, Kelly PG, Otto S, Merrill AR, Guzman-Novoa E. **2020**. Evaluation of dry and wet formulations of oxalic acid, thymol, and oregano oil for varroa mite (Acari: Varroidae) control in honey bee (Hymenoptera: Apidae) colonies. Journal of Economic Entomology. 113(6):2588–2594. doi:10.1093/jee/toaa218.

Saccà M, Lodesani M. **2020**. Isolation of bacterial microbiota associated to honey bees and evaluation of potential biocontrol agents of *Varroa destructor*. Beneficial Microbes. 11(7):641–654. doi:10.3920/BM2019.0164.

Santillán-Galicia MT, Otero-Colina G, Romero-Vera C, Cibrián-Tovar J. **2002**. *Varroa destructor* (Acari: Varroidae) infestation in queen, worker, and drone brood of *Apis mellifera* (Hymenoptera: Apidae). The Canadian Entomologist. 134(3):381–390. doi:10.4039/Ent134381-3.

Santillán-Galicia MT, Ball BV, Clark SJ, Alderson PG. **2014**. Slow bee paralysis virus and its transmission in honey bee pupae by *Varroa destructor*. Journal of Apicultural Research. 53(1):146–154. doi:10.3896/IBRA.1.53.1.16.

Schneider S, Eisenhardt D, Rademacher E. **2012**. Sublethal effects of oxalic acid on *Apis mellifera* (Hymenoptera: Apidae): changes in behaviour and longevity. Apidologie. 43:218–225. doi:10.1007/s13592-011-0102-0.

Schünemann R, Knaak N, Fiuza LM. **2014**. Mode of action and specificity of *Bacillus thuringiensis* toxins in the control of caterpillars and stink bugs in soybean culture. International Scholarly Research Notices. 2014. doi:10.1155/2014/135675.

Seeley TD, Griffin SR. **2011**. Small-cell comb does not control *Varroa* mites in colonies of honeybees of European origin. Apidologie. 42:526–532. doi:10.1007/s13592-011-0054-4.

Shen M, Yang X, Cox-Foster D, Cui L. **2005a**. The role of varroa mites in infections of Kashmir bee virus (KBV) and deformed wing virus (DWV) in honey bees. Virology. 342(1):141–149. doi:10.1016/j.virol.2005.07.012.

Shen M, Cui L, Ostiguy N, Cox-Foster D. **2005b**. Intricate transmission routes and interactions between picorna-like viruses (Kashmir bee virus and sacbrood virus) with the honeybee host and the parasitic varroa mite. Journal of General Virology. 86(8):2281–2289. doi:10.1016/j.virol.2005.07.012.

Shi T-F, Wang Y-F, Liu F, Qi L, Yu L-S. **2017**. Sublethal effects of the neonicotinoid insecticide thiamethoxam on the transcriptome of the honey bees (Hymenoptera: Apidae). Journal of Economic Entomology. 110(6):2283–2289. doi:10.1093/jee/tox262.

Singh NK, Eliash N, Raj S, Kim J, Yu Y, Plettner E, Soroker V. **2020**. Effect of the insect feeding deterrent 1-allyloxy-4-propoxybenzene on olfactory responses and host choice of *Varroa destructor*. Apidologie. 51:1133–1142. doi:10.1007/s13592-020-00791-0.

Skowronek P, Wójcik Ł, Strachecka A. **2021**. Fat body—Multifunctional insect tissue. Insects. 12(6):547. doi:10.3390/insects12060547.

Smith KM, Loh EH, Rostal MK, Zambrana-Torrelio CM, Mendiola L, Daszak P. **2013**. Pathogens, pests, and economics: drivers of honey bee colony declines and losses. EcoHealth. 10:434–445. doi:10.1007/s10393-013-0870-2.

Smith ML, Peck DT. **2023**. Dynamics of honey bee colony death and its implications for *Varroa destructor* mite transmission using observation hives. Apidologie. 54(1):13. https://hal.science/hal-04464771.

Song X-M, Zhang L-Y, Fu X-B, Wu F, Tan J, Li H-L. **2018**. Various bee pheromones binding affinity, exclusive chemosensillar localization, and key amino acid sites reveal the distinctive characteristics of odorant-binding protein 11 in the eastern honey bee, *Apis cerana*. Frontiers in Physiology. 9:422. doi:10.3389/fphys.2018.00422.

Stanimirović Z, Stevanović J, Aleksić N, Stojić V. **2010**. Heritability of grooming behaviour in grey honey bees (*Apis mellifera* carnica). Acta Veterinaria. 60(2–3):313–323. doi:10.2298/AVB1003313S.

van der Steen J, Vejsnæs F. **2021**. Varroa Control: A brief overview of available methods. Bee World. 98(2):50–56. doi:10.1080/0005772X.2021.1896196.

Steinmann N, Corona M, Neumann P, Dainat B. **2015**. Overwintering is associated with reduced expression of immune genes and higher susceptibility to virus infection in honey bees. PLoS One. 10(6):e0129956. doi:10.1371/journal.pone.0129956.

Steube X, Beinert P, Kirchner WH. **2021**. Efficacy and temperature dependence of 60% and 85% formic acid treatment against *Varroa destructor*. Apidologie. 52(3):720–729. doi:10.1007/s13592-021-00859-5.

Stevanovic J, Stanimirovic Z, Lakic N, Djelic N, Radovic I. **2012**. Stimulating effect of sugar dusting on honey bee grooming behaviour. Entomologia Experimentalis et Applicata. 143(1):23–30. doi:10.1111/j.1570-7458.2012.01231.x.

Sudo M, Yamanaka T, Miyai S. **2019**. Quantifying pesticide efficacy from multiple field trials. Population Ecology. 61(4):450–456. doi:10.1002/1438-390X.12019.

Szczurek A, Maciejewska M, Bąk B, Wilk J, Wilde J, Siuda M. **2020**. Detecting varroosis using a gas sensor system as a way to face the environmental threat. Science of the Total Environment. 722:137866. doi:10.1016/j.scitotenv.2020.137866.

Techer MA, Rane RV, Grau ML, Roberts JM, Sullivan ST, Liachko I, Childers AK, Evans JD, Mikheyev AS. **2019**. Divergent evolutionary trajectories following speciation in two ectoparasitic honey bee mites. Communications Biology. 2(1):357. doi:10.1038/s42003-019-0606-0.

Thapa R, Wongsiri S, Lee ML, Choi Y-S. **2013**. Predatory behaviour of pseudoscorpions (*Ellingsenius indicus*) associated with Himalayan *Apis cerana*. Journal of Apicultural Research. 52(5):219–226. doi:10.3896/IBRA.1.52.5.08.

The Gene Ontology Consortium, Aleksander SA, Balhoff J, Carbon S, Cherry JM, Drabkin HJ, Ebert D, Feuermann M, Gaudet P, Harris NL, et al. 2023. The Gene Ontology knowledgebase in 2023. Genetics. 224(1):iyad031. doi:10.1093/genetics/iyad031.

Tlak Gajger I, Svečnjak L, Bubalo D, Žorat T. **2019**. Control of *Varroa destructor* mite infestations at experimental apiaries situated in Croatia. Diversity. 12(1):12. doi:10.3390/d12010012.

van Toor RF, Thompson SE, Gibson DM, Smith GR. **2015**. Ingestion of *Varroa destructor* by pseudoscorpions in honey bee hives confirmed by PCR analysis. Journal of Apicultural Research. 54(5):555–562. doi:10.1080/00218839.2016.1184845.

Traynor KS, Mondet F, de Miranda JR, Techer M, Kowallik V, Oddie MAY, Chantawannakul P, McAfee A. **2020**. *Varroa destructor*: a complex parasite, crippling honey bees worldwide. Trends in Parasitology. 36(7):592–606. doi:10.1016/j.pt.2020.04.004.

Tsagou V, Lianou A, Lazarakis D, Emmanouel N, Aggelis G. **2004**. Newly isolated bacterial strains belonging to Bacillaceae (*Bacillus* sp.) and Micrococcaceae accelerate death of the honey bee mite, *Varroa destructor* (*V. jacobsoni*), in laboratory assays. Biotechnology Letters. 26:529–532. doi:10.1023/B:BILE.0000019563.92959.0e.

Tsuruda JM, Harris JW, Bourgeois L, Danka RG, Hunt GJ. **2012**. High-resolution linkage analyses to identify genes that influence *Varroa* sensitive hygiene behavior in honey bees. PLoS One. 7(11):e48276. doi:10.1371/journal.pone.0048276.

Ullah A, Gajger IT, Majoros A, Dar SA, Khan S, Shah AH, Khabir MN, Hussain R, Khan HU, Hameed M. **2021**. Viral impacts on honey bee populations: A review. Saudi Journal of Biological Sciences. 28(1):523–530. doi:10.1016/j.sjbs.2020.10.037.

Underwood RM, Currie RW. **2003**. The effects of temperature and dose of formic acid on treatment efficacy against *Varroa destructor* (Acari: Varroidae), a parasite of *Apis mellifera* (Hymenoptera: Apidae). Experimental & Applied Acarology. 29:303–313. doi:10.1023/A:1025892906393.

Underwood RM, Currie RW. **2004**. Indoor winter fumigation of *Apis mellifera* (Hymenoptera: Apidae) colonies infested with *Varroa destructor* (Acari: Varroidae) with formic acid is a potential control alternative in northern climates. Journal of Economic Entomology. 97(2):177–186. doi:10.1093/jee/97.2.177.

Underwood RM, Currie RW. **2005**. Effect of concentration and exposure time on treatment efficacy against *Varroa* mites (Acari: Varroidae) during indoor winter fumigation of honey bees (Hymenoptera: Apidae) with formic acid. Journal of Economic Entomology. 98(6):1802–1809. doi:10.1093/jee/98.6.1802.

Underwood RM, Currie RW. **2007**. Effects of release pattern and room ventilation on survival of varroa mites and queens during indoor winter fumigation of honey bee colonies with formic acid. The Canadian Entomologist. 139(6):881–893. doi:10.4039/n06-085.

Underwood R, López-Uribe M. **2022**. Methods to control *Varroa* mites: An integrated pest management approach. Penn State University Extension. Accessed 2024 June 20. https://extension.psu.edu/methods-to-control-varroa-mites-an-integrated-pest-management-approach.

Vandervalk LP, Nasr ME, Dosdall LM. **2014**. New miticides for integrated pest management of *Varroa destructor* (Acari: Varroidae) in honey bee colonies on the canadian prairies. Journal of Economic Entomology. 107(6):2030–2036. doi:10.1603/EC14048.

Veale DJ, Wium CA, Muller GJ. **2011**. Amitraz poisoning in South Africa: a two year survey (2008–2009). Clinical Toxicology. 49(1):40–44. doi:10.3109/15563650.2010.542159.

Vijverberg HPM, vanden Bercken J. **1990**. Neurotoxicological effects and the mode of action of pyrethroid insecticides. Critical Reviews in Toxicology. 21(2):105–126. doi:10.3109/10408449009089875.

Vilarem C, Piou V, Vogelweith F, Vétillard A. **2021**. *Varroa destructor* from the laboratory to the field: Control, biocontrol and IPM perspectives—A review. Insects. 12(9):800. doi:10.3390/insects12090800.

Vlogiannitis S, Mavridis K, Dermauw W, Snoeck S, Katsavou E, Morou E, Harizanis P, Swevers L, Hemingway J, Feyereisen R. **2021**. Reduced proinsecticide activation by cytochrome P450 confers coumaphos resistance in the major bee parasite *Varroa destructor*. Proceedings of the National Academy of Sciences. 118(6):e2020380118. doi:10.1073/pnas.2020380118.

Vonhoff F, Keshishian H. **2017**. In vivo calcium signaling during synaptic refinement at the Drosophila neuromuscular junction. Journal of Neuroscience. 37(22):5511–5526. doi:10.1523/JNEUROSCI.2922-16.2017.

Wallberg A, Bunikis I, Pettersson OV, Mosbech M-B, Childers AK, Evans JD, Mikheyev AS, Robertson HM, Robinson GE, Webster MT. **2019**. A hybrid de novo genome assembly of the honeybee, *Apis mellifera*, with chromosome-length scaffolds. BMC Genomics. 20:1–19. doi:10.1186/s12864-019-5642-0.

Walsh AT, Triant DA, Le Tourneau JJ, Shamimuzzaman M, Elsik CG. **2022**. Hymenoptera Genome Database: new genomes and annotation datasets for improved go enrichment and orthologue analyses. Nucleic Acids Research. 50(D1):D1032–D1039. doi:10.1093/nar/gkab1018.

Wang Z, Gerstein M, Snyder M. **2009**. RNA-Seq: a revolutionary tool for transcriptomics. Nature Reviews Genetics. 10(1):57–63. doi:10.1038/nrg2484.

Wang X, Zhang X, Zhang Z, Lang H, Zheng H. **2018**. Honey bee as a model organism to study gut microbiota and diseases. Drug Discovery Today: Disease Models. 28:35–42. doi:10.1016/j.ddmod.2019.08.010.

Wang K, Liu Z, Lin Z, Yin L, Gao F, Chen G, Ji T. **2020**. Epigenetic modifications may regulate the activation of the hypopharyngeal gland of honeybees (*Apis mellifera*) during winter. Frontiers in Genetics. 11:46. doi:10.3389/fgene.2020.00046.

Whitfield CW, Ben-Shahar Y, Brillet C, Leoncini I, Crauser D, LeConte Y, Rodriguez-Zas S, Robinson GE. **2006**. Genomic dissection of behavioral maturation in the honey bee. Proceedings of the National Academy of Sciences. 103(44):16068–16075. doi:10.1073/pnas.0606909103

Wright GA, Schiestl FP. **2009**. The evolution of floral scent: the influence of olfactory learning by insect pollinators on the honest signalling of floral rewards. Functional Ecology. 23(5):841–851. doi:10.1111/j.1365-2435.2009.01627.x.

Wu Y, Zheng Y, Chen Yanan, Wang S, Chen Yanping, Hu F, Zheng H. **2020**. Honey bee (*Apis mellifera*) gut microbiota promotes host endogenous detoxification capability via regulation of P450 gene expression in the digestive tract. Microbial Biotechnology. 13(4):1201–1212. doi:10.1111/1751-7915.13579.

Wu X, Liao C, He X, Zhang L, Yan W, Zeng Z. **2022**. Sublethal fluvalinate negatively affect the development and flight capacity of honeybee (*Apis mellifera* L.) workers. Environmental Research. 203:111836. doi:10.1016/j.envres.2021.111836.

Yang X, Cox-Foster DL. **2005**. Impact of an ectoparasite on the immunity and pathology of an invertebrate: evidence for host immunosuppression and viral amplification. Proceedings of the National Academy of Sciences. 102(21):7470–7475. doi:10.1073/pnas.0501860102.

Yilmaz HL, Yildizdas D. **2003**. Amitraz poisoning, an emerging problem: epidemiology, clinical features, management, and preventive strategies. Archives of Disease in Childhood. 88(2):130–134. doi:10.1136/adc.88.2.130.

Youssefi MR, Moghaddas E, Tabari MA, Moghadamnia AA, Hosseini SM, Farash BR, Ebrahimi MA, Mousavi NN, Fata A, Maggi F, et al. 2019. In vitro and in vivo effectiveness of carvacrol, thymol and linalool against *Leishmania infantum*. Molecules. 24(11). doi:10.3390/molecules24112072.

Yue C, Genersch E. **2005**. RT-PCR analysis of deformed wing virus in honeybees (*Apis mellifera*) and mites (*Varroa destructor*). Journal of General Virology. 86(12):3419–3424. doi:10.1099/vir.0.81401-0. doi:10.1099/vir.0.81401-0.

Zhang Z, Mu X, Cao Q, Shi Y, Hu X, Zheng H. **2022**. Honeybee gut *Lactobacillus* modulates host learning and memory behaviors via regulating tryptophan metabolism. Nature Communications. 13(1):2037. doi:10.1038/s41467-022-29760-0.

Zhang L, Shao L, Raza MF, Zhang Y, Li Z, Huang ZY, Chen Y, Su S, Han R, Li W. **2024**. Large cells suppress the reproduction of *Varroa destructor*. Pest Management Science. 80: 5224-5232. doi:10.1002/ps.8249

Zhao H, Peng Z, Huang L, Zhao S, Liu M. **2021**. Expression profile and ligand screening of a putative odorant-binding protein, AcerOBP6, from the Asian honeybee. Insects. 12(11):955. doi:10.3390/insects12110955.

Zikic B, Aleksic N, Ristanic M, Glavinic U, Vejnovic B, Krnjaic I, Stanimirovic Z. **2020**. Anti-*Varroa* efficiency of coumaphos and its influence on oxidative stress and survival of honey bees. Acta Veterinaria. 70(3):355–373. doi:10.2478/acve-2020-0027.

APPENDIX A: Chapter 3 "Differentially-expressed genes from the honey bee head dataset with unadjusted $p < 0.05$."

A.1 Table of genes from the honey bee head dataset with unadjusted *P*-values below the α = 0.05 threshold, organized by ascending log2 fold change, with the gene ID, adjusted *P*-values, and gene descriptions included.

Gene ID	Log2 Fold Change	*p*-Value	Adjusted *p*-Value	Gene Description
LOC726903	-1.674	0.011	> 0.999	uncharacterized LOC726903
LOC410107	-1.592	0.041	> 0.999	broad-complex core protein isoforms 1/2/3/4/5
LOC102654344	-1.495	0.050	> 0.999	glutamine-rich protein 2
LOC552040	-1.471	0.004	0.809	transcription activator MSS11
LOC100579026	-1.406	0.007	> 0.999	uncharacterized LOC100579026
LOC410906	-1.289	0.011	> 0.999	guanine nucleotide-binding protein subunit alpha homolog
LOC412444	-1.218	0.023	> 0.999	chymotrypsin-like elastase family member 2A
LOC100577362	-1.173	0.041	> 0.999	uncharacterized LOC100577362
Or115	-1.040	0.030	> 0.999	odorant receptor 115
LOC100577941	-1.023	0.050	> 0.999	uncharacterized LOC100577941
LOC412203	-1.021	0.049	> 0.999	protein brown
LOC725084	-0.945	0.025	> 0.999	uncharacterized LOC725084
LOC100578045	-0.942	0.022	> 0.999	uncharacterized LOC100578045
LOC102656263	-0.906	0.041	> 0.999	protein farnesyltransferase subunit beta
LOC411209	-0.902	0.049	> 0.999	uncharacterized LOC411209
LOC410747	-0.882	0.018	> 0.999	glucose dehydrogenase [FAD
LOC726737	-0.872	0.003	0.750	venom acid phosphatase Acph-1
LOC409884	-0.831	0.047	> 0.999	xylulose kinase
LOC726020	-0.779	0.022	> 0.999	protein OSCP1
LOC725351	-0.764	0.017	> 0.999	aldose 1-epimerase
LOC724561	-0.743	0.014	> 0.999	E3 ubiquitin-protein ligase DCST1
LOC102655858	-0.731	0.024	> 0.999	uncharacterized LOC102655858
LOC727129	-0.698	0.018	> 0.999	uncharacterized LOC727129
LOC551405	-0.696	0.011	> 0.999	4-nitrophenylphosphatase
LOC411301	-0.676	0.020	> 0.999	dynein heavy chain 10
LOC552523	-0.641	0.011	> 0.999	L-threonine ammonia-lyase
LOC724225	-0.628	0.015	> 0.999	sex peptide receptor-like
LOC412968	-0.604	0.047	> 0.999	putative epidermal cell surface receptor
LOC724570	-0.594	0.018	> 0.999	mpv17-like protein 2
LOC726783	-0.571	0.014	> 0.999	vitellogenin
LOC413171	-0.561	0.018	> 0.999	myosin-I heavy chain
LOC551998	-0.552	0.039	> 0.999	cell death-inducing p53-target protein 1
LOC100576972	-0.536	0.050	> 0.999	uncharacterized LOC100576972
LOC412739	-0.531	0.027	> 0.999	roundabout homolog 2
LOC102653957	-0.524	0.039	> 0.999	uncharacterized LOC102653957

LOC550958	-0.522	0.023	> 0.999	uncharacterized LOC550958
LOC727424	-0.516	0.012	> 0.999	mitochondrial thiamine pyrophosphate carrier
LOC410306	-0.512	0.007	> 0.999	ADP-ribosylation factor 2
LOC727596	-0.508	0.033	> 0.999	malectin
LOC100576638	-0.500	0.023	> 0.999	uncharacterized LOC100576638
LOC726765	-0.497	0.010	> 0.999	dynein regulatory complex protein 11
LOC409367	-0.495	< 0.001	0.234	calcyphosin-like protein
Apid1	-0.487	< 0.001	0.150	apidaecin 1
LOC408603	-0.485	0.043	> 0.999	glucose dehydrogenase [FAD
LOC100578745	-0.476	0.021	> 0.999	uncharacterized LOC100578745
LOC413833	-0.467	0.005	0.903	cytochrome P450 4C1
LOC552832	-0.467	0.008	> 0.999	glycine N-methyltransferase
LOC551902	-0.461	0.018	> 0.999	metaxin-1
LOC724993	-0.456	< 0.001	0.150	uncharacterized LOC724993
LOC410370	-0.446	0.015	> 0.999	actin-binding Rho-activating protein
LOC725036	-0.438	0.009	> 0.999	U7 snRNA-associated Sm-like protein LSm11
LOC410337	-0.434	0.037	> 0.999	venom dipeptidylpeptidase IV
LOC552418	-0.431	0.043	> 0.999	cytochrome P450 6k1
LOC412578	-0.421	0.048	> 0.999	mediator of RNA polymerase II transcription subunit 21
LOC410290	-0.414	0.024	> 0.999	anaphase-promoting complex subunit 5
LOC413746	-0.403	0.028	> 0.999	adrenodoxin
LOC102655788	-0.397	0.018	> 0.999	uncharacterized LOC102655788
LOC406146	-0.388	0.006	> 0.999	hyaluronoglucosaminidase
LOC102655538	-0.388	0.046	> 0.999	peptidyl-prolyl cis-trans isomerase C
LOC724580	-0.386	0.042	> 0.999	uncharacterized LOC724580
LOC100578162	-0.385	0.026	> 0.999	uncharacterized LOC100578162
LOC724152	-0.384	0.041	> 0.999	uncharacterized LOC724152
LOC550924	-0.374	0.024	> 0.999	cleavage stimulation factor subunit 2
Obp4	-0.373	< 0.001	0.217	odorant binding protein 4
LOC724654	-0.373	0.015	> 0.999	cytochrome b5
LOC411272	-0.373	< 0.001	0.291	putative acyl-CoA-binding protein
LOC410244	-0.371	0.024	> 0.999	uncharacterized LOC410244
LOC100578084	-0.365	0.031	> 0.999	uncharacterized LOC100578084
LOC552483	-0.364	0.039	> 0.999	ankyrin repeat domain-containing protein 54
LOC552293	-0.363	0.020	> 0.999	sialin
LOC725420	-0.354	0.037	> 0.999	sodium-dependent nutrient amino acid transporter 1
LOC410601	-0.345	0.044	> 0.999	cilia- and flagella-associated protein 206
LOC408868	-0.344	< 0.001	0.107	inositol monophosphatase 2
LOC408673	-0.344	0.046	> 0.999	maspardin
LOC113218635	-0.342	0.016	> 0.999	nuclear transcription factor Y subunit gamma-like
LOC406114	-0.340	0.033	> 0.999	alpha-amylase
LOC411406	-0.340	0.033	> 0.999	zinc metalloproteinase nas-13
LOC726724	-0.334	0.039	> 0.999	transient receptor potential channel pyrexia
LOC408269	-0.334	0.029	> 0.999	general transcription factor IIH subunit 5
LOC724835	-0.322	0.006	> 0.999	uncharacterized LOC724835
Cox6c	-0.319	0.026	> 0.999	cytochrome c oxidase subunit VIc
LOC552090	-0.318	0.028	> 0.999	transcription factor GAGA
Cat	-0.311	< 0.001	0.217	catalase
LOC413319	-0.311	0.015	> 0.999	dynein regulatory complex subunit 7

LOC412382	-0.310	0.002	0.682	excitatory amino acid transporter 3
LOC100577883	-0.309	0.007	> 0.999	cytochrome P450 4aa1-like
LOC725978	-0.309	< 0.001	0.346	translation initiation factor IF-2
LOC412318	-0.303	0.032	> 0.999	AN1-type zinc finger protein 2A
LOC552746	-0.302	0.013	> 0.999	17-beta-hydroxysteroid dehydrogenase 13
LOC726115	-0.300	0.023	> 0.999	D-2-hydroxyglutarate dehydrogenase
LOC727108	-0.299	0.048	> 0.999	rho GTPase-activating protein 26
LOC726286	-0.298	0.002	0.712	uncharacterized LOC726286
LOC725405	-0.292	0.048	> 0.999	DNA repair endonuclease XPF
LOC100576975	-0.292	0.020	> 0.999	zinc finger protein 567
LOC726040	-0.286	0.026	> 0.999	4-coumarate--CoA ligase 1
LOC100577430	-0.280	0.015	> 0.999	uncharacterized LOC100577430
LOC725997	-0.279	< 0.001	0.217	UDP-glucuronosyltransferase 2C1
Ets97D-like	-0.277	0.039	> 0.999	Ets at 97D ortholog
LOC100576555	-0.273	0.050	> 0.999	cytochrome b561 domain-containing protein 2
LOC410516	-0.272	0.036	> 0.999	cytosolic Fe-S cluster assembly factor NUBP2 homolog
LOC411978	-0.270	0.006	> 0.999	myrosinase 1
LOC100577288	-0.267	0.036	> 0.999	nudC domain-containing protein 1
LOC551268	-0.263	0.008	> 0.999	pancreatic triacylglycerol lipase
LOC408819	-0.262	0.035	> 0.999	transmembrane protein 147
LOC725186	-0.262	0.035	> 0.999	chromatin modification-related protein MEAF6
LOC551316	-0.261	0.044	> 0.999	DNA excision repair protein ERCC-1
LOC412197	-0.261	0.004	0.882	protein lethal(2)essential for life
LOC552461	-0.261	< 0.001	0.357	uncharacterized LOC552461
JHBP-1	-0.258	0.005	0.997	take-out-like carrier protein
LOC100577966	-0.253	0.030	> 0.999	probable serine/threonine-protein kinase DDB_G0283337
LOC410733	-0.253	0.007	> 0.999	glucose dehydrogenase [FAD
LOC411858	-0.250	0.043	> 0.999	ATPase family AAA domain-containing protein 1-B
LOC725204	-0.250	0.033	> 0.999	tyrosine aminotransferase
LOC410621	-0.248	0.001	0.555	multiple epidermal growth factor-like domains protein 10
Mrjp9	-0.246	0.047	> 0.999	major royal jelly protein 9
Ube2g1	-0.246	0.035	> 0.999	ubiquitin-conjugating enzyme E2G 1 (UBC7 homolog
LOC411613	-0.246	0.038	> 0.999	buffy
LOC725390	-0.244	0.023	> 0.999	leucine-rich melanocyte differentiation-associated protein
LOC410857	-0.243	0.005	0.997	protein lethal(2)essential for life
LOC408509	-0.243	0.044	> 0.999	glutamate decarboxylase 1
LOC100579015	-0.243	0.029	> 0.999	leucine-rich repeat-containing protein 15
LOC410087	-0.242	0.009	> 0.999	uncharacterized LOC410087
LOC411058	-0.240	0.028	> 0.999	uncharacterized LOC411058
LOC409269	-0.240	0.037	> 0.999	39S ribosomal protein L43
LOC551890	-0.240	0.043	> 0.999	probable serine incorporator
LOC551685	-0.238	0.019	> 0.999	uncharacterized LOC551685
LOC409932	-0.238	0.042	> 0.999	b(0
Pgrp-s2	-0.238	0.006	> 0.999	peptidoglycan recognition protein S2
LOC100578399	-0.237	0.046	> 0.999	ribonuclease P protein subunit p25-like protein
LOC409143	-0.234	0.011	> 0.999	venom serine protease 34
LOC413667	-0.233	0.044	> 0.999	G2/mitotic-specific cyclin-B3
LOC726803	-0.233	0.010	> 0.999	uncharacterized LOC726803
LOC551712	-0.231	0.023	> 0.999	lipoyltransferase 1

LOC726818	-0.231	0.022	> 0.999	beta-hexosaminidase subunit beta
LOC107965557	-0.228	0.007	> 0.999	uncharacterized LOC107965557
LOC552383	-0.228	0.049	> 0.999	PQ-loop repeat-containing protein 1
LOC408280	-0.226	0.002	0.682	cell surface glycoprotein 1
LOC412232	-0.224	0.001	0.549	dipeptidyl peptidase 3
LOC551939	-0.224	0.048	> 0.999	28S ribosomal protein S35
LOC409324	-0.224	0.011	> 0.999	short-chain-enoyl-CoA hydratase
LOC409171	-0.223	0.010	> 0.999	esterase FE4
LOC552306	-0.222	0.033	> 0.999	male-enhanced antigen 1
Obp19	-0.213	0.025	> 0.999	odorant binding protein 19
LOC552728	-0.209	0.021	> 0.999	uncharacterized LOC552728
LOC100577725	-0.207	0.003	0.784	probable chitinase 10
LOC726437	-0.203	0.043	> 0.999	tctex1 domain-containing protein 2
LOC409118	-0.203	0.038	> 0.999	translation initiation factor eIF-2B subunit alpha
LOC724703	-0.201	0.048	> 0.999	modular serine protease
LOC724421	-0.200	0.009	> 0.999	fibrillin-2
LOC102656136	-0.199	0.038	> 0.999	prefoldin subunit 4
LOC552459	-0.197	0.010	> 0.999	glycine-rich cell wall structural protein
LOC113219195	-0.196	0.007	> 0.999	clumping factor A-like
SPG11	-0.195	0.038	> 0.999	spatacsin
LOC409173	-0.194	0.034	> 0.999	esterase FE4
LOC551523	-0.191	0.046	> 0.999	adenylate kinase
LOC551496	-0.191	0.025	> 0.999	H/ACA ribonucleoprotein complex subunit GAR1
LOC409246	-0.188	0.046	> 0.999	MAP kinase-activated protein kinase 2
LOC410451	-0.186	0.012	> 0.999	venom serine carboxypeptidase
LOC552247	-0.186	0.003	0.750	nuclear factor NF-kappa-B p100 subunit
LOC100577506	-0.185	0.037	> 0.999	uncharacterized LOC100577506
LOC107965822	-0.184	0.035	> 0.999	retrovirus-related Pol polyprotein from type-1 retrotransposable element R2
LOC410993	-0.182	0.034	> 0.999	valacyclovir hydrolase
LOC409234	-0.180	0.042	> 0.999	S-phase kinase-associated protein 1
LOC409195	-0.180	0.033	> 0.999	MIP18 family protein galla-1
LOC550749	-0.180	0.020	> 0.999	C-1-tetrahydrofolate synthase
LOC409264	-0.179	0.023	> 0.999	ATPase ASNA1 homolog
LOC726361	-0.167	0.041	> 0.999	ufm1-specific protease 1
LOC408395	-0.165	0.026	> 0.999	venom carboxylesterase-6-like
LOC412445	-0.164	0.038	> 0.999	flavin reductase (NADPH)
LOC552551	-0.162	0.043	> 0.999	small integral membrane protein 14
LOC412543	-0.160	0.025	> 0.999	uncharacterized LOC412543
LOC408675	-0.160	0.049	> 0.999	probable 39S ribosomal protein L24
LOC100577644	-0.160	0.045	> 0.999	uncharacterized LOC100577644
LOC725926	-0.159	0.016	> 0.999	collagen alpha-1(IV) chain
LOC726569	-0.155	0.024	> 0.999	mitochondrial import inner membrane translocase subunit Tim21
LOC551479	-0.153	0.045	> 0.999	40S ribosomal protein S21
LOC412209	-0.152	0.041	> 0.999	probable cytochrome P450 6a17
LOC408650	-0.149	0.034	> 0.999	inositol oxygenase
LOC410012	-0.147	0.039	> 0.999	WW domain-binding protein 2
LOC724930	-0.143	0.026	> 0.999	caspase-8

LOC100576326	-0.138	0.029	> 0.999	phenoloxidase-activating factor 2
LOC726862	-0.137	0.047	> 0.999	DNA repair protein REV1
LOC552429	-0.137	0.024	> 0.999	peroxiredoxin-5
LOC551436	-0.120	0.045	> 0.999	T-complex protein 1 subunit theta
LOC725155	0.125	0.021	> 0.999	serine/arginine repetitive matrix protein 1
LOC408706	0.131	0.045	> 0.999	heat shock protein 70Cb ortholog
Cdc37	0.132	0.021	> 0.999	cell division cycle 37 homolog
LOC409196	0.133	0.036	> 0.999	alanine aminotransferase 1
LOC552519	0.134	0.035	> 0.999	clustered mitochondria protein homolog
LOC551774	0.134	0.015	> 0.999	acidic leucine-rich nuclear phosphoprotein 32 family member B
LOC413409	0.136	0.031	> 0.999	cytoplasmic dynein 1 intermediate chain
LOC724247	0.140	0.046	> 0.999	rRNA methyltransferase 3
LOC408976	0.140	0.034	> 0.999	protein kinase shaggy
LOC100576346	0.141	0.028	> 0.999	protein PFC0760c
LOC411372	0.143	0.048	> 0.999	glutathione synthetase
LOC552765	0.147	0.044	> 0.999	zinc finger CCCH domain-containing protein 13
LOC409043	0.149	0.037	> 0.999	high-affinity choline transporter 1
LOC724240	0.149	0.043	> 0.999	flap endonuclease GEN
LOC550716	0.152	0.019	> 0.999	clathrin heavy chain
LOC551973	0.153	0.034	> 0.999	cleavage and polyadenylation specificity factor subunit CG7185
Hsp90	0.156	0.017	> 0.999	heat shock protein 90
LOC410380	0.161	0.044	> 0.999	neprilysin-2
LOC411396	0.162	0.027	> 0.999	neprilysin-4
LOC102655503	0.162	0.029	> 0.999	probable WRKY transcription factor protein 1
LOC100576169	0.163	0.044	> 0.999	uncharacterized LOC100576169
LOC550930	0.166	0.018	> 0.999	TGF-beta receptor type-1
LOC551464	0.166	0.031	> 0.999	TRAF3-interacting protein 1
LOC102654653	0.168	0.044	> 0.999	dihydropyrimidinase
LOC724177	0.169	0.032	> 0.999	uncharacterized LOC724177
LOC727221	0.172	0.049	> 0.999	vacuolar protein sorting-associated protein 13C
LOC725706	0.173	0.047	> 0.999	putative mediator of RNA polymerase II transcription subunit 26
LOC411931	0.174	0.017	> 0.999	ELMO domain-containing protein C
LOC408815	0.175	0.019	> 0.999	probable DNA mismatch repair protein Msh6
LOC408601	0.181	0.022	> 0.999	aprataxin
LOC552345	0.181	0.043	> 0.999	gamma-1-syntrophin
LOC409235	0.182	0.039	> 0.999	neurotrimin
LOC100577295	0.185	0.035	> 0.999	zinc finger protein 184
LOC413001	0.186	0.028	> 0.999	extended synaptotagmin-like protein 2
LOC413837	0.187	0.018	> 0.999	kinesin 3B
LOC727165	0.189	0.047	> 0.999	flocculation protein FLO11
LOC724205	0.196	0.027	> 0.999	protein AF-9
LOC408663	0.200	0.033	> 0.999	soma ferritin
LOC412243	0.203	0.019	> 0.999	protein split ends
LOC408282	0.205	0.033	> 0.999	uncharacterized LOC408282
LOC552317	0.206	0.013	> 0.999	ATP-dependent DNA helicase Q5
LOC727127	0.208	0.018	> 0.999	NK-tumor recognition protein

LOC113218779	0.214	0.019	> 0.999	70 kDa peptidyl-prolyl isomerase-like
LOC551792	0.215	0.044	> 0.999	cytosolic carboxypeptidase 1
LOC726045	0.218	0.021	> 0.999	apoptosis-resistant E3 ubiquitin protein ligase 1
LOC726819	0.218	0.009	> 0.999	ATP-dependent RNA helicase DDX51
LOC550645	0.222	0.048	> 0.999	max-binding protein MNT
LOC410174	0.222	0.006	> 0.999	cyclin-T
LOC102654994	0.223	0.040	> 0.999	uncharacterized LOC102654994
LOC413410	0.224	0.009	> 0.999	IQ motif and SEC7 domain-containing protein 2
LOC408670	0.224	0.023	> 0.999	Down syndrome cell adhesion molecule-like protein Dscam2
LOC100578205	0.225	0.023	> 0.999	uncharacterized LOC100578205
LOC725991	0.226	0.031	> 0.999	sodium/potassium-transporting ATPase subunit beta-2
LOC408740	0.228	0.005	0.903	phosphatase and actin regulator 4
LOC411114	0.231	0.002	0.682	synaptosomal-associated protein 25
LOC724819	0.234	0.024	> 0.999	mitotic spindle assembly checkpoint protein MAD1
LOC724256	0.234	0.026	> 0.999	neuferricin
LOC551602	0.238	0.047	> 0.999	ras GTPase-activating protein-binding protein 2
LOC100576444	0.239	0.010	> 0.999	chymotrypsin inhibitor
LOC410371	0.242	< 0.001	0.234	calcium-transporting ATPase sarcoplasmic/endoplasmic reticulum type
LOC410142	0.243	0.015	> 0.999	RILP-like protein homolog
LOC409023	0.244	0.039	> 0.999	methylthioribose-1-phosphate isomerase
For	0.246	0.036	> 0.999	cGMP-dependent protein kinase foraging
LOC724991	0.246	0.015	> 0.999	phosphatidylinositol 4-phosphate 5-kinase type-1 alpha
LOC100578277	0.247	0.019	> 0.999	U11/U12 small nuclear ribonucleoprotein 25 kDa protein
LOC408809	0.249	0.008	> 0.999	diacylglycerol kinase theta
LOC413721	0.249	0.016	> 0.999	uncharacterized LOC413721
LOC725131	0.256	0.001	0.514	microtubule-associated protein futsch
LOC412594	0.257	0.013	> 0.999	uncharacterized LOC412594
LOC107964502	0.260	0.011	> 0.999	uncharacterized LOC107964502
LOC412742	0.262	0.007	> 0.999	chromatin-remodeling complex ATPase chain Iswi
LOC409682	0.264	0.008	> 0.999	NADP-dependent malic enzyme
LOC411083	0.267	< 0.001	0.234	sodium/potassium-transporting ATPase subunit alpha
LOC408471	0.268	0.033	> 0.999	brefeldin A-inhibited guanine nucleotide-exchange protein 3
LOC724803	0.269	0.048	> 0.999	neprilysin-4
LOC724497	0.270	0.018	> 0.999	protein patched homolog 3
LOC411155	0.273	0.020	> 0.999	teneurin-a
LOC408311	0.273	0.030	> 0.999	catenin delta-2
LOC410021	0.275	0.014	> 0.999	protein Skeletor
LOC551113	0.277	0.028	> 0.999	delta-1-pyrroline-5-carboxylate dehydrogenase
LOC408810	0.282	0.038	> 0.999	rap guanine nucleotide exchange factor 2
LOC725174	0.282	0.044	> 0.999	zinc finger protein 470
LOC411763	0.283	0.031	> 0.999	DNA polymerase subunit gamma-1
LOC412782	0.283	0.015	> 0.999	nucleoside diphosphate kinase 7
LOC100577004	0.285	0.020	> 0.999	probable G-protein coupled receptor CG31760
LOC725970	0.286	0.003	0.750	protein still life
LOC410796	0.287	0.048	> 0.999	histone lysine demethylase PHF8
LOC100578346	0.288	0.010	> 0.999	uncharacterized LOC100578346
LOC100576461	0.290	0.011	> 0.999	uncharacterized LOC100576461
LOC552173	0.290	0.007	> 0.999	kinesin B

LOC413793	0.295	0.017	> 0.999	enhancer of polycomb homolog 1
LOC411113	0.303	< 0.001	0.324	solute carrier family 12 member 4
LOC408680	0.303	0.003	0.765	ryanodine receptor
LOC551258	0.305	0.003	0.750	serine/threonine-protein phosphatase 2A 56 kDa regulatory subunit epsilon isoform
LOC726401	0.314	0.043	> 0.999	ras-specific guanine nucleotide-releasing factor 2
LOC414021	0.322	0.037	> 0.999	uncharacterized LOC414021
LOC410326	0.323	0.023	> 0.999	Krueppel-like factor 10
LOC411972	0.327	0.002	0.712	CTD small phosphatase-like protein 2
LOC107965037	0.328	0.038	> 0.999	probable serine/threonine-protein kinase DDB_G0278845
LOC412234	0.328	0.047	> 0.999	pyrroline-5-carboxylate reductase
LOC409441	0.329	0.024	> 0.999	transmembrane protein 53
LOC100577632	0.334	0.014	> 0.999	phosphopantothenoylcysteine decarboxylase subunit VHS3
LOC551858	0.334	0.033	> 0.999	kynurenine 3-monooxygenase
LOC102654146	0.338	0.008	> 0.999	antifreeze protein Maxi
LOC727538	0.339	< 0.001	0.217	regulator of microtubule dynamics protein 2
LOC412878	0.346	0.024	> 0.999	DNA N6-methyl adenine demethylase
LOC726972	0.347	0.034	> 0.999	uncharacterized LOC726972
LOC410001	0.352	0.009	> 0.999	regulating synaptic membrane exocytosis protein 2
LOC726251	0.356	0.043	> 0.999	uncharacterized LOC726251
LOC411181	0.360	0.024	> 0.999	sodium- and chloride-dependent glycine transporter 1
LOC727007	0.361	0.032	> 0.999	alpha-tocopherol transfer protein
LOC408839	0.362	0.049	> 0.999	uncharacterized LOC408839
LOC408887	0.362	0.025	> 0.999	ankyrin repeat and SAM domain-containing protein 1A
LOC551556	0.363	0.035	> 0.999	probable serine/threonine-protein kinase DDB_G0283337
LOC410447	0.366	0.043	> 0.999	importin subunit beta-1
LOC726240	0.372	0.045	> 0.999	globin-1
LOC102654520	0.372	0.036	> 0.999	putative uncharacterized protein DDB_G0282133
LOC724876	0.374	0.035	> 0.999	SET and MYND domain-containing protein 4
LOC724973	0.377	0.045	> 0.999	focal adhesion kinase 1
LOC411238	0.379	0.039	> 0.999	LIM domain-binding protein 2
LOC406073	0.381	0.002	0.682	homeobox protein prospero
LOC100577986	0.388	0.035	> 0.999	probable sodium/potassium/calcium exchanger CG1090
LOC410320	0.391	0.048	> 0.999	whirlin
LOC411627	0.392	0.023	> 0.999	retinoblastoma-like protein 1
LOC409379	0.396	0.035	> 0.999	eukaryotic translation initiation factor 4H
LOC411023	0.399	0.037	> 0.999	cadherin-23
LOC409598	0.401	0.008	> 0.999	uncharacterized LOC409598
LOC411642	0.401	0.026	> 0.999	NF-kappa-B inhibitor-interacting Ras-like protein
LOC411277	0.404	0.007	> 0.999	uncharacterized LOC411277
LOC725190	0.409	0.018	> 0.999	protein snail
LOC725273	0.418	0.009	> 0.999	uncharacterized LOC725273
LOC100578779	0.426	0.045	> 0.999	uncharacterized LOC100578779
LOC411046	0.434	0.011	> 0.999	serine/threonine-protein phosphatase 2B catalytic subunit 2
LOC724460	0.439	0.048	> 0.999	uncharacterized LOC724460
LOC100578990	0.442	0.003	0.750	dynein intermediate chain 3
LOC408372	0.443	0.003	0.750	poly(rC)-binding protein 3
LOC102654488	0.444	0.037	> 0.999	mpv17-like protein
LOC410317	0.447	0.033	> 0.999	small conductance calcium-activated potassium channel

				protein
LOC412308	0.450	0.012	> 0.999	flap endonuclease 1
LOC725331	0.453	0.048	> 0.999	protein hairy
LOC409525	0.461	0.003	0.750	oxysterol-binding protein-related protein 2
LOC100577107	0.465	0.006	> 0.999	uncharacterized LOC100577107
LOC411875	0.465	0.038	> 0.999	transmembrane protein 62
LOC725964	0.475	0.015	> 0.999	uncharacterized LOC725964
LOC100578774	0.491	0.001	0.514	centrosomal protein of 164 kDa
LOC102655737	0.500	< 0.001	0.217	neural-cadherin
LOC100577273	0.513	0.015	> 0.999	uncharacterized LOC100577273
LOC410689	0.541	0.036	> 0.999	ELAV-like protein 2
LOC408896	0.549	0.012	> 0.999	semaphorin-2A
LOC408430	0.567	< 0.001	0.217	voltage-dependent L-type calcium channel subunit beta-2
LOC724873	0.570	0.049	> 0.999	ras-related protein Rab-7a
LOC100578834	0.579	0.034	> 0.999	zinc finger protein 616
nAChRa7	0.586	0.015	> 0.999	nicotinic acetylcholine receptor alpha7 subunit
LOC413428	0.586	0.004	0.902	uncharacterized LOC413428
LOC411721	0.597	0.003	0.750	uncharacterized LOC411721
LOC410870	0.607	0.021	> 0.999	proton channel OtopLc
LOC113218586	0.634	0.044	> 0.999	uncharacterized LOC113218586
LOC100578476	0.671	0.017	> 0.999	uncharacterized LOC100578476
LOC411836	0.720	0.016	> 0.999	exosome complex component RRP42
LOC100578718	0.736	0.023	> 0.999	protein distal antenna
LOC406124	0.813	0.004	0.784	gamma-aminobutyric acid receptor subunit beta
LOC409869	0.845	0.043	> 0.999	kinesin 3A
LOC413738	0.846	0.034	> 0.999	uncharacterized LOC413738
LOC725803	0.858	0.016	> 0.999	protein artichoke
LOC725750	0.886	0.008	> 0.999	uncharacterized LOC725750
LOC100578524	0.899	0.042	> 0.999	uncharacterized LOC100578524
LOC102653857	0.909	0.007	> 0.999	uncharacterized LOC102653857
LOC410341	0.982	0.034	> 0.999	RNA pseudouridylate synthase domain-containing protein 2
LOC410470	1.011	0.017	> 0.999	putative polypeptide N-acetylgalactosaminyltransferase 9
LOC107964901	1.011	0.015	> 0.999	protein NATD1-like
LOC551845	1.026	0.036	> 0.999	potassium voltage-gated channel protein Shaw
LOC100577585	1.032	0.001	0.514	uncharacterized LOC100577585
LOC100577879	1.042	0.034	> 0.999	carbonic anhydrase-related protein 10
LOC726124	1.106	0.043	> 0.999	segmentation protein Runt
LOC726487	1.121	< 0.001	0.217	histone H2B
LOC100576291	1.130	0.006	> 0.999	uncharacterized LOC100576291
LOC113218939	1.182	0.038	> 0.999	uncharacterized LOC113218939
LOC409781	1.189	0.045	> 0.999	uncharacterized LOC409781
LOC551364	1.279	0.030	> 0.999	homeobox protein SIX3
LOC410624	1.402	0.044	> 0.999	serine proteinase stubble
LOC100576300	1.423	0.009	> 0.999	uncharacterized LOC100576300
LOC100576198	1.423	0.002	0.682	bromodomain-containing protein DDB_G0270170
LOC100578130	1.750	0.013	> 0.999	uncharacterized LOC100578130
LOC412762	1.753	0.002	0.682	heparan-sulfate 6-O-sulfotransferase 1-B
LOC100576738	1.826	0.027	> 0.999	uncharacterized LOC100576738
LOC113219210	2.120	0.002	0.682	RNA-binding protein 25-like

APPENDIX B: Chapter 3 "Differentially-expressed genes from the honey bee abdomen dataset with unadjusted $p < 0.05$."

B.1 Table of genes from the honey bee abdomen dataset with unadjusted *P*-values below the α = 0.05 threshold, organized by ascending log2 fold change, with the gene ID, adjusted *P*-values, and gene descriptions included.

Gene ID	Log2 Fold Change	*p*-Value	Adjusted *p*-Value	Gene Description
A4	0.152	0.041	> 0.999	apolipophorin-III-like protein
Acph-1	-0.295	0.022	> 0.999	venom acid phosphatase
Adk1	0.249	0.039	> 0.999	adenylate kinase 1
Apd-1	0.356	0.030	> 0.999	apidermin 3
Apd-3	0.464	0.022	> 0.999	C1q-like venom protein
C1q-VP	-0.160	0.041	> 0.999	cuticular protein analogous to peritrophins 3-D
Cpap3-d	-0.299	0.037	> 0.999	cuticular protein analogous to peritrophins 3-D
CPR11	-0.975	0.043	> 0.999	cuticular protein 11
Def2	-1.843	0.010	> 0.999	defensin 2
Dscam	-0.418	0.047	> 0.999	Down syndrome cell adhesion molecule
Dsx	-0.318	0.013	> 0.999	doublesex
JHBP-1	0.358	0.021	> 0.999	take-out-like carrier protein
KEF36_p03 (ND6)	0.171	0.025	> 0.999	NADH dehydrogenase subunit 6
LOC100576135	-1.090	0.008	> 0.999	glutamate receptor 1-like
LOC100576146	-1.348	0.038	> 0.999	aladin
LOC100576223	-0.388	0.045	> 0.999	myb-like protein X
LOC100576270	0.317	0.003	> 0.999	2-iminobutanoate/2-iminopropanoate deaminase
LOC100576444	0.456	0.018	> 0.999	chymotrypsin inhibitor
LOC100576497	-0.310	0.041	> 0.999	uncharacterized LOC100576497
LOC100576555	-0.461	0.040	> 0.999	cytochrome b561 domain-containing protein 2
LOC100576568	1.444	0.030	> 0.999	SWR1-complex protein 3
LOC100576700	-0.198	0.038	> 0.999	class A basic helix-loop-helix protein 15
LOC100576744	0.451	0.022	> 0.999	uncharacterized LOC100576744
LOC100576814	-1.156	0.034	> 0.999	uncharacterized LOC100576814
LOC100576882	-0.571	0.015	> 0.999	uncharacterized LOC100576882
LOC100576949	-0.266	0.048	> 0.999	uncharacterized LOC100576949
LOC100576993	-0.261	0.035	> 0.999	zinc finger protein 1
LOC100577196	-0.215	0.049	> 0.999	uncharacterized LOC100577196
LOC100577367	-0.364	0.040	> 0.999	uncharacterized LOC100577367
LOC100577488	-0.571	< 0.001	> 0.999	uncharacterized LOC100577488
LOC100577629	-0.242	0.037	> 0.999	uncharacterized LOC100577629
LOC100577667	-0.212	0.040	> 0.999	WAS/WASL-interacting protein family member 3
LOC100577798	-0.865	0.006	> 0.999	uncharacterized LOC100577798
LOC100578144	0.671	0.009	> 0.999	mitotic apparatus protein p62

LOC100578159	-0.178	0.004	> 0.999	zinc finger matrin-type protein CG9776
LOC100578191	0.190	0.016	> 0.999	uncharacterized LOC100578191
LOC100578233	-0.369	0.037	> 0.999	dynein regulatory complex protein 1
LOC100578526	0.166	0.038	> 0.999	solute carrier family 35 member E2
LOC100578624	0.338	0.021	> 0.999	delta(3,5)-Delta(2,4)-dienoyl-CoA isomerase, mitochondrial
LOC100578769	-0.178	0.031	> 0.999	uncharacterized LOC100578769
LOC102653958	2.532	0.002	> 0.999	uncharacterized LOC102653958
LOC102654436	-1.463	0.034	> 0.999	uncharacterized LOC102654436
LOC102654783	-0.775	0.044	> 0.999	uncharacterized LOC102654783
LOC102654920	0.491	0.014	> 0.999	COMM domain-containing protein 7
LOC102654930	0.484	0.047	> 0.999	uncharacterized LOC102654930
LOC102655050	0.250	0.030	> 0.999	rRNA methyltransferase 1
LOC102655120	0.371	0.025	> 0.999	hepatocyte nuclear factor 4-gamma
LOC102655189	-2.191	0.018	> 0.999	sperm flagellar protein 1-like
LOC102655228	-1.446	0.038	> 0.999	uncharacterized LOC102655228
LOC102655272	0.197	0.036	> 0.999	NHP2-like protein 1
LOC102655411	-0.208	0.041	> 0.999	nucleoside diphosphate-linked moiety X motif 8
LOC102655905	0.358	< 0.001	> 0.999	uncharacterized LOC102655905
LOC102656142	0.445	0.030	> 0.999	protein zwilch homolog
LOC102656197	0.141	0.049	> 0.999	swi5-dependent recombination DNA repair protein 1 homolog
LOC102656504	0.457	0.015	> 0.999	ethanolamine kinase 1
LOC107963965	0.339	0.039	> 0.999	zinc finger HIT domain-containing protein 1
LOC107964400	0.469	0.027	> 0.999	integrin alpha-8-like
LOC107964633	0.460	0.002	> 0.999	major antigen-like
LOC107965279	1.379	0.041	> 0.999	pancreatic lipase-related protein 2
LOC107965571	0.808	0.016	> 0.999	uncharacterized LOC107965571
LOC107965749	0.528	0.011	> 0.999	acyl-CoA Delta(11) desaturase-like
LOC113218605	-0.151	0.032	> 0.999	DNA ligase 1-like
LOC113218636	1.074	0.027	> 0.999	uncharacterized LOC113218636
LOC113218672	-1.753	0.041	> 0.999	uncharacterized LOC113218672
LOC113218738	1.677	0.049	> 0.999	uncharacterized LOC113218738
LOC113218965	0.660	0.004	> 0.999	45 kDa calcium-binding protein
LOC113219045	0.688	0.012	> 0.999	uncharacterized LOC113219045
LOC113219265	-0.383	0.011	> 0.999	trypsin-1-like
LOC113219406	1.680	0.040	> 0.999	uncharacterized LOC113219406
LOC406096	0.257	0.045	> 0.999	type I inositol 1
LOC406146	-0.457	0.013	> 0.999	hyaluronoglucosaminidase
LOC406147	0.268	0.015	> 0.999	short-chain dehydrogenase/reductase
LOC408291	0.193	0.031	> 0.999	3-ketoacyl-CoA thiolase
LOC408299	-0.186	0.042	> 0.999	purine nucleoside phosphorylase
LOC408352	0.256	0.044	> 0.999	elongation factor Ts
LOC408373	-0.518	0.027	> 0.999	phosphatidylinositol 4-kinase beta
LOC408402	-0.188	0.048	> 0.999	acetyl-coenzyme A transporter 1
LOC408457	-0.173	0.020	> 0.999	protein LSM12 homolog
LOC408465	-0.204	0.015	> 0.999	vesicle-associated membrane protein 2
LOC408470	0.195	0.021	> 0.999	NAD kinase
LOC408500	-0.243	0.045	> 0.999	endothelin-converting enzyme homolog

LOC408507	-0.191	0.039	> 0.999	WD repeat-containing protein 44
LOC408572	-0.296	0.047	> 0.999	myophilin
LOC408603	-0.329	0.010	> 0.999	glucose dehydrogenase [FAD
LOC408615	0.215	0.032	> 0.999	nuclear transcription factor Y subunit gamma
LOC408634	0.613	0.026	> 0.999	major facilitator superfamily domain-containing protein 1
LOC408635	0.354	0.041	> 0.999	BTB/POZ domain-containing protein 1
LOC408650	-0.203	0.026	> 0.999	inositol oxygenase
LOC408694	-0.175	0.023	> 0.999	plastin-2
LOC408702	0.249	0.049	> 0.999	SAGA-associated factor 29
LOC408723	-0.237	0.035	> 0.999	cerebellar degeneration-related protein 2-like
LOC408740	-0.161	0.014	> 0.999	phosphatase and actin regulator 4
LOC408843	0.221	0.026	> 0.999	F-box/WD repeat-containing protein 9
LOC408872	-0.512	0.028	> 0.999	COUP transcription factor 2
LOC408877	-0.239	0.013	> 0.999	neurogenic protein mastermind
LOC408924	-0.401	0.041	> 0.999	peptidoglycan-recognition protein LC
LOC408953	-0.192	0.023	> 0.999	peroxidase
LOC408957	-0.233	0.049	> 0.999	uncharacterized LOC408957
LOC409034	-0.751	0.009	> 0.999	uncharacterized LOC409034
LOC409117	-0.344	0.015	> 0.999	vacuolar protein sorting-associated protein 16 homolog
LOC409228	-0.468	0.039	> 0.999	scavenger receptor class B member 1
LOC409277	-0.268	0.017	> 0.999	acidic phospholipase A2 PA4
LOC409316	-0.163	0.047	> 0.999	coronin-2B
LOC409348	-0.252	0.012	> 0.999	lethal(2) giant larvae protein homolog 1
LOC409402	-0.497	0.018	> 0.999	uncharacterized LOC409402
LOC409444	-0.229	0.040	> 0.999	AMP deaminase 2
LOC409494	0.280	0.046	> 0.999	methylglutaconyl-CoA hydratase
LOC409572	-0.555	0.042	> 0.999	TWiK family of potassium channels protein 9
LOC409573	-0.234	0.010	> 0.999	zinc finger protein 2 homolog
LOC409663	0.265	0.014	> 0.999	lysozyme
LOC409666	-0.297	0.022	> 0.999	ABC transporter G family member 20
LOC409759	-0.321	0.018	> 0.999	serine-rich adhesin for platelets
LOC409793	0.191	0.016	> 0.999	NADH dehydrogenase [ubiquinone] flavoprotein 2
LOC409821	-0.146	0.029	> 0.999	twitchin
LOC409884	-0.581	0.020	> 0.999	xylulose kinase
LOC409913	-0.247	0.040	> 0.999	COMM domain-containing protein 4
LOC409961	-0.153	0.042	> 0.999	heterogeneous nuclear ribonucleoprotein 27C
LOC410059	0.182	0.044	> 0.999	probable citrate synthase 2
LOC410061	-0.160	0.038	> 0.999	type I inositol 3
LOC410103	-0.106	0.032	> 0.999	partner of Y14 and mago
LOC410114	0.208	0.028	> 0.999	solute carrier family 23 member 1
LOC410132	0.214	0.043	> 0.999	GPI transamidase component PIG-T
LOC410280	-0.610	0.036	> 0.999	GTP-binding nuclear protein Ran
LOC410295	0.637	0.027	> 0.999	queuine tRNA-ribosyltransferase accessory subunit 2
LOC410492	-0.310	< 0.001	> 0.999	cytochrome P450 9e2
LOC410609	-0.575	0.039	> 0.999	disintegrin and metalloproteinase domain-containing protein 10-like
LOC410675	-0.207	0.034	> 0.999	maternal B9.10 protein
LOC410710	-0.212	0.027	> 0.999	zinc transporter ZIP13 homolog

LOC410758	-0.603	0.031	> 0.999	mRNA decay activator protein ZFP36L3
LOC410993	0.190	0.015	> 0.999	valacyclovir hydrolase
LOC411012	-0.173	0.036	> 0.999	NF-kappa-B inhibitor cactus
LOC411046	-0.423	0.047	> 0.999	serine/threonine-protein phosphatase 2B catalytic subunit 2
LOC411156	0.534	0.017	> 0.999	putative elongator complex protein 4
LOC411223	-0.523	0.030	> 0.999	esterase FE4
LOC411234	0.659	0.011	> 0.999	aryl hydrocarbon receptor nuclear translocator homolog
LOC411272	0.198	0.049	> 0.999	putative acyl-CoA-binding protein
LOC411738	0.734	0.018	> 0.999	lutropin-choriogonadotropic hormone receptor
LOC411742	-0.174	0.033	> 0.999	transcription initiation factor TFIID subunit 8
LOC411836	1.008	0.006	> 0.999	exosome complex component RRP42
LOC411882	-0.181	0.039	> 0.999	ER membrane protein complex subunit 2-B
LOC411894	-0.439	0.032	> 0.999	dynein beta chain
LOC412070	-0.306	0.019	> 0.999	serine/threonine-protein kinase 16
LOC412108	-0.129	0.040	> 0.999	casein kinase I
LOC412155	-0.378	0.018	> 0.999	F-box/WD repeat-containing protein 5
LOC412176	-0.205	0.004	> 0.999	transcription initiation factor TFIID subunit 1
LOC412198	-0.145	0.027	> 0.999	UDP-glucose:glycoprotein glucosyltransferase
LOC412278	0.290	0.031	> 0.999	tuberin
LOC412305	0.385	0.029	> 0.999	succinate-semialdehyde dehydrogenase
LOC412394	0.188	0.039	> 0.999	alpha-L-fucosidase
LOC412397	-0.316	0.037	> 0.999	uncharacterized LOC412397
LOC412430	0.416	< 0.001	> 0.999	major facilitator superfamily domain-containing protein 6
LOC412511	-0.133	0.036	> 0.999	importin subunit alpha-3
LOC412540	0.394	0.022	> 0.999	carcinine transporter
LOC412674	0.266	0.019	> 0.999	phosphoserine phosphatase
LOC412795	0.860	0.015	> 0.999	cadherin-99C
LOC412796	0.183	0.015	> 0.999	3-hydroxyisobutyryl-CoA hydrolase
LOC412888	-2.061	0.003	> 0.999	A disintegrin and metalloproteinase with thrombospondin motifs 7
LOC413052	-0.397	0.050	> 0.999	uncharacterized LOC413052
LOC413252	-0.175	0.020	> 0.999	ATP-binding cassette sub-family F member 2
LOC413288	-1.145	0.035	> 0.999	polycomb protein Pcl
LOC413362	0.525	0.044	> 0.999	ATP-dependent DNA helicase Q1-like
LOC413441	0.523	0.011	> 0.999	dnaJ homolog subfamily C member 3
LOC413448	-1.263	0.009	> 0.999	raf homolog serine/threonine-protein kinase Raf
LOC413557	-0.627	0.004	> 0.999	syndecan
LOC413691	0.646	0.042	> 0.999	condensin complex subunit 3
LOC413789	0.222	0.033	> 0.999	elongation of very long chain fatty acids protein AAEL008004
LOC413929	-0.165	0.035	> 0.999	egl nine homolog 1
LOC413936	-0.305	0.032	> 0.999	uncharacterized LOC413936
LOC550645	0.276	0.015	> 0.999	max-binding protein MNT
LOC550914	-0.169	0.005	> 0.999	DNA ligase 1
LOC551021	-0.324	0.046	> 0.999	low-density lipoprotein receptor-related protein 6
LOC551106	-0.125	0.032	> 0.999	ubiquitin-fold modifier-conjugating enzyme 1
LOC551259	-0.172	0.016	> 0.999	titin

LOC551356	-0.154	0.036	> 0.999	nesprin-1
LOC551395	0.255	0.032	> 0.999	acetyl-CoA acetyltransferase
LOC551466	0.386	0.029	> 0.999	CAAX prenyl protease 1 homolog
LOC551562	-0.232	0.012	> 0.999	dynein beta chain
LOC551652	0.159	0.021	> 0.999	tctex1 domain-containing protein 1
LOC551728	-0.283	0.048	> 0.999	F-box/LRR-repeat protein 20
LOC551983	0.375	0.017	> 0.999	thymidylate synthase
LOC551991	-1.267	0.048	> 0.999	uncharacterized LOC551991
LOC552048	0.251	0.031	> 0.999	flocculation protein FLO11
LOC552113	0.258	0.048	> 0.999	long-chain fatty acid transport protein 4
LOC552142	-0.201	0.040	> 0.999	latrophilin Cirl
LOC552150	-0.139	0.043	> 0.999	uncharacterized LOC552150
LOC552190	0.319	0.014	> 0.999	prisilkin-39
LOC552313	-0.186	0.039	> 0.999	sterol O-acyltransferase 1
LOC552386	0.250	0.023	> 0.999	anamorsin homolog
LOC552401	-0.188	0.013	> 0.999	protein cueball
LOC552405	0.246	0.025	> 0.999	GPN-loop GTPase 2
LOC552523	-0.405	0.023	> 0.999	L-threonine ammonia-lyase
LOC552568	0.176	0.027	> 0.999	hydroxyacylglutathione hydrolase
LOC552679	0.289	0.014	> 0.999	cytochrome P450 4c3
LOC724159	-0.148	0.018	> 0.999	histone acetyltransferase KAT6B
LOC724179	0.281	0.029	> 0.999	ribosomal protein S6 kinase delta-1
LOC724221	0.155	0.047	> 0.999	uncharacterized LOC724221
LOC724227	0.580	0.004	> 0.999	synaptic vesicle glycoprotein 2B
LOC724250	0.677	0.005	> 0.999	serine protease snake
LOC724322	-0.790	0.024	> 0.999	serum response factor homolog
LOC724353	0.605	0.012	> 0.999	prion-like-(Q/N-rich) domain-bearing protein 25
LOC724408	-0.411	0.023	> 0.999	ras-related GTP-binding protein A
LOC724421	-0.143	0.040	> 0.999	fibrillin-2
LOC724464	0.462	0.034	> 0.999	cuticular protein
LOC724488	0.146	0.018	> 0.999	protein lethal(2)essential for life
LOC724535	-0.147	0.045	> 0.999	uncharacterized LOC724535
LOC724551	0.324	0.049	> 0.999	BRCA1-associated RING domain protein 1
LOC724625	0.232	0.026	> 0.999	DNA-directed RNA polymerases I
LOC724630	-0.621	0.046	> 0.999	transmembrane protein 230
LOC724752	0.917	0.047	> 0.999	E3 ubiquitin-protein ligase TRIM71
LOC724776	-0.476	0.036	> 0.999	uncharacterized LOC724776
LOC724779	-0.292	0.007	> 0.999	protein artichoke
LOC724856	0.342	0.031	> 0.999	uncharacterized LOC724856
LOC724919	-0.177	0.016	> 0.999	mitochondrial amidoxime reducing component 2
LOC725048	-0.253	0.038	> 0.999	nodal modulator 3
LOC725309	0.244	0.001	> 0.999	keratin-associated protein 19-2
LOC725498	-0.199	0.038	> 0.999	protein mesh
LOC725546	-0.175	0.044	> 0.999	DDB1- and CUL4-associated factor 6
LOC725611	0.314	0.021	> 0.999	DNA polymerase alpha catalytic subunit
LOC725633	0.210	0.033	> 0.999	probable DNA-directed RNA polymerases I and III subunit RPAC2
LOC725690	-1.030	0.039	> 0.999	tetraspanin-3
LOC725760	-0.192	0.010	> 0.999	tetraspanin-2A

LOC725797	0.232	0.032	> 0.999	NADH dehydrogenase [ubiquinone] 1 beta subcomplex subunit 3
LOC725835	-0.158	0.037	> 0.999	DNA polymerase epsilon subunit 4
LOC725925	0.315	0.019	> 0.999	prolyl 3-hydroxylase OGFOD1
LOC725936	-0.168	0.039	> 0.999	titin homolog
LOC725997	-0.249	0.021	> 0.999	UDP-glucuronosyltransferase 2C1
LOC726019	-0.269	0.029	> 0.999	protein PTHB1-like
LOC726069	-0.433	0.002	> 0.999	atrial natriuretic peptide receptor 1
LOC726071	0.359	0.025	> 0.999	uncharacterized LOC726071
LOC726149	-0.681	0.034	> 0.999	sodium channel protein Nach
LOC726165	-0.534	0.036	> 0.999	fork head domain transcription factor slp1
LOC726252	-0.287	0.019	> 0.999	titin
LOC726320	0.276	0.018	> 0.999	serine protease inhibitor 27A
LOC726329	-0.300	0.048	> 0.999	venom peptide isomerase heavy chain
LOC726330	-0.826	0.035	> 0.999	golgin subfamily A member 7
LOC726629	-0.438	0.001	> 0.999	uncharacterized LOC726629
LOC726636	0.188	0.037	> 0.999	WD repeat-containing and planar cell polarity effector protein fritz
LOC726658	0.388	0.037	> 0.999	uncharacterized LOC726658
LOC726790	-0.398	0.009	> 0.999	uncharacterized LOC726790
LOC726977	0.204	0.014	> 0.999	prostaglandin E synthase 2
LOC727001	0.293	0.037	> 0.999	solute carrier family 35 member C2
LOC727028	1.162	0.041	> 0.999	uncharacterized LOC727028
LOC727079	0.629	0.011	> 0.999	fibroblast growth factor receptor substrate 2
LOC727173	0.474	0.042	> 0.999	pancreatic triacylglycerol lipase
LOC727306	0.192	0.033	> 0.999	bolA-like protein 3
LOC727424	0.478	0.014	> 0.999	mitochondrial thiamine pyrophosphate carrier
LOC727618	0.656	< 0.001	> 0.999	farnesyl pyrophosphate synthase
Mblk-1	-0.445	0.027	> 0.999	transcription factor mblk-1-like
Obp2	-0.696	0.030	> 0.999	odorant binding protein 2
osp	-0.258	0.017	> 0.999	outspread
Per	-0.242	0.013	> 0.999	period circadian protein

APPENDIX C: Chapter 3 "Differentially-expressed genes from the varroa mite dataset with unadjusted $p < 0.05$."

C.1 Table of genes from *Varroa destructor* dataset with unadjusted *P*-values below the α = 0.05 threshold, organized by ascending log2 fold change, with the gene ID, adjusted *P*-values, and gene descriptions included.

Gene ID	Log2 Fold Change	*p*-Value	Adjusted *p*-Value	Gene Description
LOC111242946	0.285	0.014	> 0.999	probable imidazolonepropionase
LOC111243057	-0.203	0.045	> 0.999	GATOR complex protein WDR59-like isoform X1
LOC111243214	0.890	0.034	> 0.999	protein spire homolog 1-like isoform X1
LOC111243233	-0.755	0.026	> 0.999	probable serine/threonine-protein kinase tsuA isoform X1
LOC111243283	-0.242	0.033	> 0.999	thymosin beta-like
LOC111243408	0.297	0.048	> 0.999	metaxin-2-like
LOC111243433	-0.906	0.045	> 0.999	protocadherin Fat 4-like isoform X1
LOC111243470	-0.227	0.025	> 0.999	myosin heavy chain, muscle-like isoform X1
LOC111243523	0.967	0.048	> 0.999	ubiquitin carboxyl-terminal hydrolase 43-like isoform X1
LOC111243526	0.250	0.030	> 0.999	biogenesis of lysosome-related organelles complex 1 subunit 1-like isoform X1
LOC111243589	-0.648	0.029	> 0.999	calcium-binding mitochondrial carrier protein Aralar1-like isoform X1
LOC111243636	-0.617	0.039	> 0.999	regulating synaptic membrane exocytosis protein 2-like isoform X1
LOC111243661	0.669	0.012	> 0.999	cyclin-dependent kinase 10-like isoform X1
LOC111243669	-0.421	0.007	> 0.999	cGMP-dependent protein kinase, isozyme 2 forms cD4/T1/T3A/T3B-like isoform X1
LOC111243711	1.420	0.035	> 0.999	uronyl 2-sulfotransferase-like
LOC111243826	0.423	0.018	> 0.999	kinesin-like protein KIF20A
LOC111243866	-0.206	0.007	> 0.999	uncharacterized protein LOC111243866
LOC111243952	-0.322	0.021	> 0.999	UBX domain-containing protein 4-like isoform X1
LOC111244015	-0.264	0.005	> 0.999	RNA-binding protein Rsf1-like
LOC111244093	0.617	0.023	> 0.999	oxysterol-binding protein-related protein 11-like isoform X1
LOC111244100	-0.515	0.031	> 0.999	GATA zinc finger domain-containing protein 11-like
LOC111244134	-0.401	0.005	> 0.999	laminin subunit alpha-1-like isoform X1
LOC111244145	0.373	0.049	> 0.999	uncharacterized protein LOC111244145 isoform X1
LOC111244146	-0.415	0.037	> 0.999	uncharacterized protein LOC111244146 isoform X1
LOC111244156	0.237	0.049	> 0.999	alpha-N-acetylgalactosaminidase-like
LOC111244184	-0.197	0.049	> 0.999	splicing factor 3A subunit 3-like isoform X1
LOC111244198	0.338	0.032	> 0.999	cytochrome P450 3A13-like
LOC111244203	1.811	0.038	> 0.999	obscurin-like
LOC111244227	-0.274	0.001	> 0.999	ADP,ATP carrier protein 1-like
LOC111244275	1.178	0.004	> 0.999	UPF0705 protein C11orf49 homolog isoform X1
LOC111244379	-0.268	0.022	> 0.999	uncharacterized protein LOC111244379

LOC111244467	0.243	0.040	> 0.999	uncharacterized protein LOC111244467
LOC111244495	-1.749	0.039	> 0.999	importin subunit alpha-4-like
LOC111244596	-0.370	0.008	> 0.999	uncharacterized protein LOC111244596 isoform X1
LOC111244632	-1.108	0.002	> 0.999	papilin-like isoform X1
LOC111244668	-0.673	0.026	> 0.999	high mobility group protein 20A-like
LOC111244716	-1.469	0.033	> 0.999	GILT-like protein 1 isoform X1
LOC111244721	-0.247	0.002	> 0.999	calcium load-activated calcium channel-like
LOC111244738	-0.309	0.024	> 0.999	synaptotagmin 1-like isoform X1
LOC111244749	0.661	0.046	> 0.999	uncharacterized protein LOC111244749
LOC111244839	1.185	0.024	> 0.999	ceramide-1-phosphate transfer protein-like isoform X1
LOC111244877	1.119	0.039	> 0.999	chromatin-remodeling complex ATPase chain Iswi-like
LOC111244914	-0.286	0.018	> 0.999	autophagy-related protein 16-1-like isoform X1
LOC111245078	0.714	0.042	> 0.999	transmembrane protein 161B-like
LOC111245128	-1.032	0.039	> 0.999	farnesyl pyrophosphate synthase-like
LOC111245157	1.501	0.030	> 0.999	uncharacterized protein LOC111245157 isoform X1
LOC111245207	0.331	0.013	> 0.999	nuclear nucleic acid-binding protein C1D-like
LOC111245238	-1.473	0.004	> 0.999	neuroglian-like
LOC111245260	0.246	0.030	> 0.999	methyltransferase-like protein isoform X1
LOC111245261	0.367	0.043	> 0.999	surfeit locus protein 1-like
LOC111245375	0.350	0.005	> 0.999	uncharacterized protein LOC111245375 isoform X1
LOC111245385	0.260	0.040	> 0.999	tubulin gamma-1 chain-like isoform X1
LOC111245402	-0.244	0.021	> 0.999	uncharacterized protein LOC111245402
LOC111245514	0.571	0.035	> 0.999	uncharacterized protein LOC111245514 isoform X1
LOC111245596	0.233	0.014	> 0.999	serine/threonine-protein phosphatase 2A activator-like isoform X1
LOC111245627	-0.215	0.004	> 0.999	NADH dehydrogenase [ubiquinone] 1 alpha subcomplex subunit 5-like
LOC111245748	1.469	0.008	> 0.999	major facilitator superfamily domain-containing protein 4A-like
LOC111245790	0.862	0.043	> 0.999	DNA replication complex GINS protein PSF1-like
LOC111245833	-0.524	0.009	> 0.999	probable isocitrate dehydrogenase [NAD] subunit alpha, mitochondrial
LOC111245864	-0.471	0.030	> 0.999	uncharacterized protein LOC111245864 isoform X1
LOC111245879	-0.718	0.013	> 0.999	transcription initiation factor IIA subunit 1-like
LOC111245891	-0.411	0.002	> 0.999	probable peptidyl-tRNA hydrolase 2
LOC111245914	0.294	0.018	> 0.999	DNA ligase 4-like
LOC111245988	1.128	0.020	> 0.999	phospholipase A-2-activating protein-like isoform X1
LOC111246045	1.450	0.020	> 0.999	NF-kappa-B inhibitor-interacting Ras-like protein 1 isoform X1
LOC111246264	-0.470	0.008	> 0.999	uncharacterized protein LOC111246264 isoform X1
LOC111246337	0.667	0.050	> 0.999	uncharacterized protein LOC111246337 isoform X1
LOC111246351	-0.279	0.037	> 0.999	histone-lysine N-methyltransferase SMYD3-like isoform X1
LOC111246452	-1.487	0.042	> 0.999	uncharacterized protein C15orf41 homolog isoform X1
LOC111246474	-0.389	0.019	> 0.999	uncharacterized protein LOC111246474 isoform X1
LOC111246477	0.170	0.021	> 0.999	regulator of nonsense transcripts 3A-like
LOC111246488	0.837	0.013	> 0.999	syntaxin-6-like isoform X1
LOC111246493	0.875	0.037	> 0.999	vacuolar protein sorting-associated protein VTA1 homolog
LOC111246513	0.281	0.039	> 0.999	zinc phosphodiesterase ELAC protein 2-like
LOC111246518	-0.194	0.016	> 0.999	nucleolar protein 56-like

LOC111246668	-1.938	0.004	> 0.999	uncharacterized protein LOC111246668 isoform X1
LOC111246722	0.211	0.039	> 0.999	putative helicase MOV-10 isoform X1
LOC111246729	-0.594	0.047	> 0.999	chloride intracellular channel protein 2-like isoform X1
LOC111246733	0.397	0.014	> 0.999	BAI1-associated protein 3-like isoform X1
LOC111246841	-0.112	0.031	> 0.999	coiled-coil-helix-coiled-coil-helix domain-containing protein 2-like
LOC111246866	-0.768	0.003	> 0.999	WD repeat-containing protein 60-like
LOC111246886	0.224	0.035	> 0.999	dCTP pyrophosphatase 1-like
LOC111246938	-0.466	0.002	> 0.999	uncharacterized protein LOC111246938 isoform X1
LOC111246973	-0.249	0.011	> 0.999	innexin inx2-like
LOC111247001	-0.125	0.014	> 0.999	uncharacterized protein LOC111247001
LOC111247038	1.123	0.002	> 0.999	uncharacterized protein LOC111247038 isoform X1
LOC111247041	-2.390	0.036	> 0.999	zinc finger BED domain-containing protein 1-like
LOC111247069	-0.277	0.016	> 0.999	uncharacterized protein LOC111247069
LOC111247134	2.064	0.015	> 0.999	uncharacterized protein LOC111247134 isoform X1
LOC111247321	-0.779	0.025	> 0.999	golgin subfamily A member 6-like protein 22 isoform X1
LOC111247339	0.224	0.010	> 0.999	uncharacterized protein LOC111247339
LOC111247419	0.791	0.040	> 0.999	uncharacterized protein LOC111247419
LOC111247421	1.709	0.027	> 0.999	uncharacterized protein LOC111247421
LOC111247479	-0.510	0.018	> 0.999	H(+)/Cl(-) exchange transporter 5-like isoform X1
LOC111247480	-1.752	0.046	> 0.999	electron transfer flavoprotein-ubiquinone oxidoreductase, mitochondrial-like isoform X1
LOC111247486	0.288	0.033	> 0.999	atypical kinase COQ8B, mitochondrial-like
LOC111247578	0.700	0.030	> 0.999	U1 small nuclear ribonucleoprotein 70 kDa-like
LOC111247635	-0.138	0.046	> 0.999	intersectin-1-like isoform X1
LOC111247669	0.337	0.039	> 0.999	cleavage stimulation factor subunit 2-like
LOC111247743	-0.344	0.029	> 0.999	phenazine biosynthesis-like domain-containing protein
LOC111247770	-0.133	0.020	> 0.999	uncharacterized protein LOC111247770
LOC111247773	-0.391	0.005	> 0.999	LOW QUALITY PROTEIN: F-box/LRR-repeat protein 14-like
LOC111247845	0.917	0.041	> 0.999	glutathione S-transferase C-terminal domain-containing protein-like isoform X1
LOC111247882	-0.943	0.044	> 0.999	S-adenosylmethionine decarboxylase proenzyme-like
LOC111247925	0.589	0.027	> 0.999	PHD finger protein 12-like
LOC111248021	-0.436	0.050	> 0.999	protein FAM50 homolog
LOC111248062	0.479	0.044	> 0.999	potassium channel subfamily K member 1-like
LOC111248205	-0.794	0.018	> 0.999	nudC domain-containing protein 1-like
LOC111248209	-1.211	0.026	> 0.999	potassium voltage-gated channel protein Shal-like isoform X1
LOC111248272	-0.245	0.033	> 0.999	ankyrin repeat and BTB/POZ domain-containing protein BTBD11-like isoform X1
LOC111248275	-0.231	0.013	> 0.999	synaptophysin-like protein 2 isoform X1
LOC111248363	0.333	0.020	> 0.999	peptidyl-prolyl cis-trans isomerase-like 3 isoform X1
LOC111248375	-0.435	0.024	> 0.999	vacuolar protein sorting-associated protein 16 homolog isoform X1
LOC111248415	-0.446	0.048	> 0.999	TBC1 domain family member 22B-like isoform X1
LOC111248610	-0.494	0.040	> 0.999	serine/threonine-protein kinase minibrain-like
LOC111248620	0.781	0.038	> 0.999	OTU domain-containing protein 5-B-like
LOC111248647	0.275	0.039	> 0.999	uncharacterized protein LOC111248647 isoform X1
LOC111248659	0.356	0.022	> 0.999	WD repeat-containing protein 89-like isoform X1

LOC111248753	-0.510	0.020	> 0.999	extracellular serine/threonine protein CG31145-like
LOC111248774	-0.215	0.030	> 0.999	uncharacterized protein LOC111248774
LOC111248780	-0.506	0.012	> 0.999	WASH complex subunit 4-like isoform X1
LOC111248841	0.351	0.001	> 0.999	DNA replication licensing factor mcm2-like
LOC111248852	-1.631	0.023	> 0.999	RING finger protein 11-like
LOC111248903	1.140	0.011	> 0.999	uncharacterized protein LOC111248903
LOC111248979	-0.502	0.017	> 0.999	zingipain-2-like
LOC111249016	0.951	0.024	> 0.999	potential E3 ubiquitin-protein ligase ariadne-1-like isoform X1
LOC111249026	1.489	0.032	> 0.999	E3 ubiquitin-protein ligase MARCH8-like isoform X1
LOC111249076	-1.019	0.008	> 0.999	uncharacterized protein LOC111249076 isoform X1
LOC111249117	-1.305	0.045	> 0.999	uncharacterized protein LOC111249117 isoform X1
LOC111249122	-0.761	0.048	> 0.999	calcium-dependent secretion activator-like
LOC111249170	0.293	0.035	> 0.999	protein TSSC1-like
LOC111249240	0.181	0.013	> 0.999	acylphosphatase-1-like isoform X1
LOC111249312	-0.969	0.010	> 0.999	ubiquitin-associated domain-containing protein 2-like isoform X1
LOC111249335	0.660	0.045	> 0.999	zinc finger FYVE domain-containing protein 9-like isoform X1
LOC111249337	0.455	0.025	> 0.999	dnaJ homolog subfamily C member 17-like isoform X1
LOC111249377	0.232	0.031	> 0.999	uncharacterized protein LOC111249377
LOC111249395	-1.898	0.024	> 0.999	adult-specific rigid cuticular protein 15.7-like
LOC111249484	0.485	0.032	> 0.999	uncharacterized protein LOC111249484 isoform X1
LOC111249488	-1.268	0.034	> 0.999	transcriptional repressor scratch 1-like
LOC111249511	-0.749	0.027	> 0.999	uncharacterized protein LOC111249511 isoform X1
LOC111249519	-0.960	0.004	> 0.999	poly(U)-binding-splicing factor PUF60-like isoform X1
LOC111249536	1.160	0.018	> 0.999	protein kinase C-binding protein 1-like isoform X1
LOC111249664	-0.341	0.011	> 0.999	putative defense protein Hdd11-like
LOC111249745	0.895	0.015	> 0.999	mitogen-activated protein kinase 14-like isoform X1
LOC111249787	0.313	0.042	> 0.999	protein brunelleschi-like
LOC111249788	1.152	0.020	> 0.999	histone H2A deubiquitinase MYSM1-like isoform X1
LOC111249814	-0.703	0.030	> 0.999	LIM domain transcription factor LMO4-like
LOC111249837	-0.820	0.046	> 0.999	peptidyl-prolyl cis-trans isomerase FKBP4-like
LOC111249935	-0.163	0.017	> 0.999	uncharacterized protein LOC111249935 isoform X1
LOC111249952	-0.383	0.046	> 0.999	partner of xrn-2 protein 1-like
LOC111250075	0.143	0.013	> 0.999	ATP-dependent RNA helicase DDX54-like isoform X1
LOC111250111	0.269	0.013	> 0.999	protein RTF2 homolog
LOC111250128	0.659	0.013	> 0.999	cAMP-dependent protein kinase type II regulatory subunit-like isoform X1
LOC111250134	0.487	0.024	> 0.999	organic cation transporter protein-like isoform X1
LOC111250157	0.304	0.019	> 0.999	mini-chromosome maintenance complex-binding protein-like isoform X1
LOC111250176	0.478	0.022	> 0.999	zinc finger protein 235-like
LOC111250243	-0.939	0.009	> 0.999	long-chain-fatty-acid--CoA ligase 4-like isoform X1
LOC111250332	-0.572	0.003	> 0.999	acetyl-CoA carboxylase-like isoform X1
LOC111250351	0.442	0.027	> 0.999	serine/threonine-protein kinase pakA-like
LOC111250373	0.286	0.037	> 0.999	actin-like protein 6B isoform X1
LOC111250404	0.245	0.017	> 0.999	geranylgeranyl transferase type-2 subunit beta-like
LOC111250409	2.075	0.028	> 0.999	tail-anchored protein insertion receptor WRB-like isoform X1

LOC111250417	-0.250	0.011	> 0.999	kinesin-like protein KIF2A isoform X1
LOC111250439	1.349	0.006	> 0.999	FK506-binding protein 2-like
LOC111250623	0.871	0.038	> 0.999	uncharacterized protein LOC111250623 isoform X1
LOC111250643	-0.601	0.015	> 0.999	endophilin-A-like isoform X1
LOC111250648	0.178	0.041	> 0.999	calpain-B-like isoform X1
LOC111250650	-0.717	0.033	> 0.999	ornithine decarboxylase-like isoform X1
LOC111250720	-0.678	0.036	> 0.999	uncharacterized protein LOC111250720
LOC111250810	-0.769	0.029	> 0.999	pre-mRNA cleavage complex 2 protein Pcf11-like
LOC111250831	1.586	0.049	> 0.999	protein SCO1 homolog, mitochondrial-like
LOC111250975	1.086	0.037	> 0.999	uncharacterized protein LOC111250975
LOC111251030	-1.283	< 0.001	> 0.999	beta-ureidopropionase-like
LOC111251111	-0.174	0.013	> 0.999	ATP synthase lipid-binding protein, mitochondrial-like
LOC111251130	0.248	0.044	> 0.999	exosome complex component RRP43-like isoform X1
LOC111251133	0.357	0.008	> 0.999	ovostatin-like
LOC111251141	-0.164	0.023	> 0.999	14-3-3 protein zeta-like
LOC111251142	0.215	0.016	> 0.999	hydroxysteroid dehydrogenase-like protein 2
LOC111251193	0.837	0.050	> 0.999	chondroitin sulfate proteoglycan 4-like
LOC111251336	-2.008	0.022	> 0.999	uncharacterized protein LOC111251336
LOC111251396	2.691	0.002	> 0.999	serine/threonine-protein phosphatase 2A 55 kDa regulatory subunit B alpha isoform-like
LOC111251455	-0.356	0.027	> 0.999	tubulin beta chain-like
LOC111251557	-0.211	0.006	> 0.999	myosin regulatory light chain 2-like
LOC111251693	-1.365	0.034	> 0.999	enhancer of mRNA-decapping protein 4-like
LOC111251804	-0.137	0.036	> 0.999	ATP synthase subunit e, mitochondrial-like
LOC111251862	-0.795	0.043	> 0.999	MAP kinase-activating death domain protein-like isoform X1
LOC111251881	0.287	0.023	> 0.999	aldehyde dehydrogenase family 16 member A1-like isoform X1
LOC111251885	-0.935	0.048	> 0.999	uncharacterized protein LOC111251885 isoform X1
LOC111251888	0.325	0.001	> 0.999	uncharacterized protein LOC111251888 isoform X1
LOC111252026	0.650	0.033	> 0.999	carbonyl reductase [NADPH] 1-like
LOC111252232	0.608	0.044	> 0.999	uncharacterized protein LOC111252232 isoform X1
LOC111252306	0.284	0.045	> 0.999	phosphatidylglycerophosphatase and protein-tyrosine phosphatase 1-like
LOC111252329	0.159	0.047	> 0.999	calcyphosin-like protein isoform X1
LOC111252385	1.898	0.022	> 0.999	adenylate cyclase type 3-like
LOC111252439	-0.515	0.049	> 0.999	protein tweety-like isoform X1
LOC111252445	-1.321	0.030	> 0.999	SAP domain-containing ribonucleoprotein-like
LOC111252465	-0.342	0.009	> 0.999	uncharacterized protein LOC111252465 isoform X1
LOC111252601	-1.241	0.002	> 0.999	uncharacterized protein LOC111252601
LOC111252613	1.414	0.031	> 0.999	palmitoyltransferase ZDHHC5-like isoform X1
LOC111252614	-0.446	0.013	> 0.999	glucose dehydrogenase [FAD, quinone]-like isoform X1
LOC111252668	0.382	0.002	> 0.999	AP-3 complex subunit beta-2-like isoform X1
LOC111252690	-1.021	0.024	> 0.999	uncharacterized protein LOC111252690
LOC111252695	1.632	0.018	> 0.999	heterochromatin protein 1-like
LOC111252730	-0.322	0.010	> 0.999	poly(U)-binding-splicing factor PUF60-like isoform X1
LOC111252734	-0.821	0.016	> 0.999	histone-lysine N-methyltransferase 2D-like isoform X1
LOC111252780	0.711	0.036	> 0.999	pyruvate dehydrogenase protein X component, mitochondrial-like
LOC111252785	1.330	0.046	> 0.999	transmembrane protein 120A-like

LOC111252853	-0.580	0.020	> 0.999	uncharacterized protein LOC111252853
LOC111252854	-0.141	0.015	> 0.999	putative ATP synthase subunit f, mitochondrial
LOC111252865	-0.200	0.049	> 0.999	protein RRP5 homolog isoform X1
LOC111252904	-0.546	0.029	> 0.999	ubiquitin-conjugating enzyme E2 L3-like
LOC111252985	0.453	0.018	> 0.999	vacuolar protein sorting-associated protein 4A-like
LOC111253008	-0.203	0.028	> 0.999	ankyrin-2-like isoform X1
LOC111253060	-0.353	0.015	> 0.999	bifunctional 3'-phosphoadenosine 5'-phosphosulfate synthase-like isoform X1
LOC111253093	-0.430	0.041	> 0.999	nucleoside diphosphate-linked moiety X motif 19-like isoform X1
LOC111253112	-0.913	0.036	> 0.999	retinal-specific ATP-binding cassette transporter-like isoform X1
LOC111253113	1.512	0.020	> 0.999	uncharacterized protein LOC111253113 isoform X1
LOC111253152	0.267	0.006	> 0.999	uncharacterized protein LOC111253152 isoform X1
LOC111253279	0.207	0.031	> 0.999	trypsin-1-like
LOC111253309	0.216	0.026	> 0.999	U3 small nucleolar RNA-interacting protein 2-like isoform X1
LOC111253329	0.320	0.043	> 0.999	uncharacterized protein LOC111253329 isoform X1
LOC111253371	-0.646	0.008	> 0.999	zinc finger protein 133-like
LOC111253384	-1.268	0.017	> 0.999	serine/threonine-protein kinase mig-15-like isoform X1
LOC111253427	0.281	0.048	> 0.999	deoxynucleoside kinase-like isoform X1
LOC111253436	0.369	0.018	> 0.999	GATOR complex protein DEPDC5-like isoform X1
LOC111253484	-1.168	0.024	> 0.999	rhomboid-related protein 2-like
LOC111253556	-0.800	0.011	> 0.999	mucin-3A-like isoform X1
LOC111253690	-1.178	0.006	> 0.999	uncharacterized protein LOC111253690 isoform X1
LOC111253793	-0.313	0.033	> 0.999	E3 ubiquitin-protein ligase RBBP6-like isoform X1
LOC111253859	-0.287	0.003	> 0.999	ATP-binding cassette sub-family F member 1-like
LOC111254199	-0.717	0.041	> 0.999	uncharacterized protein LOC111254199
LOC111254220	1.476	0.015	> 0.999	uncharacterized protein LOC111254220
LOC111254285	-0.143	0.031	> 0.999	uncharacterized protein LOC111254285
LOC111254440	0.405	0.027	> 0.999	luc7-like protein 3
LOC111254442	-0.260	0.006	> 0.999	death-associated protein 1-like
LOC111254575	-0.362	0.040	> 0.999	pyruvate kinase PKM-like isoform X1
LOC111254711	-0.116	0.012	> 0.999	eukaryotic translation initiation factor 2 subunit 2-like isoform X1
LOC111254736	-0.937	< 0.001	> 0.999	phosducin-like protein
LOC111254752	-0.084	0.047	> 0.999	tubulin alpha-1D chain
LOC111254890	0.286	0.042	> 0.999	intraflagellar transport protein 46 homolog
LOC111254948	0.299	0.023	> 0.999	uncharacterized protein LOC111254948
LOC111254950	0.555	0.028	> 0.999	ralA-binding protein 1-like
LOC111254973	0.199	0.047	> 0.999	angiogenic factor with G patch and FHA domains 1-like isoform X1
LOC111254996	-1.303	0.011	> 0.999	ubiquitin thioesterase zranb1-B-like isoform X1
LOC111255129	-2.472	0.014	> 0.999	general vesicular transport factor p115-like
LOC111255189	-0.616	0.001	> 0.999	GAS2-like protein pickled eggs
LOC111255225	-2.042	0.029	> 0.999	myosin-15-like
LOC111255269	-0.983	0.038	> 0.999	irregular chiasm C-roughest protein-like isoform X1
LOC111255376	-1.374	0.003	> 0.999	homeobox protein CDX-1-like
LOC111255377	-0.560	0.034	> 0.999	phosphorylated CTD-interacting factor 1-like isoform X1
LOC111255486	1.313	0.006	> 0.999	uncharacterized protein LOC111255486

LOC111255491	1.456	0.047	> 0.999	graves disease carrier protein homolog isoform X1
LOC111255549	-2.511	0.009	> 0.999	heat shock protein DDB_G0288861-like